

# **Systems Biology based studies on anti-inflammatory compounds**

Proefschrift

ter verkrijging van

de graad van Doctor aan de Universiteit van Leiden,  
op gezag van de Rector Magnificus Dr. D.D. Breimer,  
hoogleraar in de faculteit der Wiskunde en  
Natuurwetenschappen en die der Geneeskunde,  
volgens besluit van het College voor Promoties  
te verdedigen op maandag 14 november 2005  
te klokke 14.15 uur

door

**Kitty Catharina Maria Verhoeckx**

geboren te Utrecht

in 1970

## Promotiecommissie

Promotor: Prof.dr. J. van der Greef

Co-promotoren: Dr. R.T.J. Rodenburg  
Dr. R.F. Witkamp

Referent: Prof.dr. R.P.H. Bischoff

Overige leden: Prof.dr. M. Danhof  
Prof.dr. T. Hankemeier  
Prof.dr. R. Verpoorte

Kaft: 360 °C foto van de binnenstad van Utrecht, beschikbaar gesteld door CycloMedia Technology B.V. ([www.cyclomedia.nl](http://www.cyclomedia.nl)). De foto symboliseert het systeem denken. Met behulp van 360 °C foto's (fish-eye foto) zijn we in staat om zoveel mogelijk van het systeem 'Utrecht binnenstad' in kaart te brengen. Het systeem bestaat niet alleen uit een paar grachten pandjes, maar ook de grachten, bruggen, straten, mensen etc behoren tot het systeem. Alle onderdelen van het systeem staan met elkaar in verbinding en beïnvloeden elkaar.

Printed by Grafisch bedrijf Ponsen & Looijen B.V., Wageningen, The Netherlands.

ISBN 9074538630

Publication of this thesis was financially supported by:

TNO Quality of Life, Zeist, The Netherlands.

Nonlinear Dynamics, Newcastle upon Tyne, UK

*Gelukkig zijn is ook een gave*

*Als het beter gaat dan ooit*

*(De Dijk)*

## Contents

<b>Chapter 1</b>	General introduction	7
1.1	Systems biology	8
1.2	Transcriptomics	10
1.3	Proteomics	11
1.4	Metabolomics	14
1.5	Multivariate data analysis	15
2.1	Inflammation	17
2.2	Macrophages	19
	Scope and outline of the thesis	20
<b>Chapter 2</b>	A combination of proteomics, principal component analysis and transcriptomics is a powerful tool for the identification of biomarkers for macrophage maturation in the U937 cell line.	27
<b>Chapter 3</b>	Categorization of anti-inflammatory compounds using transcriptomics, proteomics, and metabolomics in combination with multivariate data analysis.	53
<b>Chapter 4</b>	In search of secreted protein biomarkers for the anti-inflammatory effect of $\beta_2$ -adrenergic receptor agonists: application of DIGE technology in combination with multivariate and univariate data analysis tools.	75
<b>Chapter 5</b>	Inhibitory effects of the $\beta_2$ -adrenergic receptor agonist Zilpaterol on the LPS-induced production of TNF- $\alpha$ <i>in vitro</i> and <i>in vivo</i> .	99
<b>Chapter 6</b>	Beta-adrenergic receptor agonists induce the release of Granulocyte Chemotactic Protein-2, Oncostatin M, and Vascular Endothelial Growth Factor from macrophages.	113

<b>Chapter 7</b>	Unheated <i>Cannabis sativa</i> extracts and its major compound THC-acid have potential immuno-modulating properties not mediated by CB <sub>1</sub> and CB <sub>2</sub> receptor coupled pathways.	125
<b>Chapter 8</b>	Categorization of the anti-inflammatory properties of Cannabis extracts using transcriptomics in combination with multivariate data analysis.	145
<b>Chapter 9</b>	Concluding remarks and future perspectives	153
	Summary	159
	Samenvatting	163
	Curriculum Vitae	169
	Nawoord	171
	List of publications	173
	List of abbreviations	175



# Chapter 1

---

**General introduction**

## General Introduction

The developments in genomics have enabled fundamental changes in the drug discovery and development processes. Metabolic pathways are complex and interdependent, and diseases are rarely resulting from a single genetic or metabolic defect. Similarly, diseases often involve a plethora of biochemical and physiological responses in cells, organs and organisms.

Recognizing the complexity of normal and disturbed functioning, many laboratories active in early drug discovery are moving from rather simple “one endpoint - high throughput” screening programs towards “high content” screening strategies. These strategies are often cell-based and the aim is to obtain much more information from the same biological system in one single (micro-) experiment. In more complex systems, such as animals or humans, biomarkers have become important for the characterization of diseases and drug effects. The concept of *systems biology* is a realization that organisms do not consist of isolated subsets of genes, proteins and metabolites. It uses an integrated approach to study and understand the function of biological systems, and how perturbations of such systems, for example the administration of a drug, affect their function.

### 1.1 Systems biology

A system can be defined as a set of molecules, a cell, groups of cells working closely together (e.g. immune system), organs, individuals, or even complete ecosystems. Systems biology integrates data at the genetic, protein, and metabolite levels, as well as cellular and pathway events that are in flux and interdependent<sup>1-5</sup>. This does not necessarily imply that all elements need to be measured for a systems study, but that systems thinking and systems-based analytical strategies are important. Systems biology develops a systems level understanding by quantitatively describing the interactions among the individual components of the system under investigation. The ultimate aim of systems biology is to develop computational models of these complex systems, using the data obtained from different analytical platforms, so that the response of the biological system to any kind of perturbation, for example administration of a drug, genetic mutation, environmental perturbations etc, can be predicted.

Systems biology approaches consist of different interchangeable modules (Fig. 1)<sup>2</sup>:

- Biological question and experimental design; selection of the biological system (e.g. body fluid, cell type, organism), controls (diseased, control, treated), sample number etc.

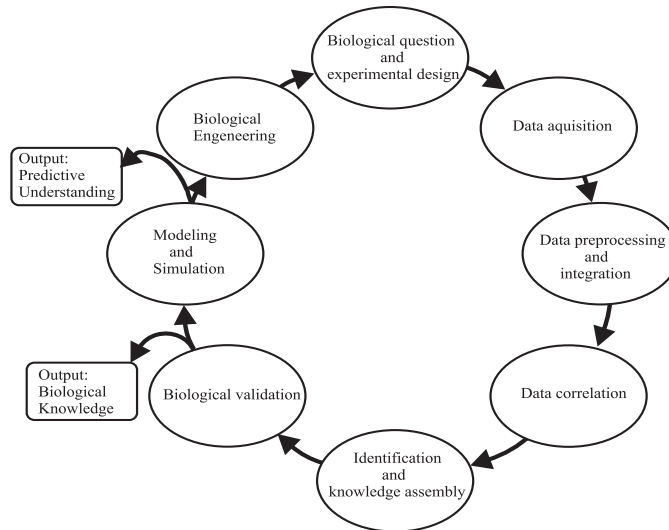


**Figure 1** Systems biology cycle contains different interchangeable modules <sup>2</sup>.

The order of the process is determined by the biological question being investigated

- Data acquisition; transcriptomics, proteomics, metabolomics, clinical, physiological data on the different groups under investigation.
- Data pre-processing and integration; data files are smoothed, aligned, and/or normalized.
- Data correlation and causality; data files are compared, and ultimately correlation and causal networks are produced.
- Component identification and knowledge assembly; statistically significant components differing between control and perturbed systems are identified and information on these components are gathered.
- Biological validation; to ensure that the correlation or causal networks have biological relevance, findings must be related back to the biology of the system under investigation (e.g. bioassays, knockout animals).
- Modelling and simulation; data and correlation networks can be used as a framework for further modelling and simulation studies of the biological processes being investigated or to predict the outcome of specific changes in the network.
- Biological engineering; once a system has been modelled and understood, it is possible to re-engineer the pathway or network to identify the optimal therapeutic agent.

In conclusion, systems biology requires the integration of biology, medicine, mathematics and chemistry with biostatistics and bioinformatics to transform complex and diverse datasets into useful knowledge. The next paragraphs describe the different analytical platforms most

frequently used in systems biology approaches. An overview of these platforms and their relationship is shown in Figure 2.

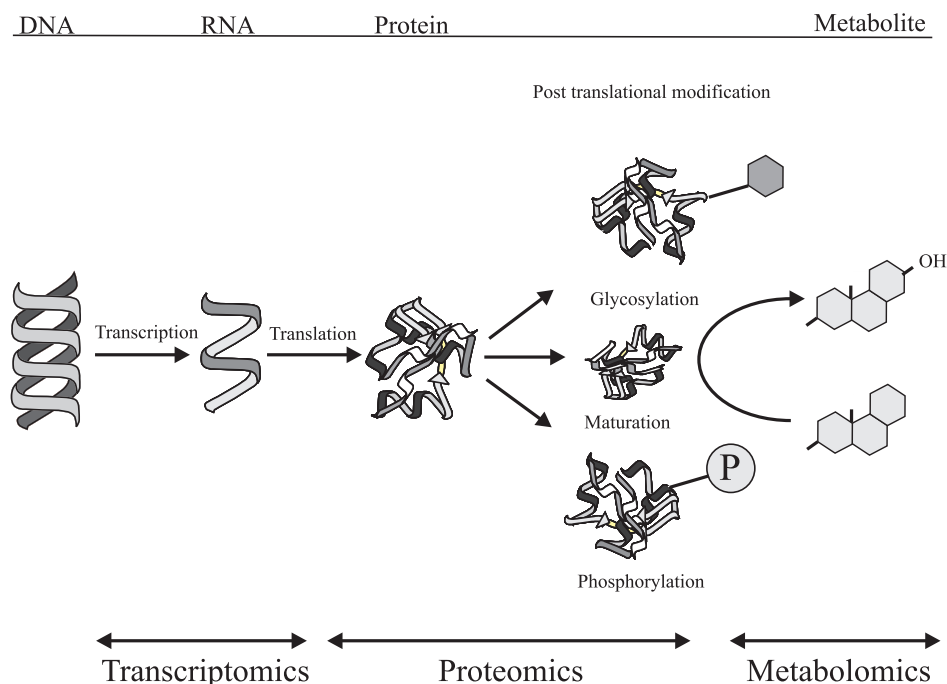


**Figure 2** Overview of the analytical platforms applied to systems biology approaches and their relationships. For the sake of simplicity, the bio feedbacks regulatory mechanisms are not drawn.

## 1.2 Transcriptomics

Many cellular processes are controlled at the gene expression level. Measurement of the mRNA expression levels can provide information on the current state of a cell or give insight in possible functions of genes.

Transcriptomics or functional genomics simultaneously monitors the transcription levels of hundred to thousands of genes. Before the development of DNA arrays that are used nowadays in transcriptomics experiments, mRNA levels were measured using Northern blot or Reversed Transcription Polymerase Chain Reaction (real time PCR). Recently the latter method has been adapted into a more quantitative method, real-time PCR<sup>6</sup> in which the amount of amplified target is followed after each amplification cycle using a fluorescent probe. However, this technology allows the analysis of the expression levels of only a few genes at the time. Microarrays<sup>7-9</sup> were developed to analyse ten thousands of gene expression levels in a single experiment. Currently, two types of microarrays are available, cDNA arrays, (DNA fragments of 500-3000 bp) and oligonucleotide arrays (25 - 70 bp fragments). A microarray consists of thousands of individual DNA/oligonucleotide sequences printed (or synthesized) in a high density array on a glass microscopic slide. Two mRNA samples are

reversed transcribed into cDNA and at the same time fluorescent dyes (usually a red fluorescent dye, Cyanine 5 (CY5) and a green fluorescent dye, Cyanine 3 (CY3) are incorporated into the cDNA strand. Subsequently, the samples are mixed in equal proportions and hybridized to the arrayed probes on the glass slide. After this competitive hybridization, the slides are imaged using a laser scanner, and fluorescent measurements are performed separately for each dye at each spot of the array. The ratio of the red and green fluorescent intensities for each spot is indicative of the relative abundance of the corresponding DNA probe in the two nucleic acid target samples. In this way the expression ratios of tens of thousands of genes can be acquired in one single analysis. Although in most cases the expression levels of the majority of genes will not differ between the samples that are compared, still many genes that are either up-or down regulated between the two samples are easily identified. The differential expression of these genes yields a wealth of information that is of great importance in studies of cellular mechanisms, in studies of diseases, in drug discovery, and in toxicological studies.

### **1.3 Proteomics**

Not all changes in cellular mechanisms can be determined by measuring the gene expression levels. In fact, proteins carry out many biological functions without any observable significant changes at the mRNA level. For example, phosphorylation of an enzyme may switch on and of enzymatic reactions, or proteolytic cleavage of membrane bound precursors may regulate the release of extra cellular signals (e.g. TNF- $\alpha$ ). Moreover, there is a limited quantitative correlation between the expression levels of mRNAs and proteins<sup>10-12</sup>. This poor correlation may for example be due to post-transcriptional (e.g. splice variants), and post translational modifications (phosphorylation, glycosylation, maturation). Therefore, the examination of the proteome is essential in order to resolve fundamental biological questions.

Proteomics has been defined as the study of all proteins, including their relative abundance, distribution, post translational modifications, functions and interactions with other macromolecules in a given cell or organism within a given environment and at a specific stage in the cell cycle<sup>11-14</sup>. Sometimes the term functional proteomics is used to describe the interactions of proteins. Proteomics can be divided in three main areas: 1) protein characterization for large scale identification of proteins and their post-translational modifications, 2) ‘differential display’ proteomics for comparison of protein levels between samples, and 3) studies of protein-protein interactions.

A simultaneous measurement of all proteins in a sample is a difficult task if not impossible, because the properties of proteins are extremely diverse (e.g. abundance, solubility, stability). Sample preparation and pre-fractionation are therefore essential steps in the proteomics workflow and determine which sub-fraction of proteins are being analysed<sup>15-17</sup>. Many different strategies for protein analysis have been developed (Table 1).

**Table 1** Commonly used technologies in proteomics

Method	Application
<b>1 and 2-Dimensional gel electrophoresis coupled to mass spectrometry</b>	Differential protein expression, Post translational modifications
<b>Mass spectrometry;</b> Matrix Assisted Laser Desorption Ionisation (MALDI), Electrospray Ionisation (ESI)	Identification of proteins after enzymatic digest Post translational modifications
<b>LC-MS/ multidimensional LC-MS</b> Multi Dimensional Protein Identification Technology (MUDPIT)	Protein identification
Isotopic labelling (e.g. Isotope Coded Affinity Tag (ICAT) , ITRAQ <sup>TM</sup> , Stable Isotope Labelling by Amino acids in Cell cultures (SILAC))	Differential protein expression Quantification
<b>Chips</b> antibody array, protein array, antigens, aptamers, carbohydrates or small molecules (e.g. drugs), Surface Enhanced Laser Desorption Ionisation (SELDI)	Protein interactions with diverse compounds Protein profiling
<b>Phage display</b>	Protein-protein interaction
<b>Yeast 2-Hybrid system</b>	Protein-protein interaction Protein-DNA interaction
<b>Imaging</b> fluorescent labels, MALDI	Protein-protein interaction Protein localization
<b>Western blot</b>	Protein identification Quantification
<b>Enzyme-linked immunosorbent assay</b>	Quantification

\* These techniques are reviewed in many publications e.g.<sup>13, 18-26</sup>

Currently, the main proteomic strategies involve: 1) two-dimensional (2-D) gel electrophoresis, followed by mass spectrometric identification, 2) liquid chromatography (LC)-based separation of enzymatically digested proteins followed by mass spectrometry and 3) antibody-based microarray technology. However, none of these techniques is favourable over the other. In fact, the techniques are complementary to each other. The separation and visualization of proteins by 2-D gel electrophoresis is the oldest and still most widely applied method<sup>23, 27</sup>. The technique was originally described by O'Farrell in 1975<sup>28</sup>, but its real

expansion as a useful technique begun with the development of analytical techniques that were able to identify proteins at the amounts available on a 2-D gel. A schematic representation is given in Figure 3. The proteins of a sample are first separated on the basis of their net charge using fixed pH gradients and then separated by mass. The separated proteins are visualized by post-electrophoretic staining methods such as Coomassie Blue, silver stain,

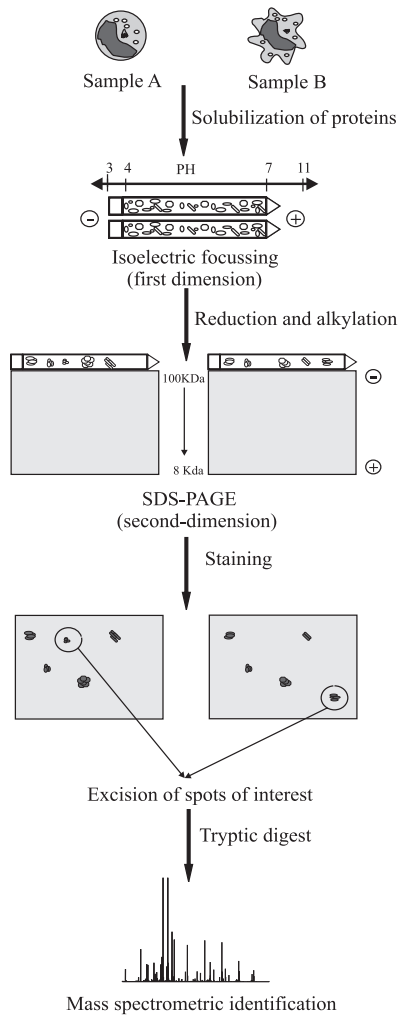


**Figure 3** Schematic presentation of the 2-D gel electrophoresis workflow

and fluorescent dyes<sup>27, 29-31</sup>. The gels are subsequently scanned and analysed using specific software that is able to determine spot positions and spot volumes. Spots of interest can be excised, enzymatically digested and subsequently identified using (LC) mass spectrometry (e.g. MALDI-MS, electrospray-MS). The peptide mass fingerprint and peptide fragmentation data can be compared to theoretically cleaved protein patterns in databases (e.g. NCBI and Swissprot). Conventional 2-D gel electrophoresis is known for its limitations with respect to reproducibility, limited dynamic range, and sensitivity. These issues have been improved with the introduction of difference gel electrophoresis (DIGE)<sup>32-34</sup>. DIGE enables the analysis of multiple protein samples on a single gel. This is achieved through the covalent binding of each protein with structurally similar but spectrally distinct fluorophores (CyDyes). Prior to electrophoresis, the samples are labelled with either CyDye 3 or CyDye 5, while CyDye 2 is used to label a pooled sample comprising equal amounts of each of the samples within the study, and acts as an internal standard. Per gel two samples and an internal standard can be separated. The internal standard is used for normalization of data between gels, thereby minimizing experimental variation and increasing the confidence in matching and quantification of different gels in complex experimental designs. Although DIGE has resolved most drawbacks of the old-fashioned 2-D gel electrophoresis technique, it is still not possible to examine all proteins, in particular hydrophobic or extremely basic proteins. To overcome these problems other gel-free approaches have been introduced. Liquid chromatography based proteomics techniques

generally involves the enzymatic digestion of the protein sample with proteases. Subsequently, the complex peptide mixture is resolved by LC or multidimensional LC (MDLC), using for example, a combination of strong cation exchange (SCX) and reverse-phase (RP) columns. The number of dimensions used depends on the complexity of the sample under investigation. The separated peptides are analyzed by mass spectrometry and the MS fragmentation patterns are matched with predicted information from genomics or proteomics databases to identify the proteins. The combination of MDLC and MS is called multi-dimensional protein identification technology (MUDPIT). The MUDPIT approach can be automated and proteins with different properties can be separated simultaneously. A drawback of MUDPIT is that quantification of proteins and peptides is more difficult. The linearity of MS response with peptide concentration may cause some difficulties, especially regarding the analysis of very complex mixtures, where peptides from highly abundant proteins may interfere with ionisation of minor compounds. Therefore other LC-MS approaches have been developed that rely on modifying the samples with a stable isotope, which changes the molecular mass but not the mass spectrometric behaviour. Quantitative differences are then determined directly as the differences in peak area between the two peptides in the mixed sample. There are basically two approaches for labelling peptides with stable isotopes: chemically incorporation of the mass tag (e.g. ICAT and iTRAQ<sup>TM</sup>), usually by reacting with cysteine after purifying the proteins; or metabolic incorporation, where labelling of the proteins is achieved by growing cells in a medium enriched with stable isotope-containing precursors (e.g. SILAC)<sup>19</sup>.

Protein microarrays are another approach for analyzing large sets of proteins<sup>18, 22, 25</sup>. In this technique, individually purified ligands (e.g. proteins, peptides, antibodies, antigens, and small molecules) can be spotted onto a derivatized surface and are generally used for examining protein expression levels. However, there are still a number of issues that need improvement, including the heterogeneity of antibody affinities, the difficulty to produce large number of specific antibodies, large protein concentration ranges and the diversity of chemical properties of proteins. Due to these issues, it is currently only possible to manufacture relatively small protein arrays containing a few different antibodies (e.g. cytokine arrays).

### **1.4 Metabolomics**

Metabolomics methods identify and quantify the levels of metabolites (small molecules) in the cell and in extra cellular fluids (e.g. plasma, urine, cell culture media), which may reflect

changes in cellular processes due to internal and external stimuli<sup>5, 12, 35</sup>. For example, processes like metabolism and biotransformation of xenobiotics can be followed in cells or plasma, and excreted metabolites can be determined in urine. The analysis of the metabolome is much more complex than that of the genome and proteome. This is due to the fact that the metabolome consists of a large number of different molecules with very diverse physical properties, and includes organic acids, lipids, amino acids, nucleotides, steroids, eicosanoids, neurotransmitters, peptides, and trace elements. Moreover, the concentration range to be covered in metabolomics can also be extremely large. These concentration ranges can even be found within a single class of compounds, such as in case of lipids that can be present in concentrations ranging from mg/ml to pg/ml within a single sample. Due to this heterogeneity and diversity it is clear that a single method or technology cannot provide the performance necessary for comprehensive metabolic studies. Metabolomics approaches use analytical techniques such as nuclear magnetic resonance (NMR), gas chromatography, and liquid chromatography, the latter two both in combination with mass spectrometry. NMR is extremely useful for global profiling of components at the higher concentration range of the metabolome, and for measuring compounds of different biosynthetic and structural natures in a single profile. MS based technologies are powerful for the separation and quantification of compound classes in complex mixtures, including amongst others lipids, steroids, and amino acids. Special data processing tools (e.g. partial linear fit algorithms) are necessary to analyse the complex raw datasets of NMR- and MS-based metabolomics techniques and to correct for minor shifts in the spectra while maintaining a high resolution.

### **1.5 Multivariate data analysis**

The methods used in systems biology generate massive amounts of complex data. Therefore, powerful biostatistics and bioinformatics tools are necessary to evaluate the complex data and to correlate the results to biological questions. Multivariate data analysis techniques and pattern recognition tools are frequently used to analyse the data from proteomics, transcriptomics and metabolomics studies to detect hidden correlations and trends. Multivariate data analysis techniques are methods that consider a group of variables together, rather than focusing on one variable at a time. In addition, these techniques in general cope better with datasets in which the number of experiments (observations) is much smaller than the number of variables (e.g. proteins, transcripts, and metabolites) with respect to univariate approaches. The most frequently used and straight forward approach for pattern recognition is principal component analysis (PCA)<sup>36-40</sup>. PCA is a mathematical procedure that summarizes

a number of possibly correlated variables into a smaller number of uncorrelated variables called principal components (PCs). The objective of principal component analysis is to reduce the dimensionality (number of variables) of the dataset while retaining most of the original variability in the data (Fig. 4).

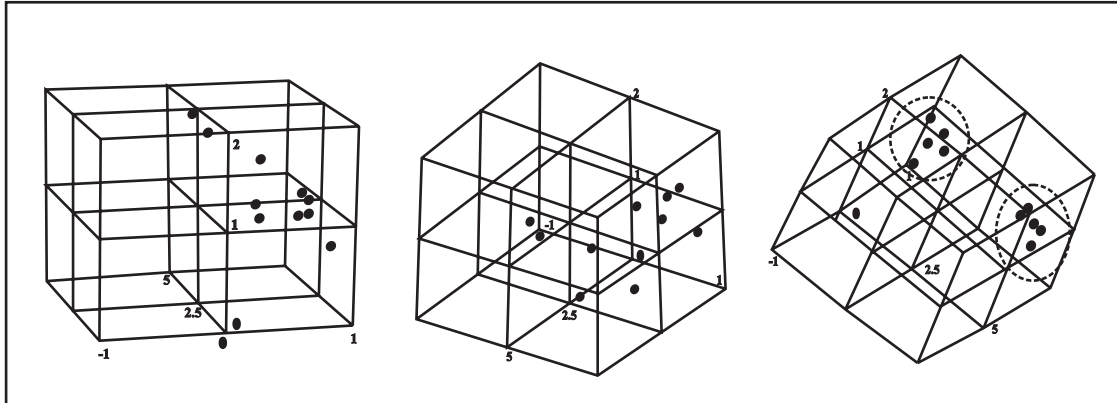


**Figure 4** Principal component analysis: Data can be visualized as a cloud of points in a multidimensional space (each axis representing an individual variable (e.g. protein, mRNA, or metabolite)). The data is rotated in such a way that the largest amount of variation in the dataset is described by the first principal component.

The first principal component accounts for as much of the variability in the data as possible, and each succeeding PC accounts for as much of the remaining variability as possible. The number of PCs needed to explain the variance in the dataset gives an indication about the complexity of the dataset. If the data are correlated and linear, a few PCs will be sufficient to reproduce the original data. For each principal component, a loading containing the influence of each original variable common for all samples is computed from the data and score values are calculated reflecting the contribution of the loading to each sample. The PCA results can be presented in a score plot in which highly correlated data is clustered together, while samples with different expression patterns will be positioned at a greater mutual distance (Fig.5).

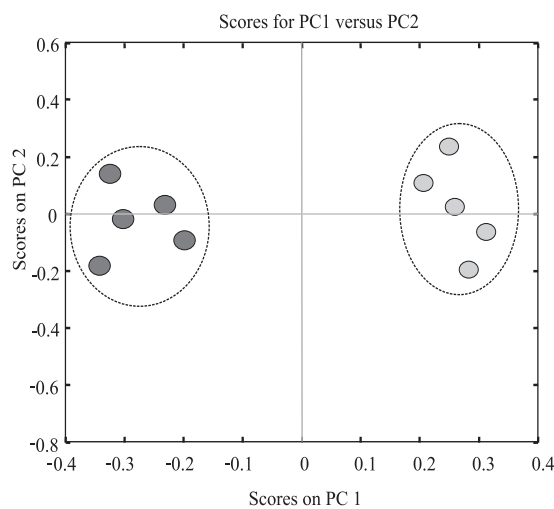


**Figure 5** Example of a score plot of a principal component analysis

PCA is an excellent explorative tool for the purpose of data overview, but it should be kept in mind that the focus is primarily on the main variation which is not necessarily the variation of interest in a given experimental situation. Therefore, additional supervised methods can be used to correlate the data to biochemical or clinical data, e.g. principal component discriminant analysis (PC-DA)<sup>41</sup>. In PC-DA (Fig. 6) the number of variables is first reduced by PCA, followed by discriminant analysis on the scores of the samples on the first PC. The discriminant functions describe the differences between the predefined groups of samples with respect to the variation within the groups.

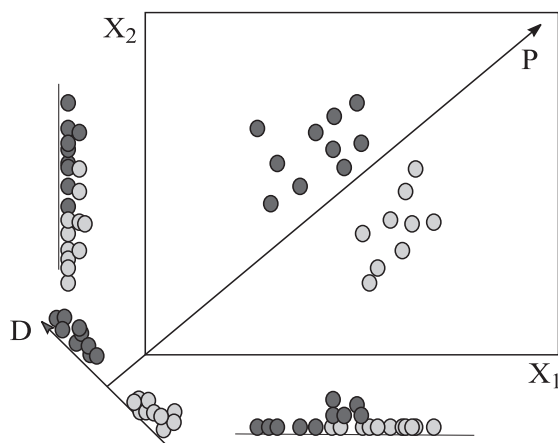


**Figure 6** Principal component discriminant analysis: D is the discriminant axis,  $X_1$  and  $X_2$  are two original variables and the dots represent the samples of two different groups (light grey and dark grey). Projection of the samples on the  $X_1$  and  $X_2$  axis shows no separation between the two groups, whereas projection on the discriminant axis shows complete separation.

## 2.1 Inflammation

In this thesis, some aspects of the inflammatory process and its response to potential anti-inflammatory drugs are explored using a systems biology approach.

Inflammation occurs as a defensive response to invasion of the host by foreign material, often of microbial nature (Fig.7)<sup>42-45</sup>. This response is normally a localized protective response that involves a complex series of events including:

- Local response of resident cells (e.g. macrophages, endothelial cells, and mast cells).
- Vasodilation, i.e. widening of the blood vessels to increase the blood flow to the infected area.
- Increased vascular permeability, which allows diffusible components to enter the site of injury.
- Cellular infiltration by chemotaxis, or the directed movement of inflammatory cells through the walls of blood vessels into the site of injury.
- Activation of cells of the immune system (e.g. monocytes, macrophages, and neutrophils) as well as of complex enzymatic systems of blood plasma.

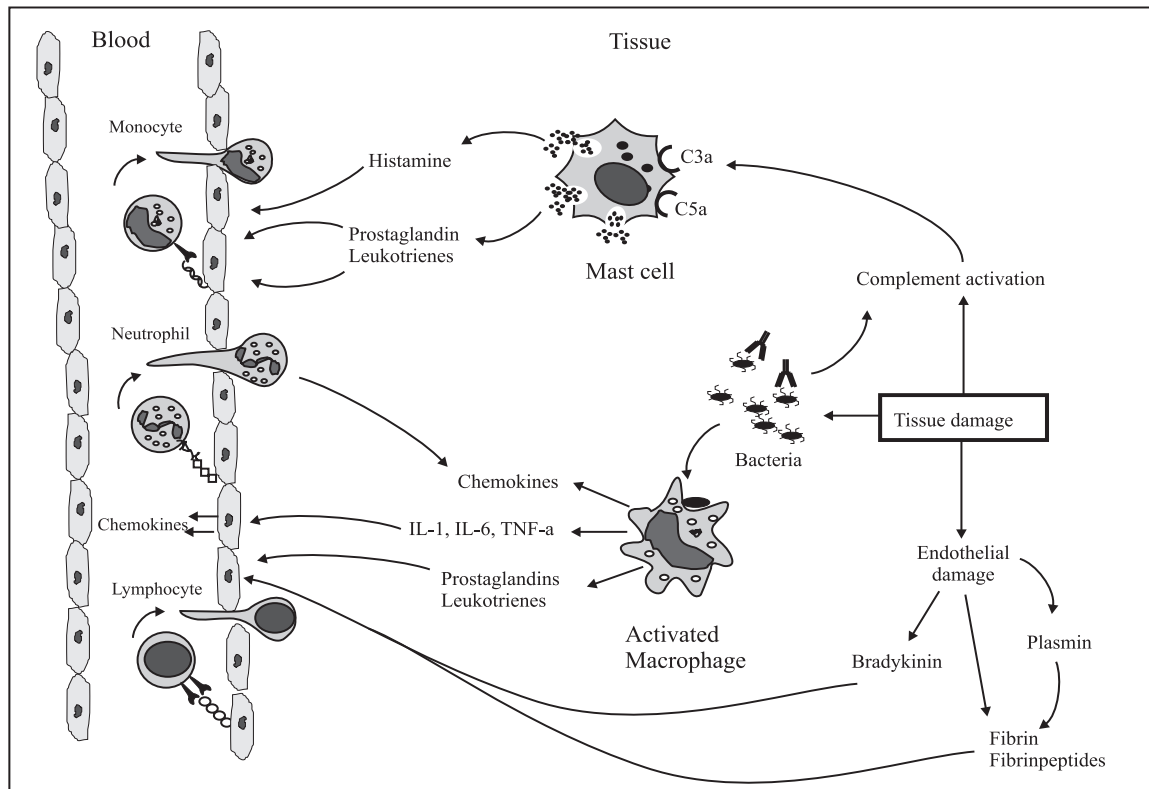


**Figure 7** Schematic presentation of the inflammatory response

The degree to which these occur is normally proportional to the severity of the injury and the extent of infection. The inflammatory response is an attempt from the body to restore and maintain homeostasis after injury. However excessive or prolonged inflammation can cause damage and may lead to chronic inflammation (e.g. asthma). In some cases the immune system attacks its own tissues, as it erroneously recognizes self as foreign, and normal as abnormal leading to autoimmune diseases like multiple sclerosis, and rheumatoid arthritis. There are many compounds that elicit inflammatory reactions. An example of such a pro-inflammatory compound is the endotoxin lipopolysaccharide (LPS), a component of the outer membrane of gram-negative bacteria. Cells of the immune system respond to LPS through a pathway involving a plasma protein, named LPS binding protein (LPB), and the CD14 receptor. Binding to this receptor on myeloid cells leads to cellular activation and triggers signal transduction pathways leading to the production of various pro- and anti-inflammatory molecules, such as cytokines (e.g.  $\text{TNF-}\alpha$ , and  $\text{IL-1}\beta$ ), chemokines (e.g.  $\text{IL-8}$ ), lipids (e.g. prostaglandins, and leukotrienes) and reactive oxygen species (e.g. super oxide). These inflammatory mediators in turn attract and activate other cells and alter many signal transduction pathways. They are key players in the onset and progression of the inflammatory cascade<sup>43, 46-48</sup>.

## 2.2 Macrophages

Macrophages play an important role during the inflammatory response. They originate from the pluripotent haematopoietic stem cell in the bone marrow. The stem cell develops into a granulocyte-monocyte progenitor cell (CFU-GM) which is the precursor for the granulocyte progenitor cell (CFU-G) and the monocyte progenitor cell (CFU-M). The monocyte progenitor cell differentiates consecutively in a monoblast, promonocyte and in a monocyte (Fig. 8).

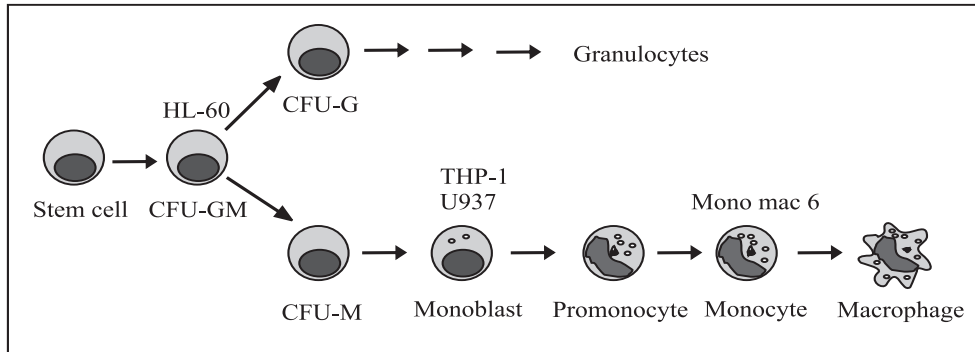


**Figure 8** Human leukaemia cell lines in haematopoiesis

The monoblast and promonocyte are immature forms of the monocyte. The monocyte leaves the bone marrow and migrates through the blood stream. Under normal steady-state conditions, monocytes migrate randomly to various organs and body cavities where they can differentiate into resident macrophages. According to their localization in tissues and body cavities, macrophages vary in their morphological and functional characteristics and therefore have different names (e.g. Kupffer cells in the liver, pulmonary and alveolar macrophages in the lungs and microglial cells in the central nervous system)<sup>49-51</sup>. Macrophages in tissues and body cavities are constantly renewed by a constant influx of monocytes and by local division of immature mononuclear phagocytes who are originally formed in the bone marrow. During a local infection or inflammation, the increase in the number of macrophages is mainly due to the influx of monocytes. These macrophages are called exudate macrophages<sup>51, 52</sup>.

Macrophages play a primary role as scavenger cells. However, macrophages are also involved in immune regulatory functions at various sites in the body. They show phagocytic activity after recognizing foreign or damaged material through cell surface receptors, and show cytotoxic activity through the production of mediators such as proteases, tumor necrosis factor- $\alpha$  (TNF- $\alpha$ ), interleukine-1 (IL-1), oxygen free radicals and nitric oxide (NO). In addition, macrophages can function as antigen-presenting cells to T- and B-lymphocytes and generate an antigen-specific immune response. They also play a role as regulators of

inflammatory responses through the production of cytokines and chemokines and attract other inflammatory cells. Macrophages are involved in a variety of diseases, including autoimmune diseases, immune deficiency diseases and infectious diseases through their various immune functions<sup>47, 49, 52-54</sup>. The macrophage is therefore an important target for some classes of anti-inflammatory drugs (e.g. corticosteroids, anti-TNF- $\alpha$  antibodies)<sup>55-59</sup>.

The human monocytic cell lines U937, HL-60, THP-1 and Mono Mac 6 are tumor cell lines that are frozen in a window of the monocytic differentiation lineage corresponding to monoblast (U937, THP-1), myeloblast (HL-60) and immature monocyte (Mono Mac 6)<sup>60-64</sup> (Fig. 8). By stimulating the cells with an inducer (e.g. phorbol 12-myristate 13-acetate, retinoic acid) the cells undergo monocytic differentiation<sup>65-69</sup>. During terminal differentiation, the cells acquire monocyte-macrophage morphology, become adhesive, express differentiation-related antigens, are not able to proliferate and become functionally monocyte-macrophage-like cells by performing phagocytosis, antibody dependent cellular cytotoxicity, antigen presenting and chemotaxis<sup>53, 54, 63</sup>. In this thesis, the U937 cell line was used as a model system for macrophage functioning.

### **Scope and outline of the thesis**

The studies described in this thesis were performed to investigate the potential of systems biology based “high-content” screening strategies in drug discovery. By analyzing many biomolecules at different levels of integration, these strategies take into account multiple pathways and mechanisms of action. This not only yields methods to classify compounds, but also provides a basis for further investigation of the mechanism of action of these compounds. Furthermore, it provides an opportunity to identify potential biomarkers in an early stage of drug discovery. The process of inflammation provides a good subject to explore the possible application of this strategy, since it involves a whole range of mediators, receptors and intracellular signalling events. As it was necessary to focus, the macrophage and more in particular the histocytic lymphoma U937 monocyte-macrophage cell line was chosen as model system in most studies.

In Chapter 2, the differentiation of U937 cells into macrophages was investigated. In Chapter 3, U937 macrophages were exposed to the endotoxin LPS to induce an inflammatory response in the absence or presence of known- and potential anti-inflammatory drugs. The cellular response was examined in detail to categorize the anti-inflammatory drugs according to their mRNA, protein and lipid expression patterns. This approach was evaluated with zilpaterol, a poorly characterized  $\beta_2$ -adrenergic receptor agonist that has only been poorly characterized so

far. Chapter 4 describes a proteomics study of the secreted proteome of U937 macrophages exposed to LPS in the absence or presence of zilpaterol and/or propranolol (a  $\beta_2$ -adrenergic receptor antagonist). This study was performed to investigate the anti-inflammatory effect of zilpaterol, and the role of the  $\beta_2$ -adrenergic receptor in this process. The data generated by the systems biology based “high-content” screening strategies provided new starting points and biomarkers for further investigation. In Chapter 5 the categorization of zilpaterol as a  $\beta_2$ -adrenergic antagonist was further explored both *in vivo* and *in vitro*. Some of the biomarkers for  $\beta_2$ -adrenergic agonists that were identified in the study described in Chapter 3 (vascular endothelial growth factor, oncostatin M and granulocyte chemotactic protein-2) were biologically validated in Chapter 6 using traditional biochemical methods.

In the second part of the thesis, Chapter 7, the immuno-modulating properties of a multi-component herbal preparation of *Cannabis sativa in vitro* was investigated using U937 macrophages and blood derived macrophages. Furthermore, the immuno-modulating effect of unheated Cannabis extract and its main constituent  $\Delta^9$ -tetrahydrocannabinoid acid (THCa) were investigated in a pilot study in an Experimental Autoimmune Encephalomyelitis (EAE) mouse model. In Chapter 8 the method described in Chapter 3 was used to categorize heated and unheated Cannabis extracts using transcriptomics in combination with PC-DA.

## References

- 1 Hood, L., *Mech Ageing Dev*, **2003**, Systems biology: Integrating technology, biology, and computation, *124*, 9-16.
- 2 Morel, N. M., Holland, J. M., van der Greef, J., Marple, E. W., *et al.*, *Mayo Clin Proc*, **2004**, Primer on medical genomics. Part xiv: Introduction to systems biology--a new approach to understanding disease and treatment, *79*, 651-658.
- 3 Provard, N. J. and McCourt, P., *Curr Opin Plant Biol*, **2004**, Systems approaches to understanding cell signaling and gene regulation, *7*, 605-609.
- 4 Tong, W., *Genomics Proteomics Bioinformatics*, **2004**, Analyzing the biology on the system level, *2*, 6-14.
- 5 van der Greef, J., Stroobant, P. and van der Heijden, R., *Curr Opin Chem Biol*, **2004**, The role of analytical sciences in medical systems biology, *8*, 559-565.
- 6 Bustin, S. A., *J Mol Endocrinol*, **2002**, Quantification of mrna using real-time reverse transcription pcr (rt-pcr): Trends and problems, *29*, 23-39.
- 7 Wang, X., Ghosh, S. and Guo, S. W., *Nucleic Acids Res*, **2001**, Quantitative quality control in microarray image processing and data acquisition, *29*, E75-75.
- 8 Brazma, A. and Vilo, J., *FEBS Lett*, **2000**, Gene expression data analysis, *480*, 17-24.
- 9 Yang, Y. H. and Speed, T., *Nat Rev Genet*, **2002**, Design issues for cdna microarray experiments, *3*, 579-588.
- 10 Anderson, L. and Seilhamer, J., *Electrophoresis*, **1997**, A comparison of selected mrna and protein abundances in human liver, *18*, 533-537.
- 11 Anderson, N. L. and Anderson, N. G., *Electrophoresis*, **1998**, Proteome and proteomics: New technologies, new concepts, and new words, *19*, 1853-1861.
- 12 Mooser, V. and Ordovas, J. M., *Curr Opin Lipidol*, **2003**, 'omic' approaches and lipid metabolism: Are these new technologies holding their promises? *14*, 115-119.
- 13 Pandey, A. and Mann, M., *Nature*, **2000**, Proteomics to study genes and genomes, *405*, 837-846.
- 14 Edwards, A., Arrowsmith, C. and des Pallieres, B., *Modern Drug Discovery*, **2000**, Proteomics: New tools for a new era bridging the gap between genomics and drug discovery, (*7*) *35*, 41-42,44.
- 15 Molloy, M. P., *Anal Biochem*, **2000**, Two-dimensional electrophoresis of membrane proteins using immobilized ph gradients, *280*, 1-10.
- 16 Herbert, B., *Electrophoresis*, **1999**, Advances in protein solubilisation for two-dimensional electrophoresis, *20*, 660-663.
- 17 Rabilloud, T. (Ed.), *Proteome research: Two dimensional gel electrophoresis and identification methods*, Springer Verlag, Berlin Heidelberg New York **2000**, p. 244.
- 18 Barry, R. and Soloviev, M., *Proteomics*, **2004**, Quantitative protein profiling using antibody arrays, *4*, 3717-3726.
- 19 De Hoog, C. L. and Mann, M., *Annu Rev Genomics Hum Genet*, **2004**, Proteomics, *5*, 267-293.
- 20 Govorun, V. M. and Archakov, A. I., *Biochemistry (Mosc)*, **2002**, Proteomic technologies in modern biomedical science, *67*, 1109-1123.
- 21 Lau, A. T., He, Q. Y. and Chiu, J. F., *Sheng Wu Hua Xue Yu Sheng Wu Wu Li Xue Bao (Shanghai)*, **2003**, Proteomic technology and its biomedical applications, *35*, 965-975.
- 22 Lopez, M. F. and Pluskal, M. G., *J Chromatogr B Analyt Technol Biomed Life Sci*, **2003**, Protein micro- and macroarrays: Digitizing the proteome, *787*, 19-27.
- 23 Rabilloud, T., *Proteomics*, **2002**, Two-dimensional gel electrophoresis in proteomics: Old, old fashioned, but it still climbs up the mountains, *2*, 3-10.
- 24 Reinders, J., Lewandrowski, U., Moebius, J., Wagner, Y. and Sickmann, A., *Proteomics*, **2004**, Challenges in mass spectrometry-based proteomics, *4*, 3686-3703.
- 25 Wilson, D. S. and Nock, S., *Curr Opin Chem Biol*, **2001**, Functional protein microarrays, *6*, 81-85.
- 26 Ross, P. L., Huang, Y. N., Marchese, J. N., Williamson, B., *et al.*, *Mol Cell Proteomics*, **2004**, Multiplexed protein quantitation in *saccharomyces cerevisiae* using amine-reactive isobaric tagging reagents, *3*, 1154-1169.
- 27 Gorg, A., Weiss, W. and Dunn, M. J., *Proteomics*, **2004**, Current two-dimensional electrophoresis technology for proteomics, *4*, 3665-3685.
- 28 O'Farrell, P. H., *J Biol Chem*, **1975**, High resolution two-dimensional electrophoresis of proteins, *250*, 4007-4021.
- 29 Patton, W. F., *J Chromatogr B Analyt Technol Biomed Life Sci*, **2002**, Detection technologies in proteome analysis, *771*, 3-31.

- 
- 30 Rabilloud, T., Strub, J. M., Luche, S., van Dorsselaer, A. and Lunardi, J., *Proteomics*, **2001**, A comparison between sypro ruby and ruthenium ii tris (bathophenanthroline disulfonate) as fluorescent stains for protein detection in gels, *1*, 699-704.
- 31 Rabilloud, T., *Electrophoresis*, **1990**, Mechanisms of protein silver staining in polyacrylamide gels: A 10-year synthesis, *11*, 785-794.
- 32 Unlu, M., Morgan, M. E. and Minden, J. S., *Electrophoresis*, **1997**, Difference gel electrophoresis: A single gel method for detecting changes in protein extracts, *18*, 2071-2077.
- 33 Shaw, J., Rowlinson, R., Nickson, J., Stone, T., *et al.*, *Proteomics*, **2003**, Evaluation of saturation labelling two-dimensional difference gel electrophoresis fluorescent dyes, *3*, 1181-1195.
- 34 Tonge, R., Shaw, J., Middleton, B., Rowlinson, R., *et al.*, *Proteomics*, **2001**, Validation and development of fluorescence two-dimensional differential gel electrophoresis proteomics technology, *1*, 377-396.
- 35 Greef, J. v. d., Davidov, E., Verheij, E., Vogels, J., *et al.*, in: Harringan, G. and Goodacre, R. (Eds.), *Metabolic profiling: Its role in biomarker discovery and gene function analysis*, Kluwer Academic Publishing, Boston **2003**, pp. 171-198.
- 36 Dillon, W. R. and Goldstein, M., *Multivariate analysis: Methods and applications*, John Wiley & Sons Inc., New York, USA **1984**, p. 608.
- 37 Joliffe, I. T., *Principal component analysis*, Springer Verlag, New York, USA **1986**.
- 38 Martens, H. and Naes, T., *Multivariate calibrations*, John Wiley & Sons, Chichester, England **1992**, p. 438.
- 39 Massart, D. L., Vandeginste, B. G. M. and De Jong, P. J., *Handbook of chemometrics and qualimetrics: Part a*, Elsevier, Amsterdam, The Netherlands **1997**.
- 40 Vandeginste, B. G. M., Massart, D. L., Buydens, L. M. C. and De Jong, P. J., *Handbook of chemometrics and qualimetrics: Part b*, Elsevier, Amsterdam, The Netherlands **1998**.
- 41 Hoogerbrugge, R., Willig, S. J. and Kistemaker, P. G., *Analytical Chemistry*, **1983**, Discriminant analysis by double stage principal component analysis, *55*, 1710-1712.
- 42 Heumann, D. and Glauser, M. P., *Scientific American science & medicine*, **1994**, Pathogenesis of sepsis, 28-37.
- 43 Decker, K., *Keio J Med*, **1998**, The response of liver macrophages to inflammatory stimulation, *47*, 1-9.
- 44 Cirino, G., *Biochem Pharmacol*, **1998**, Multiple controls in inflammation. Extracellular and intracellular phospholipase a2, inducible and constitutive cyclooxygenase, and inducible nitric oxide synthase, *55*, 105-111.
- 45 Roitt, I., Brostoff, J. and Male, D., *Immunologie*, Bohn Stafleu Van Loghum, Houten/Diegem **2000**.
- 46 Downey, J. S. and Han, J., *Front Biosci*, **1998**, Cellular activation mechanisms in septic shock, *3*, d468-476.
- 47 Decker, K., *Eur J Biochem*, **1990**, Biologically active products of stimulated liver macrophages (kupffer cells), *192*, 245-261.
- 48 Rietschel, E. T. and Brade, H., *Sci Am*, **1992**, Bacterial endotoxins, *267*, 54-61.
- 49 Burke, B. a. L., C.E. (Ed.), *The macrophage*, Oxford University Press Inc., New York, US **2002**, p. 647.
- 50 van Furth, R., *Immunobiology*, **1982**, Current view on the mononuclear phagocyte system, *161*, 178-185.
- 51 van Furth, R., *Macrophage pathogen interactions introduction* **1994**, pp. v-vii.
- 52 van Furth, R. and Sluiter, W., *Trans R Soc Trop Med Hyg*, **1983**, Current views on the ontogeny of macrophages and the humoral regulation of monocytopoiesis, *77*, 614-619.
- 53 Langermans, J. A., Hazenbos, W. L. and van Furth, R., *J Immunol Methods*, **1994**, Antimicrobial functions of mononuclear phagocytes, *174*, 185-194.
- 54 Stvrtinova, V., Jakubovsky, J. and Hulin, I., *Inflammation and fever*, Academic Electronic press, slovak **1995**.
- 55 Izeboud, C. A., Monshouwer, M., Witkamp, R. F. and van Miert, A. S., *Vet Q*, **2000**, Suppression of the acute inflammatory response of porcine alveolar- and liver macrophages, *22*, 26-30.
- 56 Joyce, D. A., Gimblett, G. and Steer, J. H., *Inflamm Res*, **2001**, Targets of glucocorticoid action on tnf-alpha release by macrophages, *50*, 337-340.
- 57 Joyce, D. A., Steer, J. H. and Abraham, L. J., *Inflamm Res*, **1997**, Glucocorticoid modulation of human monocyte/macrophage function: Control of tnf-alpha secretion, *46*, 447-451.
- 58 Mu, M. M., Chakravorty, D., Sugiyama, T., Koide, N., *et al.*, *J Endotoxin Res*, **2001**, The inhibitory action of quercetin on lipopolysaccharide-induced nitric oxide production in raw 264.7 macrophage cells, *7*, 431-438.
- 59 Steer, J. H., Kroeger, K. M., Abraham, L. J. and Joyce, D. A., *J Biol Chem*, **2000**, Glucocorticoids suppress tumor necrosis factor-alpha expression by human monocytic thp-1 cells by suppressing
-

- transactivation through adjacent nf-kappa b and c-jun-activating transcription factor-2 binding sites in the promoter, *275*, 18432-18440.
- 60 Drexler, H. G., Quentmeier, H., MacLeod, R. A., Uphoff, C. C. and Hu, Z. B., *Leuk Res*, **1995**,  
Leukemia cell lines: In vitro models for the study of acute promyelocytic leukemia, *19*, 681-691.
- 61 Rizzo, M. G., Zepparoni, A., Cristofanelli, B., Scardigli, R., *et al.*, *Br J Cancer*, **1998**, Wt-p53 action in  
human leukaemia cell lines corresponding to different stages of differentiation, *77*, 1429-1438.
- 62 Collins, S. J., *Blood*, **1987**, The hl-60 promyelocytic leukemia cell line: Proliferation, differentiation,  
and cellular oncogene expression, *70*, 1233-1244.
- 63 Tenno, T., *Department of medical sciences, Acta Universitatis Upsaliensis, Uppsala* **2001**.
- 64 Abrink, M., Gobl, A. E., Huang, R., Nilsson, K. and Hellman, L., *Leukemia*, **1994**, Human cell lines u-  
937, thp-1 and mono mac 6 represent relatively immature cells of the monocyte-macrophage cell  
lineage, *8*, 1579-1584.
- 65 Abrahm, J. and Rovera, G., *Mol Cell Biochem*, **1980**, The effect of tumor-promoting phorbol diesters on  
terminal differentiation of cells in culture, *31*, 165-175.
- 66 Huberman, E. and Callahan, M. F., *Proc Natl Acad Sci U S A*, **1979**, Induction of terminal  
differentiation in human promyelocytic leukemia cells by tumor-promoting agents, *76*, 1293-1297.
- 67 Rovera, G., O'Brien, T. G. and Diamond, L., *Science*, **1979**, Induction of differentiation in human  
promyelocytic leukemia cells by tumor promoters, *204*, 868-870.
- 68 Rovera, G., Santoli, D. and Damsky, C., *Proc Natl Acad Sci U S A*, **1979**, Human promyelocytic  
leukemia cells in culture differentiate into macrophage-like cells when treated with a phorbol diester,  
*76*, 2779-2783.
- 69 Liu, M. Y. and Wu, M. C., *Exp Hematol*, **1992**, Induction of human monocyte cell line u937  
differentiation and csf-1 production by phorbol ester, *20*, 974-979.





## Chapter 2

---

**A combination of proteomics, principal component analysis and transcriptomics is a powerful tool for the identification of biomarkers for macrophage maturation in the U937 cell line.**

Kitty C.M. Verhoeckx<sup>1,2</sup>

Sabina Bijlsma<sup>1</sup>

Els de Groene<sup>3</sup>,

Renger F. Witkamp<sup>1</sup>

Jan van der Greef<sup>1,2</sup>

Richard J.T. Rodenburg<sup>4</sup>

*Proteomics, 2004, 4, 1014-1028*

<sup>1</sup> TNO Quality of Life, Zeist, The Netherlands, <sup>2</sup> Leiden University, Leiden/Amsterdam Center for Drug Research, Leiden, The Netherlands, <sup>3</sup> Unilever Health Institute, Vlaardingen, The Netherlands, <sup>4</sup> UMC St Radboud, Nijmegen, The Netherlands

**A combination of proteomics, principal component analysis and transcriptomics is a powerful tool for the identification of biomarkers for macrophage maturation in the U937 cell line.**

*The monocyte-like human histiocytic lymphoma cell line U937 can be induced by phorbol 12-myristate 13-acetate (PMA) to undergo differentiation into a macrophage-like phenotype. We have used two-dimensional gel electrophoresis (2-D), oligonucleotide microarrays and principal component analysis (PCA) to characterize the U937 cell line as a model system for the differentiation of monocytes into macrophages. A total of 226 differentially expressed proteins were found, of which 41 were selected by PCA for identification using matrix-assisted laser desorption/ionization tandem mass spectrometry (MALDI MS/MS). Based on the PCA results, three marker proteins were selected for confirmation of the differential expression using Western blot and quantitative real time polymerase chain reaction (RT-PCR). The selected marker proteins were: gamma interferon inducible lysosomal thiol reductase (GILT), cathepsin D and adipocyte-fatty acid binding protein (A-FABP). All three were proven to be good differentiation markers for macrophage maturation of U937 cells as well as peripheral blood-derived macrophages. The transcriptomics data revealed a large number of additional putative differentiation markers in U937 macrophages, many of which are known to be expressed in peripheral blood-derived macrophages. These include osteopontin, matrix metalloproteinase 9, and HC-gp39. Our results show that the characteristics of U937 macrophages resemble those of inflammatory (exudate) macrophages, exemplified by the down-regulation of 5' nucleotidase and the up-regulation of leucine aminopeptidase mRNAs. In conclusion, using the powerful combination of transcriptomics, 2-D gel electrophoresis and PCA, our results show that U937 cells differentiated by PMA treatment are an excellent model system for monocyte derived macrophage from blood.*

---

**Introduction**

Monocytes and macrophages originate from pluripotent haematopoietic stem cells present in the bone marrow. The monocyte progenitor cells transform consecutively in monoblasts, promonocytes and finally into monocytes. The monocytes leave the bone marrow and migrate to the blood stream. Under normal steady-state conditions, monocytes migrate randomly to various organs and body cavities where they differentiate into resident macrophages<sup>1</sup>. During

a local infection or inflammation, the affected tissue is rapidly infiltrated by large numbers of exudate (inflammatory) macrophages. These inflammatory macrophages have distinct characteristics compared to the resident macrophages that are normally present in various organs<sup>2</sup>. Several cell lines are available that are widely used as model systems for monocytes and macrophages. The human monocytic cell lines U937, HL-60, THP-1, and Mono Mac 6 are tumor cell lines that originate from immature cells of the monocytic differentiation lineage corresponding to monoblast (U937, THP-1), myeloblast (HL-60), and monocyte (Mono Mac 6), respectively<sup>3-5</sup>. By stimulating the cells with phorbol 12-myristate 13-acetate, one of the most potent tumor promoting agents<sup>6</sup>, cells are induced to undergo monocytic differentiation. In this way the cells acquire the typical monocyte/macrophage morphology, become adhesive, express differentiation-related antigens and are no longer able to proliferate. Furthermore, the cells become functionally similar to monocyte/macrophage-like cells that can perform phagocytosis, antibody dependent cellular cytotoxicity, antigen presenting, and chemotaxis<sup>5</sup>. In the present study we characterized the U937 cell line as a suitable model system for monocyte to macrophage maturation. For this purpose, we compared undifferentiated U937 cells (monocytic) with U937 differentiated into a macrophage-like cell type at the level of both the proteome and the transcriptome, using 2-D gel electrophoresis<sup>7</sup> and oligonucleotide microarrays, respectively. The transcriptomics data was used to confirm our proteomics data as well as to further characterize the U937 model system at the mRNA level. The proteomics data was analyzed using a principal component analysis (PCA) method. PCA was applied as an exploratory data analysis method that is able to visualize differences between two or more complex datasets<sup>8-12</sup>. Previously, PCA has been successfully used for fingerprinting biomatrices and detection of biomarkers<sup>13</sup>. Finally, we have compared the expression of a number of identified differentially expressed genes in peripheral blood-derived monocytes that were differentiated into macrophages *ex vivo*.

### **Materials and methods**

Unless indicated otherwise, all reagents and equipment were obtained from Amersham biosciences (Uppsala, Sweden).

#### *Cell cultures and incubations*

Human monocyte-like histiocytic lymphoma cells U937<sup>14</sup> obtained from the ATCC (CRL-1593.2) were grown in RPMI-1640 medium, supplemented with 10% (v/v) fetal calf serum and 2 mM L-glutamine (Life technologies, Breda, The Netherlands) at 37 °C, 5% CO<sub>2</sub>. The

U937 monocytic cells were differentiated into macrophages using phorbol 12-myristate 13-acetate (PMA, 10 ng/ml, overnight, Omnilabo, Breda, The Netherlands) according to standard procedures<sup>15</sup>. The PMA-differentiated macrophages were allowed to recover from PMA treatment for 48 hours, during which culture medium was replaced every day. At day three after PMA treatment, the macrophages were harvested.

Peripheral blood monocytes (PB-MO) were isolated from human EDTA-blood with Rosette Sep™ human monocyte enrichment cocktail (Stemcell Technologies Inc, Meylan, France). The monocytes were cultured in culture flasks containing RPMI-1640 medium supplemented with 10% (v/v) human serum and 2 mM L-glutamine and were allowed to adhere to the bottom of the flask for two hours. This procedure yields approximately 95% pure monocytes as determined by direct immunofluorescence staining of CD14 for flow cytometric analysis. The purified monocytes were allowed to differentiate into peripheral blood macrophages (PB-MØ) for eight days<sup>16</sup>. Following this procedure, the macrophage maturation has been described to give rise to characteristic morphology and phenotype of primary macrophages<sup>17</sup>.

### **Proteomics**

#### *Two-dimensional gel electrophoresis*

The U937 monocytes and macrophages were counted and dissolved in lysis buffer containing 8 M urea, 2% (w/v) CHAPS, 0.02% (v/v) Pharmalytes, and 1% (w/v) dithiothreitol (Sigma-Aldrich chemie, Zwijndrecht, The Netherlands). After incubation at room temperature for 1 h and sonication for 5 min, the samples were diluted to  $1.5 \times 10^6$  cells/ml with rehydration buffer containing 8 M urea, 0.5% (w/v) CHAPS, 2 mM tributyl phosphine (Fluka, Buchs SG, Switzerland), and 1% (v/v) IPG ampholytes pH 4-7. For each differentiation stage the same amount of cells ( $0.5 \times 10^6$ ) were loaded on the gel. Four gels per sample were processed and analysed simultaneously. The first dimension was carried out on an IPGphor system using pH 4-7 IPG gel strips of 18 cm and 350 µl of sample solution. The IEF was performed at 20 °C under the following conditions: 12 h at 30 V; 30 min at 150 V; 1 h at 300 V; 1 h at 1500 V and 6 h at 8000 V. After isoelectric focussing, the IPG strips were equilibrated for 15 min in a buffer containing 6 M urea, 30% (v/v) glycerol, 5 mM tributyl phosphine, and 2% (w/v) SDS in 0.05 M Tris-HCl buffer, pH 8.8. The second dimensional separations were carried out on custom made 12% SDS-polyacrylamide gels and an Ettan DALT electrophoresis system. The gels were fixed in 50% (v/v) methanol and 10% (v/v) acetic acid for 20 minutes. After washing twice with water (1 min and 60 min), the gels were incubated with 0.02% (w/v) sodium thiosulfate for 1 min. The gels were washed twice with water for 10 sec and stained in

a 0.1% (w/v) silver nitrate solution for 30 min. Development was performed in a 0.18 M sodium carbonate solution with 0.01 M formaldehyde. After 1 min, the solution was replaced with fresh development solution and incubated for 6 min. The development was stopped with 1% (v/v) acetic acid. The gels were scanned on a GS-710 calibrated imaging densitometer (Bio-Rad, Veenendaal, The Netherlands).

### *Gel image and data analysis*

Scanned TIFF images were analysed using Phoretix 2-D gel analysis software version 6.01 (Nonlinear Dynamics, Newcastle upon Tyne, UK). Spots were automatically detected and visually checked for undetected or incorrectly detected spots. The protein spots detected in each experimental gel were matched to their corresponding spot in a digitized reference gel. Intensity levels were normalized between gels by dividing the spot intensity through the total intensity of all the spots in the gel. The differences in spot volumes were analysed by the Student's *t*-test (assuming normal distributions and equal variance) using MS Excel (Microsoft Corporation, Redmond, USA). A list of spots with their normalized spot volumes per gel was analyzed by PCA. PCA was performed using the PLS toolbox in Matlab (version 2.0, Eigenvector Research Inc, Washington, USA). PCA reduces the large number of dimensions of a dataset into a smaller number of dimensions without losing useful information. PCA describes data as a linear combination of so-called scores and loadings. These linear combinations are called principal components (PCs). The scores and loading vectors give a concise and simplified description of the variance present in the dataset. The data was scaled using mean-centering.

### *In-gel digestion and MALDI-TOF MS/MS*

The spots were cut out of the 2-D gel, sliced into small pieces and washed twice with 100 mM ammonium bicarbonate and acetonitril. The gel pieces were dried in a vacuum centrifuge. The proteins were digested overnight with 25 ng/ $\mu$ l trypsin (sequencing grade, Promega Benelux, Leiden, The Netherlands) in 100 mM ammonium bicarbonate and 2 mM dithiothreitol at 37 °C. The peptide fragments were extracted twice with 5  $\mu$ l water:acetonitril:formic acid (5:14:1). After drying in a vacuum centrifuge, the lyophilized digest was dissolved in 10  $\mu$ l 0.1% (v/v) trifluoro acetic acid (TFA). The peptide mixture was purified with ZipTip  $\mu$ C18 pipette tips (Millipore BV, Amsterdam, The Netherlands), following the procedure recommended by the manufacturer, except for the elution step. Peptides were eluted directly from the ZipTip onto the MALDI target in 1  $\mu$ l matrix solution. The matrix solution contained

30 mg/ml 2, 5-dihydroxybenzoic acid in 0.1% TFA/acetonitril (1:1). Peptide fingerprints and peptide sequencing data (MALDI MS/MS) were acquired on an oMALDI™ -QSTAR® XL Pulsar quadrupole time-of-flight mass spectrometer (Applied Biosystems/MDS Sciex, Nieuwerkerk a/d IJssel, The Netherlands). Full MS spectra were acquired for every spot. Major peaks in the spectra were selected for MS/MS experiments. MS/MS data could be acquired for 3-10 peptides per spot (the number of peptides being limited by sensitivity and/or by sample depletion on the MALDI target). Protein identification was performed by searching the NCBI nr protein database using the MASCOT search engine of Matrix Science Ltd (London, UK).

### *One and two-dimensional immunoblotting*

For 2-D immunoblotting, 2 mg of monocyte or macrophage protein extract was separated according to the method described above. For 1-D immunoblotting, 10 µg of sample was electrophoretically separated on a 15 % (w/v) SDS polyacrylamide gel (Bio-Rad). Subsequently, the proteins were electrophoretically transferred to a PVDF membrane. The membrane was blocked with 3.4% (w/v) milk solution (Protifar, Nutricia, Zoetermeer, The Netherlands) in Tris-Buffered Saline Tween-20 (TBST) for 1 h at room temperature. The membrane was probed with a rabbit anti-GILT anti-serum (1:500, kindly provided by Dr. Peter Cresswell, Yale University, New Haven, Connecticut, USA), mouse monoclonal anti-human cathepsin D (1:200, Oncogen, Boston, USA) or rabbit polyclonal anti-human fatty acid binding protein adipocyte (A-FABP) (1:100, Alpha diagnostic, San Antonio, USA) in 0.34% milk solution in TBST for 1 h at room temperature. Bands were visualized with alkaline phosphatase-conjugated secondary antibodies (goat anti-rabbit IgG for GILT and A-FABP and goat anti-mouse for cathepsin D) and ECF™ substrate for Western blotting. The secondary antibodies showed no non-specific binding. The blots were scanned using a Fluor S multi-imager device (Bio-Rad).

## **Transcriptomics**

### *RNA extraction*

Total RNA was extracted from the U937 monocytes and macrophages and human blood monocytes and macrophages using Trizol reagent (Life technologies, Rockville, USA) according to the manufacturer's protocol. Total RNA was further purified using RNeasy RNA purification kit (Qiagen, Westburg, Leusden, The Netherlands). DNase treatment (Qiagen) was performed on the RNeasy column.

*Oligonucleotide microarray preparation*

The Operon 70-mer oligonucleotides were suspended in 3 x saline sodium citrate (SSC) (0.45 M NaCl, 45 mM sodium citrate) and printed on aminosilane-coated UltraGAPS slides (Corning Life science, USA). In total 21,529 oligonucleotides were deposited on the slides which corresponds to 21,316 genes. The slides were UV-crosslinked in a Stratalinker.

*cDNA synthesis and labelling*

For labelling of target with Cy-3 and Cy-5 dyes an indirect amino-allyl labelling was used. The reversed transcription (RT) reaction was performed on 20 µg of total RNA with superscript II RT (Gibco/Invitrogen, California, USA) and a dNTP solution (4:1 ratio aminoallyl-dUTP (Sigma Aldrich Chemie) to dTTP). RNA was degraded by hydrolysis in 0.1 M NaOH (10 min 70 °C) and neutralized with 0.1 M HCl. After ethanol precipitation the cDNA was coupled to either Cy-3 or Cy-5 fluorophore. The reaction mixture was quenched with 4 M hydroxylamine (5 h at room temperature in the dark). Labelled cDNA was purified using the Qia-Quick PCR purification kit (Qiagen). Hybridization was carried out using Slide-Hyb Glass Array Hybridisation buffer (Ambion, Houston, USA) and hybridization station (Genomic solutions, Huntingdon Cambridgeshire, UK). The accompanying Ambion protocol was followed. Pre-hybridisation and blocking steps were not necessary. The slides were dried by centrifugation.

*Scanning and data analysis*

The dried arrays were scanned using the GenePix 4000B scanner and GenePixpro 4.0 Array analysis software (Axon Instruments, Foster City, USA). The GenePixpro 4.0 array analysis software processed the acquired images into result files. The result files were further processed in Excel (Microsoft). For each spot, the local background intensity was subtracted from the signal intensity. Only spots with a signal-to-noise ratio of 2.5 for either Cy-3 or Cy-5 or both were included in the analysis. The corrected spot intensities were normalized by dividing the signal with the mean ratio of all the genes on the array and multiplied by the mean ratio of the three arrays. Genes that failed to show similar results in the dye swap experiment were not considered to be differentially expressed. Statistical significance of the differences was tested with the Student's *t*-test (assuming normal distributions and equal variance) for each gene ( $p < 0.05$ ).

### *Experimental design*

The two differentiation stages of macrophage maturation were compared on one array. A triplicate array was run where the monocyte-derived cDNA was labelled with Cy-3 and the macrophage cDNA with Cy-5. In an additional experiment, a fourth array was run as control experiment in which the dyes were swapped. The data from the latter experiment was used to verify the data of the triplicate experiment.

### *Quantitative real time polymerase chain reaction (RT-PCR)*

Primers for GILT (forward primer; 5'GCT GTC GCC AGA CAC TAT CA 3', reverse primer; 5'AGC TGG GTC TGA TCT TCC AA 3'), cathepsin D (forward primer: 5'GAC ACA GGC ACT TCC CTC AT 3', reverse primer; 5'CCT CCC AGC TTC AGT GTG AT 3'), A-FABP (forward primer; 5'TAC TGG GCC AGG AAT TTG AC 3', reverse primer; 5'GTG GAA GTG ACG CCT TTC AT 3'), and human  $\beta$ -actin (forward primer; 5'CTG ACT GAC TAC CTC ATG AAG ATC CT 3', reverse primer; 5'CTT AAT GTC ACG CAC GAT TTC C 3') were purchased from Applied Biosystems. The RT reaction was performed on 150 ng of total RNA with avian myeloblastosis virus reverse transcriptase (Promega, Madison, WI, USA). Quantitative real time polymerase chain reactions were performed using QuantiTect™ SYBR®Green (Qiagen). QuantiTect™ SYBR®Green PCR reactions were performed in a total volume of 20  $\mu$ l 1x QuantiTect™ SYBR®Green Master Mix in the iCycler iQ™ Real-Time PCR detection system (Bio Rad). The PCR program was as follows: 1 cycle 15 min at 95°C; 45 cycles 15 s at 95°C, 30 s at 50°C (GILT, cathepsin D and  $\beta$ -actin) or 54°C (A-FABP), 20 s at 72°C; 1 cycle 5 min at 72°C. The specificity and identity of the PCR product was checked by performing a melting curve test. The absolute number of copies of the gene of interest in the experimental cDNA samples was calculated from the linear regression of a standard curve. The expression of the measured genes in each sample was normalized for  $\beta$ -actin expression. All samples were analysed in triplicate.

## **Results**

### *Proteomics*

Monocytic U937 cells were differentiated in the presence of PMA into macrophages. The proteome of the two differentiation stages were compared using 2-D gel electrophoresis. Four gels per sample were processed simultaneously and analysed with Phoretix 2-D software. Figure 1 shows two representative 2-D gel images of the monocyte stage and the macrophage stage of U937 cells. In total 788 spots were detected of which 89 spots were present in the

monocyte but absent in the macrophage. In macrophages, 226 spots were present that were not found in the monocyte. PCA was performed to identify the most relevant differences in the protein expression patterns between the two differentiation stages.

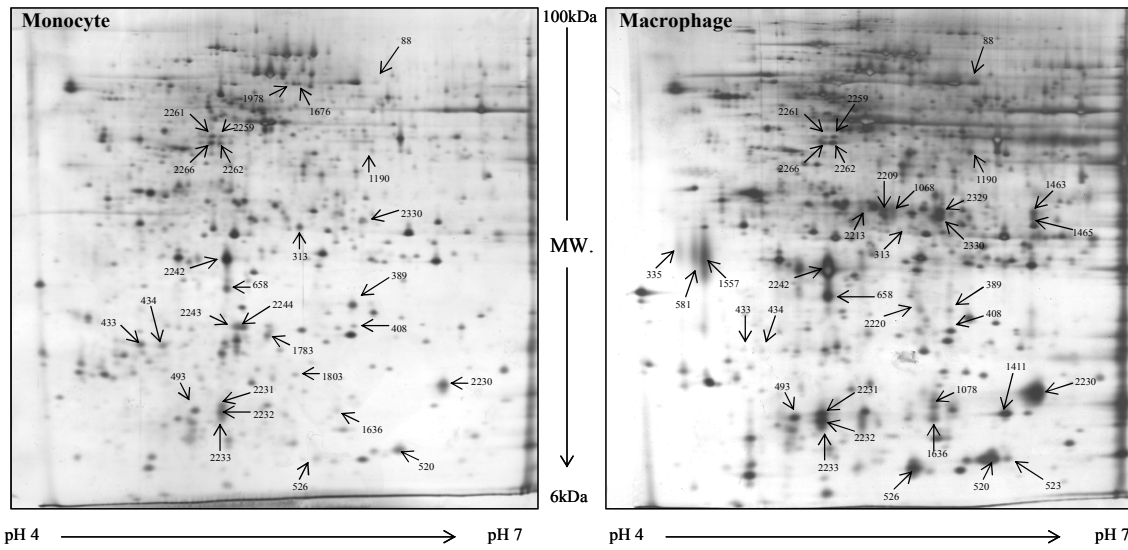


**Figure 1** Two representative 2-D gel images for U937 monocytes and macrophages. Protein extracts of  $0.5 \times 10^6$  cells were separated on a 12 % polyacrylamide gel (pH 4-7) and silver-stained. The excised spots are indicated by arrows.

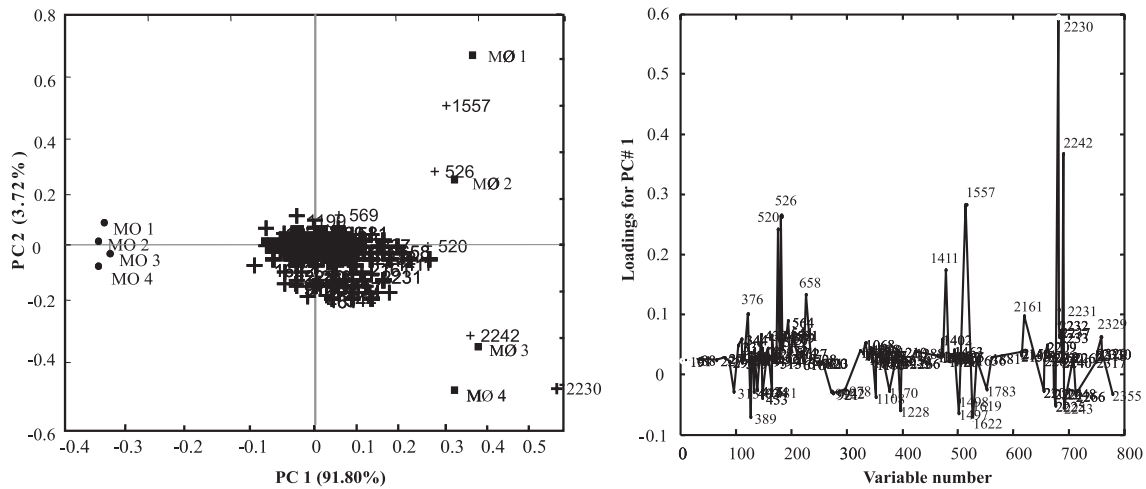


**Figure 2** Principal component analyses of the U937 monocyte and U937 macrophage proteomes. Left panel: The biplot gives an indication about clustering and trends present in the protein profiles. Scores of similar samples will tend to form clusters whereas dissimilar samples will be found at greater mutual distances. The result shows that the monocyte gels cluster near  $-0.3$  on the PC1 axis, whereas the macrophage gels cluster around  $0.3-0.4$  on the PC1 axis. Right panel: The loadings for PC1, indicating which spots are responsible for the difference between the two differentiation stages. Spot 2230 and 1557 have high loadings and therefore are very important differences between the monocyte and the macrophage according to PCA.

Protein spots that were found to be induced or inhibited during macrophage maturation (according to PCA Fig. 2) were isolated from the 2-D gel and were subjected to trypsin

digestion and MALDI MS/MS analysis. Table 1 shows the 41 most important differentially expressed proteins during macrophage differentiation according to PCA analysis. The significance of the changes was evaluated using the Student's *t*-test. For all 41 proteins the *p* value was smaller than 0.05. The mean induction factor was calculated by dividing the spot intensity of the protein spot in the macrophage (*n* = 4) by the spot intensity of the protein spot in the monocyte (*n* = 4). Thirty-eight of the 41 spots investigated spots were successfully identified.

#### *Western blot analysis*

From the protein list given in Table 1, three proteins were selected for confirmation experiments. Gamma interferon inducible lysosomal thiol reductase precursor (GILT) is synthesized as a 35 kDa soluble glycoprotein and is processed into the mature form by proteolytic cleavage<sup>18-20</sup>. According to the 2-D gel shown in Figure 3A, three forms of GILT are expressed in macrophages. All three forms were found to be glycosylated (data not shown), which is in agreement with a previous report<sup>20</sup>. We have identified 5 spots with MALDI MS/MS as cathepsin D beta chain. According to glycostaining and [<sup>33</sup>P]-labelling experiments these forms consist of both glycosylated and phosphorylated variants of cathepsin D (data not shown). This is in agreement with the notion that cathepsin D can be glycosylated and phosphorylated on several positions<sup>20-23</sup>. Both the  $\alpha$ -chain (17 kDa) and the  $\beta$ -chain (26 kDa) of cathepsin D were present on the 2-D gel from macrophages.

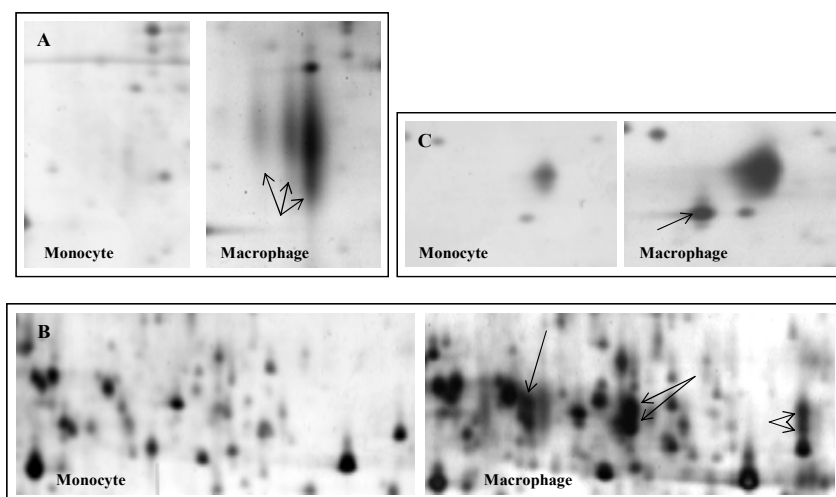


**Figure 3** 2-D gel images showing changes in protein expression during macrophage maturation. A: Three isoforms of GILT, B: Five isoforms of cathepsin D, C: A-FABP. For each protein of interest, a section of the silver stained 2-D gels is shown.

## Chapter 2

**Table 1** Protein list of differentially expressed proteins during macrophage maturation according to PCA. Negative Induction factors indicate intensity  $M\emptyset < MO$  and positive  $M\emptyset > MO$ .

Spot nr.	Protein	Mean Induction Factor	Student's <i>t</i> -test p-value	Predicted		Observed	
				MW kDa	pI	MW kDa	pI
88	Protein disulfide isomerase ER-60 precursor	6.8	3.0E-03	57.1	5.9	58.9	6.1
313	Human gamma actin partial cds	-2.9	2.4E-05	26.1	5.6	24.9	5.6
335	Gamma-interferon inducible lysosomal thiol reductase (GILT)	not in MO	2.2E-03	29.7	4.9	24.6	4.2
389	Deoxyuridine 5'-triphosphate nucleotidohydrolase (DUTP)	-6.1	1.7E-06	26.9	9.7	20.0	5.9
408	Superoxide dismutase	2.8	1.3E-05	16.0	5.7	19.2	5.9
433	Tubulin alpha-1 chain fragment	-17	2.0E-03	22.5	4.8	18.7	4.6
434	Tubulin alpha-1 chain fragment	-8.0	4.1E-03	22.5	4.8	18.7	4.7
493	Cytochrome C oxidase subunit Va	2.2	6.1E-05	16.9	6.3	17.5	4.9
520	Calgizzarin	3.0	1.0E-06	11.8	6.6	17.1	6.2
523	Cytochrome C oxidase polypeptide Vib	not in MO	2.8E-04	10.3	6.8	17.1	6.3
526	No score	25	8.9E-06			17.0	5.7
581	Gamma-interferon inducible lysosomal thiol reductase (GILT)	not in MO	9.3E-04	29.8	4.9	24.2	4.3
658	Lactoylglutathion lyase (glyoxalase I)	3.0	1.5E-06	20.9	5.1	20.7	5.1
1068	No score	not in MO	2.2E-05			27.3	5.6
1078	Cathepsin D chain A	not in MO	4.5E-04	10.9	5.6	17.7	5.9
1190	Alpha enolase	3.8	9.5E-05	47.4	7.0	36.5	6.0
1411	Adipocyte fatty acid binding protein (A-FABP)	not in MO	1.2E-07	14.7	6.6	17.6	6.3
1463	Cathepsin D chain B	not in MO	1.3E-05	26.4	5.3	27.6	6.0
1465	Cathepsin D chain B	not in MO	6.1E-07	26.4	5.3	26.8	6.5
1557	Gamma-interferon inducible lysosomal thiol reductase (GILT)	not in MO	1.6E-04	29.7	4.9	23.0	4.5
1636	Cathepsin D chain A	4.7	1.0E-04	10.9	5.6	17.5	5.8
1676	P59 (hsp binding immunophilin)	not in MØ	1.2E-05	57.9	5.2	58.0	5.6
1783	Hypothetical 17.7 kDa protein (fragment gamma actin)	not in MØ	3.3E-05	18.0	5.2	18.9	5.4
1803	TFAR 19 (PCD5_Human)	not in MØ	7.4E-07	14.2	5.8	18.0	5.6
1978	Mitochondrial matrix protein p1 precursor (P60)	not in MØ	6.5E-06	58.0	5.2	58.4	5.6
2209	Cathepsin D chain B	not in MO	2.5E-06	26.4	5.3	27.4	5.5
2213	Cathepsin B	not in MO	3.0E-07	38.7	5.9	27.1	5.9
2220	No score	not in MO	1.1E-02			20.2	5.8
2230	Fatty acid binding protein epidermal (E-FABP)	3.9	4.9E-05	15.2	6.6	17.8	6.5
2231	Galectin-1	5.1	1.3E-03	14.9	5.3	17.5	5.1
2232	Galectin-1	2.7	3.0E-04	14.9	5.3	17.4	5.1
2233	Galectin-1	6.4	1.1E-05	14.9	5.3	17.4	5.1
2242	Lactoylglutathion lyase chain A	2.5	4.7E-04	21.0	5.2	22.4	5.1
2243	Protein disulfide isomerase prolyl 4 hydroxylase beta (1MEK)	not in MØ	1.0E-06	13.4	5.9	19.2	5.2
2244	Protein disulfide isomerase prolyl 4 hydroxylase beta (1MEK)	not in MØ	4.3E-04	13.4	5.9	19.2	5.2
2259	Heterogeneous nuclear ribonucleoprotein C2	6.3	2.0E-02	33.7	4.9	39.7	5.2
2261	Heterogeneous nuclear ribonucleoprotein C2	-7.9	6.7E-06	33.7	4.9	39.8	5.1
2262	Heterogeneous nuclear ribonucleoprotein C1	9.0	4.4E-04	32.3	4.9	38.0	5.2
2266	Heterogeneous nuclear ribonucleoprotein C1	-17	2.1E-06	32.3	4.9	38.2	5.1
2329	Cathepsin D chain B	not in MO	1.2E-05	26.4	5.3	27.5	5.9
2330	Cathepsin D chain B	3.3	1.3E-04	26.4	5.3	26.2	5.8

The third protein we selected for further analysis was the 14 kDa A-FABP<sup>24,25</sup>. Similar to cathepsin D and GILT, A-FABP is not detectable in monocytes whereas it is expressed at a high level in macrophages (Fig. 3C). These results clearly show that all three proteins are suitable differentiation markers for macrophage maturation in the U937 model system.

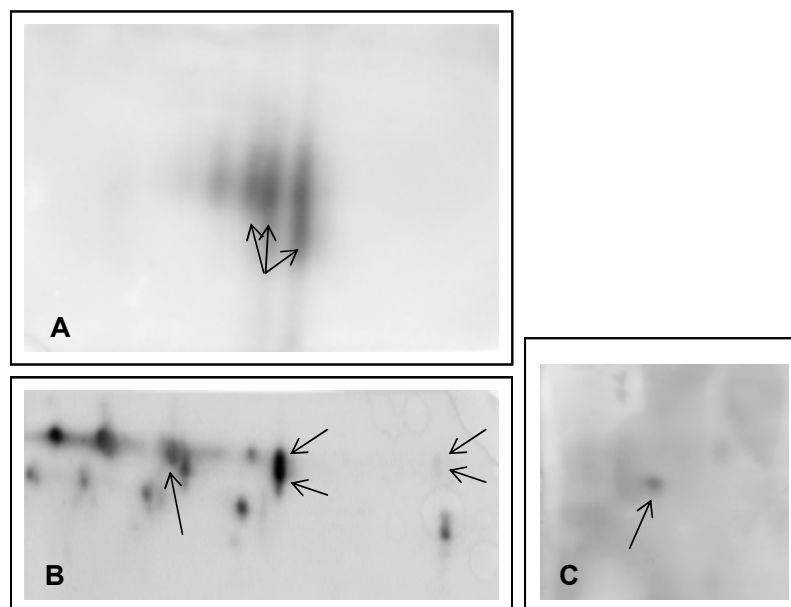


**Figure 4** Confirmation of the identity of GILT, cathepsin D, and A-FABP spots by 2-D immunoblotting. Presented are the results of 2-D immunoblots stained with anti-sera specific for GILT (A), cathepsin D (B), and A-FABP (C). The arrows indicate the spots identified with MALDI MS/MS. For GILT we have identified three spots, A-FABP one and for cathepsin D five. In addition to these 5 spots, 7 spots were stained with the specific anti-sera for cathepsin D.

The identification of the spots was confirmed by 2-D immunoblots (Fig. 4). The results show that all three proteins were correctly identified by MALDI MS/MS. The 2-D immunoblot of cathepsin D further showed that there are at least 12 forms of cathepsin D (Fig. 4B). On 1-D immunoblots (Fig. 5), U937 monocytes (MO) and macrophages (MØ) from three separately prepared batches were compared with one batch of PB-MO and PB-MØ. The results indicate that GILT is not expressed at detectable levels in monocytes, whereas it is expressed at high levels in both U937 and blood-derived macrophages. Two bands were detected in the 1-D immunoblot of cathepsin D. One is the mature (48 kDa) cathepsin D form and the other is cathepsin D  $\beta$ -chain (26 kDa). Both are clearly up-regulated in U937 macrophages and blood-derived macrophages. Unfortunately, the 2-D gel results of A-FABP could not be confirmed by 1-D Western blotting, because the available anti-A-FABP antibody was not sensitive enough to detect the protein. However, since 2-D gels are loaded with approximately 200-times more protein extract than 1D gels, A-FABP could be detected on the 2-D immunoblot

from macrophages (Fig. 4C) A-FABP was not detectable on 2-D immunoblots of monocytes (data not shown), thus confirming the differential expression pattern during monocyte to macrophage differentiation.

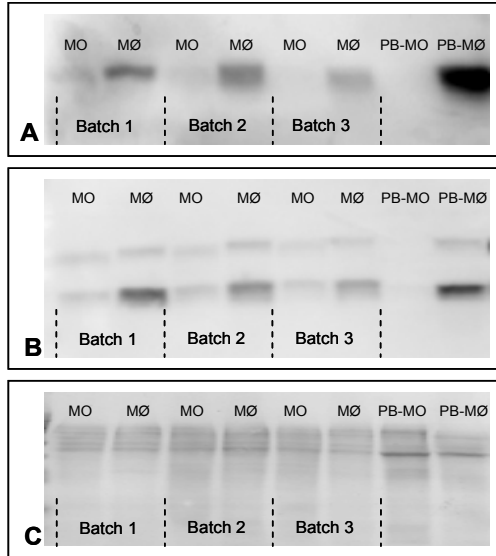


**Figure 5** Differential expressions of GILT and cathepsin D during macrophage maturation. 1-D Western blots of U937 monocytes (MO) and macrophages (MØ) of three individually prepared batches as well as one batch of PB-MO and PB-MØ. A: GILT, B: cathepsin D, and C the loading controls stained with coomassie blue.

## Transcriptomics

The mRNA expression patterns of the two differentiation stages of the U937 cell line were compared using microarrays containing 21,529 different oligonucleotides. Figure 6 gives an overview of the number of genes that are up- and down-regulated during macrophage maturation. The given ratios are the mean ratios of three arrays. In total, more than 850 genes were differentially expressed ( $p < 0.05$ ) by a factor 4 or more. Table 2 shows the genes that are down-regulated (45 genes) by more than a factor 6 and Table 3 the genes that are up-regulated (59 genes) by more than a factor 15 during monocyte differentiation to macrophage. The genes are classified into groups according to function. We have calculated the significance using the Student's  $t$ -test.

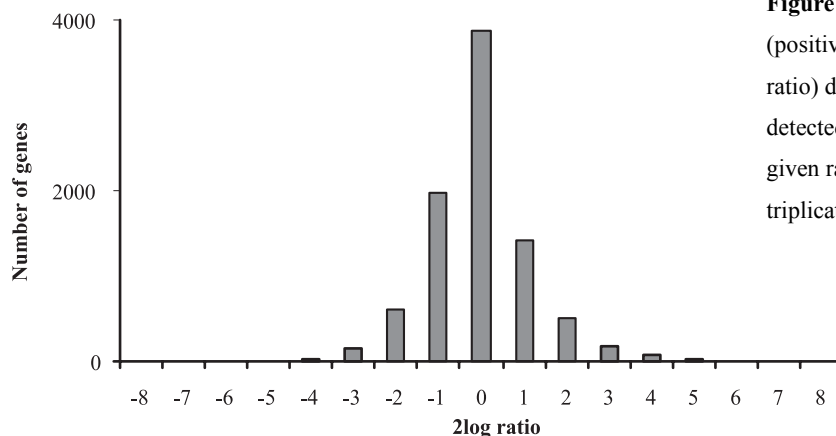


**Figure 6** Number of genes that are up- (positive ratio) and down-regulated (negative ratio) during macrophage maturation, as detected by microarray experiments. The given ratios (2log) are the average of the triplicate arrays.

## Biomarkers for macrophage maturation

**Table 2** Genes down-regulated by a factor 6 or more ( $p < 0.05$ ) during macrophage maturation in U937 cells. The genes are classified according to their function. The fold change is the mean ratio of three arrays.

GB_accession	Description	Mean fold change(n=3)	Student's <i>t</i> -test p-value	MW (kDa)	pI
<b>Immuun response/ chemotaxis</b>					
NM_005218	Defensin, beta 1	-36	6.8E-03	74.2	9.0
NM_003268	Toll-like receptor 5	-11	4.0E-03	97.7	6.2
<b>Cell growth and maintenance</b>					
NM_005563	Stathmin 1/oncoprotein 18	-8.9	3.4.E-05	17.2	5.8
<b>Cell cycle/DNA metabolism</b>					
NM_031942	C-Myc target JPO1	-30	5.6E-03	42.6	9.6
NM_002497	NIMA (never in mitosis gene a)-related kinase 2	-22	9.0E-03	51.7	9.0
NM_005263	Growth factor independent 1	-16	1.8E-06	45.6	9.5
NM_006845	Kinesin-like 6	-16	3.6E-05	81.3	8.0
NM_025259	NG23 protein	-14	1.5E-03	16.6	7.9
NM_005375	V-myb myeloblastosis viral oncogene homolog	-14	9.4E-03	72.3	6.4
NM_003542	H4 histone family, member G	-12	9.6E-05	23.7	11.6
NM_002358	MAD2 mitotic arrest deficient-like 1	-12	1.3E-05	23.5	5.0
NM_004526	MCM2 minichromosome maintenance deficient 2, mitotin	-11	1.6E-03	101.0	5.4
NM_014018	Mitochondrial ribosomal protein S28	-11	1.6E-03	20.8	9.2
NM_005432	X-ray repair complementing defective repair in Chinese hamster cells 3	-11	1.6E-03	37.9	8.8
NM_001786	Cell division cycle 2, G1 to S and G2 to M	-9.4	2.1E-03	34.1	8.4
NM_001948	Deoxyuridine 5''-triphosphate nucleotidohydrolase	-9.3	3.7E-04	26.7	9.6
NM_017518	Three prime repair exonuclease 2	-9.0	1.6E-03	30.6	6.4
NM_005322	H1 histone family, member 5	-8.8	5.2E-03	22.4	10.9
NM_005915	MCM6 minichromosome maintenance deficient 6	-8.7	3.4E-05	92.9	5.3
NM_006764	Interferon-related developmental regulator 2	-8.7	3.4E-05	48.0	6.4
NM_004336	BUB1 budding uninhibited by benzimidazoles 1	-8.6	1.3E-04	119.0	5.2
NM_002388	MCM3 minichromosome maintenance deficient 3	-8.5	3.3E-05	90.9	5.5
<b>Transport</b>					
NM_021614	Potassium intermediate/small conductance calcium-activated channel, subfamily N, member 2	-20	1.2E-02	63.8	9.5
NM_003740	Potassium channel, subfamily K, member 5	-16	2.0E-03	55.1	6.3
NM_000052	ATPase, Cu <sup>++</sup> transporting, alpha polypeptide	-8.5	1.0E-04	163	5.9
<b>Signal transduction/cell-cell signalling</b>					
BC015050	Opa-interacting protein 5	-12	2.1E-03	24.7	7
NM_005825	RAS guanyl releasing protein 2	-10	2.6E-05	73.6	8.2
NM_000956	Prostaglandin E receptor 2	-8.9	4.5E-03	39.7	9.3

## Chapter 2

**Table 3** Genes up-regulated by a factor 15 or more ( $p < 0.05$ ) during macrophage maturation in U937 cells. The genes are classified according to their function. The fold change is the mean ratio of three arrays.

GB_accession	Description	Mean fold change (n=3)	Student's <i>t</i> -test p-value	MW (kDa)	pI
<b>Immuun response/chemotaxis</b>					
NM_000582	Secreted phosphoprotein (osteopontin)	265	6.9E-03	35.4	4.4
NM_004994	Matrix metalloproteinase 9	241	3.5E-04	78.4	5.7
NM_001558	Interleukin 10 receptor, alpha	160	5.8E-04	60.7	5.2
NM_002421	Matrix metalloproteinase 1	86	6.1E-04	54.0	6.5
NM_003465	Chitinase 1 (chitotriosidase)	76	1.1E-04	21.6	6.6
NM_002659	Plasminogen activator, urokinase receptor	53	1.0E-05	36.9	6.2
NM_013439	Paired immunoglobulin-like receptor alpha	49	1.6E-04	33.9	10.1
NM_002535	2'-5'-oligoadenylate synthetase 2	41	4.2E-05	83.2	8.8
NM_000591	CD14 antigen	39	1.4E-02	40.0	5.8
NM_001548	Interferon-induced protein with tetratricopeptide repeats 1	30	7.8E-06	55.3	6.7
NM_020125	BCM-like membrane protein precursor	29	2.2E-05	27.7	8.3
Y16645	Small inducible cytokine subfamily A	26	2.0E-04	11.2	9.5
NM_000397	Cytochrome b-245, beta polypeptide	24	8.4E-03	65.2	8.9
NM_002185	Interleukin 7 receptor	22	7.8E-03	51.6	5.3
NM_003332	TYRO protein tyrosine kinase binding protein	22	2.0E-04	12.2	8.6
NM_006864	Leukocyte immunoglobulin-like receptor, subfamily B member 3	21	1.5E-05	64.1	6.9
NM_004001	Fc fragment of IgG, low affinity IIb, receptor for (CD32)	20	1.8E-04	34.0	5.7
NM_001736	Complement component 5 receptor 1 (C5a ligand)	19	4.5E-07	39.3	9.2
NM_002983	Small inducible cytokine A3	19	2.8E-04	10.0	4.8
U36759	Human pre TCR alpha mRNA, partial cds	18	4.2E-03	15.4	8.6
NM_000064	Complement component 3	18	1.8E-03	187.0	6.0
NM_005252	V-fos FBJ murine osteosarcoma viral oncogene homolog	18	2.3E-03	40.7	4.8
X52015	Interleukin 1 receptor antagonist	17	1.5E-02	20.0	5.8
AL136924	RAB5 interacting protein 2	16	3.5E-05	100.0	6.2
NM_001953	Endothelial cell growth factor 1	15	2.0E-05	50.0	5.4
NM_006889	CD86 antigen	15	4.9E-03	37.7	6.5
NM_021105	Phospholipid scramblase 1	15	2.6E-04	35.0	4.8
<b>NM_006332</b>	<b>Gamma-interferon inducible lysosomal thiol reductase (GILT)</b>	<b>15</b>	<b>2.4E-05</b>	<b>29.1</b>	<b>4.9</b>
<b>Cell growth and maintenance</b>					
NM_005651	Tryptophan 2,3-dioxygenase	153	6.6E-04	47.9	6.5
AF293462	Homo sapiens interleukin-4 induced gene-1 protein	64	1.0E-02	60.7	8.8
NM_001908	Cathepsin B	38	6.0E-07	37.8	5.9
U12767	Nuclear receptor subfamily 4, group A, member 3	32	8.4E-05	68.2	8.0
NM_004753	Short-chain dehydrogenase/reductase 1	23	9.9E-05	33.5	9.0
NM_001644	Apolipoprotein B mRNA editing enzyme, catalytic polypeptide 1	21	3.2E-03	28.2	9.0
NM_002510	Glycoprotein (transmembrane) nmb	15	5.1E-03	62.6	6.2
NM_002970	Spermidine/spermine N1-acetyltransferase	15	1.2E-03	20.0	5.1
NM_005985	Snail 1 homolog, zinc finger protein	8.4	2.4E-05	29.1	9.0
<b>Cell cycle</b>					
NM_000389	Cyclin-dependent kinase inhibitor 1A	35	3.0E-03	18.0	8.7
NM_057158	Dual specificity phosphatase 4	7.7	2.6E-03	42.9	7.1

## Biomarkers for macrophage maturation

**Table 3** Continued

GB_accession	Description	Mean fold change (n=3)	Student's t-test p-value	MW (kDa)	pI
<b>Transport</b>					
<b>NM_001442</b>	<b>Adipocyte fatty acid binding protein (A-FABP)</b>	<b>103</b>	<b>1.8E-04</b>	<b>14.6</b>	<b>6.8</b>
NM_000014	Alpha-2-macroglobulin	88	8.6E-05	163.0	6.0
NM_005502	ATP-binding cassette, sub-family A member 1	48	5.5E-03	254.0	6.4
NM_003052	Solute carrier family 34 (sodium phosphate), member 1	30	1.5E-03	68.9	9.0
NM_002959	Homo sapiens sortilin 1	26	3.1E-05	92.1	5.5
NM_000220	Potassium inwardly-rectifying channel, subfamily J, member 1	22	2.2E-04	44.8	9.0
NM_005072	Solute carrier family 12 member 4	19	6.5E-06	120.0	6.0
NM_000492	Cystic fibrosis transmembrane conductance regulator	18	3.7E-05	168.0	8.9
NM_003982	Solute carrier family 7 member 7	16	3.4E-03	56.0	5.3
<b>Cell adhesion</b>					
NM_002213	Integrin, beta 5	60	3.3E-03	88.0	5.7
NM_000632	Integrin, alpha M (CD11b)	15	4.4E-02	127.2	6.9
<b>Signal transduction</b>					
NM_023068	Sialoadhesin	90	6.2E-03	182.0	6.2
NM_005300	G protein-coupled receptor 34	59	2.4E-03	43.8	9.9
NM_003246	Thrombospondin 1	20	2.4E-04	129.0	4.7
NM_015991	Complement component 1, q subcomponent, alpha polypeptide	20	3.0E-04	26.0	9.3
NM_001881	cAMP responsive element modulator	16	1.4E-07	35.5	5.8
NM_002674	Pro-melanin-concentrating hormone	15	7.1E-03	18.7	6.2
<b>Differentiation</b>					
NM_002965	S100 calcium binding protein A9 (calgranulin B)	33	4.0E-04	13.2	5.7
NM_002964	S100 calcium binding protein A8 (calgranulin A)	33	1.4E-03	10.8	6.5
NM_000177	Gelsolin	30	2.1E-04	87.7	5.9
NM_001276	Human cartilage glycoprotein-39 (HC-gp39)	23	2.3E-02	42.6	8.7
NM_000799	Erythropoietin	15	3.4E-03	21.3	8.3

### *Quantitative real time PCR*

To confirm the microarray data by real time PCR we have selected the three genes that correspond to the proteins we have used for the 2-D gel electrophoresis confirmation, namely GILT, cathepsin D and A-FABP. In addition, we compared the U937 macrophage maturation to blood macrophage maturation. Figure 7 shows that the mRNA expression pattern of GILT and A-FABP as detected by specific real time PCR is in agreement with the array data: both are up-regulated during macrophage maturation. This is consistent with the protein expression levels (Fig. 3-5). According to the array data, cathepsin D was neither expressed in the monocyte nor in the macrophage. However, real time PCR confirmed the proteomics results (Fig. 3-5), showing that cathepsin D is also up-regulated at the genetic level in macrophages.

Most likely the oligonucleotide on the array, only  $\pm 25$  bp long and directed to only a fragment of the mRNA, did not hybridise with the cathepsin D cDNA in the sample.

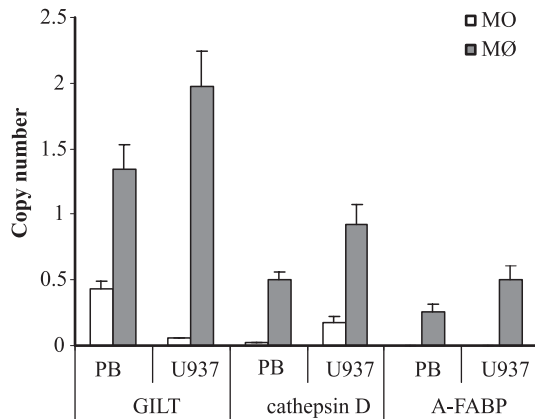


**Figure 7** Differential expression of GILT, cathepsin D, and A-FABP mRNAs during macrophage maturation. The expression of GILT, cathepsin D and A-FABP mRNA in U937 monocytes, macrophages, PB-MO and PB-MØ was determined by real time PCR. The copy number given was corrected for the expression levels of  $\beta$ -actin and is the average of three experiments.

### *Comparison of proteomics data and transcriptomics data*

Table 4 presents the comparison of the mRNA expression data obtained by oligonucleotide microarray experiments with the list of proteins identified by 2-D gel experiments. The ratios are the mean ratios of 3 arrays or four 2-D gels. The correlation between the protein ratios and the mRNA ratios was calculated according to the method of Anderson and Seilhamer<sup>26</sup>. We have found a correlation of 0.88 between the mRNA ratio of MØ divided by MO and the corresponding protein ratio.

## **Discussion**

This study describes the combination of proteomics, transcriptomics and PCA to characterize the U937 model system and to identify differentiation markers for macrophage maturation. In macrophages, we found that 226 proteins were significantly ( $p < 0.05$ ) up-regulated.

However, it is impossible to determine which proteins are the most relevant marker proteins for macrophage differentiation. The p-value determined by the Student's *t*-test only indicates which protein is significantly different between the two datasets (univariate). It provides hardly any information about the possible biological relevance. Therefore, in order to identify the most relevant marker proteins, we used PCA. Specifically, it was used as an exploratory data analysis method to quickly detect the most important markers in a huge dataset. PCA combines multiple signals that increase or decrease (multivariate) simultaneously and therefore gives more information about the possible relevance of the differentially expressed proteins as markers for macrophage differentiation. It should be noted that the number of

samples we used in this study is at the lower limit for PCA. Therefore, there was a small risk of detecting false positive markers. In order to circumvent this, the PCA results were verified by going back to the original data. The 41 most important protein spots according to PCA, were selected for identification by MALDI MS/MS. Thirty-eight spots were positively identified (Table 1). Three proteins were chosen for confirmation studies (GILT, cathepsin D and A-FABP).

**Table 4** Comparison of proteomics (23 different proteins) and transcriptomics. Negative Induction factors indicate intensity  $M\emptyset < MO$  and positive  $M\emptyset > MO$ . The standard deviations are also given in the induction factor columns. The Ag (agreement) column shows if there is a correlation between the mRNA and protein ratios. Y indicates agreement and N discrepancy.

Protein name	Accession nr	Proteomics Induction Factor (MØ/MO)(n=4)	Transcriptomics Induction factor (MØ/MO)(n=3)	Ag	References
Protein disulfide isomerase ER-60 precursor	BC010112	7 ± 3	-4.8 ± 0.5	N	a
Human gamma actin partial cds	NM_001614	-2.9 ± 0.5	-1.1 ± 0.1	N	40
Gamma-interferon inducible lysosomal thiol reductase precursor (GILT)	NM_006332	not in MO	15 ± 1	Y	19,20
Deoxyuridine 5'-triphosphate nucleotidohydrolase precursor	NM_001948	-6.1 ± 0.8	-9 ± 2	Y	41
Superoxide dismutase	NM_000636	2.8 ± 0.6	4.3 ± 0.7	Y	42
Tubulin alpha-1 chain fragment	NM_006082	-8 ± 3	-3.2 ± 0.7	Y	40
Cytochrome C oxidase subunit Va	NM_004255	2.2 ± 0.4	1.0 ± 0.2	N	a
Calgizzarin	NM_005620	3.0 ± 0.2	2.9 ± 0.6	Y	43
Cytochrome C oxidase polypeptide Vib	NM_001863	not in MO	1.1 ± 0.1	N	a
Lactoylglutathion lyase (glyoxalase I)	NM_006708	3.0 ± 0.4	1.3 ± 0.1	Y	A
Cathepsin D chain A	NM_001909	not in MO	n.d.	N	22,23
Alpha enolase	NM_001428	4 ± 1	-2.0 ± 0.4	N	a
Adipocyte fatty acid binding protein (A-FABP)	NM_001442	not in MO	103 ± 13	Y	24, 25
Cathepsin D chain B	NM_001909	not in MO	n.d.	N	22, 23
P59 (hsp binding immunophilin)	NM_002014	not in MØ	n.d.	N	44, 45
Hypothetical 17.7 kDa	NM_001614	not in MØ	-1.1 ± 0.1	N	40
TFAR 19 (PCD5_Human)	NM_004708	not in MØ	-4.0 ± 0.3	Y	a
Mitochondrial matrix protein p1 precursor (P60)	BC010112	not in MØ	-4.8 ± 0.5	Y	a
Cathepsin B	NM_001909	not in MO	38 ± 1	Y	16, 37
Fatty acid binding protein epidermal (E-FABP)	NM_001444	3.9 ± 0.7	2.6 ± 0.7	Y	24, 25
Galectin-1	NM_002305	2.7 ± 0.7	2.3 ± 0.5	Y	43, 46
Protein disulfide isomerase prolyl 4 hydroxylase beta (IMEK)	NM_000918	not in MØ	-1.45 ± 0.08	Y	a
Heterogeneous nuclear ribonucleoprotein C1/C2	NM_031314	-8 ± 1	-1.3 ± 0.2	N	28,29
Heterogeneous nuclear ribonucleoprotein C1/C2	NM_031314	6 ± 4	-1.3 ± 0.2	N	28, 29

a) No literature found on this protein to be involved in differentiation from monocyte into macrophage.

GILT catalyzes disulfide bond reduction and is involved in presentation of major histocompatibility complex (MHC) class II-peptide complexes<sup>18-20</sup>. This is an important characteristic of macrophages<sup>27</sup>. Cathepsin D is an aspartic protease and is involved in protein catabolism and is also involved in MHC class II-peptide complex presentation<sup>21-23</sup>. A-FABP is involved in the insulin sensitivity, lipid metabolism and lipolysis. It may also influence foam cell formation and atherogenesis<sup>24,25</sup>. Up-regulation of A-FABP was also detected in THP-1 cells after stimulation with PMA<sup>24</sup>. The results of the 1-D immunoblots, 2-D immunoblots, and real time PCR clearly show that all three proteins are either not present or expressed at very low levels in monocytes and are highly up-regulated in macrophages. Therefore, all three are good differentiation markers for macrophage maturation in U937 cells. We compared our findings with PB-MO and PB-MØ to confirm that these markers are really involved in macrophage maturation.

In addition to the proteome analyses, we also investigated the changes in the transcriptome that occur during macrophage maturation, using oligonucleotide microarrays. The results of these experiments were used to confirm the proteomics data and to further characterize the U937 model system. According to Anderson and Seilhamer<sup>26</sup>, there is a relatively poor correlation between mRNA and protein levels in human liver. Their study, in which the expression levels of 19 gene products were compared, yielded a correlation coefficient of 0.48 between mRNA and protein abundance. In our study we have compared the ratios of 21 proteins with the ratios of their corresponding mRNA levels. When no mRNA was available the protein was left out of the calculations. We found a correlation coefficient of 0.86, calculated according to the method described by Anderson and Seilhamer<sup>26</sup>. However, the correlation coefficient calculated in this way is biased by highly abundant proteins and mRNAs. This became clear when we omitted the most abundant mRNA, A-FABP. The resulting correlation coefficient was 0.49, which is similar to previously reported results<sup>26</sup>. A possible explanation for discrepancies between mRNA and protein expression levels is post-translational events, such as phosphorylation and glycosylation. A clear example of this is heterogeneous nuclear ribonucleoprotein (hnRNP) C1/C2, which harbours five phosphorylation sites<sup>28,29</sup>. [<sup>33</sup>P]-labelling experiments confirmed hnRNP C1/C2 phosphorylation occurs in U937 macrophages (data not shown). In our experiment, spots identified as hnRNP C1/C2 shift to the right (higher pH) during maturation (Fig. 8). This probably indicates that hnRNP C1/C2 is dephosphorylated during differentiation, as has previously been demonstrated by Stone and Collins<sup>29</sup>. The observed differential protein

expression of hnRNP C1/C2 is compatible with the notion that hnRNP C proteins undergo cell cycle dependent phosphorylation by cell cycle regulated protein kinases<sup>28</sup>. When U937 monocytes differentiate into macrophages, they are arrested in the G<sub>0</sub>/G<sub>1</sub> transition phase of the cell cycle and are therefore unable to differentiate.

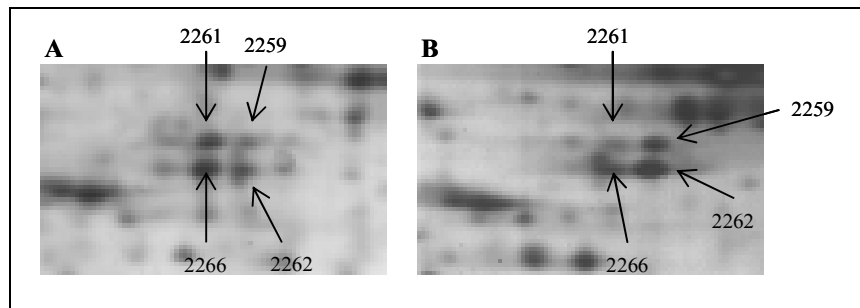


**Figure 8** HnRNP C1/C2 is dephosphorylated during macrophage maturation. A) The monocyte gel B) The gel from the macrophage. Spots 2259 and 2261 were identified as hnRNP C2. Spots 2262 and 2266 were identified as hnRNP C1 by MALDI MS/MS. The protein spots tend to shift to the right (higher pH) during macrophage maturation, indicative of dephosphorylation.

Another example of the discrepancies observed between transcriptomics and proteomics data is cathepsin D. According to the microarray data, cathepsin D was neither expressed in the monocyte nor in the macrophage. Real time PCR experiments however revealed that cathepsin D was clearly up-regulated during macrophage maturation, which is in agreement with previously published observations<sup>21,23</sup>. These results indicate that array data may not always be reliable for all genes present on the array. This is most likely due to the fact that oligonucleotide arrays contain only a very small part of each cDNA that is being tested, and in some cases this may not be specific enough to reliably detect the homologous mRNA, thereby producing false positive or false negative results.

The results of the array experiment show that almost all genes that are down-regulated in U937 macrophages are involved in cell cycle regulation. The U937 monocyte-like cell line is a proliferating tumor cell line, whereas blood monocytes are non-proliferating cells. Therefore, not all differentially up-regulated genes in U937 monocytes may be regarded as monocyte-specific genes, but could also be genes expressed in tumorigenic cells. We did not investigate this issue further as it was beyond the scope of the present study.

The genes that were found to be up-regulated during macrophage maturation are involved in many different cellular processes associated with macrophage functioning, including immune response, cell growth, cell adhesion, transport and differentiation. They may be suitable

markers for macrophage maturation, although this requires further testing. For example: secreted protein (osteopontin), up-regulated 265-fold, is involved in cell-matrix interaction. Osteopontin was also up-regulated in human blood macrophages<sup>16,30</sup>. Matrix metalloproteinase 9 is a secreted gelatinase. It degrades extra cellular matrix proteins (especially type IV and V collagens<sup>16</sup>) and is also up-regulated in blood macrophages<sup>16,30</sup>. Human cartilage glycoprotein 39 (HC-gp39) is up-regulated in U937 macrophages by a factor 23. It may play a role in the capacity of cells to respond to and cope with changes in their environment (Swissprot). HC-gp39 is expressed during the late stages of macrophage differentiation in blood macrophages<sup>16,30</sup>. Other possible markers for macrophage differentiation include gelsolin, chitinase 1(chitotriosidase), apolipoprotein E, all were previously found to be up-regulated in blood macrophages<sup>30</sup>. Alpha-2-macroglobulin<sup>30,31</sup>, thrombospondin 1<sup>32</sup>, alpha subunits (CD11a, CD11b and CD11c)<sup>5,33</sup>, sialoadhesion<sup>34</sup>, and many more not listed here were also up-regulated in blood macrophages.

Previously Juan et al.<sup>35</sup> used DNA microarrays and 2-D gels to investigate the differentiation of the human myeloid leukaemia cell line, HL-60. There are no similarities between their results with HL-60 and our results with U-937 at the protein level, except for alpha-enolase. In U937 cells, we found that alpha enolase was up-regulated at the protein level, but could not detect differential expression at the mRNA level. This suggests that the differential expression at the protein level may be the consequence of post-translational events, as was also suggested by Juan et al for differential expression of alpha-enolase protein in HL-60 cells<sup>35</sup>. A comparison of the transcriptomics data from HL-60 cells<sup>35</sup> and the data presented in this report reveals limited similarities. Forty-eight of 77 up-regulated genes in HL-60 were not found to be up-regulated in our experiment on U937 cells. The genes that are highly up-regulated during maturation of the U937 and blood derived MØ (e.g. osteopontin, matrix metalloproteinase 9, HC-gp39, etc) were not found during maturation of the HL-60 cell line. Another marked difference between the two studies was the down-regulation of cathepsin B in the HL-60 cell line. In blood monocytes<sup>16,30</sup> and U937 cell line cathepsin B is up-regulated during differentiation. Cathepsin B is a lysosomal cysteine proteinase involved in phagocytosis, a major characteristic of macrophages<sup>16,36</sup>. From a biological perspective, it can be hypothesized that the differences between HL-60 and U-937 could be explained by the fact that both cell lines are derived from monocyte-progenitors at different stages of the monocytic differentiation lineage<sup>5</sup>, thus giving rise to differences in both protein and mRNA expression patterns.

Typical characteristics of macrophages are, amongst others, the presence of Fc $\gamma$  receptors (Fc $\gamma$ R I, II and III), complement receptor for C3 components types 1 and 2 (CR1, CR2), mannose receptors (mannosyl-fructosyl receptor), antigens (CD68, CD14), and the secreted products (IL-1, IL-6, TNF) <sup>1, 17</sup>. The oligonucleotide microarray data revealed that the Fc fragments were clearly up-regulated in the macrophages (Table 3). The complement receptor CR1 was also found to be up-regulated, but due to the great variance in measured expression levels between the three arrays it was not entered into Table 3. The cytokines IL-1 and TNF were both up-regulated. Probes for complement receptor CR2 and mannosyl-fructosyl receptor were not spotted on the array. Although IL-6 was not detected using microarrays, ELISA experiments revealed that U937 macrophages do express IL-6 <sup>37</sup>. The macrophage-specific antigens CD14 and CD68 are both expressed in the U937 macrophages. These results show that the U937 macrophages express the genes that have been shown to be strongly expressed in native terminally differentiated macrophages. Furthermore, the array data shows that the 5' nucleotidase mRNA is down-regulated by a factor -4.4 in macrophages. Moreover, the mRNA encoding leucine aminopeptidase is up-regulated by a factor 2.4. The expression pattern of the latter two genes in U937 macrophages is very similar to the expression pattern in inflammatory macrophages <sup>2, 38, 39</sup>.

### **Concluding remarks**

From the results above we conclude that the U937 macrophage expressed most of the previously reported macrophage specific markers, indicating that the PMA-differentiated U937 cells are a suitable model system to study macrophages.

Finally, our results clearly show that the simultaneous application of transcriptomics and proteomics increases the chance that differentially expressed genes are identified. Since both methods produce a huge amount of data, a proper analytical tool to sort the data and to find the significant changes in the different samples is of great importance. PCA has proven in this study to be a powerful tool to identify proteins important for monocyte to macrophage differentiation.

---

**References**

- 1 van Furth, R., *Macrophage pathogen interactions introduction* **1994**, v-vii.
- 2 van Furth, R. and Sluiter, W., *Trans R Soc Trop Med Hyg*, **1983**, Current views on the ontogeny of macrophages and the humoral regulation of monocytopoiesis, *77*, 614-619.
- 3 Abrink, M., Gobl, A. E., Huang, R., Nilsson, K. and Hellman, L., *Leukemia*, **1994**, Human cell lines u-937, thp-1 and mono mac 6 represent relatively immature cells of the monocyte-macrophage cell lineage, *8*, 1579-1584.
- 4 Collins, S. J., *Blood*, **1987**, The hl-60 promyelocytic leukemia cell line: Proliferation, differentiation, and cellular oncogene expression, *70*, 1233-1244.
- 5 Tenno, T., *Department of medical sciences, Acta Universitatis Upsaliensis, Uppsala* **2001**.
- 6 Huberman, E. and Callahan, M. F., *Proc Natl Acad Sci U S A*, **1979**, Induction of terminal differentiation in human promyelocytic leukemia cells by tumor-promoting agents, *76*, 1293-1297.
- 7 Rabilloud, T., *Proteomics*, **2002**, Two-dimensional gel electrophoresis in proteomics: Old, old fashioned, but it still climbs up the mountains, *2*, 3-10.
- 8 Dillon, W. R. and Goldstein, M., *Multivariate analysis: Methods and applications*, John Wiley & Sons Inc., New York, USA **1984**, p. 608.
- 9 Joliffe, I. T., *Principal component analysis*, Springer Verlag, New York, USA **1986**.
- 10 Martens, H. and Naes, T., *Multivariate calibrations*, John Wiley & Sons, Chichester, England **1992**, p. 438.
- 11 Massart, D. L., Vandeginste, B. G. M. and De Jong, P. J., *Handbook of chemometrics and qualimetrics: Part a*, Elsevier, Amsterdam, The Netherlands **1997**.
- 12 Vandeginste, B. G. M., Massart, D. L., Buydens, L. M. C. and De Jong, P. J., *Handbook of chemometrics and qualimetrics: Part b*, Elsevier, Amsterdam, The Netherlands **1998**.
- 13 Greef, J. v. d., Davidov, E., Verheij, E., Vogels, J., *et al.*, in: Harrigan, G. and Goodacre, R. (Eds.), *Metabolic profiling: Its role in biomarker discovery and gene function analysis*, Kluwer Academic Publishing, Boston **2003**, 171-198.
- 14 Sundstrom, C. and Nilsson, K., *Int J Cancer*, **1976**, Establishment and characterization of a human histiocytic lymphoma cell line (u-937), *17*, 565-577.
- 15 Izeboud, C. A., Vermeulen, R. M., Zwart, A., Voss, H. P., *et al.*, *Naunyn Schmiedebergs Arch Pharmacol*, **2000**, Stereoselectivity at the beta2-adrenoceptor on macrophages is a major determinant of the anti-inflammatory effects of beta2-agonists, *362*, 184-189.
- 16 Krause, S. W., Rehli, M., Kreutz, M., Schwarzfischer, L., *et al.*, *J Leukoc Biol*, **1996**, Differential screening identifies genetic markers of monocyte to macrophage maturation, *60*, 540-545.
- 17 Kreutz, M., Krause, S. W., Hennemann, B., Rehm, A. and Andreesen, R., *Res Immunol*, **1992**, Macrophage heterogeneity and differentiation: Defined serum-free culture conditions induce different types of macrophages in vitro, *143*, 107-115.
- 18 Arunachalam, B., Phan, U. T., Geuze, H. J. and Cresswell, P., *Proc Natl Acad Sci U S A*, **2000**, Enzymatic reduction of disulfide bonds in lysosomes: Characterization of a gamma-interferon-inducible lysosomal thiol reductase (gilt), *97*, 745-750.
- 19 Luster, A. D., Weinshank, R. L., Feinman, R. and Ravetch, J. V., *J Biol Chem*, **1988**, Molecular and biochemical characterization of a novel gamma-interferon-inducible protein, *263*, 12036-12043.
- 20 Phan, U. T., Arunachalam, B. and Cresswell, P., *J Biol Chem*, **2000**, Gamma-interferon-inducible lysosomal thiol reductase (gilt). Maturation, activity, and mechanism of action, *275*, 25907-25914.
- 21 Baldwin, E. T., Bhat, T. N., Gulnik, S., Hosur, M. V., *et al.*, *Proc Natl Acad Sci U S A*, **1993**, Crystal structures of native and inhibited forms of human cathepsin d: Implications for lysosomal targeting and drug design, *90*, 6796-6800.
- 22 Gieselmann, V., Pohlmann, R., Hasilik, A. and Von Figura, K., *J Cell Biol*, **1983**, Biosynthesis and transport of cathepsin d in cultured human fibroblasts, *97*, 1-5.
- 23 Levy, J., Kolski, G. B. and Douglas, S. D., *Infect Immun*, **1989**, Cathepsin d-like activity in neutrophils and monocytes, *57*, 1632-1634.
- 24 Boord, J. B., Fazio, S. and Linton, M. F., *Curr Opin Lipidol*, **2002**, Cytoplasmic fatty acid-binding proteins: Emerging roles in metabolism and atherosclerosis, *13*, 141-147.
- 25 Zimmerman, A. W. and Veerkamp, J. H., *Cell Mol Life Sci*, **2002**, New insights into the structure and function of fatty acid-binding proteins, *59*, 1096-1116.
- 26 Anderson, L. and Seilhamer, J., *Electrophoresis*, **1997**, A comparison of selected mrna and protein abundances in human liver, *18*, 533-537.
- 27 Maric, M., Arunachalam, B., Phan, U. T., Dong, C., *et al.*, *Science*, **2001**, Defective antigen processing in gilt-free mice, *294*, 1361-1365.

- 28 Pinol-Roma, S. and Dreyfuss, G., *Mol Cell Biol*, **1993**, Cell cycle-regulated phosphorylation of the pre-mrna-binding (heterogeneous nuclear ribonucleoprotein) c proteins, *13*, 5762-5770.
- 29 Stone, J. R. and Collins, T., *J Biol Chem*, **2002**, Rapid phosphorylation of heterogeneous nuclear ribonucleoprotein c1/c2 in response to physiologic levels of hydrogen peroxide in human endothelial cells, *277*, 15621-15628.
- 30 Hashimoto, S., Suzuki, T., Dong, H. Y., Yamazaki, N. and Matsushima, K., *Blood*, **1999**, Serial analysis of gene expression in human monocytes and macrophages, *94*, 837-844.
- 31 Rodenburg, R. J., Brinkhuis, R. F., Peek, R., Westphal, J. R., *et al.*, *J Leukoc Biol*, **1998**, Expression of macrophage-derived chemokine (mdc) mrna in macrophages is enhanced by interleukin-1beta, tumor necrosis factor alpha, and lipopolysaccharide, *63*, 606-611.
- 32 Suchard, S. J., Mansfield, P. J. and Dixit, V. M., *J Immunol*, **1994**, Modulation of thrombospondin receptor expression during hl-60 cell differentiation, *152*, 877-888.
- 33 Corbi, A. L. and Lopez-Rodriguez, C., *Leuk Lymphoma*, **1997**, Cd11c integrin gene promoter activity during myeloid differentiation, *25*, 415-425.
- 34 Morris, L., Crocker, P. R., Hill, M. and Gordon, S., *Dev Immunol*, **1992**, Developmental regulation of sialoadhesin (sheep erythrocyte receptor), a macrophage-cell interaction molecule expressed in lymphohemopoietic tissues, *2*, 7-17.
- 35 Juan, H. F., Lin, J. Y., Chang, W. H., Wu, C. Y., *et al.*, *Electrophoresis*, **2002**, Biomic study of human myeloid leukemia cells differentiation to macrophages using dna array, proteomic, and bioinformatic analytical methods, *23*, 2490-2504.
- 36 Morland, B., *Scand J Immunol*, **1985**, Cathepsin b activity in human blood monocytes during differentiation in vitro, *22*, 9-16.
- 37 Izeboud, C. A., Mocking, J. A., Monshouwer, M., van Miert, A. S. and Witkamp, R. F., *J Recept Signal Transduct Res*, **1999**, Participation of beta-adrenergic receptors on macrophages in modulation of lps-induced cytokine release, *19*, 191-202.
- 38 Por, S. B., Cooley, M. A., Breit, S. N., Penny, R. and French, P. W., *J Histochem Cytochem*, **1991**, Antibodies to tubulin and actin bind to the surface of a human monocytic cell line, u937, *39*, 981-985.
- 39 Stvrtinova, V., Jakubovsky, J. and Hulin, I., *Inflammation and fever*, Academic Electronic press, slovak **1995**.





## Chapter 3

---

### **Categorization of anti-inflammatory compounds using transcriptomics, proteomics, and metabolomics in combination with multivariate data analysis.**

Kitty C.M. Verhoeckx<sup>1,2</sup>

Sabina Bijlsma<sup>1</sup>

Sonja Jespersen<sup>3</sup>,

Raymond Ramaker<sup>1</sup>,

Elwin R. Verheij<sup>1,2</sup>

Jan van der Greef<sup>1,2</sup>

Renger F. Witkamp<sup>1</sup>

Richard J.T. Rodenburg<sup>4</sup>

*Int Immunopharmacol, 2004, 4, p1499-1514*

<sup>1</sup> TNO Quality of Life, Zeist, The Netherlands, <sup>2</sup> Leiden University, Leiden/Amsterdam Center for Drug Research, Leiden, The Netherlands, <sup>3</sup> Ferring Pharmaceuticals, Copenhagen S, Denmark, <sup>4</sup> UMC St Radboud, Nijmegen, The Netherlands

## **Categorization of anti-inflammatory compounds using transcriptomics, proteomics, and metabolomics in combination with multivariate data analysis.**

*The discovery of new anti-inflammatory drugs is often based on an interaction with a specific target, although other pathways often play a primary or secondary role. Anti-inflammatory drugs can be categorized into classes, based on their mechanism of action. In this article we investigate the possibility to categorize novel anti-inflammatory compounds by three holistic methods. For this purpose, we make use of macrophage-like U937 cells which are stimulated with LPS in the absence or presence of an anti-inflammatory compound. Using microarrays, 2-D gel electrophoresis and a LC-MS method for lipids the effects on the transcriptome, proteome and metabolome of the exposed cells is investigated. The expression patterns are subsequently analyzed using in-house developed pattern recognition tools. Using the methods described above, we have examined the effects of 6 anti-inflammatory compounds. Our results demonstrate that different classes of anti-inflammatory compounds show distinct and characteristic mRNA, protein, and lipid expression patterns, which can be used to categorize known molecules and to discover and classify new leads. The potential of our approach is illustrated by the analysis of several beta<sub>2</sub>-adrenergic receptor agonists (β<sub>2</sub>-agonists). In addition to their primary pharmacological target, β<sub>2</sub>-AR agonists possess certain anti-inflammatory properties. We were able to show that zilpaterol, a poorly characterized β<sub>2</sub>-agonist, gives rise to an almost identical expression pattern as the β<sub>2</sub>-agonists clenbuterol and salbutamol. Furthermore we have identified specific mRNA, protein and lipid markers for the anti-inflammatory compounds investigated in this study.*

---

### **Introduction**

Inflammation plays a pivotal role in the pathogenesis of many diseases. The development of novel inflammatory modulators to support treatment of such disorders is of major interest to the pharmaceutical industry. As a consequence, the number of anti-inflammatory drugs in the pharmaceutical pipeline is increasing rapidly. The discovery of these drugs is still often based on an interaction with a specific target or by measuring single or multiple cellular endpoints such as cytokine production, e.g. TNF-α. Current anti-inflammatory drugs can be categorized into a number of classes, based on their mechanism of action. These include among others NF-κB inhibitors, corticosteroids, anti-cytokine antibodies, anti-inflammatory cytokines,

cytokine-antagonists, enzyme inhibitors, kinase-inhibitors, proteasome inhibitors, and apoptosis inducers. However, inflammation is a complex process involving a variety of cell-types and hundreds of different inflammatory mediators. Although different signal transduction pathways may share similar endpoints, such as TNF- $\alpha$  inhibition, modulating these may give rise to completely different cellular reactions. TNF- $\alpha$  was found to be regulated by different MAP kinases (e.g. p38, ERK) <sup>1</sup> and transcription factors (e.g. NF $\kappa$ B, AP-1 and CREB) <sup>2-5</sup>. These MAP kinases and transcription factors are in turn activated by other kinases in different signalling pathways. Because of this, it is increasingly recognised that more holistic, systems biology methods should be introduced in the drug discovery process.

In this paper we integrate three biological levels, the transcriptome, proteome and the metabolome, to categorize inflammatory modulators on the basis of the biological responses that they elicit. Our methodology makes use of differentiated U937 macrophages as a model system, because macrophages are the major targets of anti-inflammatory agents. The U937 cell line is widely accepted as a model system for human macrophages as exemplified in our previously published observations on the expression of macrophage maturation markers in this cell line <sup>6</sup>. The U937 cells are stimulated with the endotoxin LPS, that induces a broad range of inflammatory pathways. By using oligonucleotide microarrays, 2-D gel electrophoresis and LC-MS, the effects of LPS-exposure on the transcriptome, proteome and metabolome are readily visualized. When this procedure is performed in the presence of an anti-inflammatory compound, this leads to characteristic changes in the U937 mRNA, protein and metabolite expression patterns. The patterns of the anti-inflammatory compound under investigation are compared to those of known inflammatory modulators using principal component discriminant analysis (PC-DA) <sup>7</sup>. This mathematical tool enables the rapid classification of anti-inflammatory compounds. In this study we have examined four different classes with anti-inflammatory properties, each of which has its own specific, partially overlapping inhibitory effect. We have studied dexamethasone, a corticosteroid <sup>4, 5, 8, 9</sup>, a proteasome inhibitor (PSI) <sup>10-12</sup>, the MAP kinase inhibitor SB203580 <sup>13</sup> and two  $\beta_2$ -adrenoreceptor agonists, clenbuterol <sup>14, 15</sup> and salbutamol <sup>16</sup>. In addition to their primary pharmacological target,  $\beta_2$ -agonists possess certain anti-inflammatory properties <sup>14</sup>. Our approach was evaluated with zilpaterol, a compound originally developed as  $\beta_2$ -agonist, but later specifically being introduced for yet another effect of this class, namely as a growth promoting (anabolic) agent for use in cattle <sup>17, 18</sup>.

## **Materials and Methods**

### *Chemicals*

Lipopolysaccharide (LPS, *E.coli* 0111:B4), clenbuterol, salbutamol, formoterol, and dexamethasone were obtained from Sigma Aldrich (St. Louis, MO, USA). SB203580 and proteasome inhibitor (PSI) were purchased from Omnilabo international B.V. (Breda, The Netherlands) and zilpaterol from Intervet Inc. (Millsboro, US). The chemicals and equipment used for two-dimensional gel electrophoresis were obtained from Amersham biosciences (Uppsala, Sweden) unless stated otherwise.

### *Cell cultures and incubations*

Human monocyte-like histiocytic lymphoma cells U937<sup>19</sup> obtained from the ATCC (CRL-1593.2) were grown in RPMI-1640 medium, supplemented with 10% (v/v) fetal calf serum and 2 mM L-glutamine (Life technologies, Breda, The Netherlands) at 37 °C, 5% CO<sub>2</sub> in a humidified atmosphere. U937 monocytic cells were differentiated into macrophages using phorbol 12-myristate 13-acetate (PMA, 10 ng/ml, overnight, Omnilabo, Breda, The Netherlands) as described previously<sup>20</sup>. The PMA-differentiated macrophages were allowed to recover from PMA treatment for 48 h, during which the culture medium was replaced daily. At day three after PMA treatment, the macrophages were exposed for 6 h to LPS (*E.Coli*, 1µg/ml) in the presence or absence of an inflammatory inhibitor. The following inflammatory inhibitors were used: clenbuterol (1x10<sup>-7</sup> M), salbutamol (1x10<sup>-6</sup> M), zilpaterol (1x10<sup>-6</sup> M), dexamethasone (1x10<sup>-7</sup> M), SB203580 (1x10<sup>-6</sup> M), proteasome inhibitor (PSI, 1x10<sup>-5</sup> M) and formoterol (1x10<sup>-8</sup> M). The concentrations of inhibitors used resulted in a 15 – 30 % inhibition of TNF-α release (see results section), as determined in a dose-response experiment in which the effect on TNF-α release by U937 macrophages was measured (data not shown). The incubations were performed in duplicate.

### *Transcriptomics*

Incubations of U937 macrophages with LPS, with or without an inhibitor, were performed in triplicate and pooled afterwards. Total RNA was extracted from stimulated U937 macrophages using Trizol reagent (Life technologies, Rockville, USA) and RNeasy columns (Qiagen, Westburg, Leusden, The Netherlands) according to the manufacturer's protocol. DNase treatment (Qiagen) was performed on the RNeasy column. Each sample was analysed by oligonucleotide microarrays in triplicate, in which LPS was labelled with Cy-5 and LPS + inhibitor was labelled with Cy-3. In addition, a control experiment was performed

simultaneously by comparing LPS-Cy-5 with LPS-Cy-3 on the same array, to check the differences in labelling efficiency. Subsequently, the microarray experiments and data processing were performed as described before<sup>6</sup>. The resulting list of genes with their normalized log transformed spot volumes per array were analyzed by principal component analysis (PCA) and principal component discriminant analysis (PC-DA).

### *Proteomics*

The stimulated U937 cell pellets were dissolved in lysis buffer containing 8 M urea, 2% (w/v) CHAPS, 0.02% (v/v) Pharmalytes, and 1% (w/v) dithiothreitol (Sigma-Aldrich chemie, Zwijndrecht, The Netherlands). The protein concentration was determined using Bradford reagent (Bio-Rad, Veenendaal, The Netherlands) according to the manufacturer's protocol. The protein extract (400 µg) was further diluted to 350 µl with rehydration buffer containing 8 M urea, 0.5% (w/v) CHAPS, 2 mM tributyl phosphine (Fluka, Buchs SG, Switzerland), and 1% (v/v) IPG ampholytes pH 4-7. Per sample, two gels were processed and analyzed. In total 24 gels were run.

The first dimension was carried out on an IPGphor system using pH 4-7 IPG gel strips of 18 cm. The IEF was performed at 20 °C under the following conditions: 12 h at 30 V; 30 min at 150 V; 1 h at 300 V; 1 h at 1500 V and 7.5 h at 8000V. After isoelectric focusing, the IPG strips were equilibrated for 30 min in a buffer containing 6 M urea, 30% (v/v) glycerol, 5 mM tributyl phosphine, and 2% (w/v) SDS in 0.05 M Tris-HCl buffer, pH 8.8. The second dimensional separations were carried out on custom made 12% SDS-polyacrylamide gels using a Hoefer DALT electrophoresis system. The gels were stained with RuBPS fluorescent staining using the protocol which is described in Rabilloud et al<sup>21,22</sup>. The gels were scanned on the Typhoon laser scanner at 600 V with a green laser (532 nm) for excitation and 610 BP 30 emission filter.

Scanned TIFF images were analyzed using the Progenesis workstation software package (Nonlinear Dynamics, Newcastle upon Tyne, UK). Spots were automatically detected and visually checked for undetected or incorrectly detected spots. The protein spots detected in each experimental gel were matched to the corresponding spot in a digitized reference gel. Intensity levels were normalized between gels by dividing the spot intensity through the total intensity of all the spots in the gel. A list of spots with their normalized spot volumes per gel was analyzed by PCA and PC-DA. Protein spots were identified by in-gel digestion followed by MALDI mass mapping and/or MALDI MS/MS sequencing in combination with database search as described before<sup>6</sup>.

### *Metabolomics*

The treated U937 cell pellets containing 580  $\mu\text{g}$  of protein were dissolved in 250  $\mu\text{l}$  isopropanol and centrifuged at 1000 g for 10 min. The supernatant (75  $\mu\text{l}$ ) was injected in duplicate on a Inertsil ODS 3 (100 x 3 mm i.d. 5  $\mu\text{m}$ , Varian Chrompack, Middelburg, The Netherlands) with S2 guard column (10 x 2 mm i.d., Varian Chrompack) and a flow of 0.7 ml/min. For elution the following solvents were used: 5 % acetonitrile in water (mobile phase A), 30 % isopropanol in acetonitrile (mobile phase B), and 50 % dichloromethane in isopropanol (mobile phase C). The gradient used was as follows: A:B (70:30) at 0 min until 2 min; A:B (5:95) at 15 min; A:B:C (5:35:60) at 35 min until 40 min; A:B (5:95) at 41 min and A:B (70:30) at 50 min. The separation was performed at 20 °C. In total 24 injections were performed in randomized order. Detection was conducted on-line with a Thermo Finnigan TSQ 700 mass spectrometer (Thermo Finnigan, San Jose, USA) using electrospray interface in positive mode. The TSQ 700 operating conditions were as follows: heated capillary temperature, 225 °C; spray voltage, 4 kV; sheath gas (nitrogen), 70 psi; auxiliary gas (nitrogen) 15 psi; scan range 300-1900, and scan speed 1.5 s/scan. Internal standards, lysophosphatidylcholine (C17:0), phosphatidylcholine (di-C12:0), and triglyceride (tri-C17:0) were used to normalize the data for peak intensity and retention time alignment. The data were processed using TNO IMPRESS version 1.9, an in-house developed software package to generate peak tables of all files. Alignment of retention times was performed using TNO – EQUEST 2.1. A list of aligned retention times, m/z values and peak areas were analyzed with PCA and PC-DA.

### *Data analysis*

The datasets were analysed by PCA using the PLS tool box for Matlab (version 2.0; Eigenvector Research, Washington, USA). Only with the transcriptomics data we obtained clustering and separation of the different classes of anti-inflammatory inhibitors. Additionally, the datasets (transcriptomics, proteomics and metabolomics) were analysed with PC-DA using an in house developed function for Matlab (version 6.5.1, release 13, The Mathworks, Inc., 2003).

PCA describes data as a linear combination of so-called scores and loadings. These linear combinations are called principal components. The scores and loadings vectors give a concise and simplified description of the variance present in the dataset<sup>23, 24</sup>.

PC-DA is based on the assumption that samples of the same group are more similar compared to samples of other groups<sup>7</sup>. The goal of PC-DA is to find and identify structures in the

original data that show large differences in the group means. This process involves a priori knowledge of which samples are similar. Therefore, PC-DA is said to be a supervised analysis technique. The data of the individual datasets were mean-centered<sup>23,24</sup>. The combined dataset was scaled on the range of the variables followed by mean-centering.

*Quantitative real time polymerase chain reaction (PCR)*

Primers for human CXCR5 (forward primer; 5'-TCA GAC TGG TTG AGT TCA GGT AGC T-3', reverse primer; 5' ACC CAG GAT CCG GTG ACA T-3', TaqMan<sup>®</sup> probe; 5' CCC CTG GCT CTG ACC GAA ACA GC-3'), human CXCL6 (forward primer; 5'-AAT TTT GGA CAG TGG AAA CAA GAA A-3', reverse primer; 5'-AGA AAA CTG CTC CGC TGA AGA CT -3', TaqMan<sup>®</sup> probe; 5'-ACT GAG TAA CAA AAA AGA CCA TGC ATC ATA AAA TTG C-3'), and human  $\beta$ -actin (forward primer; 5'CTG ACT GAC TAC CTC ATG AAG ATC CT 3', reverse primer; 5'CTT AAT GTC ACG CAC GAT TTC C 3', TaqMan<sup>®</sup> probe; TAC AGC TTC ACC ACC ACG GCC GA-3') were purchased from Applied Biosystems (Nieuwerkerk a/d IJssel, The Netherlands). The RT reaction was performed on 500 ng of total RNA with avian myeloblastosis virus reverse transcriptase (Promega, Madison, WI, USA). Quantitative real time polymerase chain reactions were performed using TaqMan<sup>®</sup> probes. PCR reactions were performed in a total volume of 20  $\mu$ l 1x TaqMan<sup>®</sup> Universal Mastermix in the iCycler iQ<sup>™</sup> Real-Time PCR detection system (Bio Rad). The PCR program was as follows: 1 cycle 2 min at 50 °C, 1 cycle 10 min at 95 °C; 50 cycles 15 sec at 95 °C, 60 sec at 60 °C. The absolute number of copies of the gene of interest in the experimental cDNA samples was calculated from the linear regression of a standard curve. The expression of the measured genes in each sample was normalized for  $\beta$ -actin expression.

*Enzyme-Linked Immunosorbent Assay (ELISA) and enzyme activity measurements*

Immunoassays for CXCL6 and oncostatin M were purchased from R&D systems (Oxon, UK). The VEGF ELISA was obtained from Preprotech (London, UK) and the cytoset antibody pair kit for TNF- $\alpha$  from Biosource (Etten-Leur, The Netherlands). The immunoassays were performed according to the manufactures instructions. All samples were analyzed in duplicate. The enzyme activity of lactate dehydrogenase (LDH) was quantitatively determined using the *in vitro* assay for LDH activity from Roche Diagnostics (Mannheim, Germany) for automated clinical chemistry analyzer Hitachi 911 (Hitachi, Japan).

## Results

The effect of the inhibitors on LPS activated U937 cells was tested by measuring the TNF- $\alpha$  release and LDH activity in the cell culture media (Fig. 1.). After 6 h of LPS stimulation both early inflammatory effects (e.g. TNF- $\alpha$  release) and late inflammatory effects (e.g. IL-10 release) were detectable (data not shown). The concentrations of the various inhibitors were chosen as such to achieve similar levels of TNF- $\alpha$  inhibition. At these concentrations, none of the inhibitors induced LDH release significantly above the level obtained with LPS alone. The one exception to this is PSI, which did lead to a 2 to 3-fold increase in LDH release. The PSI concentration used in this experiment was chosen in order to minimise the apoptotic effect while still generating a clear anti-inflammatory effect, although it was not possible to separate the two effects (data not shown).

### *Transcriptomics*

The same experimental conditions were used to test the effects of the inhibitors on the mRNA expression levels in U937 macrophages stimulated by LPS. The microarrays used contained 21,529 oligonucleotides which correspond to 21,316 genes. After data pre-processing and normalisation a dataset of 9,436 genes remained and was used in the PC-DA. Figure 2 shows the results of the PC-DA of the microarray dataset.

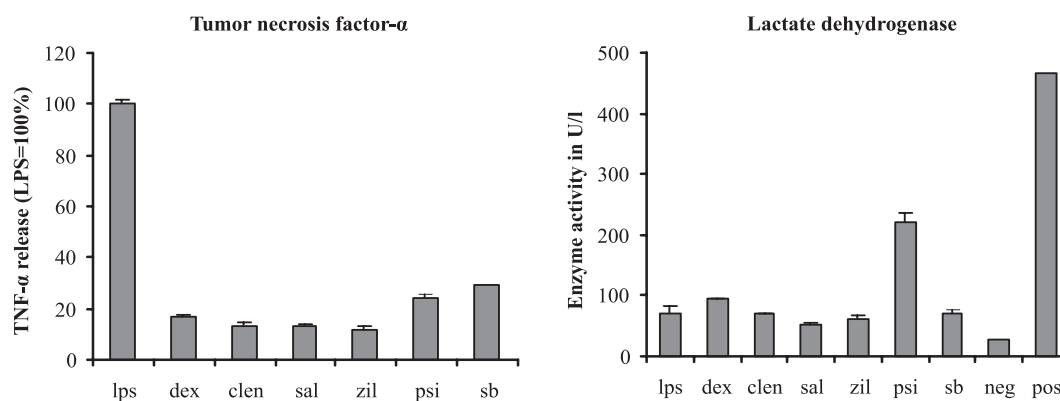


**Figure 1** Release of TNF- $\alpha$  (left panel) and LDH enzyme activity (right panel) from U937 macrophages incubated for 6 h with LPS with or without an anti-inflammatory inhibitor, dexamethasone (dex,  $1 \times 10^{-7}$  M), clenbuterol (clen,  $1 \times 10^{-7}$  M), salbutamol (sal,  $1 \times 10^{-6}$  M), zilpaterol (zil,  $1 \times 10^{-6}$  M), proteasome inhibitor (psi,  $1 \times 10^{-5}$  M) and SB203580 (sb,  $1 \times 10^{-6}$  M). The release of TNF- $\alpha$  is given with respect to the TNF- $\alpha$  release of LPS stimulated cells. The enzyme activity of LDH in the culture media reflects the extent of cell death. As control incubations either culture media not incubated with cells (negative control, neg) or culture media from U937 cells lysed by repeated freeze-thawing (positive control, pos) were used. The results are presented as means  $\pm$  SD of duplicate measurements.

The four classes of inhibitors were separated from each other. The two known  $\beta_2$ -agonists clenbuterol and salbutamol gave rise to overlapping clusters, which illustrates that the separation of the datasets reflects the biological responses elicited by the various inhibitors. Zilpaterol showed a similar pattern as clenbuterol and salbutamol. This was illustrated by the clustering of the array data from zilpaterol near to the array data from clenbuterol and salbutamol (Fig. 2). The data points of the PSI array data were positioned at a relatively great distance from the other data points, which may reflect the fact that the U937 transcriptome in response to PSI is very different from the transcriptome obtained after incubation with the other inflammatory inhibitors.

To further explore the specificity of the response to  $\beta_2$ -agonists compared to the other inhibitors, the microarray data was examined using PC-DA by defining two new groups (Fig. 3). Group one contained the microarray data from the two  $\beta_2$ -agonists, clenbuterol, and salbutamol and the poorly characterized  $\beta_2$ -agonist, zilpaterol. The second group consisted of the microarray data of dexamethasone, SB203580, and PSI. The results show that the data was separated in only one dimension in a score plot of two groups (Fig. 3A). From the loading plot, the individual genes responsible for the separation of the complete datasets could be derived (Fig. 3B).

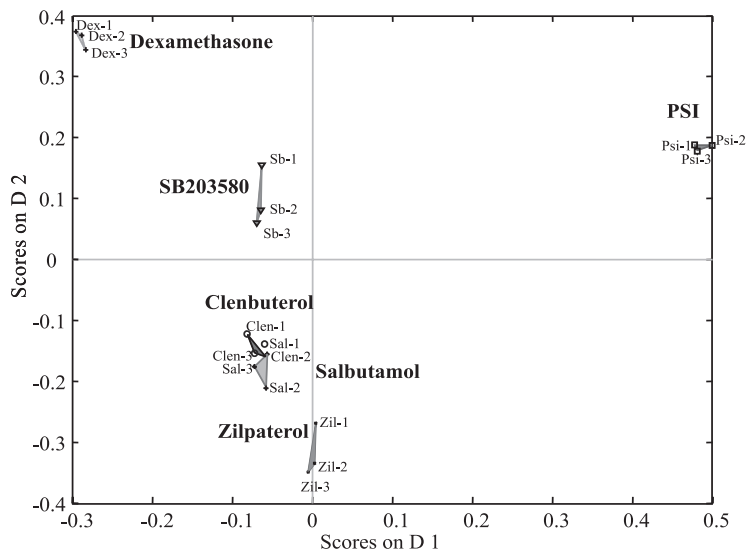


**Figure 2** Graphical presentation of the microarray data analyzed by PC-DA. The arrays of zilpaterol (zil  $\times$ ), clenbuterol (clen  $\circ$ ), salbutamol (sal\*) SB203580 (sb  $\Delta$ ), dexamethasone (dex +), and proteasome inhibitor (PSI  $\square$ ) are represented as dots, asterisks or crosses and array ID code. For every inhibitor three symbols are shown, each representing a separate micro-array. The anti-inflammatory inhibitors show different mRNA expression patterns. The arrays form the three  $\beta_2$ -agonists are clustered in the lower left corner in the score plot. This indicates that the mRNA expression patterns are comparable.

Negative loadings indicated the genes that are important in the clustering of the array data of the  $\beta_2$ -agonists, and are putative markers for this class of inhibitors. Figure 4 represents the differential expression of the first nine genes that showed the highest negative loadings in the loading plot. The three  $\beta_2$ -agonists were found to regulate seven out of nine genes (CXCR5, CXCL6, VEGF, oncostatin M, Mitogen induced nuclear orphan receptor, and small breast epithelial mucin) in a similar manner. The effects of the other inflammatory inhibitors on the

expression of these genes, was either opposite to the effect of the  $\beta_2$ -agonists or showed no regulation at all. These seven genes could therefore be specific markers for the  $\beta_2$ -agonists compared to PSI, dexamethasone and SB203580.

The differential expression of the two marker genes that were found to be regulated in a similar way by zilpaterol, clenbuterol, and salbutamol according to the microarray data analyzed by PC-DA, was confirmed by real time PCR experiments (Fig. 5). For this experiment, cells were incubated with the same inflammatory inhibitors as used in the microarray experiment. In addition, a fourth well-characterized  $\beta_2$ -agonist, formoterol<sup>25</sup>, was tested to further confirm the specificity of the markers found. The results clearly showed that CXCL6 and CXCR5 are specifically induced in cells exposed to LPS and a  $\beta_2$ -agonist (clenbuterol, salbutamol, zilpaterol, and formoterol), compared to cells treated with LPS alone. Cells incubated with LPS and dexamethasone, PSI or SB203580 showed a down-regulation compared to cells treated with LPS alone. This confirms the observations made in the microarray experiments.

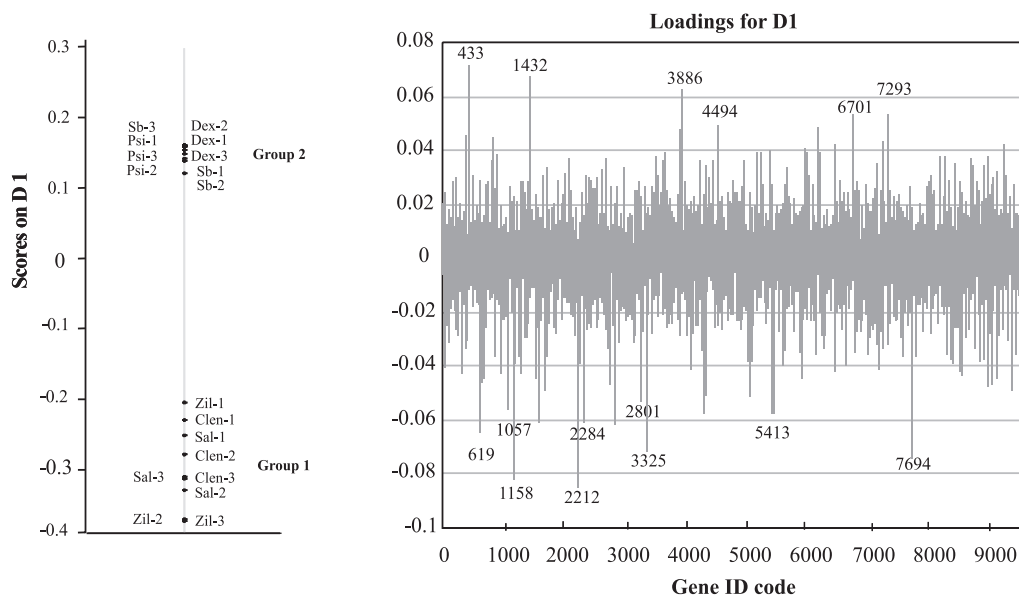


**Figure 3** PC-DA of the microarray data whereby the arrays from the three  $\beta_2$ -agonists are combined in group 1. Group 2 contains the array data from dexamethasone, SB203580 and PSI. Left panel: The score plot gives an indication about clustering and trends present in the mRNA profiles. The individual arrays are represented as asterisks. The result shows that the arrays from group 1 cluster between -0.2 and -0.4 on the D1 axis, and the arrays from group 2 cluster between 0.1 and 0.2, indicating that the two groups can be separated on the basis of their mRNA expression profiles. Right panel: The loadings for D1 from the score plot (left panel). The loading plot indicates which genes are responsible for the difference between the two defined groups. Genes with high positive and high negative loadings represent the genes that are differentially regulated between the two groups. The negative loadings represent genes that are involved in group 1. Genes coded 1158 and 2212 have high loadings and are therefore important determinants for the separation of the two groups by PC-DA.

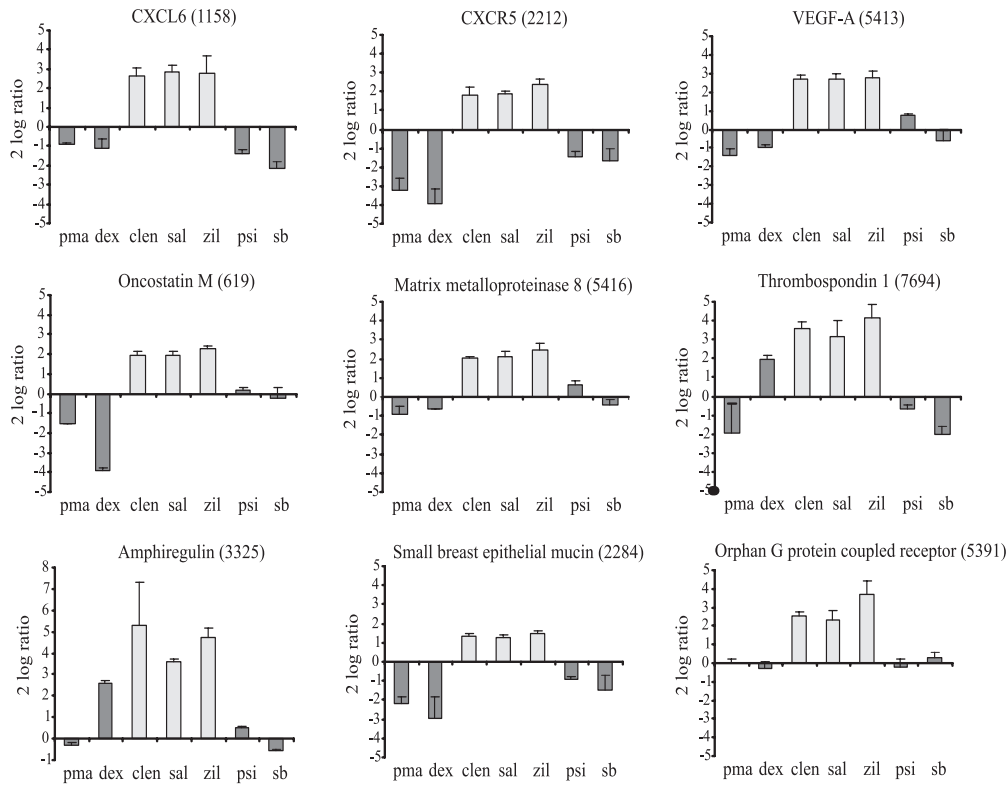


**Figure 4** Differential mRNA expression of the 9 genes that showed the highest negative loadings according to PC-DA. The induction factor is presented as a 2 log ratio value. The 9 genes were found to be regulated in a similar manner by zilpateterol (zil), salbutamol (sal) and clenbuterol (clen) according to PC-DA analysis (light grey bars). The expression levels are compared to proteasome inhibitor (PSI), dexamethasone (dex), and SB203580 (sb) (dark grey bars). The numbers between brackets indicate the gene ID code used in PC-DA.

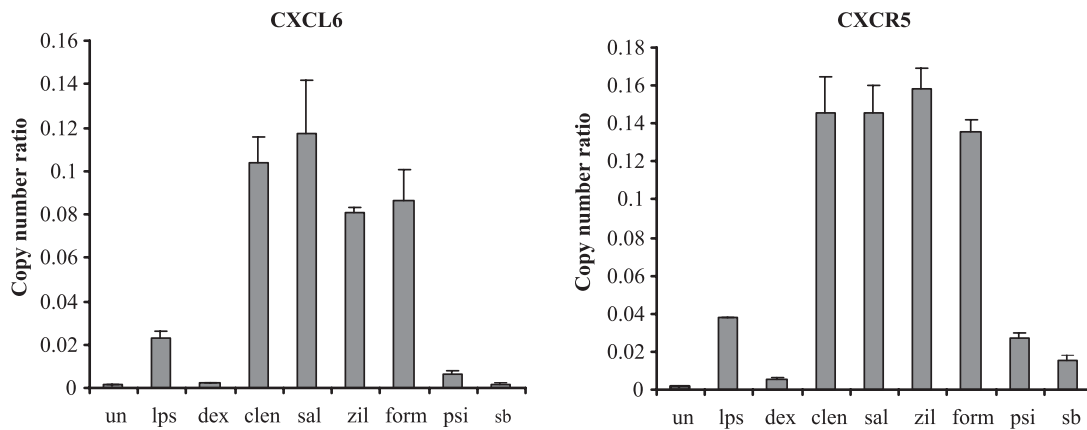


**Figure 5** mRNA expression levels of CXCL6 and CXCR5 determined in untreated U937 macrophages (un) and after a 6 hours incubation with LPS with or without an anti-inflammatory inhibitor, dexamethasone (dex), clenbuterol (clen), salbutamol (sal), zilpateterol (zil), formoterol (form), proteasome inhibitor (PSI), and SB203580 (sb). The expression levels of CXCL6 and CXCR5 mRNA were determined by real time real time PCR. The copy number given was corrected for the expression levels of the reference mRNA  $\beta$ -actin and is the mean + SD of two experiments.

To test whether the identified  $\beta_2$ -agonists marker genes are also specifically regulated at the protein level, a limited number of identified marker genes were selected to determine their regulation at the protein level. These included three secreted proteins, Oncostatin M, VEGF, and CXCL6, which expression in U937 cells was analysed by using specific immunoassays. U937 macrophages were stimulated in duplicate according to a time series (6, 8, 16, and 24 h) without LPS or with LPS in the presence or absence of an inflammatory inhibitor. The results show that Oncostatin M, VEGF, and CXCL-6 were all up-regulated in cells treated with the combination of LPS and a  $\beta_2$ -agonist compared to cells treated with LPS alone (Fig. 6). The highest level of expression of all three proteins was detected after 16 to 24 h incubation.

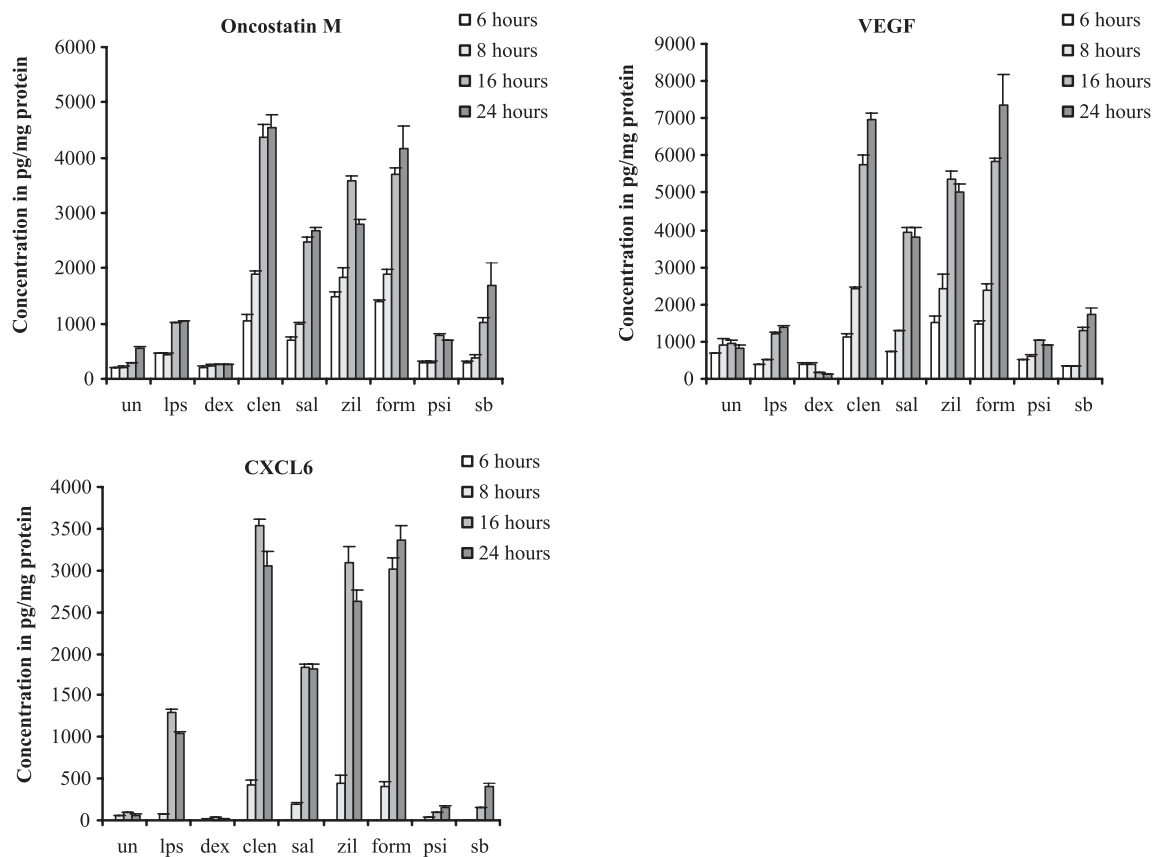


**Figure 6** Protein expression levels of oncostatin M, VEGF, and CXCL6 determined using specific immunoassays. The levels of these proteins released by the macrophages in the culture medium were determined at the time points indicated. The following incubations were performed: untreated macrophages (un), macrophages treated with LPS alone (LPS) and LPS with an anti-inflammatory inhibitor, dexamethasone (dex), clenbuterol (clen), salbutamol (sal), zilpaterol (zil), formoterol (form), proteasome inhibitor (PSI), and SB203580 (sb). The expression levels given are the average + SD of duplicate incubations.

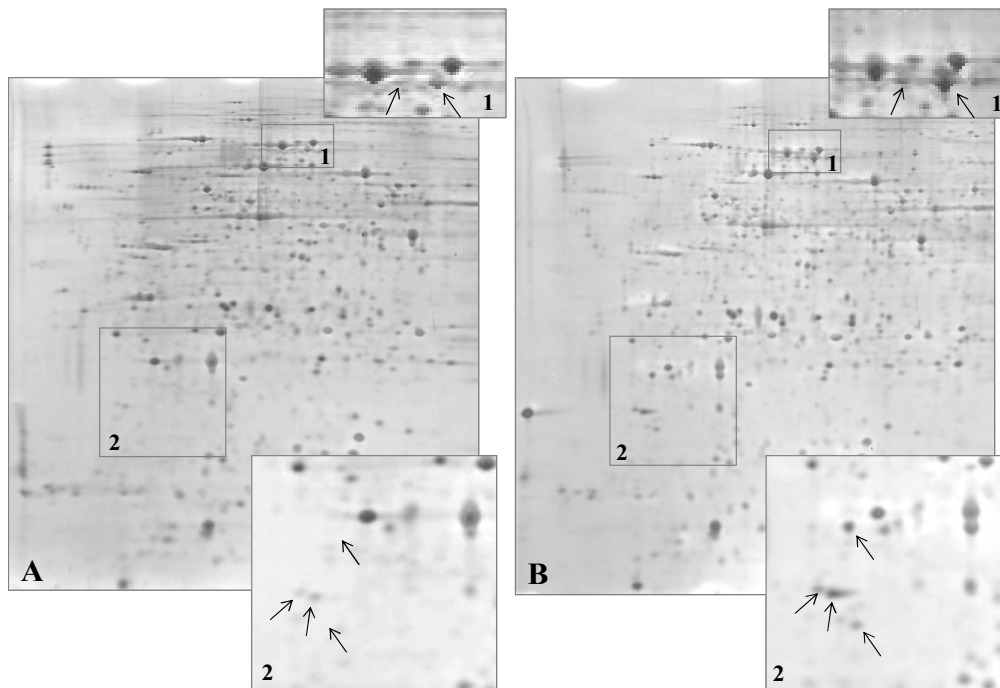


**Figure 7** Representative 2-D gel image for U937 macrophages stimulated with LPS (Panel A) and stimulated with LPS and PSI (Panel B). Protein extracts of 400  $\mu\text{g}$  were separated on a 12 % polyacrylamide gel, pH 4-7 and stained with RuBps stain. The arrows indicate the marker protein spots for PSI, according to PC-DA. The protein spots in panel 1 were identified by mass spectrometry as Heat shock protein 70 and in panel 2 as fragments of vimentin.

### *Proteomics*

The proteomes of macrophages incubated with LPS or with LPS combined with one of the 6 anti-inflammatory inhibitors were compared using 2-D gel electrophoresis. In total 999 different spots were detected in the various gels. Figure 7 shows two representative 2-D gel images of U937 macrophages stimulated with LPS and LPS in combination with PSI. PC-DA was performed to find differences in the protein patterns.

The PC-DA of the proteomics data (Fig. 8) revealed distinct positioning of clenbuterol from salbutamol and zilpaterol. Similar to what was seen with the transcriptomics data, the gels from PSI were placed at a greater mutual distance in the score plot compared to the gels from the other inhibitors. The effect of PSI on the protein dataset was stronger than seen with the microarray dataset. In the score plot of discriminant 1 against discriminant 2 (data not shown), there was no separation between dexamethasone, SB203580 and the three  $\beta_2$ -agonists, meaning that PSI has a great impact on the model. Plotting discriminant 1 against discriminant 3 (Fig. 8) showed a better separation between the 6 inhibitors. Further analysis by defining new groups in the PC-DA, revealed only specific markers for PSI, e.g. vimentin and heat shock protein 70. These markers were confirmed by univariate analysis of the gel

spots in the 2-D gels (Fig. 7) and identified by in-gel digestion followed by MALDI mass mapping and/or MALDI MS/MS sequencing in combination with database search. From the results of these experiments we concluded that with the exception of PSI, no specific marker proteins could be detected.

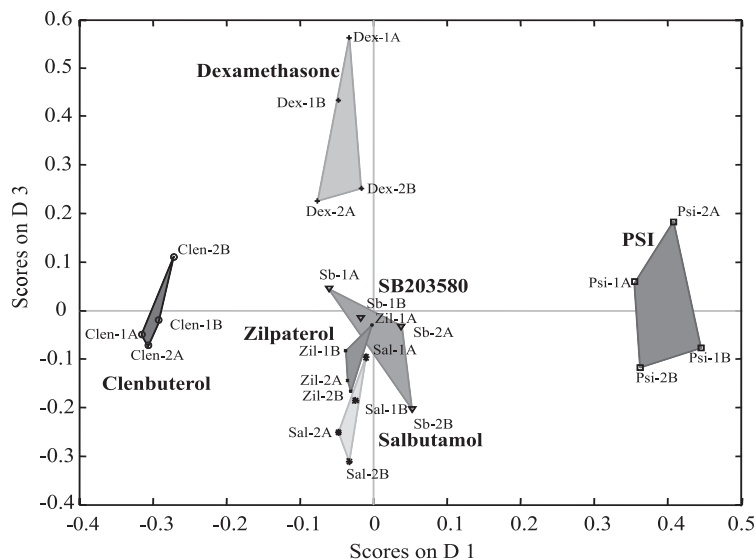


**Figure 8** Score plot of the 24 2-D gels analyzed with PC-DA. The graphic represents the gels of zilpaterol (zil ×), clenbuterol (clen ○), salbutamol (sal\*) SB203580 (sb Δ), dexamethasone (dex +), and proteasome inhibitor (PSI □) as dots, asterisks or crosses. For every inhibitor four symbols can be found, each representing the results of a single gel. In all cases, the four gels of the anti-inflammatory inhibitors are clustered, showing that the gel-to-gel variation is acceptable. The PC-DA revealed distinct positioning of the two  $\beta_2$ -agonists, clen and sal.

### Metabolomics

The lipid profiles of U937 cells after incubation with LPS in the absence or presence of an inflammatory inhibitor were analyzed by LC-MS. Figure 9 shows a representative chromatogram of the lipid extract of macrophages incubated with LPS and zilpaterol.

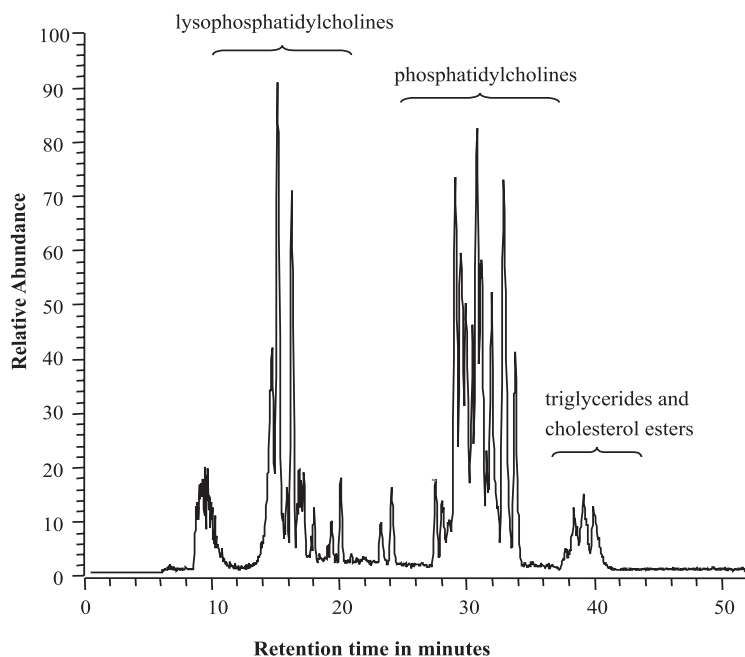


**Figure 9** Base peak chromatogram (m/z 400-1900) of the lipid extract obtained from macrophages incubated with LPS and zilpaterol. The elution order of the lipid compounds was as follows: lysophosphatidylcholines, phosphatidylcholines, triglycerides and cholesterol esters.

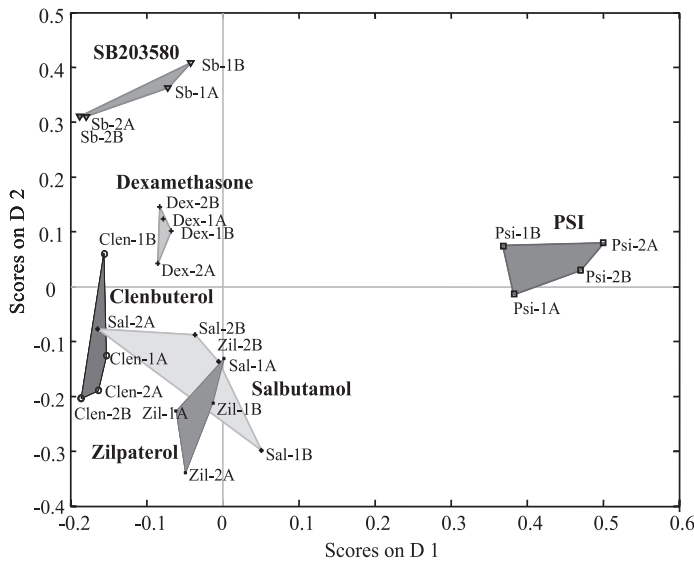


**Figure 10** Score plot of the lipid patterns of zilpateterol (zil ×), clenbuterol (clen ○), salbutamol (sal\*) SB203580 (sb Δ), dexamethasone (dex +), and proteasome inhibitor (PSI □). The lipid expression patterns of zil, sal and clen are clustered together in the lower left corner; this indicates a similarity in lipid expression pattern of the three  $\beta_2$ -agonists.

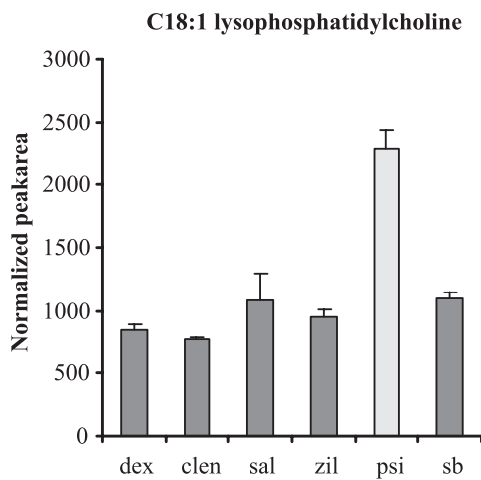
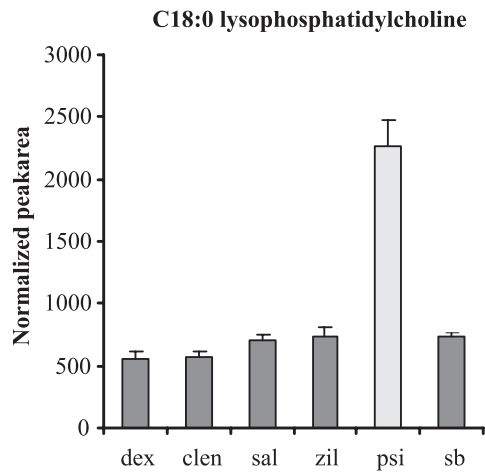
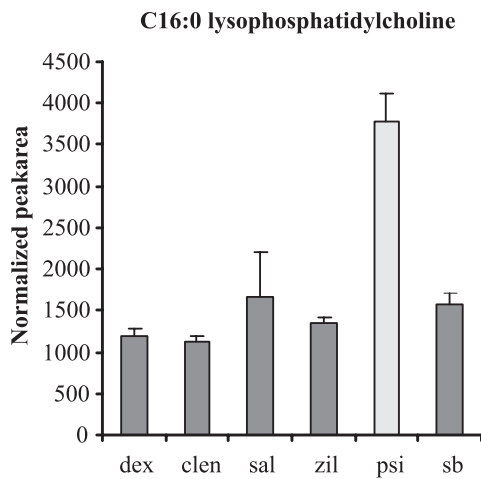


**Figure 11** Expression levels of three lysophosphatidylcholines (LPC) (C16:0, C18:0 and C18:1). The three LPC's are up-regulated according to student's *t*-test ( $p < 0.05$ ) for macrophages treated with LPS and PSI (light grey bars) with respect to macrophages treated with LPS in combination with dexamethasone (dex),  $\beta_2$ -agonist (clen, zil and sal) or SB203580 (sb). The expression levels given are the average + SD of four measurements.

Comparison of the lipid expression patterns of the 6 anti-inflammatory compounds using PC-DA (Fig. 10) resulted in a separation of the inflammatory inhibitors SB203580, PSI, dexamethasone and  $\beta_2$ -agonists. The lipid expression patterns of zilpaterol, clenbuterol and salbutamol were similar, which is demonstrated by their clustering in the lower left corner of the coordinate system. Similar to the transcriptomics and the proteomics data, PSI showed a completely different expression pattern. However, definition of two new groups in the PC-DA in order to detect markers for the different inhibitors did not reveal individual marker lipids. For the  $\beta_2$ -agonists we found a group of lipids that were regulated in a similar way. This group was identified as triglycerides. The induction of the triglycerides was not statistically different from the other anti-inflammatory compounds according to the univariate Student's *t*-test (assuming normal distributions and equal variance). Nevertheless, by using multivariate analysis we were able to separate the  $\beta_2$ -agonists from the other inhibitors. Only PSI gave rise to an induction of several individual lipids compared to the other inhibitors (Fig. 11). By applying LC-MS/MS, the lipids shown in Figure 11 were identified as various forms of lysophosphatidylcholine (LPC).

Figure 12 shows the PC-DA of the combination of the transcriptomics, proteomics and metabolomics dataset. As expected, the score plot again revealed a clustering of the three  $\beta_2$ -agonists in the upper left corner, indicating that there is a clear resemblance in mRNA, protein, and lipid patterns for the three compounds. The combination of the three datasets showed the best separation of the different anti-inflammatory inhibitors after PC-DA with respect to the separate techniques. However, evaluation of the data for individual marker molecules did not reveal important marker molecules in addition to those found on the basis of transcriptomics, proteomics or metabolomics datasets alone.

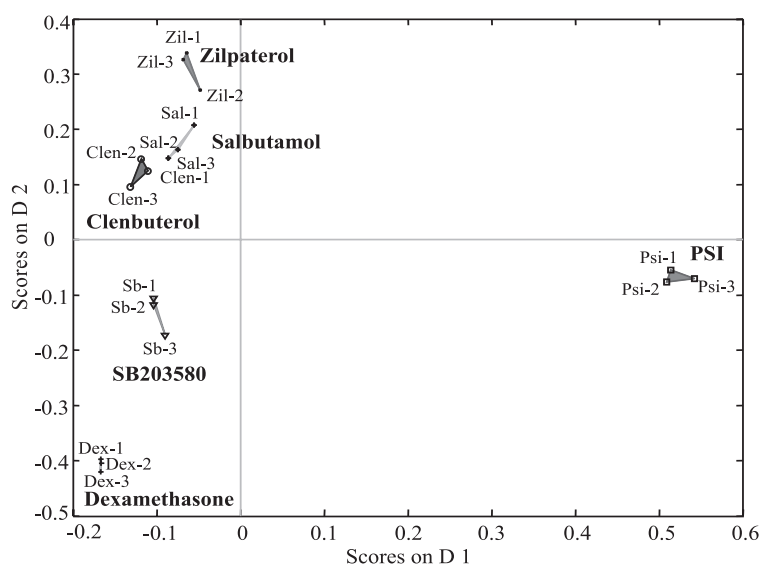


**Figure 12** PC-DA score plot of the combination of the mRNA, protein and lipid datasets. Data points are represented as dots, asterisks and crosses; zilpaterol (zil ×), clenbuterol (clen ○), salbutamol (sal\*) SB203580 (sb Δ), dexamethasone (dex +), and proteasome inhibitor (PSI □). The combination of expression patterns shows a clustering of clen, sal and zil in the upper left corner; this indicates a similarity of the three  $\beta_2$ -agonists.

**Discussion**

The data of the microarray analysis of U937 cells incubated with the various anti-inflammatory compounds, which was analysed by PC-DA, showed that the different classes of inhibitors could be separated from each other. In spite of the marked structural differences, zilpaterol appears to evoke a response in U937 cells very similar to salbutamol and clenbuterol. This, combined with the fact that zilpaterol is reported to be a  $\beta_2$ -agonist<sup>17, 18</sup>, suggest that this effect is  $\beta_2$ -receptor associated. Further studies, for example including specific antagonists, should elucidate this. By defining two new groups in the PC-DA, group 1; clenbuterol, salbutamol and zilpaterol and group 2; dexamethasone, PSI, and SB203580, we were able to find specific markers for the  $\beta_2$ -agonists with respect to PSI, dexamethasone and SB203580, (e.g. CXCL6, CXCR5, VEGF, and oncostatin M). These markers were confirmed by real time PCR and ELISA experiments to be specific for  $\beta_2$ -agonists. Since PC-DA is a mathematical tool, finding a false positive marker can't be ruled out beforehand, especially when the number of data points is at the lower limit. For example amphiregulin and thrombospondin (Fig. 4) showed the same regulation for clenbuterol, salbutamol and zilpaterol, but was also up-regulated by dexamethasone, although to a lesser extent than achieved by the  $\beta_2$ -agonists (induction factor is 2-8 times lower). For this reason the markers found by PC-DA were verified by univariate analysis of the original dataset. Specific markers for the other inhibitors, dexamethasone, PSI and SB203580 were also found by using the same approach (data not shown). It can be envisioned that these markers could be useful in screenings methods, where these markers are used for the screening of newly synthesized anti-inflammatory compounds.

Remarkably, the proteome of the cell lysates obtained from U937 macrophages incubated with LPS and an anti-inflammatory compound revealed no similarities between clenbuterol and salbutamol, although both are known to be  $\beta_2$ -agonists and also evoked a very similar transcriptome in U937 cells. We speculate that the differences in the proteomes are not related to  $\beta_2$ -receptor effects. In the score plot of discriminant 1 versus discriminant 2 the proteome data from PSI was the most dominant factor. PSI was separated from the other inhibitors that were all clustered together (data not shown). Even in the score plot of discriminant 3 versus 1 (Fig. 8) the effect of PSI is still quite dominant, although there is a better separation of the other inhibitors as well. Interestingly, the PSI-marker proteins we identified by mass spectrometry included heat shock protein 70 and different fragments of vimentin. Vimentin is known to be cleaved in different fragments during apoptosis<sup>26, 27</sup>, while heat shock protein 70 is up-regulated in apoptotic cells to perform their protective function against cell death<sup>28-30</sup>.

These two markers indicate that apoptosis is a major determinant for the separation by PC-DA of the proteome data. This is compatible with the notion that PSI is able to induce apoptosis in various cell types<sup>10, 11</sup>. Apart from PSI, the 2-D PAGE technique appeared to be not very suitable for categorization of the anti-inflammatory compounds based on their anti-inflammatory mechanism of action. When this technique is applied to whole cell lysates, only abundant proteins can be detected, e.g. cytoskeleton proteins like actin. Many of these ubiquitously expressed proteins are modified during apoptosis. Unfortunately, the proteins involved in other more specific pathways (e.g. the pathways involved in the inflammatory response) are more difficult to detect, because of their low abundance<sup>31</sup>. Possibly, pre-fractionation of the protein sample may overcome this. The markers found with the microarray experiment were mostly mRNAs encoding secreted or membrane-bound proteins. Membrane bound proteins are difficult to dissolve in the standard buffers used for 2-D gel electrophoresis<sup>31, 32</sup>. The secreted proteins are present at the pg/ml level in the culture media. Therefore, the culture medium has to be concentrated at least a thousand times before secreted proteins are detectable on a 2-D gel. It has already been shown that this concentrating step will cause problems in the first dimension of 2-D gel electrophoresis (e.g. high salt concentration)<sup>33</sup>. Moreover, pre-fractionation will make 2-D gel electrophoresis not suitable for relatively fast screening of inflammatory inhibitors. Whether alternative proteomics techniques (e.g. 2-D LC-MS), are more suitable than 2-D gel electrophoresis for this type of screening approach remains to be established.

The LC-MS method for lipids was found to be the fastest method for categorizing anti-inflammatory compounds. The PC-DA of the lipid expression patterns of the 6 anti-inflammatory compounds gave a similar result as the PC-DA of the mRNA expression patterns. The lipid expression patterns of zilpaterol, clenbuterol and salbutamol are similar according to multivariate analysis and are therefore clustered in the score plot. Surprisingly further analysis of the lipid data by PC-DA by defining two new groups (group1; clenbuterol, zilpaterol, and salbutamol, group 2; dexamethasone, PSI, and SB203580) revealed no specific markers for the  $\beta_2$ -agonists. There is no significant up- or down-regulation of individual lipids with respect to the other inhibitors according to univariate analysis. This means that the combination of several lipids together is responsible for the differences in the lipid expression patterns found by PC-DA. This underlines the power of multivariate analysis, namely the capacity to find hidden correlation and trends. By contrast, the PC-DA of PSI versus the other inhibitors did reveal a few individual marker lipids. These markers were identified as lysophosphatidylcholines (LPC). These lipids are known to be involved in apoptosis<sup>34-36</sup>.

LPC is generated upon phospholipase A<sub>2</sub> (PLA<sub>2</sub>) mediated hydrolysis of membranous phosphatidylcholine into LPC and arachidonic acid. PLA<sub>2</sub> is activated by means of caspase-3 cleavage during apoptosis. The secreted forms of LPC are involved in attraction of phagocytes to the apoptotic cells (secreted form)<sup>35</sup>, in the recognition of apoptotic cells (membrane bound form)<sup>37</sup> and is even known to be able to induce apoptosis by itself<sup>34,36</sup>. The PC-DA of the combination of the three datasets showed the best separation. The three  $\beta_2$ -agonists, clenbuterol, salbutamol and zilpaterol are clustered as one group, whereas the other inhibitors are clearly separated from the  $\beta_2$ -agonists and from each other. The transcriptomics data is the dominant factor in this model. This is not only explained by the large amount of data points (9585 of the 13208 variables belong to the microarray dataset) but is also influenced by the number of variables that are specifically regulated by the different anti-inflammatory compounds. In other words, the number of mRNA's that is regulated by the anti-inflammatory compounds is much greater than the number of detectable proteins or lipids. This is compatible with the notion that there are more pathways that have the same end point. For example TNF- $\alpha$ , all tested anti-inflammatory compounds inhibited the TNF- $\alpha$  expression at the protein level, but the metabolic pathways leading to this effect are different. Nevertheless, we expect that the number of proteins that is regulated is larger than we have found in our experiment, but may have been missed due to the limited fraction of proteins that was analysed. Although the microarray data dominated the PC-DA model, the incorporation of the lipid and protein data clearly improved the clustering of the datasets. From a practical point of view, PC-DA of microarray data alone already gives satisfactory results.

In conclusion, our results demonstrate that different classes of anti-inflammatory compounds show distinct and characteristic mRNA, protein and lipid expression patterns in our model system. Furthermore, our model system shows that zilpaterol, a compound originally developed as a  $\beta_2$ -agonist but later specifically introduced as a growth promoting (anabolic) agent, gives rise to an almost identical mRNA and lipid expression pattern as the well-characterized  $\beta_2$ -agonists clenbuterol and salbutamol. This shows that the approach presented here is suitable to classify new or poorly characterized anti-inflammatory compounds that act on macrophages by using mRNA and lipid expression data both in combination with PC-DA. However it should be mentioned that the success of classification depends on the compounds that are used as reference compounds in the experiment and the effect on other cells of the immune system has to be tested additionally, but with the results of the categorization method, it is possible to apply a more targeted research.

More rapid screening is possible when the specific markers from the microarray experiments are used in simplified experiments. For example CXCL6, VEGF, and oncostatin M could be used as markers for  $\beta_2$ -agonists.

## References

- 1 Dong, C., Davis, R. J. and Flavell, R. A., *Annu Rev Immunol*, **2002**, Map kinases in the immune response, *20*, 55-72.
- 2 Baldwin, A. S., Jr., *Annu Rev Immunol*, **1996**, The nf-kappa b and i kappa b proteins: New discoveries and insights, *14*, 649-683.
- 3 Gupta, D., Wang, Q., Vinson, C. and Dziarski, R., *J Biol Chem*, **1999**, Bacterial peptidoglycan induces cd14-dependent activation of transcription factors creb/atf and ap-1, *274*, 14012-14020.
- 4 Almawi, W. Y. and Melemedjian, O. K., *J Mol Endocrinol*, **2002**, Negative regulation of nuclear factor-kappab activation and function by glucocorticoids, *28*, 69-78.
- 5 Joyce, D. A., Gimblett, G. and Steer, J. H., *Inflamm Res*, **2001**, Targets of glucocorticoid action on tnf-alpha release by macrophages, *50*, 337-340.
- 6 Verhoeckx, K. C., Bijlsma, S., de Groene, E. M., Witkamp, R. F., *et al.*, *Proteomics*, **2004**, A combination of proteomics, principal component analysis and transcriptomics is a powerful tool for the identification of biomarkers for macrophage maturation in the u937 cell line, *4*, 1014-1028.
- 7 Hoogerbrugge, R., Willig, S. J. and Kistemaker, P. G., *Analytical Chemistry*, **1983**, Discriminant analysis by double stage principal component analysis, *55*, 1710-1712.
- 8 Steer, J. H., Kroeger, K. M., Abraham, L. J. and Joyce, D. A., *J Biol Chem*, **2000**, Glucocorticoids suppress tumor necrosis factor-alpha expression by human monocytic thp-1 cells by suppressing transactivation through adjacent nf-kappa b and c-jun-activating transcription factor-2 binding sites in the promoter, *275*, 18432-18440.
- 9 Joyce, D. A., Steer, J. H. and Abraham, L. J., *Inflamm Res*, **1997**, Glucocorticoid modulation of human monocyte/macrophage function: Control of tnf-alpha secretion, *46*, 447-451.
- 10 Adams, J., *Curr Opin Oncol*, **2002**, Proteasome inhibitors as new anticancer drugs, *14*, 628-634.
- 11 Wojcik, C., *Cell Mol Life Sci*, **1999**, Proteasomes in apoptosis: Villains or guardians? *56*, 908-917.
- 12 Griscavage, J. M., Wilk, S. and Ignarro, L. J., *Proc Natl Acad Sci U S A*, **1996**, Inhibitors of the proteasome pathway interfere with induction of nitric oxide synthase in macrophages by blocking activation of transcription factor nf-kappa b, *93*, 3308-3312.
- 13 Lee, J. C., Kassisi, S., Kumar, S., Badger, A. and Adams, J. L., *Pharmacol Ther*, **1999**, P38 mitogen-activated protein kinase inhibitors--mechanisms and therapeutic potentials, *82*, 389-397.
- 14 Izeboud, C. A., Monshouwer, M., van Miert, A. S. and Witkamp, R. F., *Inflamm Res*, **1999**, The beta-adrenoceptor agonist clenbuterol is a potent inhibitor of the lps-induced production of tnf-alpha and il-6 in vitro and in vivo, *48*, 497-502.
- 15 Izeboud, C. A., Mocking, J. A., Monshouwer, M., van Miert, A. S. and Witkamp, R. F., *J Recept Signal Transduct Res*, **1999**, Participation of beta-adrenergic receptors on macrophages in modulation of lps-induced cytokine release, *19*, 191-202.
- 16 Libretto, S. E., *Arch Toxicol*, **1994**, A review of the toxicology of salbutamol (albuterol), *68*, 213-216.
- 17 Plascencia, A., Torrentera, N. and Zinn, R. A., *Proceedings, Western Section, American Society of animal science*, **1999**, Influence of the beta-agonist, zilpaterol, on growth performance and carcass characteristics of feedlot steers, *50*, 331-334.
- 18 Intervet, **1998**, Zilmax technical brochure.
- 19 Sundstrom, C. and Nilsson, K., *Int J Cancer*, **1976**, Establishment and characterization of a human histiocytic lymphoma cell line (u-937), *17*, 565-577.
- 20 Izeboud, C. A., Vermeulen, R. M., Zwart, A., Voss, H. P., *et al.*, *Naunyn Schmiedebergs Arch Pharmacol*, **2000**, Stereoselectivity at the beta2-adrenoceptor on macrophages is a major determinant of the anti-inflammatory effects of beta2-agonists, *362*, 184-189.
- 21 Rabilloud, T., Strub, J. M., Luche, S., van Dorsselaer, A. and Lunardi, J., *Proteomics*, **2001**, A comparison between sypro ruby and ruthenium ii tris (bathophenanthroline disulfonate) as fluorescent stains for protein detection in gels, *1*, 699-704.
- 22 Rabilloud, T., Strub, J. M., Luche, S., Girardet, J. L., *et al.*, Springer-Verlag Heidelberg | Tiergartenstr. 17 | D-69121 Heidelberg | Germany **2000**, 1-6.
- 23 Vandeginste, B. G. M., Massart, D. L., Buydens, L. M. C. and De Jong, P. J., *Handbook of chemometrics and qualimetrics: Part b*, Elsevier, Amsterdam, The Netherlands **1998**.

- 
- 24 Massart, D. L., Vandeginste, B. G. M. and De Jong, P. J., *Handbook of chemometrics and qualimetrics: Part a*, Elsevier, Amsterdam, The Netherlands **1997**.
- 25 Lotvall, J., *Pulm Pharmacol Ther*, **2002**, The long and short of beta2-agonists, *15*, 497-501.
- 26 Byun, Y., Chen, F., Chang, R., Trivedi, M., *et al.*, *Cell Death Differ*, **2001**, Caspase cleavage of vimentin disrupts intermediate filaments and promotes apoptosis, *8*, 443-450.
- 27 Muller, K., Dulku, S., Hardwick, S. J., Skepper, J. N. and Mitchinson, M. J., *Atherosclerosis*, **2001**, Changes in vimentin in human macrophages during apoptosis induced by oxidised low density lipoprotein, *156*, 133-144.
- 28 Beere, H. M. and Green, D. R., *Trends Cell Biol*, **2001**, Stress management - heat shock protein-70 and the regulation of apoptosis, *11*, 6-10.
- 29 Jaattela, M., Wissing, D., Kokholm, K., Kallunki, T. and Egeblad, M., *Embo J*, **1998**, Hsp70 exerts its anti-apoptotic function downstream of caspase-3-like proteases, *17*, 6124-6134.
- 30 Garrido, C., Gurbuxani, S., Ravagnan, L. and Kroemer, G., *Biochem Biophys Res Commun*, **2001**, Heat shock proteins: Endogenous modulators of apoptotic cell death, *286*, 433-442.
- 31 Rabilloud, T., *Proteomics*, **2002**, Two-dimensional gel electrophoresis in proteomics: Old, old fashioned, but it still climbs up the mountains, *2*, 3-10.
- 32 Molloy, M. P., *Anal Biochem*, **2000**, Two-dimensional electrophoresis of membrane proteins using immobilized ph gradients, *280*, 1-10.
- 33 Rabilloud, T. (Ed.), *Proteome research: Two dimensional gel electrophoresis and identification methods*, Springer Verlag, Berlin Heidelberg New York **2000**, p. 244.
- 34 Jostarndt, K., Gellert, N., Rubic, T., Weber, C., *et al.*, *Biochem Biophys Res Commun*, **2002**, Dissociation of apoptosis induction and cd36 upregulation by enzymatically modified low-density lipoprotein in monocytic cells, *290*, 988-993.
- 35 Lauber, K., Bohn, E., Krober, S. M., Xiao, Y. J., *et al.*, *Cell*, **2003**, Apoptotic cells induce migration of phagocytes via caspase-3-mediated release of a lipid attraction signal, *113*, 717-730.
- 36 Masamune, A., Sakai, Y., Satoh, A., Fujita, M., *et al.*, *Pancreas*, **2001**, Lysophosphatidylcholine induces apoptosis in ar42j cells, *22*, 75-83.
- 37 Kim, S. J., Gershov, D., Ma, X., Brot, N. and Elkon, K. B., *J Exp Med*, **2002**, I-pla(2) activation during apoptosis promotes the exposure of membrane lysophosphatidylcholine leading to binding by natural immunoglobulin m antibodies and complement activation, *196*, 655-665.



## Chapter 4

---

**In search of secreted protein biomarkers for the anti-inflammatory effect of  $\beta_2$ -adrenergic receptor agonists: application of DIGE technology in combination with multivariate and univariate data analysis tools.**

Kitty C.M. Verhoeckx<sup>1,2</sup>

Marco Gaspari<sup>1,2</sup>

Sabina Bijlsma<sup>1</sup>

Robert P. Doornbos<sup>1</sup>

Jan van der Greef<sup>1,2</sup>

Renger F. Witkamp<sup>1</sup>

Richard J.T. Rodenburg<sup>3</sup>

*Accepted for publication in J Proteome Res*

<sup>1</sup> TNO Quality of Life, Zeist, The Netherlands, <sup>2</sup> Leiden University, Leiden/Amsterdam Center for Drug Research, Leiden, The Netherlands, <sup>3</sup> UMC St Radboud, Nijmegen, The Netherlands

**In search of secreted protein biomarkers for the anti-inflammatory effect of  $\beta_2$ -adrenergic receptor agonists: application of DIGE technology in combination with multivariate and univariate data analysis tools.**

*Two-dimensional difference gel electrophoresis (DIGE) in combination with univariate (Student's t-test) and multivariate data analysis, principal component analysis (PCA) and partial least squares discriminant analysis (PLS-DA) were used to study the anti-inflammatory effects of the  $\beta_2$ -adrenergic receptor ( $\beta_2$ -AR) agonist zilpaterol. U937 macrophages were exposed to the endotoxin lipopolysaccharide (LPS) to induce an inflammatory reaction, which was inhibited by the addition of zilpaterol (LZ). This inhibition was counteracted by addition of the  $\beta_2$ -AR antagonist propranolol (LZP). The extracellular proteome of the U937 cells induced by the three treatments were examined by DIGE. PCA was used as an explorative tool to investigate the clustering of the proteome dataset. Using this tool, the dataset obtained from cells treated with LPS and LZP were separated from those obtained from LZ treated cells. PLS-DA, a multivariate data analysis tool that also takes correlations between protein spots and class assignment into account, correctly classified the different extracellular proteomes and showed that many proteins were differentially expressed between the proteome of inflamed cells (LPS and LZP) and cells in which the inflammatory response was inhibited (LZ). The Student's t-test revealed 8 potential protein biomarkers, each of which was expressed at a similar level in the LPS and LZP treated cells, but differently expressed in the LZ treated cells. Two of the identified proteins, macrophage inflammatory protein-1beta (MIP-1 $\beta$ ) and macrophage inflammatory protein-1alpha (MIP-1 $\alpha$ ) are known secreted proteins. The inhibition of MIP-1 $\beta$  by zilpaterol and the involvement of the  $\beta_2$ -AR and cAMP were confirmed using a specific immunoassay.*

---

**Introduction**

Inflammation occurs as a defensive response to invasion of the host by foreign intruders, often of microbial nature. This response normally involves a complex series of events including macrophage activation, secretion of inflammatory mediators e.g. cytokines and chemotactic cytokines (chemokines) and recruitment of leukocytes into the inflamed area<sup>1,2</sup>. Cytokines (e.g. TNF- $\alpha$ , IL-1 $\beta$ , and IFN- $\gamma$ ) and chemokines (e.g. IL-8 and RANTES) are small secreted proteins that are involved in regulation of the network of interactions between cells during inflammation. They are involved in the onset and development of inflammation, recruit, and

activate a range of immune cells<sup>3</sup>. Regulation of the expression of these secreted inflammatory mediators is of therapeutic importance in many inflammatory diseases like asthma, rheumatoid arthritis and many others.

Beta<sub>2</sub>-adrenergic receptor ( $\beta_2$ -AR) agonists are widely used in the treatment of pulmonary diseases, e.g. asthma. Their effect on the airways primarily involves relaxation of airway smooth muscle<sup>4-6</sup>. Binding of  $\beta_2$ -AR agonists to the  $\beta_2$ -AR activates adenylate cyclase, which subsequently elevates the intracellular level of cyclic adenosine-3',5'-cyclic monophosphate (cAMP)<sup>7-12</sup>. Cyclic AMP is a second messenger that exerts its effects via many different metabolic pathways and regulates the production of various inflammatory mediators<sup>13,14</sup>.

In the present study we examined proteins that are secreted by macrophages in response to LPS in combination with a  $\beta_2$ -AR agonist and that are regulated via the  $\beta_2$ -AR. These proteins are potential biomarkers in monitoring the effect of  $\beta_2$ -AR agonists in the treatment of inflammatory diseases and may further elucidate the mechanism of action of these compounds. For this purpose we used the human monocytic U937 cell line that expresses the  $\beta_2$ -AR<sup>15</sup> and that has previously proved to be a suitable model system to study the effect of  $\beta_2$ -AR agonists on the inflammation response induced by the endotoxin lipopolysaccharide (LPS)<sup>15-18</sup>. The extracellular proteome of U937 macrophages exposed to LPS, LPS in combination with zilpaterol ( $\beta_2$ -AR agonist)<sup>18,19</sup>, and LPS in combination with zilpaterol and propranolol ( $\beta_2$ -AR antagonist) were compared using 2-D difference gel electrophoresis (DIGE). The DIGE technology enables the analysis of multiple protein samples within one gel. This is achieved through covalent modification of each protein with structurally similar but spectrally distinct fluorophores (CyDye2, CyDye3, and CyDye5). On each gel two samples and an internal standard comprising an equal amount of each sample within the study can be examined. This process reduces the gel-to-gel variation and allows more accurate and sensitive quantitative proteomics studies<sup>20-22</sup>. The proteomics data was analyzed using a classical univariate data analysis tool (Student's *t*-test) and two multivariate data analysis tools (principal component analysis (PCA) and partial least squares discriminant analysis (PLS-DA)). PCA<sup>23-27</sup> was used as an explorative tool to visualize differences between the complex datasets. PLS-DA<sup>28</sup> on two groups (inflammation and inhibition of inflammation), was used to discover potential biomarkers for anti-inflammatory effects of  $\beta_2$ -AR agonists. In the literature, little attention has been paid to the validation of potential biomarkers found by multivariate data analysis, especially the biological validation. In this study the PLS-DA was

validated by cross validation, and the permutation test. Finally a biological validation was performed using enzyme-linked immunoassay.

## **Materials and methods**

### *Chemicals*

Unless indicated otherwise, all reagents and equipment were obtained from Amersham Biosciences (Uppsala, Sweden). Lipopolysaccharide (LPS, *E.coli* 0111:B4), propranolol, formoterol, salbutamol, dibutyryl cAMP, prostaglandin E<sub>2</sub>, and forskolin were obtained from Sigma Aldrich (St. Louis, MO, USA) and zilpaterol from Intervet Inc. (Millsboro, US).

### *Cell cultures*

Human monocyte-like histiocytic lymphoma cells U937<sup>29</sup> obtained from the ATCC (CRL-1593.2) were grown in RPMI-1640 medium, supplemented with 10% (v/v) fetal calf serum and 2 mM L-glutamine (Life technologies, Breda, The Netherlands) at 37 °C, 5% CO<sub>2</sub> in a humidified atmosphere. U937 monocytic cells were differentiated into macrophages using phorbol 12-myristate 13-acetate (PMA, 10 ng/ml, overnight, Omnilabo, Breda, The Netherlands) as described previously<sup>18,30</sup>. The PMA-differentiated macrophages were allowed to recover from PMA treatment for 48 h, during which the culture medium was replaced daily.

Peripheral blood monocytes (PB-MO) were isolated from human EDTA-blood with Rosette Sep<sup>TM</sup> human monocyte enrichment cocktail (Stemcell Technologies Inc, Meylan, France) as described previously<sup>30</sup>. The monocytes were cultured in 24-well cell culture plates containing RPMI-1640 medium supplemented with 10% (v/v) human serum and 2 mM L-glutamine and were allowed to differentiate into peripheral blood macrophages (PB-MØ) for 8 days.

Following this procedure, the macrophage maturation has been shown to give rise to the morphology and phenotype that is characteristic of primary macrophages<sup>31</sup>.

### *Incubations for proteome analysis*

Per incubation 40x10<sup>6</sup> U937 monocytic cells in a 175 cm<sup>3</sup> culture flask were differentiated into macrophages using PMA. At day three after PMA treatment, the macrophages were washed 5 times with serum free culture medium. Subsequently, the cells were exposed to 1 µg/ml LPS, LPS in combination with 1x10<sup>-6</sup> M zilpaterol or LPS in combination with zilpaterol and 1x10<sup>-6</sup> M propranolol respectively, for 16 h at 37 °C, 5% CO<sub>2</sub> in a humidified atmosphere. The incubation time of 16 h was chosen based on the results of microarray

---

experiments<sup>18</sup> and time course experiments<sup>32</sup>. The incubations were performed in duplicate. Finally, a protease inhibitor cocktail was added and the culture medium was filtered over a 0.45  $\mu\text{M}$  filter. The samples were stored at  $-80\text{ }^{\circ}\text{C}$  until further analysis.

#### *Incubations for MIP-1 $\beta$ analysis*

PB-M $\emptyset$  and U937 cells ( $1 \times 10^6$  cells per well) were exposed for 16 h to 1  $\mu\text{g/ml}$  LPS in the presence or absence of  $\beta_2$ -adrenergic receptor agonists; clenbuterol ( $1 \times 10^{-7}$  M), formoterol ( $1 \times 10^{-8}$  M), salbutamol ( $1 \times 10^{-6}$  M), and zilpaterol ( $1 \times 10^{-6}$  M). Furthermore, U937 macrophages were incubated with other cAMP elevating compounds, dibutyryl cAMP ( $1 \times 10^{-4}$  M), forskolin ( $1 \times 10^{-5}$  M), and prostaglandin E<sub>2</sub> ( $1 \times 10^{-4}$  M) in the presence of 1  $\mu\text{g/ml}$  LPS. The concentrations of the various compounds were chosen as such to achieve similar levels of TNF- $\alpha$  inhibition. Culture medium was collected and diluted 500 fold. The concentration of MIP-1 $\beta$  in the culture supernatants was determined using the cytoseet antibody pair kit for MIP-1 $\beta$  from Biosource (Etten-Leur, The Netherlands) according to the manufacturer's protocol. The cells were lysed in 0.1 M NaOH and used for protein determination by the modified method of Bradford (Bio-Rad, Veenendaal, The Netherlands). All incubations were performed in triplicate and were corrected for protein content.

#### *Two-dimensional gel electrophoresis*

Culture media (10 ml) was thawed on ice and the proteins were precipitated by adding 1.8 ml of a 100% (w/v) TCA solution. After 45 min, the mixture was centrifuged at 3000 g and  $4\text{ }^{\circ}\text{C}$ . The pellet was washed twice with 1 ml of cold acetone and air-dried for a few minutes. The proteins were dissolved in 100  $\mu\text{l}$  of DIGE lysis buffer (8M Urea, 4% w/v CHAPS and 30 mM Tris) and the pH was adjusted to 8.5. The protein content was determined using the modified method of Bradford. Each sample (50  $\mu\text{g}$ ) was labelled with 0.8  $\mu\text{l}$  of CyDye 3 and CyDye 5 CyDye<sup>TM</sup> DIGE fluors minimal dyes (400  $\mu\text{M}$ ). The experimental design is shown in Table 1. After 30 min, the incubation was stopped by adding 1  $\mu\text{l}$  of 10 mM Lysine. The labelled samples were further diluted with an equal volume of 2 x sample buffer containing 8 M urea, 4% w/v CHAPS, 130 mM DTT (Sigma Aldrich), and 2% Pharmalyte<sup>TM</sup> 3-10. The internal standard included 50  $\mu\text{g}$  of each sample (6 samples in total) labelled with CyDye 2. Two samples (CyDye 3 and CyDye 5) and the internal standard (CyDye 2) were run per gel. The three labelled samples were mixed and the volume was adjusted to 350  $\mu\text{l}$  with rehydration buffer containing 8 M urea, 4% w/v CHAPS, 2 mM tributyl phosphine (Fluka, Buchs SG, Switzerland), and 1% (v/v) IPG ampholytes pH 4-7.

All gels, 6 in total, were processed and analyzed simultaneously.

The first dimension was carried out on an IPGphor system using pH 4-7 IPG gel strips of 18 cm. The IEF was performed at 20 °C under the following conditions: 12 h at 30 V; 30 min at 150 V; 1 h at 300 V; 1 h at 1500 V and 6 h at 8000 V. After isoelectric focussing, the IPG strips were equilibrated for 15 min in reduction buffer (6 M urea, 30% (v/v) glycerol, 1% w/v DTT, and 2% (w/v) SDS in 0.05 M Tris-HCl buffer, pH 8.8) and subsequently alkylated for 15 min in alkylation buffer containing 6 M urea, 30% (v/v) glycerol, 4.7% (w/v) iodoacetamide, and 2% (w/v) SDS in 0.05 M Tris-HCl buffer, pH 8.8. The second dimensional separations were carried out on custom made 12% SDS-polyacrylamide gels and a Hoefer DALT electrophoresis system.

**Table 1** Experimental design of the 2-D DIGE experiment

Incubation	Labeling	Gel code	Progenesis analysis	Statistical analysis
1-LPS	CyDye-3	1	3 images:	2 data sets:
	CyDye-5	1	CyDye2, CyDye3, and CyDye5	CyDye3/CyDye2 and CyDye5/CyDye2
2-LPS	CyDye-3	2	3 images:	2 data sets:
	CyDye-5	2	CyDye2 CyDye3, and CyDye5	CyDye3/CyDye2 and CyDye5/CyDye2
1-LZ	CyDye-3	3	3 images:	2 data sets:
	CyDye-5	3	CyDye2 CyDye3, and CyDye5	CyDye3/CyDye2 and CyDye5/CyDye2
2-LZ	CyDye-3	4	3 images:	2 data sets:
	CyDye-5	4	CyDye2 CyDye3, and CyDye5	CyDye3/CyDye2 and CyDye5/CyDye2
1-LZP	CyDye-3	5	3 images:	2 data sets:
	CyDye-5	5	CyDye2 CyDye3, and CyDye5	CyDye3/CyDye2 and CyDye5/CyDye2
2-LZP	CyDye-3	6	3 images:	2 data sets:
	CyDye-5	6	CyDye2 CyDye3, and CyDye5	CyDye3/CyDye2 and CyDye5/CyDye2
1-LPS + 2-LPS + 1-LZ + 2-LZ + 1-LZP + 2-LZP	CyDye-2	1 - 6		
Total	13	6	18	12

### *Gel imaging and data analysis*

The gels were scanned using the Typhoon 9400 laser scanner at three different settings (CyDye2, blue laser 488 nm and 520 bp 40 filter; CyDye3, green laser 532 nm and 580 bp 30 filter; CyDye5, red laser 633 nm and 670 bp 30 filter). Three images per gel were obtained

(18 in total). The scanned images were analyzed using Progenesis workstation 2004 with the special cross stain analysis (CSA) module for analysing multi-labelled gels (Nonlinear Dynamics, Newcastle upon Tyne, UK). Spots were automatically detected and visually checked for undetected or incorrectly detected spots. The protein spots detected in each image were automatically linked between the three images per gel. All gels were matched to a digitized reference gel, containing all the protein spots present in all 6 internal standard images.

Per image the intensity levels were normalized by dividing the spot volume through the total intensity of all the spots in the image and multiplying it by the average of the total spot intensity of all 18 gel images. Subsequently, the CyDye3 and CyDye5 labelled spot volumes were divided by the spot volume of the corresponding protein spot in the internal standard (CyDye2) image. The differences in spot ratios were analyzed by multivariate data analysis tools and the Student's *t*-test (assuming normal distributions and equal variance) using MS Excel (Microsoft Corporation, Redmond, USA).

### *Multivariate data analysis*

A list of spots with their normalized spot volumes per gel was mean-centered<sup>27</sup>.

Subsequently, the dataset was examined by PCA and PLS-DA. PCA was applied as an exploratory data analysis method that is able to visualize differences between complex samples. The dataset can be visualized as a cloud of data points, where each data point represents a sample in a multidimensional space. The coordinates of these data points are represented by the spot intensities (dimensions). PCA reduces the large number of dimensions of a dataset into a smaller number of dimensions in such a way that most of the variance of the dataset is described by the first principal component (PC)<sup>33, 34</sup>.

PLS-DA was used to cluster the gels from LPS treated U937 cells and cells treated with LPS in combination with zilpaterol and propranolol. These two groups resemble the same biological state of the cell, namely inflammation. The second group contained the gels from cells treated with LPS in combination with zilpaterol (inhibition of inflammation). Using PLS-DA a regression model can be formed between the intensity of the proteins spots (X-block) and class assignment (Y-block). In PLS-DA the scores and loadings are described as latent variables (LV).

PCA and PLS-DA were performed using the PLS toolbox (3.0.2 (2003), Eigenvector Research, Inc.) in Matlab (Version 7.0 (R14) Service Pack 1 (2004), The Mathworks).

### *Validation*

Full leave one out cross-validation was used to validate statistically the PLS-DA model. The class assignment of one sample was predicted from a calibration model consisting of the rest of the samples (11 gels). This validation was repeated for every sample. The percentage misclassification was calculated from the class predictions for all individual samples for each LV.

A permutation test was performed to test if the separation between the two assigned groups (inflammation/no inflammation) was significant. Therefore only the Y-block (class assignment) was permuted 1000 times, whereas the X-block was left unchanged. For every permutation of the Y-block, a PLS-DA model was built between the X-block (protein spot intensities) and the new class assignment (Y-block) using the same number of LV's (lowest number of misclassifications) as was used with the correct Y-block (the 'real class' assignment). For every PLS-DA model built, a ratio of the distance between the two assigned groups (sum of squares between) and the distance within a group (sum of squares within) was calculated (B/W). The ratio of all class assignment permutations can be plotted, resulting in a distribution of nonsense. When the B/W value of the 'real class' assignment is positioned outside the distribution of nonsense, the separation between the assigned groups can be considered as significant.

The biological validation was performed using an ELISA.

### *In-gel digestion and nLC-MS/MS*

Preparative gels were run with 1 mg of protein and stained with RuBPS fluorescent staining using the protocol which is described by Rabilloud et al <sup>35,36</sup>. Spots were excised and sliced into small pieces. The gel pieces were washed twice with 100 mM ammonium bicarbonate and acetonitrile. Next, the pieces were dried in a vacuum centrifuge and digested overnight with 25 ng/ $\mu$ l trypsin (sequencing grade, Promega Benelux, Leiden, The Netherlands) in 50 mM ammonium bicarbonate and 2 mM dithiothreitol at 37 °C. The peptide fragments were extracted twice with 5  $\mu$ l water:acetonitrile:formic acid (5:14:1). After drying in a vacuum centrifuge, the lyophilized digest was dissolved in 25  $\mu$ l of 4 M Urea buffered at pH 8.0 with 25 mM tris.

Nanobore chromatography was performed on an Ultimate nano LC system from LC Packings (Amsterdam, The Netherlands). Ten microliters of the peptide mixture was injected on a 300  $\mu$ m ID X 0.5 mm Pepmap C<sub>18</sub> trap column (LC Packings) and washed at 30  $\mu$ l/min for 10 minutes with 0.05% trifluoroacetic acid in water before the RP trap was switched on-line in

back-flush mode to a 75  $\mu\text{m}$  X 150 mm Pepmap C<sub>18</sub> nano LC column. Gradient elution of peptides was achieved at 300 nl/min going from 95% mobile phase A (water:acetonitrile:formic acid 97.9:2:0.08 v/v/v) and 5% mobile phase B (water:acetonitrile:formic acid 19.9:80:0.1 v/v/v) to 45% B in 35 minutes, then to 60% B in 10 minutes.

The nano LC column was coupled to a LCQ DECA ion trap MS (Thermo Electron, San Jose, CA, USA) via a nano electrospray interface from Proxeon (Odense, Denmark). Electrospray was performed by applying 1.3 kV to the electrospray pico tip (20  $\mu\text{m}$  ID, 10  $\mu\text{m}$  tip ID, distal coated from New Objective, Cambridge, MA, USA) via a Pt wire; ions were introduced in the mass spectrometer through a heated capillary kept at 180° C.

The ion trap was operated in data-dependent mode, selecting top two ions for MS/MS scans at 35 % collision energy units. Protein identification was performed by searching MS/MS spectra against the NCBI database (accessed on August 2004) using Mascot search engine ([www.matrixscience.com](http://www.matrixscience.com)). Search parameters used were as follows: peptide mass tolerance 0.8 Da; MS/MS tolerance 1.2 Da; allowed missed cleavages 1; enzyme trypsin; taxonomy human; fixed modification, carbamidomethyl (C) variable modifications, oxidation (M).

## Results

### *Proteomics*

The proteome of the secreted proteins of three different incubations, U937 macrophages treated with LPS (inflammation), treated with LPS and zilpaterol (inhibition of inflammation) and treated with LPS, zilpaterol and propranolol (antagonism of the inflammatory inhibition), were compared to each other by using the DIGE technology.

Figure 1 shows a representative 2-D gel image of the internal standard, which consisted of a CyDye2-labelled mixture of all samples analyzed in this experiment. In total 586 different spots could be detected on all the internal standard images of the experiment. The expression ratios were calculated for each spot by dividing the normalized spot intensity of the CyDye3 or CyDye5 labelled spot by the normalized spot intensity of the corresponding reference spot labelled with CyDye2.

The obtained dataset containing the expression ratios of each spot in each sample was analysed by multivariate data analysis tools, PCA and PLS-DA, and a univariate data analysis tool, Student's *t*-test.

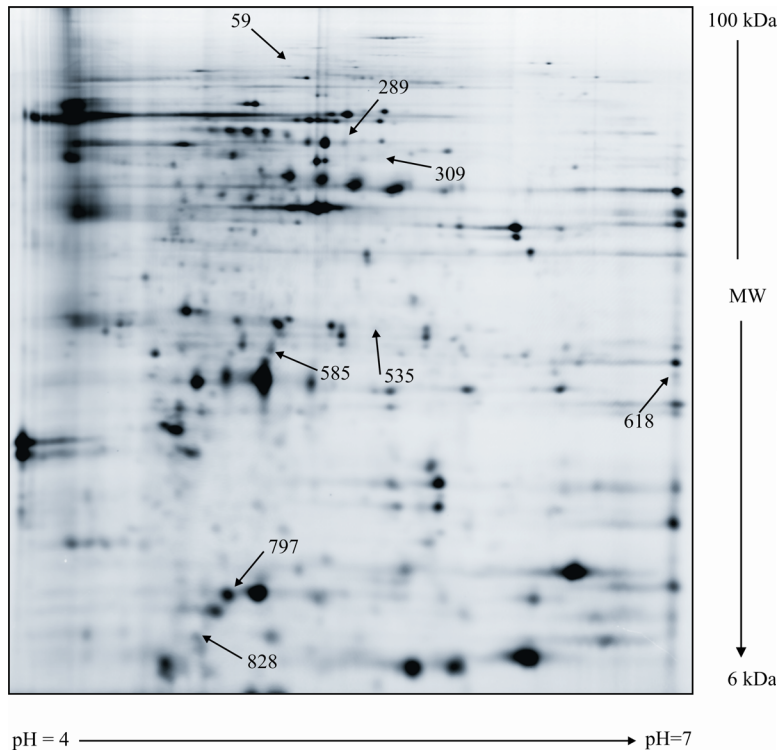


**Figure 1** A representative 2-D gel image of a CyDye2 labelled mixture of U937 macrophages treated with LPS alone, LPS in combination with zilpaterol and LPS in combination with zilpaterol and propranolol. The proteins were separated on a 12% polyacrylamide gel (pH 4-7). The excised spots for identification are indicated by arrows.

#### *Multivariate data analysis*

PCA was used as an explorative data analysis tool. This unsupervised method resulted in a separation visible between the data of the gels from cells treated with LPS in combination with zilpaterol and those from cells treated with LPS alone or in the presence of zilpaterol and propranolol. Figure 2 shows that PC 1 mainly describes differences induced by the labelling with either CyDye3 or CyDye5. A similar result was obtained for PC 2 (data not shown). By contrast, PC 3 predominantly describes differences that appear to be due to the treatments of the U937 cells. Although the number of samples analysed is relatively small, it seems that there are no outliers present in the dataset. Because the number of variables (586) is much larger than the number of samples analysed, the interpretation of the loadings of the PCA for identification of potential biomarkers is limited and the observation can only serve as a first exploratory result.

In order to find specific protein biomarkers for the anti-inflammatory properties of zilpaterol mediated by the  $\beta_2$ -adrenergic receptor, PLS-DA was applied to the same proteome dataset. Two groups for PLS-DA were defined. Group one, labelled “inflammation”, consisted of the DIGE-gel images belonging to the U937 cells treated with LPS or LPS in combination with zilpaterol and propranolol (LZP), while the second group labelled, “no inflammation” consisted of the gel images from U937 cells treated with LPS in combination with zilpaterol

(LZ). A PLS-DA model was generated from the data, containing 586 protein spots and 12 gels (X-block) using the classes inflammation and no inflammation as the response variable (Y-block).

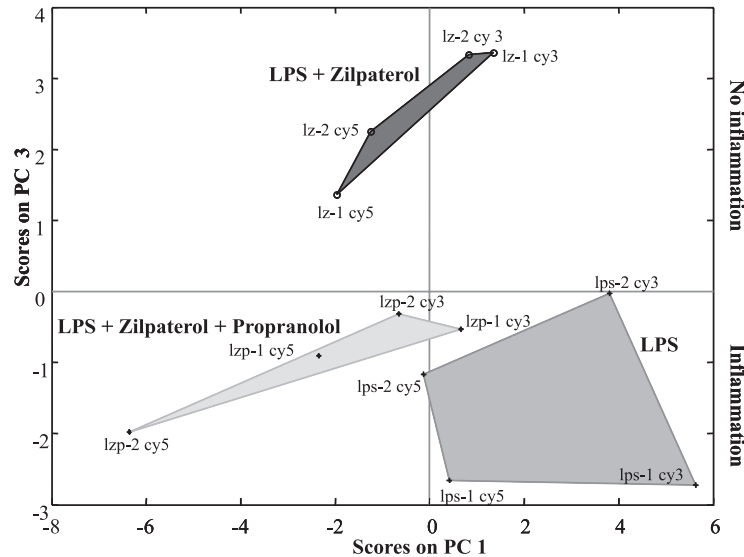


**Figure 2** Graphical presentation of the proteomics data analyzed with Principal Component Analysis (score plot). The gel images of U937 cells treated with LPS (LPS, +), LPS in combination with zilpaterol (LZ, ○) or LPS in combination with zilpaterol and propranolol (LZP, \*) are represented as crosses, dots or stars and image ID code. Each group consists of 4 data points, comprising two separate incubations (1 and 2) each labelled with CyDye 3 and CyDye 5. The images of the LZ group are clustered in the upper part of the score plot and the LPS and LZP group are positioned at the lower part. This indicates that the LPS and LZP group share a similar protein expression pattern whereas the LZ group has a distinct pattern.

The score plot of LV 1 versus LV 2 is presented in Figure 3. By using 4 LV's, no misclassifications were observed. The class assignment considered was reliable according to the permutation test results. The B/W value was positioned outside the distribution of nonsense. Figure 3 shows that LV 1 mainly describes differences that appear to involve the inflammatory status of the U937 cells, while LV 2 appears to describe differences related to the labelling of samples with either CyDye3 or CyDye5.

The influences of the individual protein spots on the PLS-DA model are described by regression values. In this particular case the high regression values indicated proteins that were down-regulated in the “no inflammation” group (LZ) with respect to the “inflammation” group (LPS and LZP), whereas low regression values indicated the up-regulated proteins. Figure 4 shows the mean expression ratios of the protein spots with successively the lowest and highest regression values.

From Figure 4 can be concluded that the differential expression of many proteins are assigned by PLS-DA as relevant to the separation of the proteomes of the “inflammation group” and

the “no inflammation” group. However, with PLS-DA we tried to identify proteins that were regulated in a similar manner in the LZP treated cells and LPS treated cells. Figure 4A and 4B show that some proteins do not meet this criterion (e.g. proteins in spots 21, 163, 310, 660, and 784). These discrepancies are most probably caused by the limited number of samples analysed in this study. Moreover, the differences in the expression levels of several other proteins do not appear to be significant (Fig. 4). Proper validation of these results is therefore necessary.

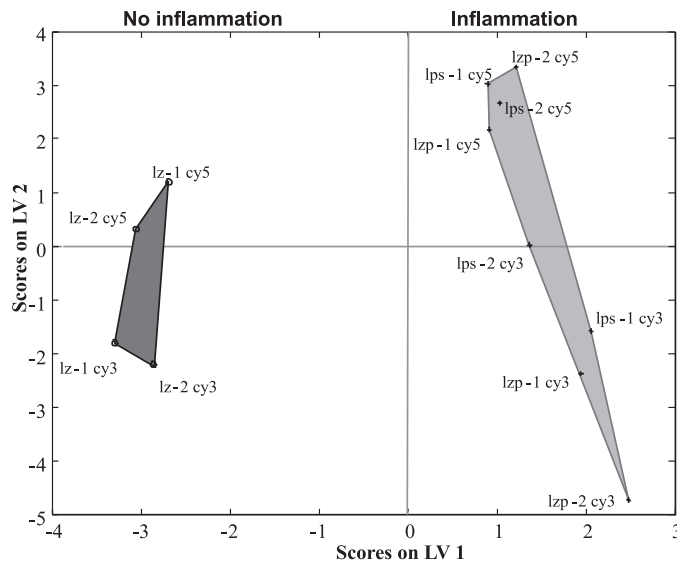


**Figure 3** Score plot of 12 protein samples. The samples were divided into two groups; “inflammation” containing all the gel images of the cells treated with LPS (LPS) or LPS in combination with zilpaterol and propranolol (LZP) and “no inflammation” containing only the gel images belonging to U937 cells treated with LPS in combination with zilpaterol (LZ). The gel images are represented as dots (no inflammation,  $\circ$ ) or crosses (inflammation,  $\times$ ) and image ID code. The images of the “no inflammation” group are clustered in the left part, whereas the images of the “inflammation” group are positioned at the right of the score plot.

### Univariate data analysis

The differences in protein expression levels were also analyzed by the Student’s *t*-test to identify potential biomarkers for the anti-inflammatory effect of zilpaterol, which were regulated via the  $\beta_2$ -AR. For this purpose the following requirements were set: i) the protein had to be regulated in a similar manner ( $p > 0.05$ ) by LPS alone and by LPS in combination with zilpaterol and propranolol ii) the protein had to be significantly up- or down-regulated in U937 macrophages treated with LPS in combination with zilpaterol with respect to the other two treatments according to the Student’s *t*-test ( $p < 0.05$ ). Eight proteins met these requirements. Moreover, some of these proteins (59, 535, 797, and 828) were also marked as potential biomarkers by PLS-DA (Fig.4). The other protein spots (289, 309, 618, and 585)

were also important in the PLS-DA model (data not shown), but were not found in the top 10 of protein spots with the highest or lowest regression values.

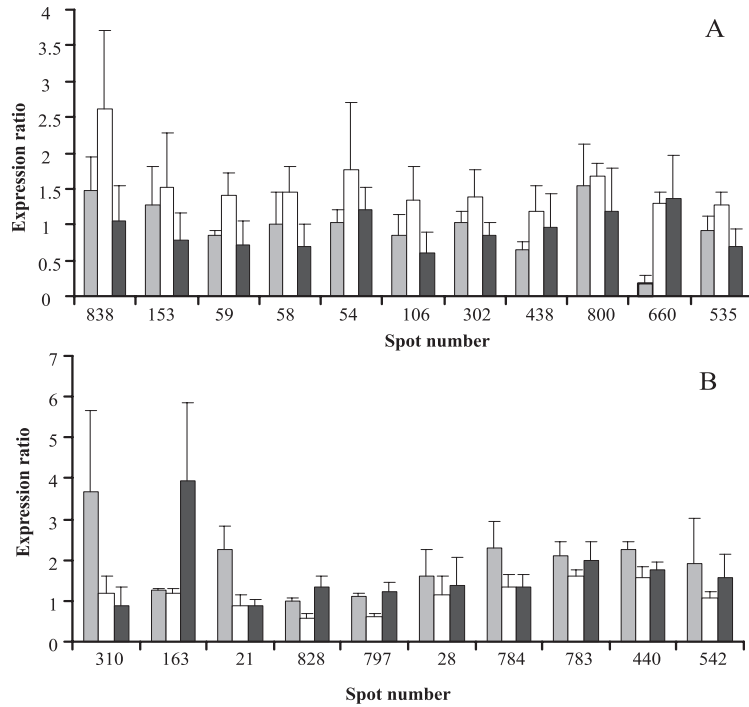


**Figure 4** Expression ratios of 10 protein spots with the A) lowest and B) highest regression values. Protein spots with high regression values are down-regulated in culture media of U937 macrophages treated with LPS and zilpaterol (white bars) with respect to LPS (light grey bars) and LPS in combination with zilpaterol and propranolol (dark grey bars), whereas the low regression values indicate up-regulation.

**Table 2** List of proteins up- or down-regulated in culture media from LPS plus zilpaterol treated U937 macrophages with respect to U937 macrophages exposed to LPS alone or LPS in combination with zilpaterol and propranolol according to the Student's *t*-test ( $p < 0.05$ ).

Spot no.	Protein identification	Accession nr.	Experimental MW	Experimental Ip	Theoretical MW	Theoretical Ip	Peptides identified	Coverage %	Total score*
59	Heat shock protein apg-2	P34932	83.3	5.2	95.1	5.2	7	8	344
289	60 kDa heat shock protein	P10809	62.1	4.8	61.2	4.8	5	18	372
309	No identification		59.3	5.6					
535	No identification		32.8	5.6					
585	Rho-gdp-dissociation inhibitor 2	P52566	29.4	5.1	23.0	5.1	10	67	378
618	Phosphoglycerate mutase	P18669	26.5	6.9	28.9	6.8	8	51	289
	Adenylate kinase iso enzym	P54819	26.5	6.9	26.6	7.9	4	17	177
797	Macrophage inflammatory protein 1-beta	P13236	11.9	4.9	10.5	5.3	1	25	81
828	Macrophage inflammatory protein 1-alpha	P10147	10.1	4.8	10.1	4.8	2	43	85

\*Total score is the sum of the individual peptide scores. Individual peptide score >39 indicate identity or extensive homology ( $p < 0.05$ ) according to mascot database search program.

Figure 5 shows the differences between the expression levels of the eight proteins in the three different treatments of U937 cells, as represented by the mean spot intensity on the DIGE gels. In order to identify the proteins in the eight selected protein spots, the spots were excised and subjected to trypsin digestion followed by identification using nLC-MS/MS. Six out of 8 spots could be identified (Table 2). The identification was impossible for faint spots (spot 309, and 535). Spot 618 was found to consist of two proteins, phosphoglycerate mutase and adenylate kinase. The individual contribution of the two proteins to the spot intensity was not further investigated.

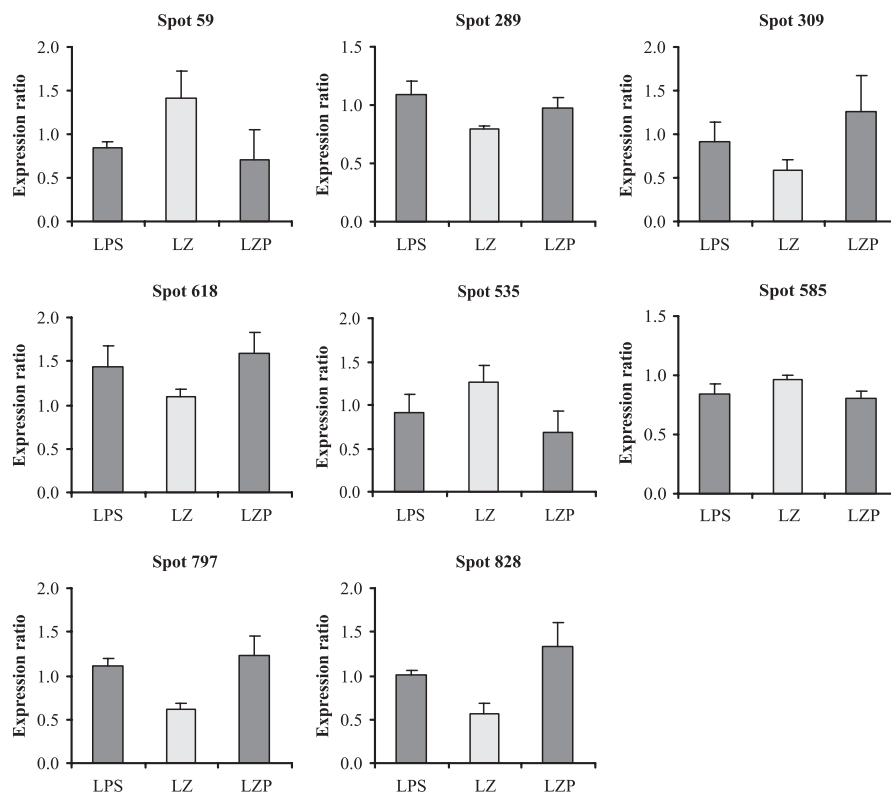


**Figure 5** Differential expressions of 8 protein spots in culture media of U937 macrophages treated with LPS alone (LPS), LPS in combination with zilpaterol (LZ) or LPS in combination with zilpaterol and propranolol (LZP). The protein spots were equally expressed in LPS treated macrophages and macrophages treated with LZP. The expressions of LZ treated macrophages were opposite to the above mentioned treatments. The expressions are given as ratios (spot intensity sample/spot intensity internal standard). The ratios are expressed as the mean of 4 expression ratios  $\pm$  SD.

Two out of eight spots were identified as a known secreted protein, macrophage inflammatory protein-1beta (MIP-1 $\beta$ ) and macrophage inflammatory protein-1alpha (MIP-1 $\alpha$ ). The other proteins are known to be involved in the maintenance of the cell, protein folding or development and are located in the cytoplasm or mitochondrial matrix (i.e. intracellular locations) (Table 3).

**Table 3** List of protein function and cellular location of proteins identified using nLC-MS/MS. More information can be found on <http://us.expasy.org>, using the accession no. from Table 2

Protein name	Function	Sub cellular location
Heat shock protein apg-2	ATP binding, protein folding	Cytoplasm
60 kDa heat shock protein	ATP binding, protein folding, mitochondrial matrix protein transport	Mitochondrial matrix
Rho-gdp-dissociation inhibitor 2	Actin cytoskeleton organisation, development	Cytoplasm
Phosphoglycerate mutase	Enzyme in glycolysis	Cytosol
Adenylate kinase iso enzym	Enzyme, maintenance and cell growth	Mitochondrial
Macrophage inflammatory protein -1beta	Chemokine, cell-cell signalling, inflammatory response	Secreted
Macrophage inflammatory protein -1alpha	Chemokine, cell-cell signalling, inflammatory response	Secreted

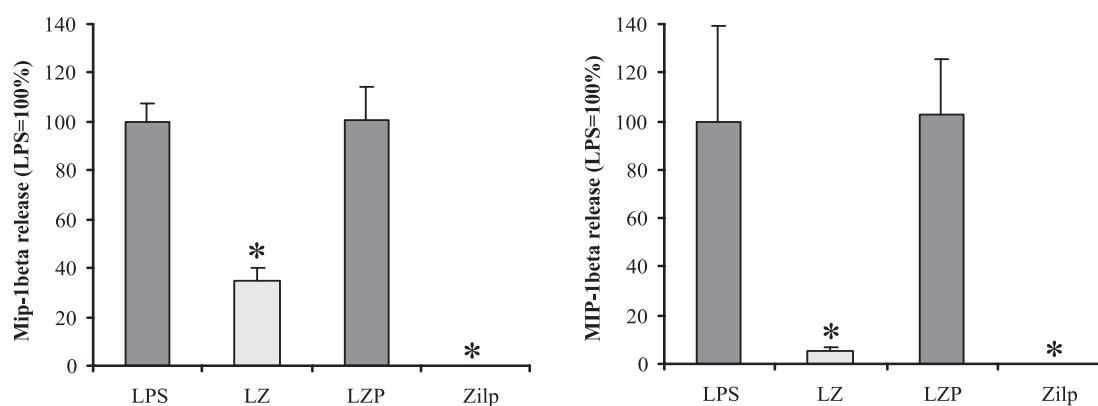


**Figure 6** Release of MIP-1 $\beta$  from U937 macrophages (left panel) and PB-MØ (right panel) incubated for 16 h with 1  $\mu$ g/ml LPS (LPS), LPS in combination with  $1 \times 10^{-6}$  M zilpaterol (LZ), LPS in combination with zilpaterol and  $1 \times 10^{-6}$  M propranolol (LZP) or  $1 \times 10^{-6}$  M zilpaterol alone (Zilp), respectively. The release of MIP-1 $\beta$  is corrected for protein content and represented as mean percentage of LPS induction (LPS = 100%)  $\pm$  SD of triplicate measurements. \* Different with respect to LPS (based on Student's *t*-test).

### Biological validation

The down-regulation of MIP-1 $\beta$  was confirmed by the analysis of the culture media using a specific ELISA for MIP-1 $\beta$  (Fig. 6, left panel). MIP-1 $\beta$  was up-regulated in LPS-treated U937 macrophages and this up-regulation was inhibited by the addition of zilpaterol. Using an antagonist for the  $\beta$ -AR, propranolol this inhibition could be blocked, indicating that the inhibitory effect of zilpaterol on MIP-1 $\beta$  production is mediated via the  $\beta$ -AR. When human peripheral blood macrophages were incubated with LPS, LPS in combination with zilpaterol and LPS in combination with zilpaterol and propranolol, the effect was more pronounced (Fig. 6, right panel).

In order to confirm that the inhibition of MIP-1 $\beta$  is mediated by the  $\beta_2$ -AR, U937 macrophages were exposed to LPS in combination with other known  $\beta_2$ -receptor agonists. Figure 7 shows the inhibitory effect of zilpaterol, clenbuterol, formoterol and salbutamol on the production of MIP-1 $\beta$ . Since the main pathway by which activation of the  $\beta_2$ -AR exerts its effect is related to the elevation of intracellular cyclic AMP, we determined the effect of other agents that elevate intracellular cAMP levels. From the right panel of Figure 7, it can be concluded that forskolin, dibutyryl cAMP and PGE<sub>2</sub> were also capable of inhibiting the LPS induced MIP-1 $\beta$  production in U937 macrophages.

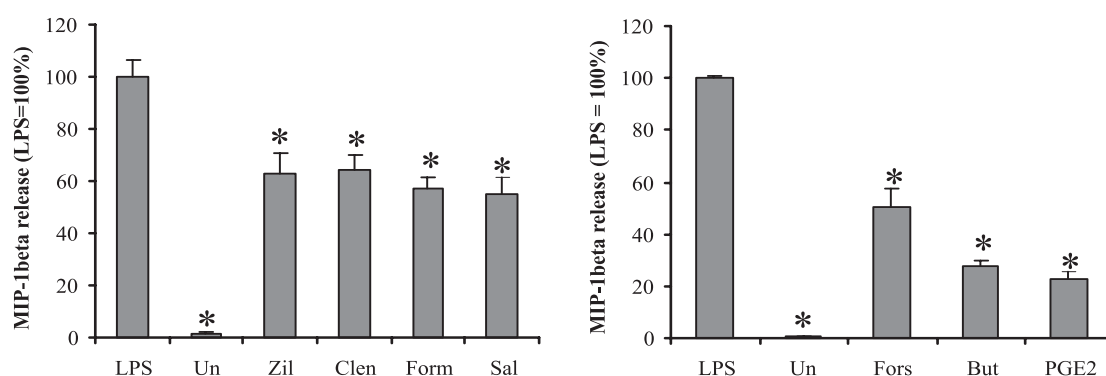


**Figure 7** Release of MIP-1 $\beta$  from U937 macrophages incubated for 16 h with 1  $\mu$ g/ml LPS (LPS), no treatment (Un) or LPS in the presence of  $\beta_2$ -adrenergic agonists, zilpaterol  $1 \times 10^{-6}$  M (Zil), clenbuterol  $1 \times 10^{-7}$  M (Clen), formoterol  $1 \times 10^{-8}$  M (Form) and salbutamol  $1 \times 10^{-6}$  M (Sal), respectively (left panel). The right panel shows the release of MIP-1 $\beta$  from U937 macrophages exposed for 16 h with 1  $\mu$ g/ml LPS (LPS), no treatment (Un), or LPS in the presence of cAMP elevating agents, forskolin  $1 \times 10^{-5}$  M (Fors), dibutyryl cAMP  $1 \times 10^{-4}$  M (But), or prostaglandin E<sub>2</sub>  $1 \times 10^{-4}$  M (PGE<sub>2</sub>) respectively. The release of MIP-1 $\beta$  is corrected for protein content and represented as mean percentage of LPS induction (LPS = 100%)  $\pm$  SD of triplicate measurements. \* Different with respect to LPS according to Student's *t*-test.

## Discussion

Conventional two-dimensional gel electrophoresis (2-D PAGE) allows the resolution of several thousand proteins in a single gel<sup>37,38</sup>. The well known limitations of this technique are low sensitivity (Coomassie and Sypro Ruby), limited dynamic range (silver) and gel to gel variability. Difference gel electrophoresis (DIGE) circumvents these issues associated with traditional 2-D PAGE and allows sensitive and more accurate quantitative proteomics studies<sup>20-22</sup>. However, with minimal labelling, only 5 % of the proteins will be labelled, the bulk unlabelled proteins will run with a higher mobility during the electrophoresis<sup>39</sup>. Preparative gels, stained with less sensitive stains as Coomassie blue or Sypro Ruby are therefore necessary in order to be able to excise the protein spots out of the gel for spot identification.

Using this procedure we encountered that some of the protein spots of interest, identified by DIGE, could not be found back on the fluorescent-stained gels. This is in line with the previously published observation that approximately 40 % of the proteins spots from a Cydye labelled gel could not be found back on Coomassie stained gels, this was somewhat better with Sypro Ruby<sup>39</sup>. An additional limiting step in spot identification is the insufficient amount of peptides being generated after in-gel digestion and their low signal intensity. This is especially true for hydrophobic, low abundant proteins or proteins with low MW. Several recent reports have described improved digestion protocols, signal intensities and recoveries of peptides<sup>40-45</sup>. However, at present there is no universal protocol suitable for every type of protein that may be present on a 2-D gel. Improving the sensitivity of protein stains also requires a better recovery of proteins out of the gel and improved peptide signals for mass spectrometry.

In this study we compared the secreted protein pattern of U937 macrophages exposed to LPS (inflammation), LPS in combination with zilpaterol (LZ; inhibition of inflammation) and LPS in combination with zilpaterol and propranolol (LZP; counteraction of the anti-inflammatory effect of zilpaterol), by using 2-D DIGE. The datasets generated after scanning of the 2-D gels were analysed by univariate (Student's *t*-test) and multivariate data analysis tools (PCA and PLS-DA). PCA showed clustering of the gel images obtained from LPS and LZP group (inflammation) and separated these gels from the images obtained from the LZ group (no inflammation). The first two principal components mainly described the effect of the different CyDyes used (CyDye 3 and CyDye 5). This dye bias has also been observed by Karp et al<sup>34</sup> who analysed *Erwinia carotovora* samples using DIGE in combination with PCA and PLS-DA. It is therefore important to label samples with both dyes in order to counteract the dye bias effect.

PLS-DA was used to correlate class assignment (“inflammation” and “non-inflammation”) with spot data to discover potential biomarkers for the anti-inflammatory effect of  $\beta_2$ -agonists. The use of PCA or PLS-DA to cluster data and discover potential biomarkers is not justified in cases where the number of samples is much smaller than the number of variables, as is the case with most proteomic studies. Nevertheless, cautious use for exploratory studies can be helpful as a first guidance in the biomarker discovery trajectory<sup>30, 33, 34, 46</sup>. Using the multivariate approach, up- or down-regulated markers are easily identified, although it should be noted that these would also have been identified by more straightforward univariate tools, such as the Student's *t*-test. In this study, we only identified the proteins that were assigned by PLS-DA as an important protein in the separation between the groups “inflammation” and

“non-inflammation”, and that were significantly altered according to the Student’s *t*-test. A major drawback of the Student’s *t*-test is its sensitivity to false positive results ( $p < 0.05$ ), especially when large numbers of variables are analysed. Protein markers that are found to be correlated either to each other or to a class assignment (PLS-DA) or identified by the Student’s *t*-test have to be additionally validated, both statistically as well as biologically. In addition to the statistical arguments, another reason to biologically validate putative marker proteins is that uncertainties arise in each step of the proteomics workflow (e.g. accidental modifications introduced by sample preparation, spot shifts in gels which may result in missing values and false spot identification).

The aim of this study was to identify protein biomarkers for the anti inflammatory properties of zilpaterol mediated by the  $\beta_2$ -AR. By examining the secreted fraction of proteins, we identified 8 proteins as putative biomarkers. Two of the eight proteins were identified as secreted proteins, namely macrophage inflammatory protein-1beta (MIP-1 $\beta$ ) and macrophage inflammatory protein-1alpha (MIP-1 $\alpha$ ). The other 6 proteins were previously reported to be intra-cellular proteins. Most likely, the culture media samples that were examined in these experiments were contaminated with intracellular proteins. When comparing the protein pattern of the secreted proteins with the pattern of the cell lysate<sup>30</sup>, many similarities could be observed. Other studies performed on secreted proteins reported the same phenomenon<sup>47-49</sup>. This contamination is unfortunately inevitable, because a few dead cells are already enough to mask the very low abundant proteins present in the culture media.

The down-regulation of MIP-1 $\beta$  by zilpaterol was confirmed in U937 macrophages as well as human peripheral blood macrophages by using a specific ELISA. The  $\beta$ -adrenergic blockade by propranolol counteracted the inhibitory effect of zilpaterol on the MIP-1 $\beta$  production. Furthermore, the down-regulation of MIP-1 $\beta$  was also achieved by other  $\beta_2$ -AR agonists like clenbuterol, salbutamol and formoterol. These data demonstrate the involvement of the  $\beta$ -AR. The involvement of cAMP was investigated by incubating U937 macrophages with LPS in combination with cAMP elevating agents. The release of MIP-1 $\beta$  was inhibited by prostaglandin E<sub>2</sub> (PGE<sub>2</sub>) which augments cyclic AMP by binding to its own receptor, forskolin, a direct activator of adenylate cyclase and the membrane permeable stable derivate of cAMP, dibutyryl cAMP. This observation suggests that the inhibition of MIP-1 $\beta$  production is most probably due to the elevation of intracellular cAMP. The  $\beta$ -AR belongs to the family of G-protein coupled receptors that activate Gs proteins. Gs proteins activate adenylate cyclase that subsequently catalyses the conversion of ATP into cAMP<sup>7-12</sup>. Cyclic

AMP is known to be involved in the induction and inhibition of many inflammatory genes encoding proteins involved in inflammation<sup>13, 14, 50</sup>. The results described above suggest that zilpaterol inhibits the LPS induced production of MIP-1 $\beta$  via the  $\beta_2$ -AR by elevating the cAMP production. This finding is in agreement with those of Martin et al<sup>51</sup>, who discovered that PGE<sub>2</sub> inhibited the production of MIP-1 $\beta$  mRNA levels in murine macrophage cell line partially via a cAMP mediated pathway of signal transduction.

MIP-1 $\beta$  belongs to the chemokine family and is involved in endotoxin induced inflammation. Chemokines play a major role in the recruitment of leukocytes to sites of infection. In addition they often activate these cells resulting in an enhanced local inflammatory response<sup>3</sup>. MIP-1 $\beta$  is a chemoattractant for natural killer cells and has been found in inflamed tissues of patients with rheumatoid arthritis, Multiple Sclerosis, and respiratory system disorders<sup>52-54</sup>. Interestingly, MIP-1 $\alpha$  (chemokine CC), which shows 68% homology with MIP-1 $\beta$ , was also inhibited by  $\beta_2$ -AR agonists and other cAMP elevating compounds<sup>52, 55, 56</sup>. This inhibition was also found in this report using 2-D DIGE. The regulation of MIP-1 $\alpha$ , MIP-1 $\beta$  and perhaps other chemoattractants by  $\beta_2$ -AR agonists could therefore be of therapeutic importance and could in part explain the mechanism of action of  $\beta_2$ -AR agonist in the treatment of asthma.

### **Acknowledgements**

The authors thank Age Smilde and Carina Rubingh for there helpful discussion on statistical data analysis and Ian Sanders and Louise Vickers from Nonlinear Dynamics (Newcastle upon Tyne, UK) for their support in the implementation of the Progenesis software

---

**References**

- 1 Heumann, D. and Glauser, M. P., *Scientific American science & medicine*, **1994**, Pathogenesis of sepsis, 28-37.
- 2 Cirino, G., *Biochem Pharmacol*, **1998**, Multiple controls in inflammation. Extracellular and intracellular phospholipase a2, inducible and constitutive cyclooxygenase, and inducible nitric oxide synthase, *55*, 105-111.
- 3 Henderson, B., Poole, S. and Wilson, M., *Microbiol Rev*, **1996**, Bacterial modulins: A novel class of virulence factors which cause host tissue pathology by inducing cytokine synthesis, *60*, 316-341.
- 4 Lotvall, J., *Pulm Pharmacol Ther*, **2002**, The long and short of beta2-agonists, *15*, 497-501.
- 5 Libretto, S. E., *Arch Toxicol*, **1994**, A review of the toxicology of salbutamol (albuterol), *68*, 213-216.
- 6 Barnes, P. J., *J Allergy Clin Immunol*, **1999**, Effect of beta-agonists on inflammatory cells, *104*, S10-17.
- 7 Liggett, S. B., *J Allergy Clin Immunol*, **2002**, Update on current concepts of the molecular basis of beta2-adrenergic receptor signaling, *110*, S223-227.
- 8 Strosberg, A. D., *Protein Sci*, **1993**, Structure, function, and regulation of adrenergic receptors, *2*, 1198-1209.
- 9 Lombardi, M. S., Kavelaars, A. and Heijnen, C. J., *Crit Rev Immunol*, **2002**, Role and modulation of g protein-coupled receptor signaling in inflammatory processes, *22*, 141-163.
- 10 Ji, T. H., Grossmann, M. and Ji, I., *J Biol Chem*, **1998**, G protein-coupled receptors. I. Diversity of receptor-ligand interactions, *273*, 17299-17302.
- 11 Nurnberg, B., Gudermann, T. and Schultz, G., *J Mol Med*, **1995**, Receptors and g proteins as primary components of transmembrane signal transduction. Part 2. G proteins: Structure and function, *73*, 123-132.
- 12 Neer, E. J., *Protein Sci*, **1994**, G proteins: Critical control points for transmembrane signals, *3*, 3-14.
- 13 Zidek, Z., *Eur Cytokine Netw*, **1999**, Adenosine - cyclic amp pathways and cytokine expression, *10*, 319-328.
- 14 Sekut, L., Champion, B. R., Page, K., Menius, J. A., Jr. and Connolly, K. M., *Clin Exp Immunol*, **1995**, Anti-inflammatory activity of salmeterol: Down-regulation of cytokine production, *99*, 461-466.
- 15 Izeboud, C. A., Mocking, J. A., Monshouwer, M., van Miert, A. S. and Witkamp, R. F., *J Recept Signal Transduct Res*, **1999**, Participation of beta-adrenergic receptors on macrophages in modulation of lps-induced cytokine release, *19*, 191-202.
- 16 Izeboud, C. A., Vermeulen, R. M., Zwart, A., Voss, H. P., *et al.*, *Naunyn Schmiedebergs Arch Pharmacol*, **2000**, Stereoselectivity at the beta2-adrenoceptor on macrophages is a major determinant of the anti-inflammatory effects of beta2-agonists, *362*, 184-189.
- 17 Izeboud, C. A., Monshouwer, M., van Miert, A. S. and Witkamp, R. F., *Inflamm Res*, **1999**, The beta-adrenoceptor agonist clenbuterol is a potent inhibitor of the lps-induced production of tnf-alpha and il-6 in vitro and in vivo, *48*, 497-502.
- 18 Verhoeckx, K. C., Bijlsma, S., Jespersen, S., Ramaker, R., *et al.*, *Int Immunopharmacol*, **2004**, Characterization of anti-inflammatory compounds using transcriptomics, proteomics, and metabolomics in combination with multivariate data analysis, *4*, 1499-1514.
- 19 Intervet, **1998**, Zilmax technical brochure.
- 20 Alban, A., David, S. O., Bjorkesten, L., Andersson, C., *et al.*, *Proteomics*, **2003**, A novel experimental design for comparative two-dimensional gel analysis: Two-dimensional difference gel electrophoresis incorporating a pooled internal standard, *3*, 36-44.
- 21 Unlu, M., Morgan, M. E. and Minden, J. S., *Electrophoresis*, **1997**, Difference gel electrophoresis: A single gel method for detecting changes in protein extracts, *18*, 2071-2077.
- 22 Tonge, R., Shaw, J., Middleton, B., Rowlinson, R., *et al.*, *Proteomics*, **2001**, Validation and development of fluorescence two-dimensional differential gel electrophoresis proteomics technology, *1*, 377-396.
- 23 Massart, D. L., Vandeginste, B. G. M. and De Jong, P. J., *Handbook of chemometrics and qualimetrics: Part a*, Elsevier, Amsterdam, The Netherlands **1997**.
- 24 Vandeginste, B. G. M., Massart, D. L., Buydens, L. M. C. and De Jong, P. J., *Handbook of chemometrics and qualimetrics: Part b*, Elsevier, Amsterdam, The Netherlands **1998**.
- 25 Dillon, W. R. and Goldstein, M., *Multivariate analysis: Methods and applications*, John Wiley & Sons Inc., New York, USA **1984**, p. 608.
- 26 Joliffe, I. T., *Principal component analysis*, Springer Verlag, New York, USA **1986**.
- 27 Martens, H. and Naes, T., *Multivariate calibrations*, John Wiley & Sons, Chichester, England **1992**, p. 438.
- 28 Barker, M. and Rayens, W., *J. Chemometrics*, **2003**, Partial least squares for discrimination, *17*, 166-173.

- 
- 29 Sundstrom, C. and Nilsson, K., *Int J Cancer*, **1976**, Establishment and characterization of a human histiocytic lymphoma cell line (u-937), *17*, 565-577.
- 30 Verhoeckx, K. C., Bijlsma, S., de Groene, E. M., Witkamp, R. F., *et al.*, *Proteomics*, **2004**, A combination of proteomics, principal component analysis and transcriptomics is a powerful tool for the identification of biomarkers for macrophage maturation in the u937 cell line, *4*, 1014-1028.
- 31 Kreutz, M., Krause, S. W., Hennemann, B., Rehm, A. and Andreesen, R., *Res Immunol*, **1992**, Macrophage heterogeneity and differentiation: Defined serum-free culture conditions induce different types of macrophages in vitro, *143*, 107-115.
- 32 Verhoeckx, K. C. M., Doorenbos, R. P., Witkamp, R. F., Van der Greef, J. and Rodenburg, R. J., *Int Immunopharmacol*, **2005**, Beta-adrenergic receptor agonists induce the release of granulocyte chemotactic protein-2, oncostatin m, and vascular endothelial growth factor from macrophages., *in press*.
- 33 Kleno, T. G., Leonardsen, L. R., Kjeldal, H. O., Laursen, S. M., *et al.*, *Proteomics*, **2004**, Mechanisms of hydrazine toxicity in rat liver investigated by proteomics and multivariate data analysis, *4*, 868-880.
- 34 Karp, N. A., Griffin, J. L. and Lilley, K. S., *Proteomics*, **2005**, Application of partial least squares discriminant analysis to two-dimensional difference gel studies in expression proteomics, *5*, 81-90.
- 35 Rabilloud, T., Strub, J. M., Luche, S., van Dorsselaer, A. and Lunardi, J., *Proteomics*, **2001**, A comparison between sypro ruby and ruthenium ii tris (bathophenanthroline disulfonate) as fluorescent stains for protein detection in gels, *1*, 699-704.
- 36 Rabilloud, T., Strub, J. M., Luche, S., Girardet, J. L., *et al.*, Springer-Verlag Heidelberg | Tiergartenstr. 17 | D-69121 Heidelberg | Germany **2000**, pp. 1-6.
- 37 Gorg, A., Weiss, W. and Dunn, M. J., *Proteomics*, **2004**, Current two-dimensional electrophoresis technology for proteomics, *4*, 3665-3685.
- 38 Rabilloud, T., *Proteomics*, **2002**, Two-dimensional gel electrophoresis in proteomics: Old, old fashioned, but it still climbs up the mountains, *2*, 3-10.
- 39 Shaw, J., Rowlinson, R., Nickson, J., Stone, T., *et al.*, *Proteomics*, **2003**, Evaluation of saturation labelling two-dimensional difference gel electrophoresis fluorescent dyes, *3*, 1181-1195.
- 40 Katayama, H., Nagasu, T. and Oda, Y., *Rapid Commun Mass Spectrom*, **2001**, Improvement of in-gel digestion protocol for peptide mass fingerprinting by matrix-assisted laser desorption/ionization time-of-flight mass spectrometry, *15*, 1416-1421.
- 41 Soskic, V. and Godovac-Zimmermann, J., *Proteomics*, **2001**, Improvement of an in-gel tryptic digestion method for matrix-assisted laser desorption/ionization-time of flight mass spectrometry peptide mapping by use of volatile solubilizing agents, *1*, 1364-1367.
- 42 Zischka, H., Gloeckner, C. J., Klein, C., Willmann, S., *et al.*, *Proteomics*, **2004**, Improved mass spectrometric identification of gel-separated hydrophobic membrane proteins after sodium dodecyl sulfate removal by ion-pair extraction, *4*, 3776-3782.
- 43 Nomura, E., Katsuta, K., Ueda, T., Toriyama, M., *et al.*, *J Mass Spectrom*, **2004**, Acid-labile surfactant improves in-sodium dodecyl sulfate polyacrylamide gel protein digestion for matrix-assisted laser desorption/ionization mass spectrometric peptide mapping, *39*, 202-207.
- 44 Katayama, H., Tabata, T., Ishihama, Y., Sato, T., *et al.*, *Rapid Commun Mass Spectrom*, **2004**, Efficient in-gel digestion procedure using 5-cyclohexyl-1-pentyl-beta-d-maltoside as an additive for gel-based membrane proteomics, *18*, 2388-2394.
- 45 Lui, M., Tempst, P. and Erdjument-Bromage, H., *Anal Biochem*, **1996**, Methodical analysis of protein-nitrocellulose interactions to design a refined digestion protocol, *241*, 156-166.
- 46 Jessen, F., Lametsch, R., Bendixen, E., Kjaersgard, I. V. and Jorgensen, B. M., *Proteomics*, **2002**, Extracting information from two-dimensional electrophoresis gels by partial least squares regression, *2*, 32-35.
- 47 Watt, S. A., Wilke, A., Patschkowski, T. and Niehaus, K., *Proteomics*, **2005**, Comprehensive analysis of the extracellular proteins from xanthomonas campestris pv. Campestris b100, *5*, 153-167.
- 48 Kubota, K., Wakabayashi, K. and Matsuoka, T., *Proteomics*, **2003**, Proteome analysis of secreted proteins during osteoclast differentiation using two different methods: Two-dimensional electrophoresis and isotope-coded affinity tags analysis with two-dimensional chromatography, *3*, 616-626.
- 49 Dupont, A., Tokarski, C., Dekeyser, O., Guihot, A. L., *et al.*, *Proteomics*, **2004**, Two-dimensional maps and databases of the human macrophage proteome and secretome, *4*, 1761-1778.
- 50 Kast, R. E., *Int J Immunopharmacol*, **2000**, Tumor necrosis factor has positive and negative self regulatory feed back cycles centered around camp, *22*, 1001-1006.
- 51 Martin, C. A. and Dorf, M. E., *Cell Immunol*, **1991**, Differential regulation of interleukin-6, macrophage inflammatory protein-1, and je/mcp-1 cytokine expression in macrophage cell lines, *135*, 245-258.
- 52 Menten, P., Wuyts, A. and Van Damme, J., *Cytokine Growth Factor Rev*, **2002**, Macrophage inflammatory protein-1, *13*, 455-481.
-

- 53 Schall, T. J., Bacon, K., Camp, R. D., Kaspari, J. W. and Goeddel, D. V., *J Exp Med*, **1993**, Human macrophage inflammatory protein alpha (mip-1 alpha) and mip-1 beta chemokines attract distinct populations of lymphocytes, *177*, 1821-1826.
- 54 O'Grady, N. P., Tropea, M., Preas, H. L., 2nd, Reda, D., *et al.*, *J Infect Dis*, **1999**, Detection of macrophage inflammatory protein (mip)-1alpha and mip-1beta during experimental endotoxemia and human sepsis, *179*, 136-141.
- 55 Li, C. Y., Chou, T. C., Lee, C. H., Tsai, C. S., *et al.*, *Anesth Analg*, **2003**, Adrenaline inhibits lipopolysaccharide-induced macrophage inflammatory protein-1 alpha in human monocytes: The role of beta-adrenergic receptors, *96*, 518-523, table of contents.
- 56 Hasko, G., Shanley, T. P., Egnaczyk, G., Nemeth, Z. H., *et al.*, *Br J Pharmacol*, **1998**, Exogenous and endogenous catecholamines inhibit the production of macrophage inflammatory protein (mip) 1 alpha via a beta adrenoceptor mediated mechanism, *125*, 1297-1303.





## Chapter 5

---

### **Inhibitory effects of the $\beta_2$ -adrenergic receptor agonist Zilpaterol on the LPS-induced production of TNF- $\alpha$ *in vitro* and *in vivo*.**

Kitty C.M. Verhoeckx<sup>1,2</sup>

Robert P. Doornbos<sup>1</sup>

Jan van der Greef<sup>1,2</sup>

Renger F. Witkamp<sup>1</sup>

Richard J.T. Rodenburg<sup>3</sup>

*Accepted for publication in J. Vet Pharmacol Ther*

<sup>1</sup> TNO Quality of Life, Zeist, The Netherlands, <sup>2</sup> Leiden University, Leiden/Amsterdam Center for Drug Research, Leiden, The Netherlands, <sup>3</sup> UMC St Radboud, Nijmegen, The Netherlands

## **Inhibitory effects of the $\beta_2$ -adrenergic receptor agonist Zilpaterol on the LPS-induced production of TNF- $\alpha$ *in vitro* and *in vivo*.**

*In this study the immuno-modulating properties of zilpaterol, a  $\beta_2$ -adrenergic receptor ( $\beta_2$ -AR) agonist specifically developed as a growth promoter in cattle were investigated. Although zilpaterol has a different structure compared to the  $\beta_2$ -adrenergic receptor agonists known to date, it was noted that it was able to bind to both the  $\beta_2$ -adrenergic receptor ( $K_i = 1.1 \times 10^{-6}$  M) and the  $\beta_1$ -adrenergic receptor ( $K_i = 1.0 \times 10^{-5}$  M). Using lipopolysaccharide (LPS) exposed U937 macrophages, the production of cyclic adenosine-3',5'-cyclic monophosphate (cAMP) and tumor necrosis factor alpha (TNF- $\alpha$ ) were investigated. Zilpaterol inhibited TNF- $\alpha$  release and induced intracellular cAMP level in a dose-dependent manner. The inhibition of TNF- $\alpha$  release and the induction of cAMP production was mainly mediated via the  $\beta_2$ -AR, as indicated by addition of  $\beta_1$ - and  $\beta_2$ -selective antagonists. The effects of zilpaterol were investigated in LPS-treated male Wistar rats. Zilpaterol dosed at 500  $\mu$ g/kg bodyweight reduced TNF- $\alpha$  plasma levels. In conclusion, zilpaterol is a  $\beta_2$ -adrenergic agonists and an inhibitor of TNF- $\alpha$  production induced by LPS both *in vivo* and *in vitro*.*

---

### **Introduction**

Beta-adrenergic agonists can be used as so-called repartitioning agents. In muscle tissue,  $\beta$ -agonists promote protein synthesis and cell hypertrophy by inhibition of proteolysis, whereas in adipose tissue they promote lipolysis. On the basis of these properties,  $\beta$ -agonists can be used in cattle industry to increase feeding efficiency, increase carcass leanness, and promote animal growth<sup>1,2</sup>. In most countries this is illegal. In addition,  $\beta$ -agonists have been shown to be abused to enhance athletic performance<sup>3,4</sup>. In clinical practice,  $\beta_2$ -adrenergic agonists are used as bronchodilators in both humans and horses<sup>5-9</sup>. The predominant effect of  $\beta_2$ -agonists on the airways is relaxation of airway smooth muscle. Although some authors have suggested that  $\beta_2$ -agonists possess anti-inflammatory characteristics, these anti-inflammatory effects have mainly been observed *in vitro*<sup>10,11</sup>. However previous studies demonstrated that clenbuterol suppressed the release of TNF- $\alpha$  by LPS activated U937 macrophages and in rats treated with LPS. Evidence for the involvement of the  $\beta_2$ -AR in this effect was also presented<sup>12,13</sup>. Zilpaterol was originally designed as a growth promoter in cattle<sup>14</sup>. The use of zilpaterol has been approved in South Africa and Mexico, but is forbidden in the EU, USA and Asia<sup>15,16</sup>. Little is known about the mechanism of action of zilpaterol. Although it has been claimed

by the manufacturer that zilpaterol acts via the  $\beta_2$ -adrenergic receptor ( $\beta_2$ -AR)<sup>14</sup>, there are as far as we know no data in the open literature that support this basic property.

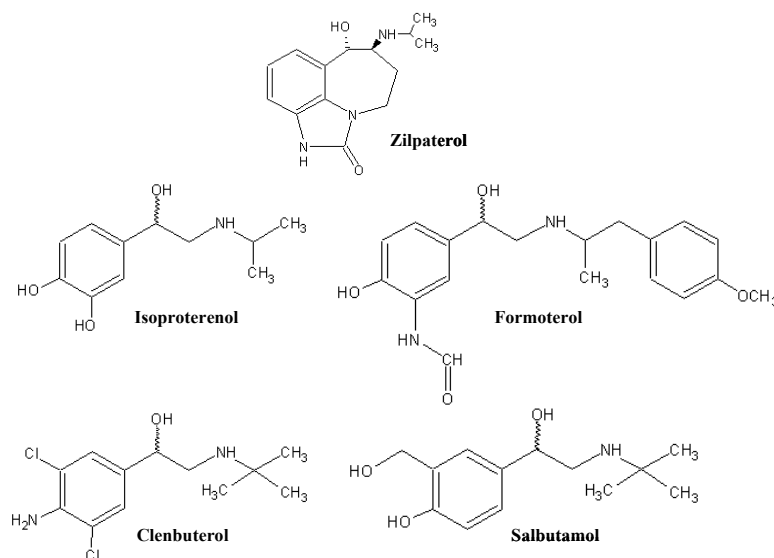


**Figure 1** Comparison of the chemical structure of zilpaterol with several other  $\beta_2$ -AR agonists.

In this study it was investigated whether zilpaterol, which shows little structural resemblance to other  $\beta_2$ -agonists (e.g. clenbuterol, formoterol, salbutamol, and isoproterenol) (Fig. 1), has affinity for the  $\beta_1$ -AR and/or  $\beta_2$ -AR. Beta-ARs belong to the family of GTP-binding protein-coupled receptors (GPCR). Beta<sub>1</sub>-AR and  $\beta_2$ -AR augment the activity of adenylate cyclase via Gs regulatory proteins. Binding to the  $\beta_1$ -AR or  $\beta_2$ -AR results in the production of the second messenger cyclic adenosine-3',5'-cyclic monophosphate (cAMP)<sup>17-22</sup>.

This study also investigates the potential immuno-modulating effects of zilpaterol. Although results from previous studies from our laboratory<sup>12, 13</sup> and others<sup>10, 11</sup> suggest that this might be a general property of all  $\beta_2$ -agonists, it would be interesting to establish if such an effect is also induced by this compound of differing structure. It has been suggested that cAMP is involved in the inhibition of tumor necrosis factor-alpha (TNF- $\alpha$ ) synthesis and release<sup>23, 24</sup>. Therefore, the study investigated the anti-inflammatory properties of zilpaterol by examining its effects on the production of cAMP and TNF- $\alpha$ . For this purpose the human monocyte-like histiocytic lymphoma cell line U937 was used as a model system. Furthermore, the roles of the  $\beta_1$ - and  $\beta_2$ -adrenergic receptors on the effects of zilpaterol on cAMP and TNF- $\alpha$  were examined. Finally, an endotoxemic rat model system was used to investigate the inhibitory effect of zilpaterol on the LPS-induced TNF- $\alpha$  plasma levels *in vivo*.

## Material en Methods

### *Chemicals*

Lipopolysaccharide (LPS, *E.coli* 0111:B4), propranolol, ICI 118551 and atenolol were obtained from Sigma Aldrich (St. Louis, MO, USA) and zilpaterol from Intervet Inc. (Millsboro, US).

### *Receptor radioligand binding*

Cell membrane homogenates from  $\beta_2$ -adrenergic receptor-transfected Sf9 cells or  $\beta_1$ -adrenergic receptor transfected HEK-293 cells (15-20  $\mu\text{g}$  protein) were incubated for 60 min at 22 °C with 0.15 nM CGP 12177 in the absence or presence of varying concentrations of zilpaterol ( $1 \times 10^{-9}$  -  $1 \times 10^{-4}$  M) and clenbuterol ( $1 \times 10^{-10}$  -  $1 \times 10^{-5}$  M) in a buffer containing 50 mM Tris-HCl (pH 7.4), 10mM  $\text{MgCl}_2$ , and 2 mM EDTA. Non-specific binding was determined in the presence of 50  $\mu\text{M}$  alprenolol. Following incubation, the samples were filtered rapidly under vacuum through GF/B glass fibre filters (Packard, Rungis, France) using a Unifilter 96-sample cell harvester (Packard). The filters were dried and subsequently counted for radioactivity in a Topcount scintillation counter (Packard) using Microscint scintillation cocktail (Packard). ICI 118551 was used as standard reference compound for the  $\beta_2$  adrenergic receptor and atenolol for the  $\beta_1$ -adrenergic receptor.

The specific binding of ligands to the receptors was defined as the difference between the total binding and the non-specific binding determined in the presence of an excess of unlabelled ligand. The results are expressed as a percentage of control specific binding obtained in the presence of zilpaterol inhibition of the control radioligand specific binding. Binding studies were performed in triplicate. Using Graphpad Prism Software (San Diego, USA), the inhibition constants ( $K_i$ ) were calculated from the Cheng Prushoff equation ( $K_i = \text{IC}_{50}/(1 + (L/K_D))$ ), in which L = the concentration radioligand in the assay, and  $K_D$  = the affinity of the radioligand for the receptor.

### *Cell cultures*

Human monocyte-like histiocytic lymphoma cells U937<sup>25</sup> obtained from the ATCC (CRL-1593.2) were grown in RPMI-1640 medium, supplemented with 10% (v/v) fetal calf serum and 2 mM L-glutamine (Life technologies, Breda, The Netherlands) at 37 °C and 5%  $\text{CO}_2$  in a humidified atmosphere. U937 monocytic cells were differentiated into macrophages using phorbol 12-myristate 13-acetate (PMA, 10 ng/ml, overnight, Omnilabo, Breda, The Netherlands) as described previously<sup>26</sup>.

The PMA-differentiated macrophages were allowed to recover from the PMA treatment for 48 h, during which the culture medium was replaced daily.

*Macrophage activation and TNF- $\alpha$  assay*

U937 macrophages were cultured at a concentration of  $1 \times 10^6$  cells per well. Cells were incubated for 4 h with LPS (*E. Coli* 0111:B4,  $1 \mu\text{g/ml}$ ), LPS in the presence of a dilution series of zilpaterol ( $1 \times 10^{-8}$  -  $1 \times 10^{-4}$  M), LPS in the presence of a dilution series of clenbuterol ( $1 \times 10^{-10}$  -  $1 \times 10^{-6}$  M) or LPS plus zilpaterol ( $1 \times 10^{-6}$  M) in combination with a dilution series of  $\beta$ -AR antagonists ( $1 \times 10^{-8}$  -  $1 \times 10^{-5}$  M), respectively. The following  $\beta$ -AR antagonists were used; ICI 118551 ( $\beta_2$ -AR), atenolol ( $\beta_1$ -AR), and propranolol (non-selective antagonist for  $\beta_1$ -AR and  $\beta_2$ -AR). The incubations were performed in 6-fold.

The concentration of TNF- $\alpha$  in the culture supernatants was determined by ELISA using the cytoset antibody pair kit for TNF- $\alpha$  from Biosource (Etten-Leur, The Netherlands) according to the manufacturer's protocol. After removal of culture medium the cells were lysed in 0.1 M NaOH and used for protein determination by the modified method of Bradford (Bio-Rad, Veenendaal, The Netherlands). The toxicity of the zilpaterol concentration used was determined by measuring the enzyme activity of lactate dehydrogenase (LDH). LDH activity was quantitatively determined using the *in vitro* assay for LDH activity from Roche Diagnostics (Mannheim, Germany) for automated clinical chemistry analyzer Hitachi 911 (Hitachi, Japan).

*Measurements of intracellular cAMP formation*

U937 macrophages were cultured in 24 well cell culture plates at a concentration of  $1 \times 10^6$  cells per well. Cells were incubated for 10 minutes at 37 °C with  $1 \mu\text{g/ml}$  LPS in the absence or presence of a dilution series of zilpaterol ( $1 \times 10^{-8}$  -  $1 \times 10^{-4}$  M). In addition, cells that were used for antagonism studies were incubated with  $1 \mu\text{g/ml}$  LPS and  $1 \times 10^{-5}$  M zilpaterol in combination with a dilution series of  $\beta$ -AR antagonists ( $1 \times 10^{-8}$  -  $1 \times 10^{-4}$  M). The following  $\beta$ -AR antagonists were used; ICI 118551, atenolol, and propranolol. The incubations were performed in 6-fold. The culture medium was aspirated and the cells were placed directly on ice. The cells were lysed in 0.25 ml 0.1 M HCl and after centrifugation the samples were assayed directly using the cyclic AMP EIA kit from Cayman Chemical (Ann Arbor, USA).

*In Vivo effect of zilpaterol on TNF- $\alpha$  release*

Twenty four male Wistar rats (200-250 g) were purchased from Charles River Inc. (Sulzfeld, Germany). The animals were randomized into four groups of 6 animals and received food and water *ad libitum*. Room temperature was kept constant and light was maintained at a 12 h cycle. The rats were fasted the night before the experiment (only water available, *ad libitum*). Saline (Eurovet animal health BV, Bladel, The Netherlands) was used for administration either as control or as vehicle for the following doses: LPS-solution (2 mg/kg bodyweight) and zilpaterol (500  $\mu$ g/kg bodyweight). The doses and observation period were based on previously performed *in vivo* experiments<sup>12,27</sup> and for zilpaterol a dose was estimated based on the data obtained in the *in vitro* data presented. The control group and LPS group were administered saline orally, one hour before an intra-peritoneal injection of saline or LPS respectively. The LZ (LPS + zilpaterol) group and Zil (zilpaterol) group received both an oral dose of zilpaterol followed after 1 hour by an intra-peritoneal injection of LPS or saline respectively. Blood samples from all rats were drawn at 2 h after LPS challenge. Blood was collected in EDTA containing tubes and centrifuged for 15 min (3000g, 4 °C). Plasma was stored at -80 °C until analysis. The concentration of TNF- $\alpha$  in rat plasma was determined by ELISA using the Rat TNF- $\alpha$  Ultrasensitive kit from Biosource (Etten-Leur, The Netherlands) according to the manufacturer's protocol. The study protocol was approved by the Ethical Committee for experiments on Animals of our Institute.

*Statistical evaluation*

All values presented are means  $\pm$  SD of 6 individual incubations unless stated otherwise. For the comparison of receptor-binding data and the dose response curves (logEC-50) the F-test was performed. The levels of TNF- $\alpha$  and cAMP were compared using the Student's *t*-test assuming normal distributions and equal variance. TNF- $\alpha$  results from the *in vivo* study were compared using one-way ANOVA followed by the Bonferroni's multiple comparison test. The effect on bodyweight of animals treated with zilpaterol and the control group were analysed using the Mann-Whitney test (nonparametric). The results were considered significantly different if  $p < 0.05$ . All analyses were performed using Graphpad prism 4.0 software package (Graph Pad Software Inc., San Diego, USA).

## Results

### Receptor-binding

Specific receptor-binding assays for the  $\beta_1$ -AR and  $\beta_2$ -AR were used to measure the affinity of zilpaterol to these receptors. The binding curves in Figure 2 show that zilpaterol did bind to the  $\beta_2$ -AR ( $K_i = 1.0 \times 10^{-6}$  M), although with a lower affinity compared to ICI 118551 ( $K_i = 1.3 \times 10^{-9}$  M) and clenbuterol ( $K_i = 4.2 \times 10^{-8}$  M). The  $K_i$  of the three compounds were significantly different ( $p < 0.05$ , F-test). The binding of zilpaterol to the  $\beta_1$ -AR ( $K_i = 1.0 \times 10^{-5}$  M) was found to be weaker than to the  $\beta_2$ -AR in this assay. The difference in  $K_i$  was significantly different ( $p < 0.05$ , F-test).

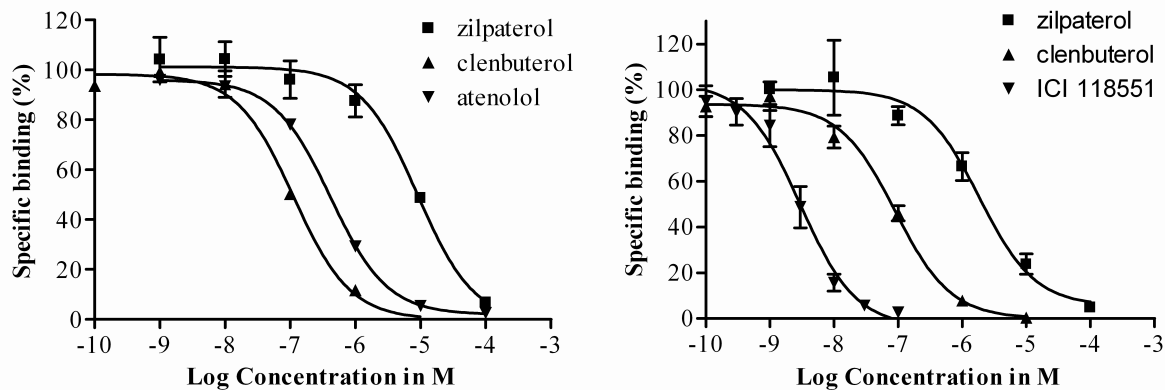


**Figure 2** Receptor binding curves of zilpaterol to the  $\beta_1$ -AR (left panel) and to the  $\beta_2$ -AR (right panel). Cell membrane homogenates of HEK293 cells transfected with  $\beta_1$ -AR or Sf9 cells transfected with  $\beta_2$ -AR were incubated with [ $^3$ H] CGP 12177 (control radioligand) in the absence or presence of zilpaterol (■), clenbuterol (▲) or reference compound (▼). ICI 118551 was used as reference compound for binding to the  $\beta_2$ -AR and atenolol for  $\beta_1$ -AR binding. The results are expressed as percentage inhibition of control radioligand-specific binding (mean  $\pm$  SD of a triplicate measurement).

### Macrophage activation and TNF- $\alpha$ assay

Although binding to the  $\beta_1$ - and  $\beta_2$ -AR was found to be relatively weak, the role of the two receptors in the biological response of the cell to zilpaterol was investigated. Because other  $\beta_2$ -adrenergic agonists are known to inhibit pro-inflammatory responses of cells in *in vitro* experiments, we investigated if zilpaterol was able to inhibit the TNF- $\alpha$  production of U937 macrophages exposed to LPS. Figure 3 indicates that zilpaterol inhibited the TNF- $\alpha$  release of U937 cells exposed to LPS in a dose-dependent manner. The inhibition was not due to a toxic effect induced by zilpaterol, as indicated by LDH activity in the culture medium of exposed cells. Untreated cells had an LDH activity of  $50.6 \pm 3.4$  U/l, whereas U937 macrophages treated with LPS in combination with  $1 \times 10^{-4}$  M zilpaterol (highest dose) had an LDH activity of  $55.0 \pm 3.1$  U/l. The LDH activities induced by the two treatments were not significantly different ( $p > 0.05$ ). However the inhibition of the LPS-induced TNF- $\alpha$  production by

zilpaterol ( $EC_{50} = 5.8 \times 10^{-9}$  M) was less pronounced than the inhibition by clenbuterol ( $EC_{50} = 7.1 \times 10^{-10}$  M).

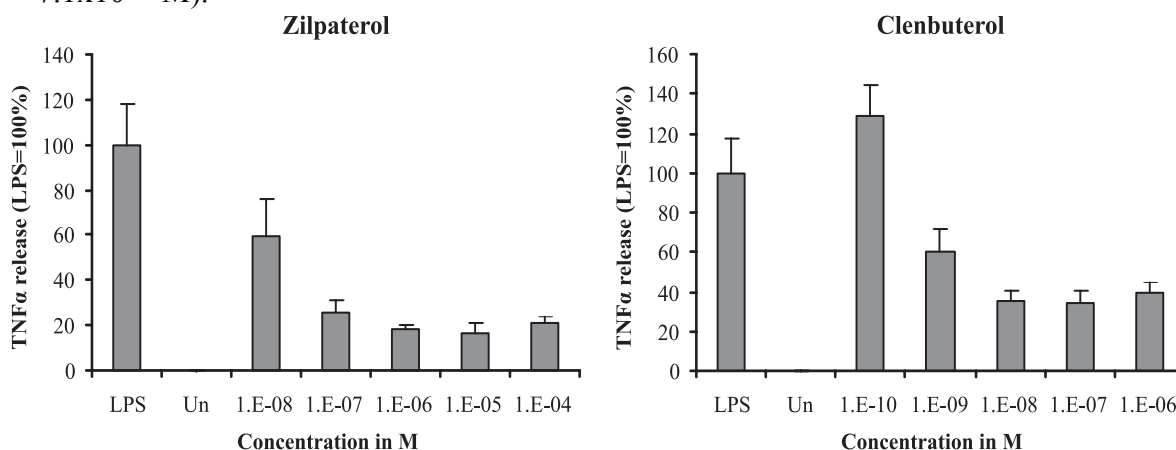


**Figure 3** Inhibition of TNF- $\alpha$  release from untreated U937 macrophages (Un) and macrophages incubated for 4 h with 1  $\mu$ g/ml LPS in the absence (LPS) or presence of a dilution series of zilpaterol ( $1 \times 10^{-8}$ ,  $1 \times 10^{-7}$ ,  $1 \times 10^{-6}$ ,  $1 \times 10^{-5}$ , and  $1 \times 10^{-4}$  M, respectively (left panel) or a dilution series of clenbuterol ( $1 \times 10^{-10}$ ,  $1 \times 10^{-9}$ ,  $1 \times 10^{-8}$ ,  $1 \times 10^{-7}$ , and  $1 \times 10^{-6}$  M, respectively (right panel). The release of TNF- $\alpha$  is corrected for protein content and calculated with respect to the TNF- $\alpha$  release from U937 cells exposed to LPS alone ( $17.3 \pm 5.5$  ng/ml). The results are presented as means  $\pm$  SD (n=6).

This difference in inhibitory effect was statistically significant ( $p < 0.05$ , F-test). The involvement of  $\beta$ -ARs in the inhibitory effect of zilpaterol on the TNF- $\alpha$  production was investigated by using a selective  $\beta_2$ -AR antagonist, ICI 118551, a selective  $\beta_1$ -AR antagonist, atenolol, and a non-selective  $\beta$ -AR antagonist, propranolol ( $\beta_1$  and  $\beta_2$ ). From Figure 4 it can be concluded that the inhibition of the TNF- $\alpha$  release was reversed in a dose-dependent manner by both ICI 118551 and propranolol, whereas atenolol did not affect the inhibitory effect of zilpaterol on the TNF- $\alpha$  production completely. The inhibitory effect was slightly reversed at a concentration of  $1 \times 10^{-5}$  M.

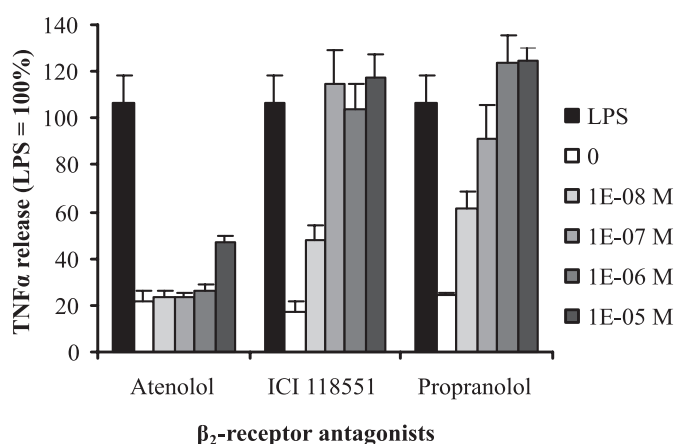


**Figure 4** Effect of  $\beta_2$ -AR antagonists on the inhibition of TNF- $\alpha$  production by zilpaterol. U937 macrophages were exposed to 1  $\mu$ g/ml LPS (black bars), LPS in combination with  $1 \times 10^{-6}$  M zilpaterol (white bars) or LPS in combination with zilpaterol in the presence of a dilution series of atenolol, ICI 118551 or propranolol (from left to right;  $1 \times 10^{-8}$ ,  $1 \times 10^{-7}$ ,  $1 \times 10^{-6}$ , and  $1 \times 10^{-5}$  M respectively). The release of TNF- $\alpha$  is corrected for protein content and calculated with respect to the TNF- $\alpha$  release from U937 cells exposed to LPS alone ( $22.2 \pm 6.8$  ng/ml). The results are presented as means  $\pm$  SD (n=6).

### Measurements of intracellular cAMP formation

$\beta$ -ARs belong to the GPCR family and are known to activate Gs proteins, which subsequently stimulate the production of cAMP. Therefore it was investigated if zilpaterol was able to induce intracellular cAMP levels. As shown in Figure 5 (left panel), zilpaterol induced the cAMP production in a dose-dependent manner. The addition of LPS alone had no effect on the cAMP production. Propranolol, ICI 118551, and atenolol inhibited the production of cAMP by zilpaterol in combination with LPS. However the effect of atenolol was less pronounced (Fig. 5). From these results can be concluded that the stimulation of cAMP production by zilpaterol was mainly mediated by the  $\beta_2$ -AR and weakly by the  $\beta_1$ -AR.

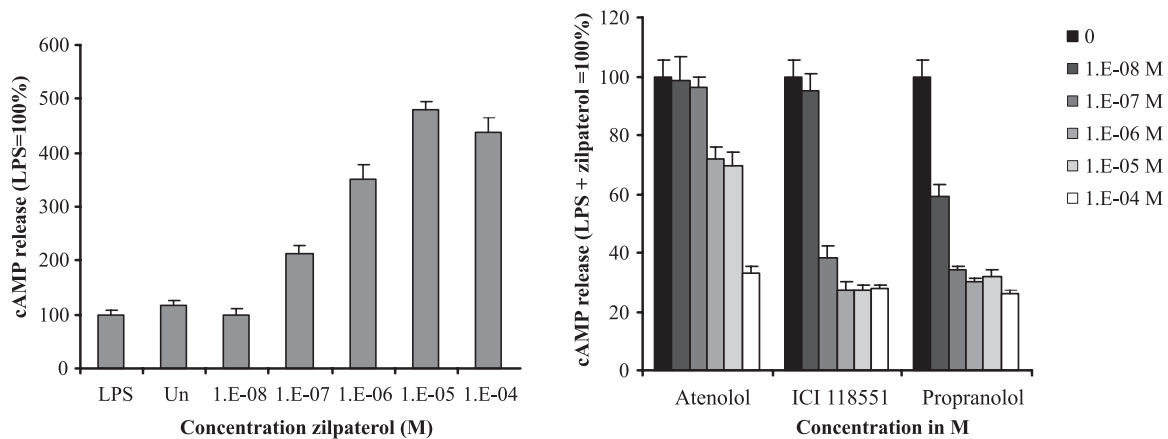


**Figure 5** Left panel: induction of cAMP release by U937 macrophages untreated (Un) and treated with 1  $\mu$ g/ml LPS in the absence (LPS) or presence of a dilution series of zilpaterol ( $1 \times 10^{-8}$ ,  $1 \times 10^{-7}$ ,  $1 \times 10^{-6}$ ,  $1 \times 10^{-5}$  and  $1 \times 10^{-4}$  M, respectively). Right panel: the effect of  $\beta$ -AR antagonists, atenolol, ICI 118551 and propranolol on the inducing effect of zilpaterol on cAMP production. U937 macrophages were exposed to 1  $\mu$ g/ml LPS in combination with  $1 \times 10^{-5}$  M zilpaterol (black bars) or LPS in combination with zilpaterol in the presence of a dilution series of the three  $\beta$ -AR antagonists mentioned above (from left to right;  $1 \times 10^{-8}$ ,  $1 \times 10^{-7}$ ,  $1 \times 10^{-6}$ ,  $1 \times 10^{-5}$ , and  $1 \times 10^{-4}$  M, respectively). The release of cAMP is calculated with respect to the cAMP release from U937 cells exposed to LPS alone (left panel) or LPS in combination with zilpaterol (right panel). The highest cAMP level measured was  $85.4 \pm 6.8$  pmol/ml for U937 macrophages incubated with LPS in combination with  $1 \times 10^{-4}$  M zilpaterol. The data are represented as means  $\pm$  SD (n=6).

### In vivo effect of zilpaterol on TNF- $\alpha$ release

The inhibitory effect of zilpaterol on the TNF- $\alpha$  production *in vitro* reflects the effects of other  $\beta_2$ -AR agonist, such as clenbuterol<sup>12, 13</sup>. In order to investigate whether zilpaterol could also inhibit the TNF- $\alpha$  production *in vivo*, the effects of zilpaterol on rats exposed to LPS was examined. Two hours after administration of LPS, rats showed high plasma levels of TNF- $\alpha$  (Fig. 6). TNF- $\alpha$  production was markedly inhibited by the treatment of rats with 500  $\mu$ g/kg zilpaterol. The treatment of rats with saline or zilpaterol alone had no effect on the TNF- $\alpha$  production; however the administration of zilpaterol alone did have a clear effect on the

bodyweight of the animals. The increase in bodyweight (mean increase in bodyweight  $12.7 \pm 5.5$  g) was significantly ( $p = 0.026$ , Mann-Whitney test, two tailed) enhanced with respect to the control group (mean increase in bodyweight:  $4.9 \pm 4.0$  g). As zilpaterol was originally designed for this purpose, it is therefore of interest to note that this effect is already visible after one day of treatment of rats with only a single dose of 500  $\mu\text{g}/\text{kg}$  zilpaterol.

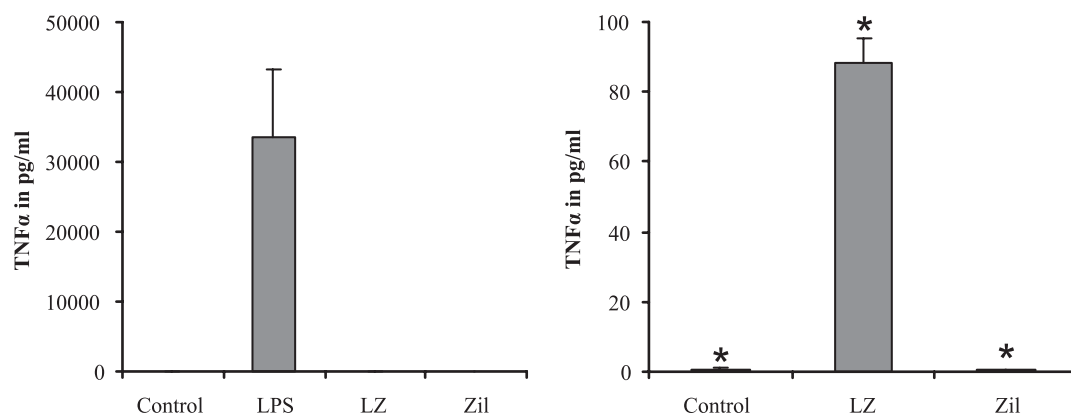


**Figure 6** Effect of zilpaterol on TNF- $\alpha$  plasma levels, 2 hours after administration of LPS or saline. Rats were orally administered with saline one hour before intra-peritoneal injection of saline (Control) or before intra-peritoneal injection of 2 mg/kg bodyweight LPS (LPS), orally administered zilpaterol (500  $\mu\text{g}/\text{kg}$  bodyweight) one hour before LPS-challenge (LZ) or orally administered zilpaterol (500  $\mu\text{g}/\text{kg}$  bodyweight) one hour before intra-peritoneal injection of saline (Zil). The left panel shows the results of all treated groups and in the right panel the LPS group is omitted. The TNF- $\alpha$  plasma levels are presented as means of 6 animals  $\pm$  SEM. \* indicates significant difference with respect to LPS ( $p < 0.05$ ) according to one way ANOVA followed by the Bonferroni's multiple Comparison Test.

## Discussion

In this study, the affinity of zilpaterol for the  $\beta_1$ -AR and  $\beta_2$ -AR was investigated using specific receptor-binding assays. Like clenbuterol, zilpaterol binds to the  $\beta_1$ -AR as well as the  $\beta_2$ -AR, although clenbuterol binds to both receptors more potently.

Furthermore the U937 macrophage was used to investigate the immuno-modulating properties of zilpaterol and its mechanisms of action. The U937 cell line is a well established in vitro model system for human macrophages that express both the  $\beta_1$ -AR as well as the  $\beta_2$ -AR<sup>13</sup>. Zilpaterol inhibits TNF- $\alpha$  release from U937 macrophages exposed to LPS in a dose-dependent manner and this inhibitory effect is mainly mediated by the  $\beta_2$ -AR. To achieve the same inhibitory effect as clenbuterol on the TNF- $\alpha$  release, at least a ten times higher dose for zilpaterol is needed.

Activation of the  $\beta$ -ARs results in a Gs protein-mediated activation of adenylate cyclase, which subsequently catalyses the conversion of ATP in to cAMP<sup>17-22</sup>. Enhanced levels of

cAMP have been found to result in the inhibition of TNF- $\alpha$  production stimulated either *in vivo* or *in vitro* with LPS<sup>23,24</sup>. This is in line with our findings that zilpaterol inhibits the TNF- $\alpha$  production and augments the cAMP production in a dose-dependent manner. The induction of cAMP can be mediated by both the  $\beta_1$ -AR and the  $\beta_2$ -AR, but our results demonstrate that the induction of cAMP by zilpaterol in U937 macrophages is mediated by the  $\beta_2$ -AR and to a lesser extent by the  $\beta_1$ -AR. This study demonstrates that the inhibitory effect on the TNF- $\alpha$  production is mainly mediated via the  $\beta_2$ -receptor. The effect of zilpaterol on TNF- $\alpha$  production and cAMP reflects the effects of other  $\beta_2$ -AR agonists *in vitro*. Salmeterol inhibits the release of TNF- $\alpha$  from LPS-stimulated THP-1 cells and inhibits the LPS-induced increase of murine serum TNF- $\alpha$  levels *in vivo*<sup>28</sup>. Moreover, isoproterenol which inhibits the TNF- $\alpha$  production in THP-1 cells, also increases intracellular cAMP levels<sup>29</sup>. Similar results have been observed for clenbuterol both *in vivo* and *in vitro*<sup>12,13</sup>. Our results show that zilpaterol is a potent inhibitor of TNF- $\alpha$  plasma levels of rats exposed to LPS. Clinical observations were in line with the TNF- $\alpha$  data, as the animals receiving zilpaterol did not show the typical effects of LPS e.g. low body temperature, in-appetite and lower activity. In conclusion, this study demonstrates that zilpaterol is a  $\beta_2$ -adrenergic receptor agonist and an inhibitor of TNF- $\alpha$  release, both *in vitro* and *in vivo*.

### **Acknowledgement**

The authors thank the collaborators from the animal department at TNO in Zeist for performing the animal study.

---

**References**

- 1 Birkelo, C. P., *Vet Clin North Am Food Anim Pract*, **2003**, Pharmaceuticals, direct-fed microbials, and enzymes for enhancing growth and feed efficiency of beef, *19*, 599-624, vi.
- 2 Ricks, C. A., Dalrymple, R. H., Baker, P. K. and Ingle, D. L., *Journal of animal science*, **1984**, Use of a beta-agonist to alter fat and muscle deposition in steers, *59*, 1247-1255.
- 3 Spann, C. and Winter, M. E., *Ann Pharmacother*, **1995**, Effect of clenbuterol on athletic performance, *29*, 75-77.
- 4 Goubault, C., Perault, M. C., Leleu, E., Bouquet, S., *et al.*, *Thorax*, **2001**, Effects of inhaled salbutamol in exercising non-asthmatic athletes, *56*, 675-679.
- 5 Torneke, K., Ingvast Larsson, C. and Appelgren, L. E., *J Vet Pharmacol Ther*, **1998**, A comparison between clenbuterol, salbutamol and terbutaline in relation to receptor binding and in vitro relaxation of equine tracheal muscle, *21*, 388-392.
- 6 Diamant, Z. and Dekhuijzen, P. N. R., *Ned. Tijdschr Geneesk*, **2003**, Behandeling van matig, persisterend astma: Inhalatiecorticosteroiden combineren met langwerkende beta2adrenerge agonisten (luchtwegverwijders) dan wel met leukotrienreceptoragonisten (ontstekingsremmers); het 'stap-3-dilemma', *147*, 1681-1685.
- 7 Johnson, M., *Agents Actions Suppl*, **1993**, Beta 2-agonists as anti-inflammatory therapies in the lung, *41*, 27-45.
- 8 Sears, M. R., *Can Respir J*, **1998**, Asthma treatment: Inhaled beta-agonists, *5 Suppl A*, 54A-59A.
- 9 Settignano, R. A., *Allergy Asthma Proc*, **2003**, Defining the effects of an inhaled corticosteroid and long-acting beta-agonist on therapeutic targets, *24*, 85-89.
- 10 Barnes, P. J., *J Allergy Clin Immunol*, **1999**, Effect of beta-agonists on inflammatory cells, *104*, S10-17.
- 11 Johnson, M., *J Allergy Clin Immunol*, **2002**, Effects of beta2-agonists on resident and infiltrating inflammatory cells, *110*, S282-290.
- 12 Izeboud, C. A., Monshouwer, M., van Miert, A. S. and Witkamp, R. F., *Inflamm Res*, **1999**, The beta-adrenoceptor agonist clenbuterol is a potent inhibitor of the lps-induced production of tnf-alpha and il-6 in vitro and in vivo, *48*, 497-502.
- 13 Izeboud, C. A., Mocking, J. A., Monshouwer, M., van Miert, A. S. and Witkamp, R. F., *J Recept Signal Transduct Res*, **1999**, Participation of beta-adrenergic receptors on macrophages in modulation of lps-induced cytokine release, *19*, 191-202.
- 14 Intervet, **1998**, Zilmax technical brochure.
- 15 Shelver, W. L. and Smith, D. J., *J Agric Food Chem*, **2004**, Enzyme-linked immunosorbent assay development for the beta-adrenergic agonist zilpaterol, *52*, 2159-2166.
- 16 Bocca, B., Di Mattia, M., Cartoni, C., Fiori, M., *et al.*, *J Chromatogr B Analyt Technol Biomed Life Sci*, **2003**, Extraction, clean-up and gas chromatography-mass spectrometry characterization of zilpaterol as feed additive in fattening cattle, *783*, 141-149.
- 17 Strosberg, A. D., *Protein Sci*, **1993**, Structure, function, and regulation of adrenergic receptors, *2*, 1198-1209.
- 18 Liggett, S. B., *J Allergy Clin Immunol*, **2002**, Update on current concepts of the molecular basis of beta2-adrenergic receptor signaling, *110*, S223-227.
- 19 Lombardi, M. S., Kavelaars, A. and Heijnen, C. J., *Crit Rev Immunol*, **2002**, Role and modulation of g protein-coupled receptor signaling in inflammatory processes, *22*, 141-163.
- 20 Neer, E. J., *Protein Sci*, **1994**, G proteins: Critical control points for transmembrane signals, *3*, 3-14.
- 21 Nurnberg, B., Gudermann, T. and Schultz, G., *J Mol Med*, **1995**, Receptors and g proteins as primary components of transmembrane signal transduction. Part 2. G proteins: Structure and function, *73*, 123-132.
- 22 Ji, T. H., Grossmann, M. and Ji, I., *J Biol Chem*, **1998**, G protein-coupled receptors. I. Diversity of receptor-ligand interactions, *273*, 17299-17302.
- 23 Zidek, Z., *Eur Cytokine Netw*, **1999**, Adenosine - cyclic amp pathways and cytokine expression, *10*, 319-328.
- 24 Kast, R. E., *Int J Immunopharmacol*, **2000**, Tumor necrosis factor has positive and negative self regulatory feed back cycles centered around camp, *22*, 1001-1006.
- 25 Sundstrom, C. and Nilsson, K., *Int J Cancer*, **1976**, Establishment and characterization of a human histiocytic lymphoma cell line (u-937), *17*, 565-577.
- 26 Verhoeckx, K. C., Bijlsma, S., de Groene, E. M., Witkamp, R. F., *et al.*, *Proteomics*, **2004**, A combination of proteomics, principal component analysis and transcriptomics is a powerful tool for the identification of biomarkers for macrophage maturation in the u937 cell line, *4*, 1014-1028.
- 27 Izeboud, C. A., Hoebe, K. H., Grootendorst, A. F., Nijmeijer, S. M., *et al.*, *Inflamm Res*, **2004**, Endotoxin-induced liver damage in rats is minimized by beta 2-adrenoceptor stimulation, *53*, 93-99.

- 28 Sekut, L., Champion, B. R., Page, K., Menius, J. A., Jr. and Connolly, K. M., *Clin Exp Immunol*, **1995**, Anti-inflammatory activity of salmeterol: Down-regulation of cytokine production, *99*, 461-466.
- 29 Severn, A., Rapson, N. T., Hunter, C. A. and Liew, F. Y., *J Immunol*, **1992**, Regulation of tumor necrosis factor production by adrenaline and beta-adrenergic agonists, *148*, 3441-3445.



## Chapter 6

---

### **Beta-adrenergic receptor agonists induce the release of Granulocyte Chemotactic Protein-2, Oncostatin M, and Vascular Endothelial Growth Factor from macrophages.**

Kitty C.M. Verhoeckx<sup>1,2</sup>

Robert P. Doornbos<sup>1</sup>

Jan van der Greef<sup>1,2</sup>

Renger F. Witkamp<sup>1</sup>

Richard J.T. Rodenburg<sup>3</sup>

*Accepted for publication in Int Immunopharmacol*

<sup>1</sup> TNO Quality of Life, Zeist, The Netherlands, <sup>2</sup> Leiden University, Leiden/Amsterdam Center for Drug Research, Leiden, The Netherlands, <sup>3</sup> UMC St Radboud, Nijmegen, The Netherlands

## **Beta-adrenergic receptor agonists induce the release of Granulocyte Chemotactic Protein-2, Oncostatin M, and Vascular Endothelial Growth Factor from macrophages.**

*Vascular endothelial growth factor (VEGF), oncostatin M (OSM), and granulocyte chemotactic protein-2 (GCP-2/CXCL6) are up-regulated in U937 macrophages and peripheral blood macrophages exposed to LPS, beta<sub>2</sub>-adrenergic receptor ( $\beta_2$ -AR) agonists (e.g. zilpaterol, and clenbuterol) and some other agents that induce intracellular cAMP (prostaglandin E<sub>2</sub>, forskolin, and dibutyryl cAMP). LPS in combination with  $\beta_2$ -agonists and cAMP elevating agents had an additional effect on the release of VEGF, OSM, and CXCL6. These proteins are up-regulated after 16-24 h of exposure and this is mediated by the  $\beta_2$ -AR, as determined by time course experiments and the use of a selective  $\beta_2$ -AR antagonist (ICI 118551). Beta<sub>2</sub>-AR agonists are used as bronchodilators in the treatment of asthma, but appear to have no effect on the chronic inflammation of the disease. However, the up-regulation of VEGF, OSM, and CXCL6 may have adverse effects on the inflammatory process of asthma. These mediators are involved in the recruitment of neutrophils, airway remodelling and angiogenesis, known features of chronic inflammatory diseases. We propose that the up-regulation of these proteins could play a role in the adverse effects of prolonged excessive usage of  $\beta_2$ -AR agonists on the airways besides the desensitization of the  $\beta_2$ -AR.*

---

### **Introduction**

Beta<sub>2</sub>-adrenergic agonists are used as bronchodilators in the treatment of pulmonary diseases<sup>1-5</sup>. Although the major action of  $\beta_2$ -agonists on the airways is relaxation of airway smooth muscle, these drugs have several other effects mediated through  $\beta_2$ -adrenergic receptors ( $\beta_2$ -AR) expressed on other cells as well. These additional actions of  $\beta_2$ -agonists may contribute to the efficacy of  $\beta_2$ -agonists in relieving asthma symptoms. Beta<sub>2</sub>-agonists inhibit plasma exudation in the airways by acting on  $\beta_2$ -AR on capillary venule cells. They inhibit the secretion of bronchoconstrictor mediators from eosinophils, macrophages, T-lymphocytes, and neutrophils. Despite these inhibitory effects on inflammatory cells *in vitro*,  $\beta_2$ -agonists do not appear to reduce the chronic inflammation of asthma. Desensitization is more readily seen in inflammatory cells than in airway smooth muscle cells and may account for this discrepancy<sup>6,7</sup>. In a previous paper<sup>8</sup> we described a genomics-based screening methodology to categorize anti-inflammatory drugs. For this purpose, we used U937 macrophages which

were stimulated with LPS in the absence or presence of different classes of anti-inflammatory compounds (e.g. MAP kinase inhibitor, corticosteroid, proteasome inhibitor, and  $\beta_2$ -agonists). Using microarrays the effects on the transcriptome of the exposed cells were investigated. The expression patterns were subsequently analyzed using pattern recognition tools, which revealed that different classes of anti-inflammatory drugs show distinct and characteristic mRNA expression patterns that can be used to categorize known compounds and to discover and classify new leads. We were able to show that zilpaterol, a poorly characterized  $\beta_2$ -agonist, gives rise to an almost identical expression pattern as the  $\beta_2$ -agonists clenbuterol and salbutamol. Furthermore, we identified specific biomarkers, vascular endothelial growth factor (VEGF), oncostatin M (OSM), and granulocyte chemotactic protein-2 (GCP-2/CXCL6) which were exclusively up-regulated by U937 macrophages exposed to LPS in combination with  $\beta_2$ -agonists, compared to the treatment with LPS alone or LPS in combination with other anti-inflammatory compounds (e.g. dexamethasone, SB203580 and proteasome inhibitor). In the present study we investigated if these mRNA markers were also up-regulated at the protein level by peripheral blood macrophages and if these markers are up-regulated by U937 macrophages in a dose-dependent manner. Furthermore, we established if this up-regulation was mediated by the  $\beta_2$ -AR and we followed the course of this regulation in time. In our experiments we used two  $\beta_2$ -AR agonists of a different chemical structure: clenbuterol and zilpaterol.

Clenbuterol was originally designed as a potent bronchodilator but only reached the clinic in a few countries. Nowadays it is mostly known for its anabolic action in athletes and cattle and approved as bronchodilator in horses <sup>1,9</sup>. Zilpaterol is a relatively new and rather unknown  $\beta_2$ -AR agonist which was originally designed as an growth promoter in cattle <sup>10</sup>.

$\beta_2$ -agonists signal through  $\beta_2$ -AR receptors which belong to the family of GTP-binding protein-coupled receptors (GPCRs).  $\beta_2$ -AR activates adenylate cyclase via Gs regulatory proteins. Binding to the  $\beta_2$ -AR results in the production of the second messenger cyclic adenosine-3',5'-cyclic monophosphate (cAMP) <sup>11-16</sup>, which is involved in many metabolic pathways <sup>13, 16-20</sup>. We investigated if cAMP is involved in the up-regulation of VEGF, OSM, and CXCL6. Therefore we incubated U937 macrophages with cAMP elevating agents; prostaglandin E<sub>2</sub> (PGE<sub>2</sub>) which induces cyclic AMP by binding to its own receptor, forskolin, a direct activator of adenylate cyclase and the membrane permeable stable derivate of cAMP, dibutyryl cAMP, in the absence or presence of LPS.

## Materials and Methods

### *Chemicals*

Lipopolysaccharide (LPS, *E.coli* 0111:B4), ICI 118551, clenbuterol, dibutyryl cAMP, prostaglandin E<sub>2</sub>, forskolin were obtained from Sigma Aldrich (St. Louis, MO, USA) and zilpaterol from Intervet Inc. (Millsboro, US).

### *Cell cultures*

Human monocyte-like histiocytic lymphoma cells U937<sup>21</sup> obtained from the ATCC (CRL-1593.2) were grown in RPMI-1640 medium, supplemented with 10% (v/v) fetal calf serum and 2 mM L-glutamine (Life technologies, Breda, The Netherlands) at 37 °C and 5% CO<sub>2</sub> in a humidified atmosphere. U937 monocytic cells were differentiated into macrophages using phorbol 12-myristate 13-acetate (PMA, 10 ng/ml, overnight, Omnilabo, Breda, The Netherlands) as described previously<sup>22</sup>. The PMA-differentiated macrophages were allowed to recover from the PMA treatment for 48 h, during which the culture medium was replaced daily.

Peripheral blood monocytes (PB-MO) were isolated from human EDTA-blood with Rosette Sep<sup>TM</sup> human monocyte enrichment cocktail (Stemcell Technologies Inc, Meylan, France) as described previously<sup>22</sup>. The monocytes (0.5x10<sup>6</sup> cells per well) were cultured in 24 well cell culture plates containing RPMI-1640 medium supplemented with 10% (v/v) human serum and 2 mM L-glutamine and were allowed to differentiate into peripheral blood macrophages (PB-MØ) for eight days. Following this procedure, the macrophage maturation has been described to give rise to the characteristically morphology and phenotype of primary macrophages<sup>23</sup>.

### *Macrophage activation*

U937 macrophages were cultured at a concentration of 1x10<sup>6</sup> cells per well. Cells were incubated for 16 h with LPS (1 µg/ml), LPS in the presence of a dilution series of zilpaterol (1x10<sup>-8</sup> - 1x10<sup>-4</sup> M), or LPS in the presence of a dilution series of clenbuterol (1x10<sup>-10</sup> - 1x10<sup>-6</sup> M) respectively.

Human PB-MØ were cultured in 12 well plates at a concentration of 1x10<sup>6</sup> cells per well and pre-incubated with 1x10<sup>-6</sup> M zilpaterol or 1x10<sup>-7</sup> M clenbuterol at 37 °C. After 30 minutes LPS (1 µg/ml) was added and the cells were incubated for a further 16 h at 37 °C. For the time course experiments U937 cells (1x10<sup>6</sup> cells per well) were incubated with LPS (1 µg/ml), LPS in the presence of  $\beta_2$ -AR agonists (1x10<sup>-6</sup> M zilpaterol or 1x10<sup>-7</sup> M clenbuterol), or LPS in the

presence of  $\beta_2$ -AR agonists in combination with ICI 118551 (equal concentration as  $\beta_2$ -AR agonist). Culture medium was collected at 8, 16, and 24 h respectively. Furthermore, U937 macrophages were incubated with cAMP elevating compounds, dibutyryl cAMP ( $1 \times 10^{-4}$  M), forskolin ( $1 \times 10^{-5}$  M), prostaglandin E<sub>2</sub> ( $1 \times 10^{-4}$  M), zilpaterol ( $1 \times 10^{-6}$  M), and clenbuterol ( $1 \times 10^{-7}$  M) in the presence or absence of 1  $\mu$ g/ml LPS. The concentrations of the various compounds were chosen as such to achieve similar levels of TNF- $\alpha$  inhibition. All incubations were performed in triplicate. The culture medium was collected and stored at -20 °C until analysis. The cells were lysed in 0.1 M NaOH and used for protein determination by the modified method of Bradford (Bio-Rad, Veenendaal, The Netherlands).

#### *Enzyme-Linked Immunosorbent Assays (ELISA)*

The concentration of VEGF, OSM and CXCL6 in the culture supernatants were determined by ELISA. Immunoassays for CXCL6 and oncostatin M were purchased from R&D systems (Oxon, UK). The VEGF ELISA was obtained from Prepotech (London, UK). The immunoassays were performed according to the manufactures instructions. The enzyme activity of lactate dehydrogenase (LDH) was quantitatively determined using the *in vitro* assay for LDH activity from Roche Diagnostics (Mannheim, Germany) for automated clinical chemistry analyzer Hitachi 911 (Hitachi, Japan).

#### **Results**

Beta<sub>2</sub>-AR agonists, zilpaterol and clenbuterol induced the release of VEGF, OSM and CXCL6 by U937 macrophages exposed to LPS in a dose-dependent manner (Fig. 1). The concentrations used were not toxic, as was determined by measuring LDH activity in the culture medium of exposed cells (data not shown). Clenbuterol induced the release of the three proteins more potently than zilpaterol, as was demonstrated by the lower concentration needed, but a lower maximum was obtained.

To investigate if the release of these compounds was not restricted to tumor cells like the human monocyte-like histiocytic lymphoma U937 cells, we used macrophages derived from freshly isolated peripheral blood monocytes from healthy donors, in order to confirm the inducing effect of  $\beta_2$ -AR agonists on the VEGF, OSM and CXCL6 release. The concentrations of zilpaterol and clenbuterol used showed maximum up-regulation of the three compounds and equally inhibited the TNF- $\alpha$  release (data not shown). From Figure 2 it can be concluded that the release of VEGF, OSM as well as CXCL6 were significantly augmented by zilpaterol as well as clenbuterol, both in combination with LPS.

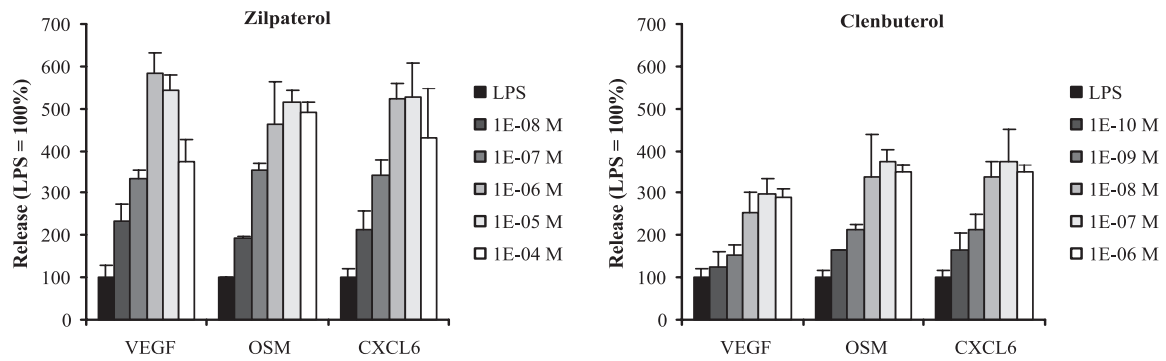


**Figure 1** Induction of VEGF, OSM, and CXCL6 release from U937 macrophages incubated for 16 h with 1  $\mu$ g/ml LPS in the absence (black bars) or presence of a dilution series of zilpaterol ( $1 \times 10^{-8}$ ,  $1 \times 10^{-7}$ ,  $1 \times 10^{-6}$ ,  $1 \times 10^{-5}$ , and  $1 \times 10^{-4}$  M respectively) or a dilution series of clenbuterol ( $1 \times 10^{-10}$ ,  $1 \times 10^{-9}$ ,  $1 \times 10^{-8}$ ,  $1 \times 10^{-7}$ , and  $1 \times 10^{-6}$  M respectively). The release of VEGF, OSM, and CXCL6 was determined by ELISA, corrected for protein content and calculated with respect to the release from U937 cells exposed to LPS alone. The results are presented as means  $\pm$  SD of a triplicate measurement.

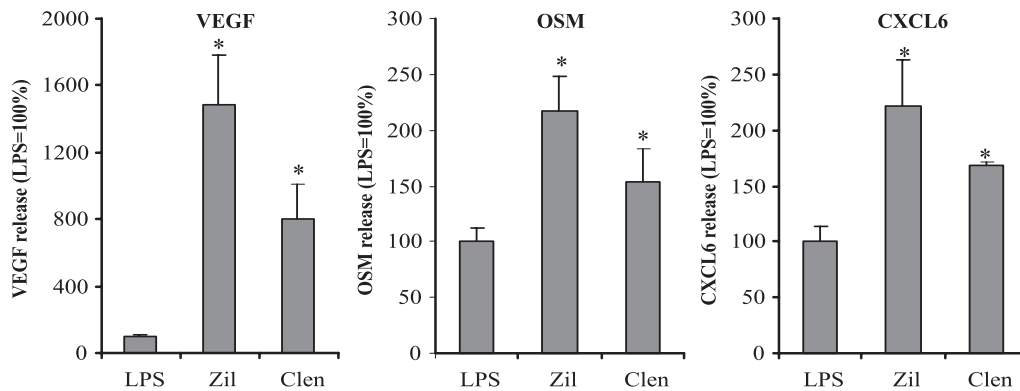


**Figure 2** Release of VEGF, OSM, and CXCL6 by peripheral blood macrophages exposed to 0.1  $\mu$ g/ml LPS in the absence (LPS) or presence of  $1 \times 10^{-6}$  M zilpaterol (Zil) or  $1 \times 10^{-7}$  M clenbuterol (Clen). The release of VEGF, OSM, and CXCL6 is corrected for protein content and calculated with respect to the release from PB-M $\emptyset$  exposed to LPS alone. The results are presented as means  $\pm$  SD of a triplicate measurement. \* Different according to Student's *t*-test (assuming normal distributions and equal variance,  $p < 0.05$ ). The *p*-values are calculated with respect to PB-M $\emptyset$  cells treated with LPS alone.

Since  $\beta_2$ -AR agonists mediate their effect via the  $\beta_2$ -AR, we investigated if the  $\beta_2$ -AR was involved in the inducing effect of zilpaterol and clenbuterol on the VEGF, OSM, and CXCL6 production by using a selective  $\beta_2$ -AR antagonist ICI 118551. From Figure 3 it can be concluded that the induction of the three compounds was reversed by the addition of ICI 118551. Figure 3 also shows that the release of VEGF, OSM and CXCL6 was particularly induced at longer incubation times and that this induction was also achieved by U937 cells exposed to LPS in the absence of the  $\beta_2$ -AR agonists, or LPS in combination with a  $\beta_2$ -AR agonist and ICI 118551.

Since the main pathway by which activation of  $\beta$ -ARs exerts their effects is related to the elevation of intracellular cyclic AMP levels, we determined the effect of other agents which are known to elevate intracellular cyclic AMP levels. U937 macrophages were incubated in the presence or absence of LPS with or without  $\beta$ -AR agonists or cAMP elevating compounds.

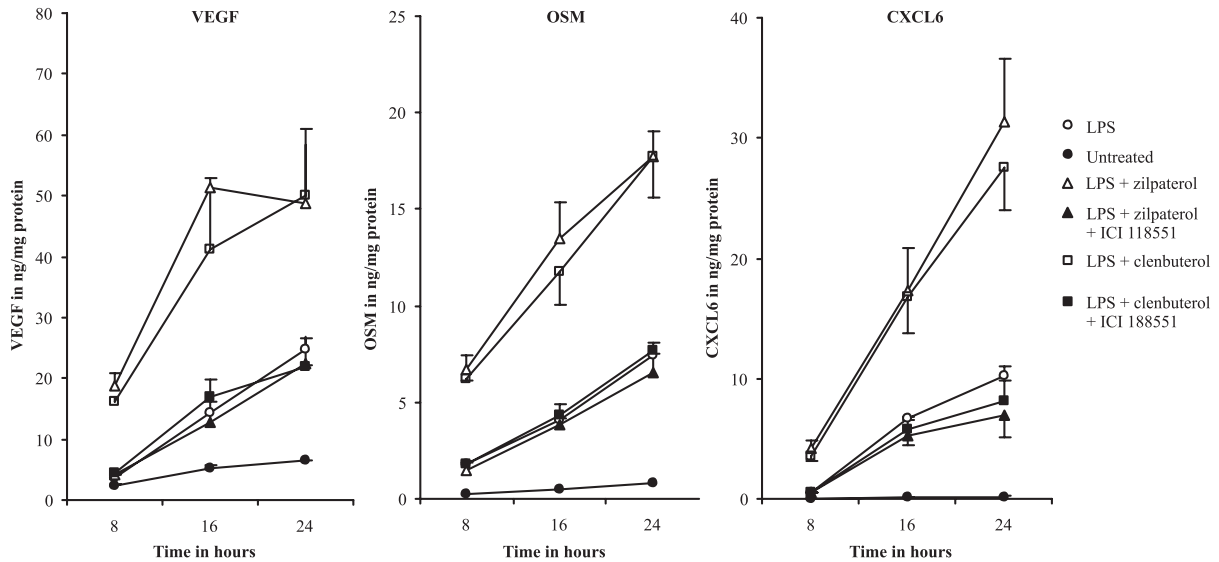


**Figure 3** Release of VEGF, OSM, and CXCL6 from untreated U937 macrophages, U937 macrophages after exposure to LPS (1  $\mu$ g/ml) alone, LPS in combination with  $1 \times 10^{-6}$  M zilpaterol, LPS in combination with  $1 \times 10^{-7}$  M clenbuterol, LPS in combination with zilpaterol and  $1 \times 10^{-6}$  M ICI 118551, or LPS in combination with clenbuterol and  $1 \times 10^{-7}$  M ICI 118551. The levels of VEGF, OSM, and CXCL6 released by the macrophages in the culture medium were determined at the time points indicated and are corrected for protein content. The results are presented as means  $\pm$  SD of triplicate measurements.

Figure 4 shows that forskolin, butyryl cAMP,  $PGE_2$ , the two  $\beta$ -AR agonists all significantly induced the release of VEGF, OSM and CXCL6 from U937 macrophages. Exposure to LPS also gave rise to an increase in the release of these proteins. Interestingly, exposure of U937 cells to a combination of LPS and either a  $\beta$ -AR agonist or a c-AMP elevating compound resulted in an even higher induction of the release of the three proteins. Only the addition of  $PGE_2$  to LPS exposed U937 macrophages had no significant additional effect on the VEGF release compared to U937 macrophages exposed to LPS alone. These results indicate that VEGF, OSM, and CXCL6 were induced via a cAMP-dependent pathway. The release of the three proteins was elevated by LPS,  $\beta$ -AR agonists and cAMP-elevating agents. The production is induced even more when the U937 macrophages are simultaneously treated with LPS and cAMP-elevated agents or  $\beta$ -AR agonists.

## Discussion

Our results demonstrate that VEGF, OSM and GCP-2/CXCL6 release from U937 macrophages and peripheral blood macrophages exposed to LPS are up-regulated by  $\beta_2$ -AR agonists via the  $\beta_2$ -AR and a cAMP dependent pathway. The expression of these markers is a relatively late event, as they become apparent 16 h after addition of the  $\beta_2$ -AR agonists. This contrasts the immediate effects of  $\beta_2$ -AR agonists on smooth muscle. Relaxation of smooth muscle, the main action of  $\beta_2$ -agonists, occurs directly after inhalation until approximately 20 hours after inhalation<sup>3-5</sup>.

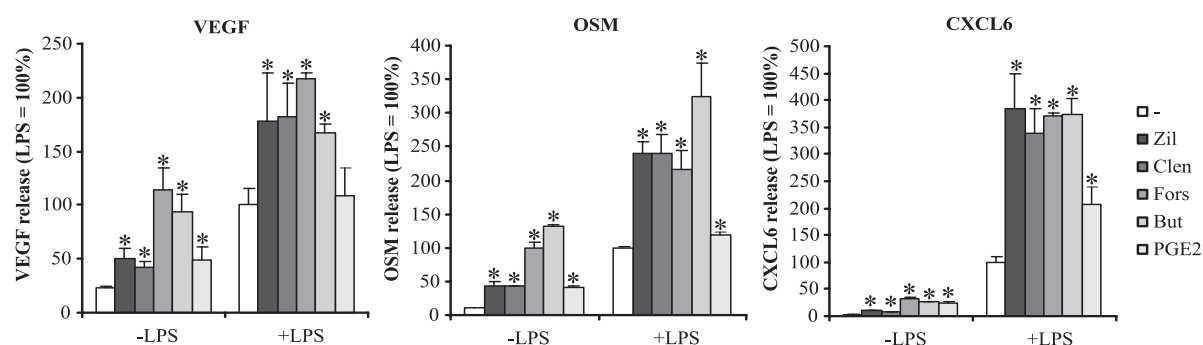


**Figure 4** Release of VEGF (A), OSM (B), and CXCL6 (C) from U937 macrophages (-) or U937 macrophages incubated for 24 h with  $\beta_2$ -adrenergic agonists;  $1 \times 10^{-6}$  M zilpaterol (Zil),  $1 \times 10^{-7}$  M, clenbuterol (Clen), or cAMP elevating agents;  $1 \times 10^{-5}$  M forskolin (Fors),  $1 \times 10^{-4}$  M butyryl cAMP (Butyl), or  $1 \times 10^{-4}$  M prostaglandin E<sub>2</sub> (PGE<sub>2</sub>) respectively in the absence (-LPS) or presence of 1  $\mu$ g/ml LPS (+LPS). The concentrations of the various compounds were chosen as such to achieve similar levels of TNF- $\alpha$  inhibition. The release of VEGF, OSM, and CXCL6 is corrected for protein content and represented as mean percentage of LPS induction (LPS=100%)  $\pm$  SD of triplicate measurements. \* Significant difference according to Student's *t*-test (assuming normal distributions and equal variance,  $p < 0.05$ ). The *p*-values of the +LPS group were calculated with respect to U937 cells treated with LPS alone, and for -LPS group with respect to untreated U937 macrophages.

VEGF is a growth factor and is involved in angiogenesis, lymphangiogenesis, endothelial cell growth<sup>24</sup>, and is mainly produced by macrophages. VEGF stimulates inflammatory cell recruitment and promotes the expression of proteases implicated in pericellular matrix degradation in angiogenesis<sup>25</sup>. Angiogenesis and microvascular remodelling are known features of chronic inflammatory diseases<sup>26</sup>. The newly formed vessels facilitate leukocyte influx and leak plasma proteins into the airway mucosa.<sup>27</sup> VEGF is highly expressed in asthmatic airways<sup>28</sup>, and it can be envisioned that VEGF plays a role in the formation of new vessels and remodelling in asthmatic tissue<sup>26</sup>. However,  $\beta_2$ -agonists have been shown to decrease the plasma protein leakage and reduce the infiltration of inflammatory cells (e.g. neutrophils)<sup>26</sup>. This suggests that the effects of  $\beta_2$ -agonists on VEGF release are counterbalanced by other, more favourable effects of  $\beta_2$ -agonists. In previously published

reports, VEGF was shown to be up-regulated by LPS, cAMP, PGE<sub>2</sub>, and forskolin in human macrophages<sup>27, 29, 30</sup> with a peak release after 24 h. This is in line with our findings that cAMP is involved in the up-regulation of VEGF and that it is a relatively late biomarker. OSM belongs to the Interleukin (IL)-6 subfamily and is involved in growth regulation, differentiation, inflammatory response, hematopoiesis, tissue remodelling, and development<sup>31</sup>. OSM is secreted from activated T cells, monocytes and macrophages<sup>31, 32</sup>. The role of OSM is ambiguous. OSM is considered to be a late phase cytokine that inhibits the production or modulates the activities of initiators of the inflammatory response (e.g. IL-1 and TNF- $\alpha$ )<sup>33</sup>. On the other hand it has been shown that OSM also possesses pro-inflammatory properties<sup>32, 34</sup>. O'Hara et al<sup>34</sup> suggested that OSM may play a role in the development of airway wall remodelling by deposition of collagen in the sub-epithelial basement membrane and, as a consequence, may be a suitable target for further research in the pathogenesis of asthma and its treatment. Furthermore, OSM is able to increase VEGF release and thus indirectly may contribute to airway remodelling observed in chronic airways disease<sup>32, 35</sup>. Our results suggesting that cAMP is involved in the induction of OSM is in agreement with previous findings that PGE<sub>2</sub>, and forskolin up-regulate the release of OSM in human airway smooth muscles<sup>34</sup>, and microglia, the resident macrophages of the brain<sup>36</sup>. CXCL6 or GCP-2 is a CXC chemokine and is closely related to Interleukin 8. CXCL6 predominantly exert stimulatory and chemotactic activities towards neutrophils<sup>37, 38</sup>. The CXCL6 expression has been reported to be regulated by a variety of inflammatory mediators, including IL-1 $\beta$  and TNF- $\alpha$ <sup>37, 39</sup>. Recently it has been shown that Interleukin 17 levels are increased in the airways of patients with asthma. Furthermore, it was suggested that Interleukin 17 may play a role in the recruitment of airway neutrophils by releasing CXCL6 and IL-8 in human bronchial epithelial cells<sup>40</sup>. Accumulation and activation of neutrophils can lead to a release of proteases and reactive oxygen free radicals that can contribute to mucus secretion, airway remodelling and lung tissue destruction, key characteristics of severe acute asthma<sup>40</sup>. The induction of CXCL6 by cAMP has to our knowledge not been published to date.

In conclusion, our results revealed that VEGF, OSM and CXCL6 were up-regulated in macrophages exposed to LPS and  $\beta_2$ -AR agonists via the  $\beta_2$ -AR and a cAMP dependent pathway. We can only speculate about the possible adverse effects of the release of VEGF, OSM, and CXCL6 on the development of asthma. In spite of inhibiting the inflammatory response, these proteins induce the recruitment of neutrophils, cause airway remodelling and

angiogenesis, known features of chronic inflammatory diseases. The up-regulation of these proteins in a late stadium may play a role in the increased airway hyper-responsiveness to allergen after prolonged excessive usage of  $\beta_2$ -agonists, besides the desensitization of the  $\beta_2$ -AR<sup>3-5</sup>. In a previous study<sup>8</sup> we already showed that VEGF, OSM and CXCL6 were significantly down-regulated by the corticosteroid dexamethasone. This may provide an additional explanation for the preferred usage of inhaled corticosteroids in combination with  $\beta_2$ -adrenergic agonists besides the usage of the  $\beta_2$ -ARs alone.

## References

- 1 Torneke, K., Ingvast Larsson, C. and Appelgren, L. E., *J Vet Pharmacol Ther*, **1998**, A comparison between clenbuterol, salbutamol and terbutaline in relation to receptor binding and in vitro relaxation of equine tracheal muscle, *21*, 388-392.
- 2 Diamant, Z. and Dekhuijzen, P. N. R., *Ned. Tijdschr Geneesk*, **2003**, Behandeling van matig, persisterend astma: Inhalatiocorticosteroiden combineren met langwerkende beta2adrenerge agonisten (luchtwegverwijders) dan wel met leukotrieenreceptoragonisten (ontstekingsremmers); het 'stap-3-dilemma', *147*, 1681-1685.
- 3 Johnson, M., *Agents Actions Suppl*, **1993**, Beta 2-agonists as anti-inflammatory therapies in the lung, *41*, 27-45.
- 4 Sears, M. R., *Can Respir J*, **1998**, Asthma treatment: Inhaled beta-agonists, *5 Suppl A*, 54A-59A.
- 5 Settupane, R. A., *Allergy Asthma Proc*, **2003**, Defining the effects of an inhaled corticosteroid and long-acting beta-agonist on therapeutic targets, *24*, 85-89.
- 6 Barnes, P. J., *J Allergy Clin Immunol*, **1999**, Effect of beta-agonists on inflammatory cells, *104*, S10-17.
- 7 Johnson, M., *J Allergy Clin Immunol*, **2002**, Effects of beta2-agonists on resident and infiltrating inflammatory cells, *110*, S282-290.
- 8 Verhoeckx, K. C., Bijlsma, S., Jespersen, S., Ramaker, R., *et al.*, *Int Immunopharmacol*, **2004**, Characterization of anti-inflammatory compounds using transcriptomics, proteomics, and metabolomics in combination with multivariate data analysis, *4*, 1499-1514.
- 9 Chodorowski, Z. and Sein Anand, J., *Przegl Lek*, **1997**, Acute poisoning with clenbuterol--a case report, *54*, 763-764.
- 10 Intervet, **1998**, Zilmax technical brochure.
- 11 Wisdom, R., *Exp Cell Res*, **1999**, Ap-1: One switch for many signals, *253*, 180-185.
- 12 Zidek, Z., *Eur Cytokine Netw*, **1999**, Adenosine - cyclic amp pathways and cytokine expression, *10*, 319-328.
- 13 Lombardi, M. S., Kavelaars, A. and Heijnen, C. J., *Crit Rev Immunol*, **2002**, Role and modulation of g protein-coupled receptor signaling in inflammatory processes, *22*, 141-163.
- 14 Zidek, Z., *Eur Cytokine Netw*, **2001**, Role of cytokines in the modulation of nitric oxide production by cyclic amp, *12*, 22-32.
- 15 Hasko, G., Nemeth, Z. H., Szabo, C., Zsilla, G., *et al.*, *Brain Res Bull*, **1998**, Isoproterenol inhibits il-10, tnf-alpha, and nitric oxide production in raw 264.7 macrophages, *45*, 183-187.
- 16 Liggett, S. B., *J Allergy Clin Immunol*, **2002**, Update on current concepts of the molecular basis of beta2-adrenergic receptor signaling, *110*, S223-227.
- 17 Strosberg, A. D., *Protein Sci*, **1993**, Structure, function, and regulation of adrenergic receptors, *2*, 1198-1209.
- 18 Neer, E. J., *Protein Sci*, **1994**, G proteins: Critical control points for transmembrane signals, *3*, 3-14.
- 19 Nurnberg, B., Gudermann, T. and Schultz, G., *J Mol Med*, **1995**, Receptors and g proteins as primary components of transmembrane signal transduction. Part 2. G proteins: Structure and function, *73*, 123-132.
- 20 Ji, T. H., Grossmann, M. and Ji, I., *J Biol Chem*, **1998**, G protein-coupled receptors. I. Diversity of receptor-ligand interactions, *273*, 17299-17302.
- 21 Sundstrom, C. and Nilsson, K., *Int J Cancer*, **1976**, Establishment and characterization of a human histiocytic lymphoma cell line (u-937), *17*, 565-577.

- 
- 22 Verhoeckx, K. C., Bijlsma, S., de Groene, E. M., Witkamp, R. F., *et al.*, *Proteomics*, **2004**, A combination of proteomics, principal component analysis and transcriptomics is a powerful tool for the identification of biomarkers for macrophage maturation in the u937 cell line, *4*, 1014-1028.
- 23 Kreutz, M., Krause, S. W., Hennemann, B., Rehm, A. and Andreesen, R., *Res Immunol*, **1992**, Macrophage heterogeneity and differentiation: Defined serum-free culture conditions induce different types of macrophages in vitro, *143*, 107-115.
- 24 McColl, B. K., Stacker, S. A. and Achen, M. G., *Apmis*, **2004**, Molecular regulation of the vegf family - inducers of angiogenesis and lymphangiogenesis, *112*, 463-480.
- 25 Tammela, T., Enhalm, B., Alitalo, K. and Paavonen, K., *Cardiovasc Res*, **2005**, The biology of vascular endothelial growth factors, *65*, 550-563.
- 26 McDonald, D. M., *Am J Respir Crit Care Med*, **2001**, Angiogenesis and remodeling of airway vasculature in chronic inflammation, *164*, S39-45.
- 27 Mukutmoni, M., Hubbard, N. E. and Erickson, K. L., *Prostaglandins Leukot Essent Fatty Acids*, **2001**, Prostaglandin e(2) modulation of vascular endothelial growth factor production in murine macrophages, *65*, 123-131.
- 28 Kanazawa, H., Hirata, K. and Yoshikawa, J., *Thorax*, **2002**, Involvement of vascular endothelial growth factor in exercise induced bronchoconstriction in asthmatic patients, *57*, 885-888.
- 29 Bamba, H., Ota, S., Kato, A., Kawamoto, C. and Fujiwara, K., *Biochem Biophys Res Commun*, **2000**, Prostaglandins up-regulate vascular endothelial growth factor production through distinct pathways in differentiated u937 cells, *273*, 485-491.
- 30 Bamba, H., Ota, S., Kato, A., Miyatani, H., *et al.*, *Aliment Pharmacol Ther*, **2003**, Effect of rebamipide on prostaglandin receptors-mediated increase of inflammatory cytokine production by macrophages, *18 Suppl 1*, 113-118.
- 31 Tanaka, M. and Miyajima, A., *Rev Physiol Biochem Pharmacol*, **2003**, Oncostatin m, a multifunctional cytokine, *149*, 39-52.
- 32 Chen, S. H. and Benveniste, E. N., *Cytokine Growth Factor Rev*, **2004**, Oncostatin m: A pleiotropic cytokine in the central nervous system, *15*, 379-391.
- 33 Wahl, A. F. and Wallace, P. M., *Ann Rheum Dis*, **2001**, Oncostatin m in the anti-inflammatory response, *60 Suppl 3*, iii75-80.
- 34 O'Hara, K. A., Kedda, M. A., Thompson, P. J. and Knight, D. A., *Clin Exp Allergy*, **2003**, Oncostatin m: An interleukin-6-like cytokine relevant to airway remodelling and the pathogenesis of asthma, *33*, 1026-1032.
- 35 Faffe, D. S., Flynt, L., Mellema, M., Whitehead, T. R., *et al.*, *Am J Physiol Lung Cell Mol Physiol*, **2005**, Oncostatin m causes vegf release from human airway smooth muscle: Synergy with il-1 $\beta$ , *in press*.
- 36 Repovic, P. and Benveniste, E. N., *J Neurosci*, **2002**, Prostaglandin e2 is a novel inducer of oncostatin-m expression in macrophages and microglia, *22*, 5334-5343.
- 37 Mine, S., Nasu, K., Fukuda, J., Sun, B. and Miyakawa, I., *Fertil Steril*, **2003**, Secretion of granulocyte chemotactic protein-2 by cultured human endometrial stromal cells, *79*, 146-150.
- 38 Van Damme, J., Wuyts, A., Froyen, G., Van Coillie, E., *et al.*, *J Leukoc Biol*, **1997**, Granulocyte chemotactic protein-2 and related cxc chemokines: From gene regulation to receptor usage, *62*, 563-569.
- 39 Wuyts, A., Struyf, S., Gijssbers, K., Schutyser, E., *et al.*, *Lab Invest*, **2003**, The cxc chemokine gcp-2/cxcl6 is predominantly induced in mesenchymal cells by interleukin-1beta and is down-regulated by interferon-gamma: Comparison with interleukin-8/cxcl8, *83*, 23-34.
- 40 Prause, O., Laan, M., Lotvall, J. and Linden, A., *Eur J Pharmacol*, **2003**, Pharmacological modulation of interleukin-17-induced gcp-2-, gro-alpha- and interleukin-8 release in human bronchial epithelial cells, *462*, 193-198.
-



## Chapter 7

---

### **Unheated *Cannabis sativa* extracts and its major compound THC-acid have potential immuno-modulating properties not mediated by CB<sub>1</sub> and CB<sub>2</sub> receptor coupled pathways.**

Kitty C.M. Verhoeckx<sup>1,3</sup>

Henrie A.A.J. Korthout<sup>2</sup>

Karl A. Ehlert<sup>1</sup>

Tonny Lagerweij<sup>2</sup>

Lex Nagelkerken<sup>2</sup>

Mei Wang<sup>2</sup>

Jan van der Greef<sup>1,3</sup>

Richard J.T. Rodenburg<sup>4</sup>

Renger F. Witkamp<sup>1</sup>

*Part of the work described in this chapter has been submitted for publication*

<sup>1</sup> TNO Quality of Life, Zeist, The Netherlands, <sup>2</sup> TNO Quality of Life, Leiden, The Netherlands, <sup>3</sup> Leiden University, Leiden/Amsterdam Center for Drug Research, Leiden, The Netherlands, <sup>4</sup> UMC St Radboud, Nijmegen, The Netherlands

**Unheated *Cannabis sativa* extracts and its major compound THC-acid have potential immuno-modulating properties not mediated by CB<sub>1</sub> and CB<sub>2</sub> receptor coupled pathways.**

*There is a great interest in the pharmacological properties of cannabinoid like compounds that are not linked to the adverse effects of  $\Delta^9$ -tetrahydrocannabinol (THC), e.g. psychoactive properties. The present paper describes the potential immuno-modulating activity of unheated Cannabis sativa extracts and its main non-psychoactive constituent  $\Delta^9$ -tetrahydrocannabinoid acid (THCa). By heating Cannabis extracts, THCa was shown to be converted into THC. Unheated Cannabis extract and THCa were able to inhibit the tumor necrosis factor alpha (TNF- $\alpha$ ) release from U937 macrophages and peripheral blood macrophages after stimulation with LPS in a dose-dependent manner. The inhibition of TNF- $\alpha$  release was prolonged over a longer period of time, whereas THC and heated extracts induced TNF- $\alpha$  release at longer incubation times. Furthermore we demonstrated that THCa and THC show distinct effects on phosphatidylcholine specific phospholipase C (PC-PLC) activity. Unheated Cannabis extract and THCa inhibit the PC-PLC activity in a dose-dependent manner, while THC induced PC-PLC activity at high concentrations. These results suggest that THCa and THC exert their immuno-modulating effects via different metabolic pathways. In order to study the possible in vivo implications of these findings, a pilot study in an Experimental Autoimmune Encephalomyelitis (EAE) mouse model was performed. Unheated Cannabis extract and THCa had a favourable effect on the clinical and histological signs of EAE. These preliminary results are auspicious, but further extensive investigation is necessary.*

---

**Introduction**

*Cannabis sativa* and its primary psychoactive constituent,  $\Delta^9$ -tetrahydrocannabinol (THC) have shown therapeutic benefits in the relief of nausea and vomiting associated with cancer and its treatments, stimulation of appetite in AIDS patients and patients with anorexia and wasting syndromes, analgesia, muscle relaxation<sup>1-6</sup>. These positive effects are partially linked to the presence of the CB<sub>1</sub> receptor, but are over shadowed by the psychotropic effects which have thus far also been attributed to the CB<sub>1</sub> receptor<sup>7-9</sup>. Besides the psychotropic effect, THC and Cannabis exert several additional adverse effects on health. For example chronic inflammatory and precancerous changes in the airways have been demonstrated in Cannabis

smokers. Overdosing Cannabis manifests itself in anxiety and panic attacks, increased heart rate, and changes in blood pressure <sup>1,10</sup>.

Cannabinoids are known to bind to cannabinoid receptors CB<sub>1</sub> and CB<sub>2</sub> with different affinity <sup>4,5</sup>. The CB<sub>1</sub> receptor is predominantly expressed in the brain as well as several tissues of the periphery, whereas the CB<sub>2</sub> receptor is primarily expressed on cells of the immune system <sup>4-6</sup>. Both receptors have shown to be involved in immuno-modulating actions <sup>7,11-13</sup>, but not all actions could be linked to these receptors, suggesting that non-cannabinoid receptors and metabolic pathways are involved <sup>1,8,14</sup>. The psychotropic effect of CB<sub>1</sub> receptor agonists and the stigma of cannabinoids as a recreational and addicting drug are still major obstacles to legalize the drug in certain countries for therapeutic use <sup>1</sup>. So there is great interest in cannabinoids and other compounds that have a reduced ability to activate CB<sub>1</sub> receptors but maintain the therapeutic effects of THC and lack the unwanted effect of these drugs.

In the Cannabis plant, cannabinoids are synthesized and accumulated as cannabinoid acids <sup>1,15,16</sup>. The cannabinoid acids are devoid of psychotropic effects and have to be decarboxylated to phenols to produce psychotropic effects e.g. by smoking the dried plant matter. MS patients using Cannabis preparations other than by smoking or that contain low THC content claim positive health effects and fewer side effects. For this reason we investigated the relation between cannabinoid content of heated and unheated Cannabis extracts and their inhibitory effect on tumor necrosis factor alpha (TNF- $\alpha$ ) production after stimulation of U937 macrophages with endotoxin lipopolysaccharide (LPS). TNF- $\alpha$  is a well known pro-inflammatory cytokine which plays an important role in inflammatory responses. It has been shown that TNF- $\alpha$  production can be inhibited by various pathways. In the present study we focussed on the role of the CB receptors in this process and investigated the involvement of adenosine-3',5'-cyclic monophosphate (cAMP) and phosphatidylcholine specific phospholipase C (PC-PLC).

Finally we studied the effect of THCa and unheated Cannabis extract in an Experimental Autoimmune Encephalomyelitis (EAE) mouse model. Cannabinoids have shown to have a positive effect on inhibiting the development of clinical signs of MS in some animal models <sup>9,17,18</sup>. EAE is a demyelinating disease of the central nervous system (CNS) that can be induced by immunization with various myelin-derived antigens, including myelin basic protein (MBP) and proteolipid protein (PLP) <sup>19,20</sup>. Evidence has been obtained both in rats and mice showing that infiltration of macrophages and CD4<sup>+</sup> T cells in the CNS play an important role in the pathogenesis of the disease through the secretion of a variety of cytokines, in particular TNF- $\alpha$ , TNF- $\beta$ , and IFN- $\gamma$  <sup>21,22</sup>.

## Materials and Methods

### *Chemicals*

Lipopolysaccharide (Escherichia coli O111:B4) and D609 were obtained from Sigma-Aldrich (St. Louis, MO, USA). The pure cannabinoid compounds:  $\Delta^9$ -tetrahydrocannabinol (THC) and  $\Delta^9$ -tetrahydrocannabinoid acid (THCa) were purified as described previously<sup>23</sup> and provided by the University of Leiden (Leiden, The Netherlands). The CB<sub>1</sub> antagonist, AM281 and CB<sub>2</sub> antagonist AM630 were obtained from Tocris Cookson Ltd. (Bristol, UK).

### *Cannabis extracts*

The *Cannabis sativa* plant materials were obtained from a local grower (The Netherlands). About 3.1 g of dried flower tops were ground in liquid nitrogen and extracted with 40 mL chloroform/methanol/water (50:25:25) for 30 minutes. The mixture was centrifuged for 20 minutes (2000 g) allowing the separation of the polar from the non-polar liquid phase. The non-polar chloroform-phase that contained the cannabinoids was isolated. For cell based studies, the chloroform phase was evaporated using a vacuum centrifuge and re-dissolved in an equal volume of DMSO. This extract will be referred to as the 'unheated' extract. For the heated extracts, the chloroform extracts were evaporated, heated for 7 minutes at 200 °C and re-dissolved in an equal volume of DMSO. The concentration of THC, THCa, CBD and CBDa in Cannabis extracts were analysed using LC-IT-MS<sup>n</sup> as described previously<sup>24</sup>. Metabolite profiles were obtained using a gas chromatographic instrument from Agilent (6890N) with a mass spectrometric detector (5973). The extracts were dried using sodium sulphate and subsequently derivatized with N-Methyl-N-(trimethylsilyl) trifluoroacetamide (MSTFA). The derivatized extracts (1  $\mu$ l) were separated on a HP-5MS column (30 m \* 0.25 mm \* 0.25  $\mu$ m, Agilent technologies, Amstelveen, The Netherlands).

### *Cell cultures*

Human monocyte-like histiocytic lymphoma cells U937<sup>25</sup> obtained from the ATCC (CRL-1593.2) were grown in RPMI-1640 medium, supplemented with 10% (v/v) fetal calf serum and 2 mM L-glutamine (Life technologies, Breda, The Netherlands) at 37 °C, 5% CO<sub>2</sub> in a humidified atmosphere. U937 monocytic cells (1x10<sup>6</sup> cells per well) were differentiated into macrophages using phorbol 12-myristate 13-acetate (PMA, 10 ng/ml, overnight, Omnilabo, Breda, The Netherlands) as described previously<sup>26</sup>. The PMA-differentiated macrophages were allowed to recover from PMA treatment for 48 h, during which the culture medium was replaced daily.

Peripheral blood monocytes (PB-MO) were isolated from human EDTA-blood with Rosette Sep<sup>TM</sup> human monocyte enrichment cocktail (Stemcell Technologies Inc, Meylan, France) as described previously<sup>27</sup>. The monocytes ( $5 \times 10^5$  cells per well) were cultured in 24 well cell culture plates containing RPMI-1640 medium supplemented with 10% (v/v) human serum and 2 mM L-glutamine and were allowed to differentiate into peripheral blood macrophages (PB-MØ) for eight days. Following this procedure, the macrophage maturation has been described to give rise to the characteristically morphology and phenotype of primary macrophages<sup>28</sup>.

#### *Macrophage activation and TNF- $\alpha$ assay*

PB-MØ and U937 cells were exposed to LPS (1  $\mu\text{g/ml}$ ) in the presence or absence of THC and THCa (12.5, 25, 50, 100 and 200 nM) or *Cannabis sativa* plant extracts (250, 500, 1000, 2000 and 4000 fold diluted) for 4 h. For the time course experiments U937 cells ( $1 \times 10^6$  cells per well) were incubated with LPS (1  $\mu\text{g/ml}$ ) in combination with 80 nM THC, THCa or 500 fold diluted heated Cannabis extract or unheated Cannabis extract. Culture medium was collected at 1, 2, 4, 6, 8, 16 and 24 h respectively. All incubations were performed in triplicate.

The concentration of TNF- $\alpha$  in the culture supernatants was determined by ELISA using the cytoset antibody pair kit for TNF- $\alpha$  from Biosource (Etten-Leur, The Netherlands) according to the manufacturer's protocol. The cells were lysed in 0.1 M NaOH and used for protein determination by the modified method of Bradford (Bio-Rad, Veenendaal, The Netherlands).

#### *CB<sub>1</sub> and CB<sub>2</sub> antagonism*

U937 macrophages were incubated with LPS (1  $\mu\text{g/ml}$ ) together with 80 nM THC, THCa or 500 fold diluted unheated Cannabis extract in combination with a concentration series ( $1 \times 10^{-8}$  -  $1 \times 10^{-4}$  M) of AM281, a CB<sub>1</sub> antagonist<sup>29,30</sup> or AM630, a CB<sub>2</sub> antagonist<sup>31</sup>. After 4 h the culture medium was collected and the cells lysed in 1 ml 0.1 M NaOH.

#### *Measurement of intracellular cAMP formation*

U937 macrophages were cultured in 24 well cell culture plates at a concentration of  $1 \times 10^6$  cells per well. Cells were incubated for 10 minutes at 37 °C with a concentration series of THC, THCa (12.5, 25, 50, 100, and 200 nM) or unheated Cannabis extract (250, 500, 1000, 2000 and 4000 fold diluted) in combination with LPS (1  $\mu\text{g/ml}$ ). Zilpaterol (Intervet Inc., Millsboro, US), a  $\beta_2$ -adrenergic receptor agonist at a concentration of  $1 \times 10^{-6}$  M was used as a

positive control for cAMP induction. The culture medium was aspirated and the cells were placed directly on ice. The cells were lysed in 0.25 ml 0.1 M HCl. After centrifugation, the samples were assayed directly using the cyclic AMP EIA kit from Cayman Chemical (Ann Arbor, USA). The incubations were performed in duplicate.

#### *Determination of phospholipase C activity*

The medium of U937 macrophages ( $1 \times 10^6$  cells per well) was changed into RPMI-1640 medium, without fetal calf serum, 24 h before incubation with THC, THCa (25, 50, 100, and 200 nM), or unheated Cannabis extract (250, 500, 1000, and 2000 fold diluted). D609 at a concentration of 200  $\mu$ M was used as a positive control for inhibition of PC-PLC activity. After 15 minutes LPS (1  $\mu$ g/ml) was added and the cells were incubated for a further 5 minutes at 37 °C. Supernatant was aspirated and the cells were washed with ice cold PBS. The cells were lysed in 0.2 ml reaction buffer and 100  $\mu$ g of cell lysate was further analyzed using the Amplex® Red Phosphatidylcholine-Specific Phospholipase C assay Kit (Molecular Probes, Eugene, USA) according to the manufacturer's protocol.

#### *EAE in SJL mice*

Female SJL mice (Harlan, Horst, The Netherlands) 9 weeks of age, were randomized and divided over three groups (n = 10) and immunized subcutaneously with 75  $\mu$ g of synthetic peptide comprising amino acid 139 through 151 from proteolipid protein (PLP<sub>139-151</sub>) dissolved in PBS and emulsified with an equal volume of complete Freund's adjuvant containing 1 mg/ml *Mycobacterium tuberculosis* H37Ra (Difco, Detroit, MI). After one and three days, mice were injected i.v. with  $10^{10}$  heat-inactivated *Bordetella pertussis* organisms (Institute of Public Health, Bilthoven, The Netherlands). Development of EAE was monitored daily by assessment of bodyweight and a disability score. The score ranges from 0: no signs, 0.5: partial loss of tail tonus, 1: complete loss of tail tonus, 2: limb weakness, 2.5: partial paresis, 3: complete paralysis from diaphragm to hind limbs, 3.5: complete paralysis from diaphragm to hind limbs, incontinence, 4: moribund, to 5: death due to EAE. The animals received daily an oral dose of the following compounds for 21 consecutive days from immunization until day 20: group 1: placebo (olive oil), group 2: THCa (50 mg/kg) in olive oil and group 3: unheated Cannabis extract (50 mg THCa/kg) in olive oil. After 42 days the animals were sacrificed. Brains and spinal cords were fixed in 10 % formalin and paraffin embedded. Six sections per animal, each comprising three different areas of the nervous system (cerebellum, brain stem) and three sections of spinal cord were analyzed for infiltrates

after staining with haematoxylin. The severity of the inflammatory reaction was indicated using the following histological score; 0: no infiltrates, 1: sporadic, mild perivascular infiltration (less than two inflammatory lesions per section), 2: multifocal, mild perivascular infiltration, 3: multifocal, severe perivascular infiltration, 4: multifocal, severe perivascular infiltration accompanied by spreading into the parenchyma. The study protocol was approved by the Ethical Committee for experiments on Animals of our Institute.

## Results

### *Cannabis extracts*

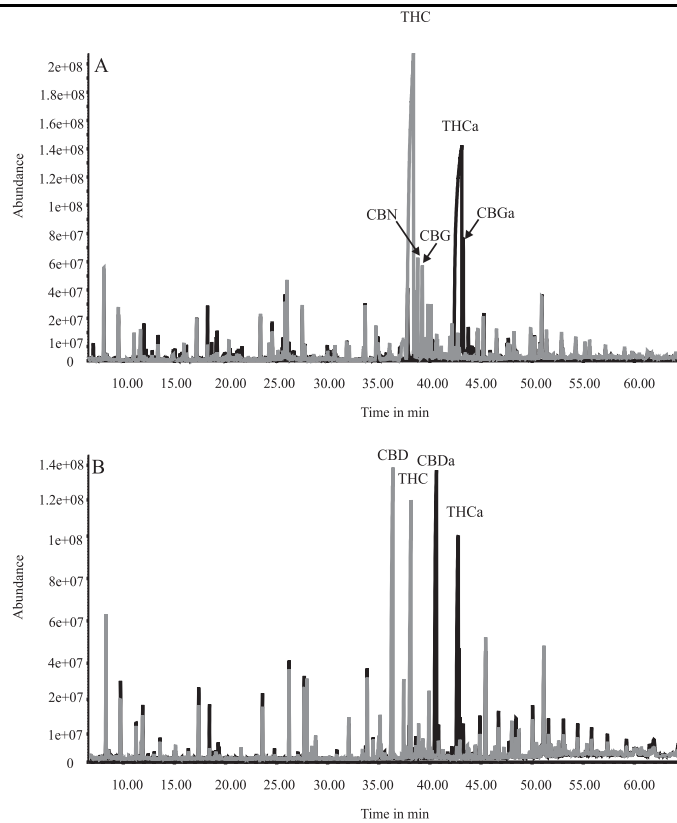
Two different plant cultivars; a cultivar with a high THCa content (Table 1 A; no CBDa) and one with a low THCa content (Table 1, B; CBDa : THCa 1:1) were extracted with chloroform/methanol/water. The chloroform phase containing the cannabinoid acids is referred to as the unheated Cannabis extract. The same extract was heated at 200 °C for 7 minutes and this extract is referred to as the heated extract.

Table 1 shows the concentrations of the main cannabinoid acids (THCa and CBDa) and cannabinoid compounds (THC and CBD) in the two plant extracts (unheated) and when heated as determined using LC-IT-MS<sup>n</sup>.

**Table 1** Concentration of the main cannabinoids; THC, THCa, CBD and CBDa in unheated and heated plant extracts (3.1 g per 40 ml), determined by LC-MS. The concentrations are given in µg/ml.

Plant extract	Treatment	THC	THCa	CBD	CBDa
A	unheated	90	14500	3.9	28
A	heated	10060	150	29	17
B	untreated	48	3300	26	3500
B	heated	1100	9.3	1900	0.9

In the unheated extracts the cannabinoid acids of THC and CBD (THCa and CBDa) were most dominant, whereas after heating these compounds were decarboxylated into THC and CBD. The metabolite profiles of the different Cannabis extracts (Fig.1) obtained by GC-MS show that THCa and THC are the main constituents of unheated and heated Cannabis extracts respectively.



**Figure 1** Total ion currents from unheated (black) and heated (grey) Cannabis extract A (A) and Cannabis extract B (B) obtained with GC-MS.

*Macrophage activation and TNF- $\alpha$  assay*

U937 macrophages were exposed for 4 h to LPS in the presence or absence of different concentrations of Cannabis extracts. The immuno-modulating effect of three plant extracts, unheated A (high THCa content), heated A (low THCa content) and unheated B (low THCa content) on LPS activated U937 cells was tested by measuring the TNF- $\alpha$  release in the cell culture media (Fig. 2). The release of TNF- $\alpha$  was clearly inhibited in a concentration dependent manner by all three plant extracts.

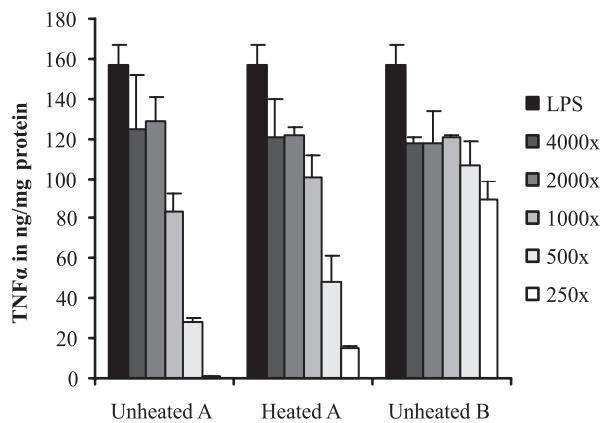


**Figure 2** Release of TNF- $\alpha$  from U937 macrophages incubated for 4 h with LPS (black bars) with a dilution series (from left to right successively; 4000, 2000, 1000, 500 and 250 fold diluted) of unheated Cannabis extract A (high THCa content), heated Cannabis extract A (low THCa content), and unheated Cannabis extract B (low THCa content), respectively. The release of TNF- $\alpha$  is corrected for protein content. The results are presented as means  $\pm$  SD of triplicate measurements.

The inhibition was not due to a toxic effect induced by the Cannabis extracts according to LDH activity determinations (data not shown). The inhibitory effect of the 250, 500 and 1000 fold dilutions of the unheated Cannabis extract A was larger than the effect of the heated Cannabis extract A and the unheated Cannabis extract B according to the Student's *t*-test ( $p < 0.05$ ).

Because the main difference between the three extracts was the THCa/THC content (Fig. 1), we investigated whether THCa could be responsible for the TNF- $\alpha$ -inhibitory effect. THCa (pure compound) was added to the heated Cannabis extract A as well as the unheated Cannabis extract B in such a way that the concentration THCa was equal to the level of THCa in the unheated Cannabis extract A. Figure 3 shows the effect of THCa addition on the TNF- $\alpha$  release.

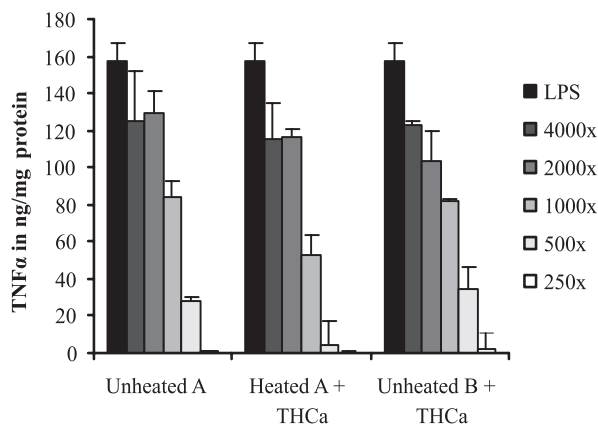


**Figure 3** Release of TNF- $\alpha$  from U937 macrophages incubated for 4 h with LPS (black bars) with a dilution series (from left to right successively; 4000, 2000, 1000, 500 and 250 fold diluted) of unheated Cannabis extract A, heated Cannabis extract A + THCa addition, and unheated Cannabis extract B + THCa addition, respectively. The concentration of THCa is equal in the three plant extracts. The release of TNF- $\alpha$  is corrected for protein content. The results are presented as means  $\pm$  SD of triplicate.

The addition of THCa to the heated Cannabis extract A and the unheated Cannabis extract B augmented the inhibitory effect on the TNF- $\alpha$  release. The effect of the unheated Cannabis extract B + THCa addition was similar to the effect induced by the unheated Cannabis extract A, this may suggest that THCa is one of the main compounds involved in the inhibitory effect of the unheated Cannabis extracts. For this reason it was interesting to see if pure THCa also exhibited this TNF- $\alpha$  inhibitory property. From this point we only used the Cannabis extract containing a high amount of THCa (Cannabis extract A).

U937 macrophages and PB-M $\emptyset$  were exposed to LPS in the absence or presence of pure THC, THCa or unheated Cannabis extract. Figure 4 shows the results of the comparison of the effects of the pure compounds on the TNF- $\alpha$  release in U937 macrophages and PB-M $\emptyset$ . The concentration of the pure compounds was chosen in such a way that the concentration of the pure compound equals the concentration of THCa in the unheated Cannabis extract.

THC, THCa as well as unheated Cannabis extract were capable of inhibiting the TNF- $\alpha$  release from U937 macrophages and blood macrophages exposed to LPS in a dose-dependent manner. The inhibitory effect of pure THCa was comparable to the effect induced by the unheated Cannabis extract on both U937 macrophages and PB-M $\emptyset$ .

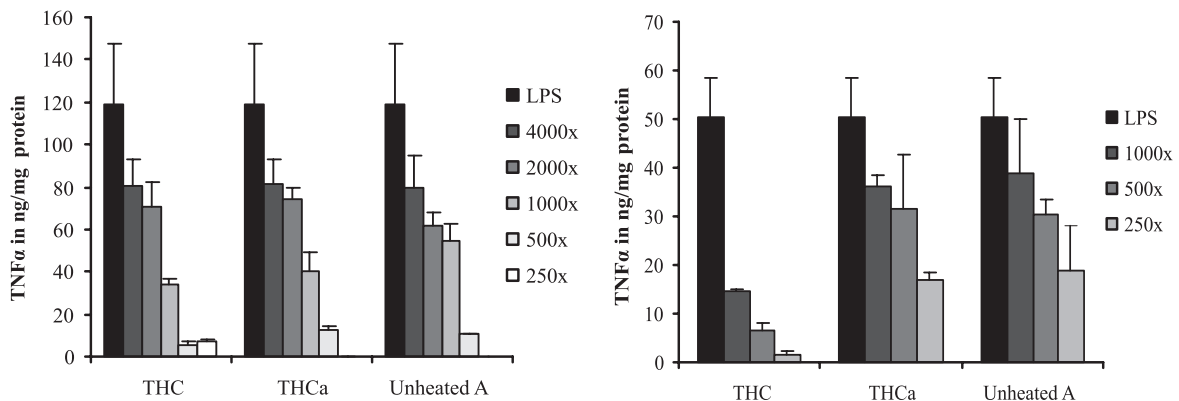


**Figure 4** Release of TNF- $\alpha$  from U937 macrophages (left panel) and PB-M $\emptyset$  (right panel) incubated for 4 h with LPS or LPS in combination with a concentration series of THC, THCa and unheated Cannabis extract A (from left to right 4000, 2000, 1000, 500, and 250 fold diluted respectively for U937 macrophages and 1000, 500, and 250 fold diluted respectively for PB-M $\emptyset$ ). The concentrations of THC and THCa are equal to the concentration of THCa in the unheated Cannabis extract. The release of TNF- $\alpha$  is corrected for protein content. The results are presented as means  $\pm$  SD of triplicate measurements.

The TNF- $\alpha$  release from U937 macrophages after treatment with THC showed an analogous effect to THCa, whereas the effect of THC on the TNF- $\alpha$  release from PB-M $\emptyset$  was markedly stronger. TNF- $\alpha$  release was more inhibited with respect to THCa. At higher THC concentration (200 nM), the inhibition of the TNF- $\alpha$  release tended to become weaker. Considerable information can be found on the anti-inflammatory effect of THC.

Unfortunately these results are often contradictory, because different cells, incubation times and concentrations were used. We postulated that the incubation time could be an important factor for these discrepancies in the literature and therefore we investigated the TNF- $\alpha$  inhibitory effect of pure THC, THCa, unheated and heated Cannabis extract in time. U937 macrophages were incubated with LPS in the presence or absence of THC, THCa, unheated or heated Cannabis extract. Culture media was collected at different time points for the determination of TNF- $\alpha$  (Fig. 5). THC, THCa, unheated and heated Cannabis extract all inhibited the TNF- $\alpha$  release. As opposed to TNF- $\alpha$  production by cells stimulated in the presence of heated extract or THC, the TNF- $\alpha$  production in the presence of unheated extract or THCa was delayed and showed a lower maximum.

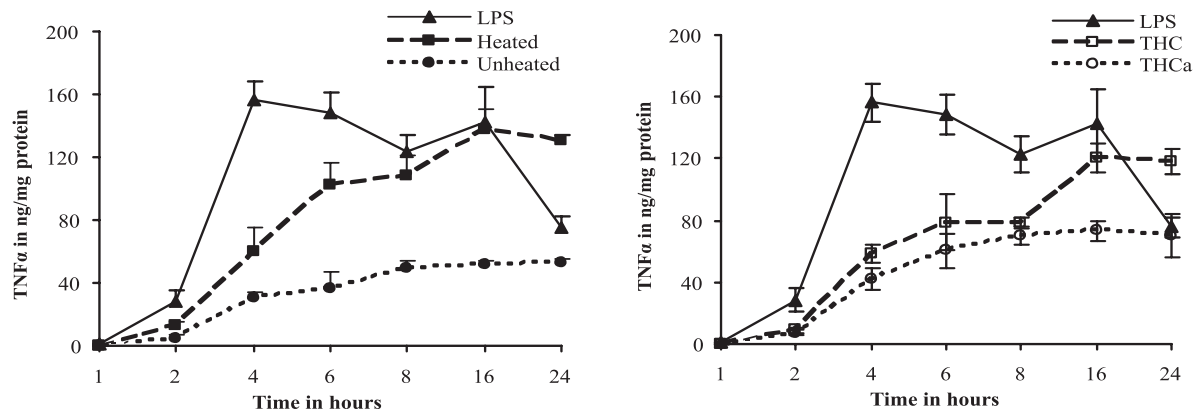


**Figure 5** Left panel: release of TNF- $\alpha$  from U937 macrophages after exposure to LPS (1  $\mu$ g/ml) alone and in combination with unheated extract A (500 fold diluted) or heated Cannabis extract A (500 fold diluted). Right panel: release of TNF- $\alpha$  from U937 macrophages after exposure to LPS (1  $\mu$ g/ml) alone and in combination with THC (80 nM) or THCa (80 nM). The levels of TNF- $\alpha$  released by the U937 macrophages in the culture medium were determined at the time points indicated and are corrected for protein content. The results are presented as means  $\pm$  SD of triplicate measurements.

### *CB<sub>1</sub> and CB<sub>2</sub> antagonism*

To further investigate the possible differences in the TNF- $\alpha$  inhibitory properties of THC and THCa we investigated if the inhibition of TNF- $\alpha$  production was mediated via the cannabinoid receptors CB<sub>1</sub> and CB<sub>2</sub> (Fig. 6).

Western blot experiments with specific antibodies for CB<sub>1</sub> and CB<sub>2</sub> confirmed the presence of these receptors on the membranes of U937 cells (data not shown). This is in line with previous reports that mention the presence of CB receptors on human leukocytes<sup>1, 6, 32</sup>. U937 macrophages were exposed to LPS plus a fixed concentration of THC, THCa or unheated Cannabis extract in combination with a concentration series of the CB<sub>1</sub> receptor antagonist AM281 or the CB<sub>2</sub> receptor antagonist AM630. The results presented in Figure 6 revealed that THC, THCa and the unheated Cannabis extract inhibited the TNF- $\alpha$  release induced by LPS. Both the CB<sub>1</sub> antagonist and the CB<sub>2</sub> antagonist were not able to reverse this inhibitory effect. The antagonists themselves had no effect on the TNF- $\alpha$  release induced by LPS (data not shown).

The results suggested that the inhibitory effect on the TNF- $\alpha$  release by THC, THCa and unheated Cannabis extract involved different mechanisms. We therefore investigated whether the TNF- $\alpha$  inhibitory properties were mediated via cAMP induction, which is also known to be linked to TNF- $\alpha$  inhibition.

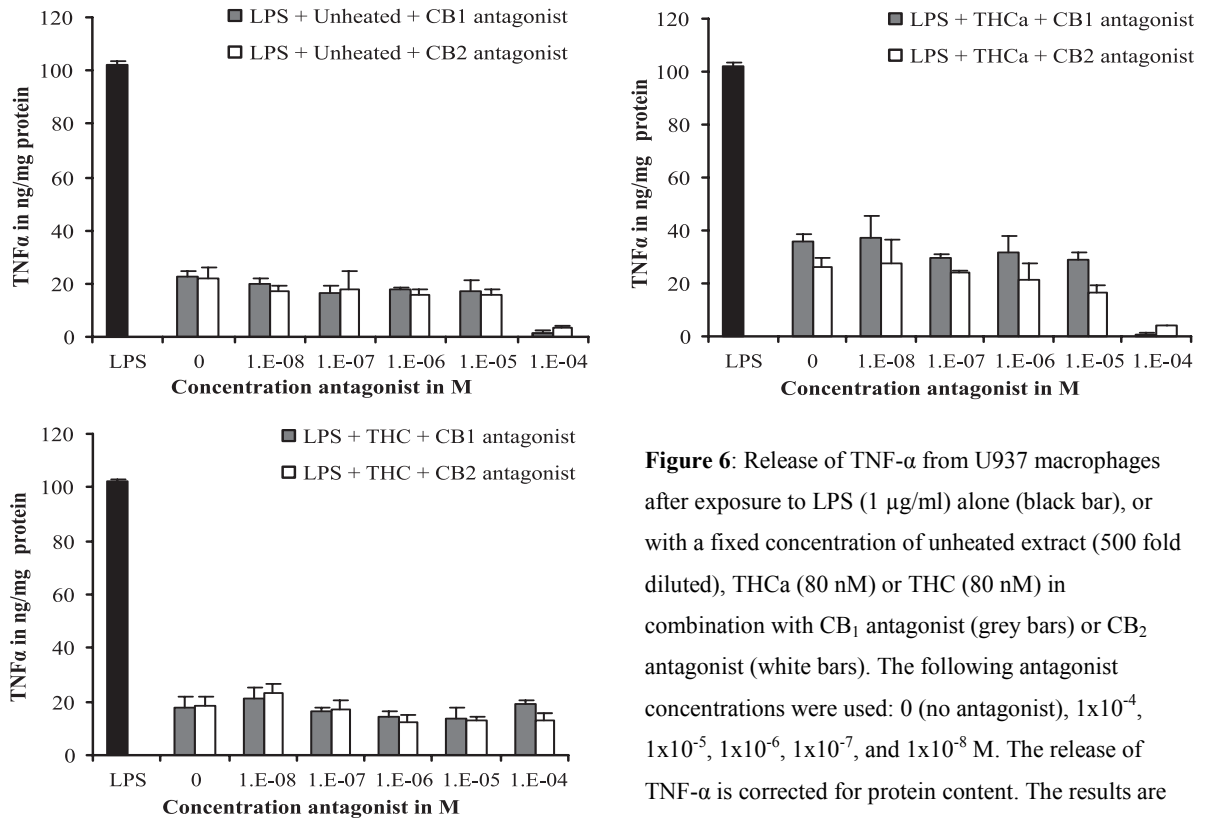


**Figure 6:** Release of TNF- $\alpha$  from U937 macrophages after exposure to LPS (1  $\mu$ g/ml) alone (black bar), or with a fixed concentration of unheated extract (500 fold diluted), THCa (80 nM) or THC (80 nM) in combination with CB<sub>1</sub> antagonist (grey bars) or CB<sub>2</sub> antagonist (white bars). The following antagonist concentrations were used: 0 (no antagonist),  $1 \times 10^{-4}$ ,  $1 \times 10^{-5}$ ,  $1 \times 10^{-6}$ ,  $1 \times 10^{-7}$ , and  $1 \times 10^{-8}$  M. The release of TNF- $\alpha$  is corrected for protein content. The results are presented as means  $\pm$  SD of triplicate measurements.

*Measurement of intracellular cAMP formation*

The concentration of cAMP was measured after treatment of U937 macrophages with LPS in the presence or absence of a concentration series of THC, THCa and unheated Cannabis extract. From Figure 7 it can be concluded that cAMP is not induced by THC, THCa or unheated Cannabis extract according to the Student's *t*-test. As a positive control we used zilpaterol, a  $\beta_2$ -adrenergic receptor agonist, which induced the cAMP release more obviously, as determined by using the Student's *t*-test ( $p < 0.05$ ). Beta<sub>2</sub>-agonists inhibit the production of LPS induced TNF- $\alpha$  via the induction of cAMP.

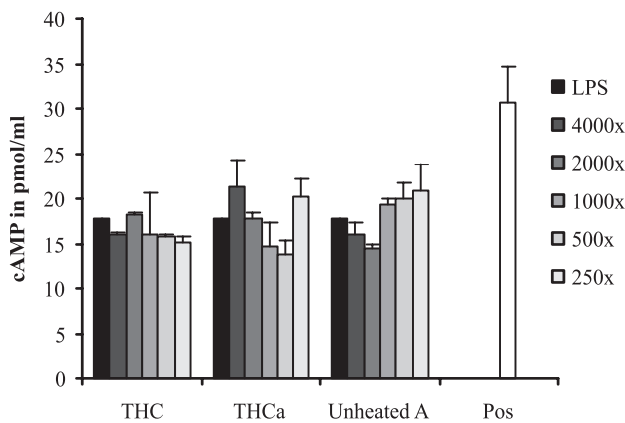


**Figure 7** Release of cAMP from U937 macrophages exposed to LPS in combination with a concentration series of THC, THCa or unheated Cannabis extract A (4000, 2000, 1000, 500, and 250 fold diluted, respectively). The concentrations of THC and THCa are equal to the concentration of THCa in the unheated Cannabis extract. Zilpaterol ( $1 \times 10^{-6}$  M) was used as a positive control for cAMP induction (Pos). The results are presented as means  $\pm$  SD of duplicate measurements.

As THC, THCa and unheated Cannabis extract did not mediate their inhibitory effect on TNF- $\alpha$  via cAMP, we examined if the inhibitory effect was established via the inhibition of PC-PLC activity.

#### *Determination of phospholipase C activity*

Tricyclodecan-9-yl-xanthogenate (D609), a selective inhibitor of phosphatidylcholine specific phospholipase C (PC-PLC), inhibits the activity of PC-PLC induced by LPS stimulation and subsequently inhibits the production of TNF- $\alpha$  via a complex signalling pathway. We therefore investigated if THC, THCa and unheated Cannabis extract inhibit TNF- $\alpha$  release after LPS exposure via the induction of PC-PLC. Macrophages were pre-incubated with THC, THCa and unheated Cannabis extract in serum free culture media. Subsequently the cells were exposed to LPS for 5 minutes after which the cells were lysed and the PC-PLC activity was determined directly. The results presented in Figure 8 revealed that THCa and unheated Cannabis extract both inhibited the PC-PLC activity in a dose-dependent manner. The induction of PC-PLC activity at high THC concentration (80 nM) correlates with the induction of TNF- $\alpha$  in Figure 4 (left panel).

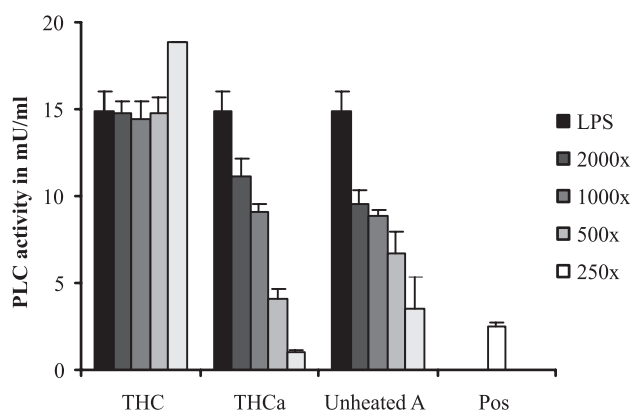


**Figure 8** Phosphatidylcholine specific phospholipase C activity of U937 macrophages exposed to LPS alone or in combination with a concentration series of THC, THCa or unheated Cannabis extract A (2000, 1000, 500, and 250 fold diluted respectively). The concentrations of THC and THCa are equal to the concentration of THCa in the unheated Cannabis extract. D609 (200  $\mu$ M) was used as a positive control for inhibition of PC-PLC activity (Pos). For every sample 100  $\mu$ g of cell lysate was assayed. The results are presented as means  $\pm$  SD of duplicate measurements.

#### *Effects of THCa and unheated Cannabis extract on EAE*

Like THC, THCa and unheated Cannabis extracts were able to inhibit the TNF- $\alpha$  release *in vitro*, although this effect was obviously regulated via different pathways it was interestingly to know if THCa and unheated Cannabis extracts were also immuno-modulating *in vivo*. Previous studies have shown that THC had a positive effect on the clinical and histological signs of EAE in rat models. We therefore investigated the effect of THCa and unheated Cannabis extract on the severity of EAE immunized mice. Table 2 summarizes the clinical data on EAE incidence, day of disease onset, disease severity and loss of bodyweight. Both treatments resulted in a slightly more favourable disease course than treatment with placebo,

evident from a lower incidence of disease, a lower maximal or cumulative EAE score or lower loss of bodyweight. However, these results failed to reach statistical significance when evaluated with the non-parametric Kruskal Wallis test for multiple groups

**Table 2** Clinical evaluation of *in vivo* treatment with THCa and unheated Cannabis extract on the development of EAE. The concentration of unheated Cannabis extract was chosen in such a way that the THCa concentration in the unheated Cannabis extract was equal to the THCa concentration of the pure compound (1mg). The results are presented as means  $\pm$  SEM.

Treatment	Incidence	Day of onset*	Max. clinical score day 0-20	Max. cumulative score day 0-20**	Max. clinical score day 21-42	Max. cumulative score day 21-42**	Max. % loss of bodyweight
Placebo	9/10	11.4 $\pm$ 0.2	2.1 $\pm$ 0.2	13.4 $\pm$ 2.3	1.8 $\pm$ 0.4	16.6 $\pm$ 3.8	19.6 $\pm$ 1.9
THCa	8/9	12.8 $\pm$ 0.6	1.5 $\pm$ 0.3	9.0 $\pm$ 2.5	0.9 $\pm$ 0.2	11.8 $\pm$ 4.6	16.3 $\pm$ 2.6
Unheated Cannabis	6/10	12.0 $\pm$ 0.3	1.4 $\pm$ 0.4	9.8 $\pm$ 3.2	1.5 $\pm$ 0.5	17.0 $\pm$ 5.9	13.5 $\pm$ 3.0

\* The mean day of onset is calculated for the animals that developed clinical signs of EAE (N=8 for THCa, N=6 for unheated Cannabis extract and N=9 for placebo)

\*\* For each individual mouse the cumulative disability score (sum of daily disability scores) was calculated from day 0 up to day 20 and from day 21 up to day 42 and included in the mean.

To establish if THCa and unheated Cannabis extract had a sub-clinical effect on the inflammatory response within the CNS, different regions of the CNS were (cerebellum, brain stem and spinal cord) analysed using haematoxylin staining (Fig. 9). These areas of the brain were infiltrated by immune cells in the majority of the animals. In mice treated with THCa and unheated Cannabis extract the severity of the inflammation in the brainstem was decreased (Kruskall-Wallis,  $p < 0.05$ ), a significant inhibition was observed for THCa (post-hoc Mann-Witney U-test,  $p = 0.004$ ) and unheated Cannabis extract (post-hoc Mann-Whitney U-test,  $p = 0.006$ ) as compared to the placebo group.

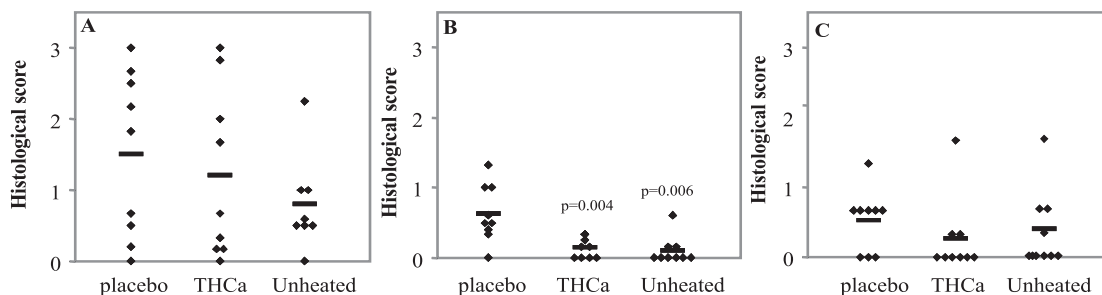


**Figure 9** Effect of THCa and unheated Cannabis extract on the inflammatory response in the cerebellum (A), brain stem (B) and spinal cord (C). The severity of the inflammatory response was expressed on a scale of 0 (no infiltrates) to 4 (severe

---

inflammatory response) as indicated in Material and Methods. Each symbol (◆) represents one individual mouse. — represents the mean value of histological score.

These data thus suggest that both THCa and unheated Cannabis extract have the potential to inhibit inflammatory responses within the CNS and may possibly inhibit the development of clinical disease when administered at a different dosage.

## Discussion

In the Cannabis plant, cannabinoids are synthesized and accumulated as cannabinoid acids<sup>1, 15</sup>. The main constituent of *Cannabis Sativa* is  $\Delta^9$ -THCa.  $\Delta^9$ -THCa and other cannabinoid acids are devoid of psychotropic effects<sup>1, 33</sup>. When the plant is heated (e.g. by smoking),  $\Delta^9$ -THCa decarboxylizes into  $\Delta^9$ -THC, the main psychoactive compound of heated Cannabis extract. The bioavailability of  $\Delta^9$ -THC depends on the way of administration, but eventually  $\Delta^9$ -THC is metabolized into its psychoactive metabolite 11-hydroxy- $\Delta^9$ -THC (11-OH-THC), which in turn is further oxidized into the non-psychoactive compound THC-COOH (11-nor-9-carboxy- $\Delta^9$ -THC). THC-COOH is secreted after glucuronidation and must not be mistaken for THCa in the Cannabis plant<sup>1, 32, 34</sup>. The psychoactive properties of  $\Delta^9$ -THC and 11-OH-THC are mediated by the CB<sub>1</sub> receptor. Cannabinoid receptors (CB<sub>1</sub> and CB<sub>2</sub>) are the main receptors of the endogenous cannabinoid system<sup>4-6</sup>. THCa is compared to THC, a weak agonist for the CB<sub>1</sub> (K<sub>i</sub> = 6.3 x10<sup>-7</sup> M vs. 3.5x10<sup>-9</sup> M) and CB<sub>2</sub> receptor (K<sub>i</sub> = 8.9x10<sup>-7</sup> M vs. 3.2x10<sup>-9</sup> M) as determined with receptor expressing membranes from cells transfected with cloned CB receptors (data not shown).

In this study we showed for the first time that THCa and unheated *Cannabis sativa* extracts were capable of inhibiting the production of TNF- $\alpha$  by LPS induced macrophages in a dose-dependent manner. Our results indicate that THCa is probably the major component responsible for this effect. However, other constituents might contribute as well but this remains to be investigated. The TNF- $\alpha$  inhibitory effect of the heated Cannabis extract was less pronounced, whereas the effects of the pure compounds (THC and THCa) were comparable. This discrepancy can be explained by the fact that the amount of THC in the heated extracts was lower with respect to the THCa content in the unheated extracts, but an effect of other metabolites in the unheated extract should not be ruled out beforehand. THCa as well as unheated Cannabis extract were also capable of inhibiting the TNF- $\alpha$  release from blood macrophages in a dose-dependent manner. However, the effect of THC on the TNF- $\alpha$  release from PB-M $\emptyset$  was more pronounced than observed in U937 macrophages. This discrepancy can be caused by the fact that U937 cells and PB-MO are originating from

different differentiation stages of the mononuclear myeloid cell line<sup>28, 35, 36</sup>.

The effect of THC concentration (Fig. 4) and its time-course (Fig. 5) on TNF- $\alpha$  release differed from that of THCa. At the higher THC concentration tested, the inhibition of the TNF- $\alpha$  release tended to become weaker. This phenomenon has been reported before, Berdyshec et al<sup>37</sup> reported that THC exerted a biphasic action on pro-inflammatory cytokines in human PB-MO. Low amounts of THC (nM) inhibited the TNF- $\alpha$  production, whilst high concentrations ( $\mu$ M) stimulated TNF- $\alpha$ . After prolonged exposure time THC and heated Cannabis extract tend to induce the TNF- $\alpha$  production. Cannabinoids have demonstrated effects *in vivo* and *in vitro* on the production and function of a variety of cytokines. Depending upon the model system used, these effects are often conflicting<sup>11, 14</sup>. The dose and duration of incubation time, as mentioned above are possible explanations for these discrepancies.

Using a selective antagonist AM281 for the CB<sub>1</sub> receptor<sup>29, 30</sup> and a selective antagonist for the CB<sub>2</sub> receptor, AM630<sup>31</sup> we showed that the inhibitory effect on TNF- $\alpha$  production by THC, THCa and unheated Cannabis extract is not mediated via these receptors (Fig. 6). From these results it can not be concluded whether THCa acts via another receptor or via non-receptor mediated mechanisms. There have been many speculations about a third type of CB receptor<sup>1, 8, 37</sup> but many other options could be possible as well. As one pathway leading to TNF- $\alpha$  inhibition is linked to cAMP induction<sup>38, 39</sup> the possibility that THCa acts via this route was investigated. Accumulation of cAMP may result from the stimulation of receptors which activate Gs proteins<sup>38, 39</sup>. Figure 7 shows that cAMP was not significantly induced by THC, THCa or unheated Cannabis extract. Another possibility is that receptors that couple to Gq proteins are involved. Binding to this receptor will activate phospholipase C. LPS can induce TNF- $\alpha$  production via the following pathway: LPS activates PC-PLC, which hydrolyses phosphatidylcholine resulting in the formation of cholinephosphate and diacylglycerol (DAG). DAG stimulates ceramide, which in turn activates successively raf1, MEK, ERK, and TNF- $\alpha$ <sup>40</sup>. We therefore investigated if THC, THCa and unheated Cannabis extract had any effect on the PC-PLC activity. From Figure 8 we can conclude that there is indeed a difference in the effect on PC-PLC activity of THC and THCa. THCa and unheated Cannabis extract inhibited both the PC-PLC activity in a dose-dependent manner. This could be an explanation for the difference in TNF- $\alpha$  inhibitory effect. D609 was used as a positive control for inhibition of PC-PLC activity. D609 is a selective PC-PLC inhibitor and inhibits the production of TNF- $\alpha$  induced by LPS<sup>40-42</sup> via a PC-PLC dependent pathway. The question is if THCa exerts its effect via a Gq receptor or directly on PC-PLC itself. These

results merit further investigation. Interesting is the induction of PC-PLC activity at high THC concentration (80 nM). This induction reflects the increase in TNF- $\alpha$  production shown in Figure 4. Ho et al<sup>43</sup> found that the CB<sub>1</sub> receptor coupled positively to phospholipase C activity. We can only speculate that high levels of THC bind to the CB<sub>1</sub> receptor, which couples to PC-PLC and via a complex pathway, induces TNF- $\alpha$  production. Further investigation would be necessary to support this.

The cannabinoids,  $\Delta^9$ -THC and  $\Delta^8$ -THC showed in previous *in vivo* studies to have a positive effect on the onset, incidence and severity of EAE in Lewis rats immunized with myelin basic protein or autologous spinal cord.<sup>17, 18</sup>  $\Delta^9$ -THC, not  $\Delta^8$ -THC also inhibited the inflammatory infiltrates in brain tissue. In this study we investigated if THCa and unheated Cannabis extract are able to reflect the positive effect of THC on the clinical and histological signs of EAE. In this pilot study we used, the EAE-SJL mice model system. EAE induced by PLP<sub>139-151</sub> in SJL mice follows a reliable relapsing-remitting course with acute clinical signs first appearing about 11 days after immunization and relapses first appear after 28 days<sup>21, 44</sup>. During the relapsing period (20-42 days) the animals were not treated with medication, so the effect over a longer period can be investigated. Table 2 revealed that unheated Cannabis extract and THCa had a slight effect on the severity of the disease, which failed to reach significance. Since no information on the pharmacokinetics of THCa and unheated Cannabis extract was available for mice, the dosing schedule could be further optimized. Nevertheless, both treatments resulted in significantly less inflammatory infiltrates in the brain stem, supporting that THCa and unheated Cannabis extract may have the potential to inhibit inflammatory responses *in vivo* and to suppress clinical symptoms when administered at a different dosage. More detailed analysis of inflammatory infiltrates is required at earlier time points for a better appreciation of the efficacy of treatment on sub-clinical aspects of the disease.

### **Concluding remarks**

This is the first report describing the immuno-modulating properties of THCa and unheated Cannabis extracts, which lack the psychoactive properties of THC. Our results suggest that THCa and unheated Cannabis extracts are acting via different metabolic pathways than THC, but we can only speculate if they are devoid of the adverse effects of THC and heated Cannabis extracts on health. The immuno-modulating effect of THCa and unheated Cannabis extracts was not only observed *in vitro*, but also *in vivo*. In a pilot EAE animal study the effects of THCa and unheated Cannabis extracts on the clinical and histological signs of EAE

collectively suggest that these may have therapeutic potential, but more attention has to be paid to the way and amount of dosing, because little is known about the pharmacokinetics of THCa and unheated Cannabis extracts.

### Acknowledgements

The authors thank Inge Haspels for her assistance in performing the EAE animal study.

### References

- 1 Grotenhermen, F., *Clin Pharmacokinet*, **2003**, Pharmacokinetics and pharmacodynamics of cannabinoids, *42*, 327-360.
- 2 Kalant, H., *Pain Res Manag*, **2001**, Medicinal use of cannabis: History and current status, *6*, 80-91.
- 3 Mechoulam, R. and Hanu, L., *Pain Res Manag*, **2001**, The cannabinoids: An overview. Therapeutic implications in vomiting and nausea after cancer chemotherapy, in appetite promotion, in multiple sclerosis and in neuroprotection, *6*, 67-73.
- 4 Pertwee, R. G. and Ross, R. A., *Prostaglandins Leukot Essent Fatty Acids*, **2002**, Cannabinoid receptors and their ligands, *66*, 101-121.
- 5 Howlett, A. C., Barth, F., Bonner, T. I., Cabral, G., *et al.*, *Pharmacol Rev*, **2002**, nion of pharmacology. Xxvii. Classification of cannabinoid receptors, *54*, 161-202.
- 6 Klein, T. W., Newton, C., Larsen, K., Lu, L., *et al.*, *J Leukoc Biol*, **2003**, The cannabinoid system and immune modulation, *74*, 486-496.
- 7 Bonhaus, D. W., Chang, L. K., Kwan, J. and Martin, G. R., *J Pharmacol Exp Ther*, **1998**, Dual activation and inhibition of adenylyl cyclase by cannabinoid receptor agonists: Evidence for agonist-specific trafficking of intracellular responses, *287*, 884-888.
- 8 Wiley, J. L. and Martin, B. R., *Chem Phys Lipids*, **2002**, Cannabinoid pharmacology: Implications for additional cannabinoid receptor subtypes, *121*, 57-63.
- 9 Pertwee, R. G., *Pharmacol Ther*, **2002**, Cannabinoids and multiple sclerosis, *95*, 165-174.
- 10 Kalant, H., *Prog Neuropsychopharmacol Biol Psychiatry*, **2004**, Adverse effects of cannabis on health: An update of the literature since 1996, *28*, 849-863.
- 11 Klein, T. W., Lane, B., Newton, C. A. and Friedman, H., *Proc Soc Exp Biol Med*, **2000**, The cannabinoid system and cytokine network, *225*, 1-8.
- 12 Herring, A. C. and Kaminski, N. E., *J Pharmacol Exp Ther*, **1999**, Cannabinol-mediated inhibition of nuclear factor-kappab, camp response element-binding protein, and interleukin-2 secretion by activated thymocytes, *291*, 1156-1163.
- 13 Bidaut-Russell, M., Devane, W. A. and Howlett, A. C., *J Neurochem*, **1990**, Cannabinoid receptors and modulation of cyclic amp accumulation in the rat brain, *55*, 21-26.
- 14 Klein, T. W., Newton, C. A. and Friedman, H., *Pain Res Manag*, **2001**, Cannabinoids and the immune system, *6*, 95-101.
- 15 De Meijer, E. P., Bagatta, M., Carboni, A., Crucitti, P., *et al.*, *Genetics*, **2003**, The inheritance of chemical phenotype in cannabis sativa l, *163*, 335-346.
- 16 Pate, D. W., *Journal of the international Hemp association*, **1994**, Chemical ecology of cannabis, *2*, 32-37.
- 17 Lyman, W. D., Sonett, J. R., Brosnan, C. F., Elkin, R. and Bornstein, M. B., *J Neuroimmunol*, **1989**, Delta 9-tetrahydrocannabinol: A novel treatment for experimental autoimmune encephalomyelitis, *23*, 73-81.
- 18 Wirguin, I., Mechoulam, R., Breuer, A., Schezen, E., *et al.*, *Immunopharmacology*, **1994**, Suppression of experimental autoimmune encephalomyelitis by cannabinoids, *28*, 209-214.
- 19 Satoh, J., Sakai, K., Endoh, M., Koike, F., *et al.*, *J Immunol*, **1987**, Experimental allergic encephalomyelitis mediated by murine encephalitogenic t cell lines specific for myelin proteolipid apoprotein, *138*, 179-184.
- 20 Nagelkerken, L., Blauw, B. and Tielemans, M., *Int Immunol*, **1997**, Il-4 abrogates the inhibitory effect of il-10 on the development of experimental allergic encephalomyelitis in sjl mice, *9*, 1243-1251.
- 21 Begolka, W. S., Vanderlugt, C. L., Rahbe, S. M. and Miller, S. D., *J Immunol*, **1998**, Differential expression of inflammatory cytokines parallels progression of central nervous system pathology in two clinically distinct models of multiple sclerosis, *161*, 4437-4446.

- 
- 22 Issazadeh, S., Ljungdahl, A., Hojeberg, B., Mustafa, M. and Olsson, T., *J Neuroimmunol*, **1995**, Cytokine production in the central nervous system of lewis rats with experimental autoimmune encephalomyelitis: Dynamics of mrna expression for interleukin-10, interleukin-12, cytolysin, tumor necrosis factor alpha and tumor necrosis factor beta, *61*, 205-212.
- 23 Hazekamp, A., Choi, Y. H. and Verpoorte, R., *Chem Pharm Bull (Tokyo)*, **2004**, Quantitative analysis of cannabinoids from cannabis sativa using 1h-nmr, *52*, 718-721.
- 24 Stolker, A. A., van Schoonhoven, J., de Vries, A. J., Bobeldijk-Pastorova, I., *et al.*, *J Chromatogr A*, **2004**, Determination of cannabinoids in cannabis products using liquid chromatography-ion trap mass spectrometry, *1058*, 143-151.
- 25 Sundstrom, C. and Nilsson, K., *Int J Cancer*, **1976**, Establishment and characterization of a human histiocytic lymphoma cell line (u-937), *17*, 565-577.
- 26 Verhoeckx, K. C., Bijlsma, S., Jespersen, S., Ramaker, R., *et al.*, *Int Immunopharmacol*, **2004**, Characterization of anti-inflammatory compounds using transcriptomics, proteomics, and metabolomics in combination with multivariate data analysis, *4*, 1499-1514.
- 27 Verhoeckx, K. C., Bijlsma, S., de Groene, E. M., Witkamp, R. F., *et al.*, *Proteomics*, **2004**, A combination of proteomics, principal component analysis and transcriptomics is a powerful tool for the identification of biomarkers for macrophage maturation in the u937 cell line, *4*, 1014-1028.
- 28 Kreutz, M., Krause, S. W., Hennemann, B., Rehm, A. and Andreesen, R., *Res Immunol*, **1992**, Macrophage heterogeneity and differentiation: Defined serum-free culture conditions induce different types of macrophages in vitro, *143*, 107-115.
- 29 Gatley, S. J., Lan, R., Volkow, N. D., Pappas, N., *et al.*, *J Neurochem*, **1998**, Imaging the brain marijuana receptor: Development of a radioligand that binds to cannabinoid cb1 receptors in vivo, *70*, 417-423.
- 30 Cosenza, M., Gifford, A. N., Gatley, S. J., Pyatt, B., *et al.*, *Synapse*, **2000**, Locomotor activity and occupancy of brain cannabinoid cb1 receptors by the antagonist/inverse agonist am281, *38*, 477-482.
- 31 Ross, R. A., Brockie, H. C., Stevenson, L. A., Murphy, V. L., *et al.*, *Br J Pharmacol*, **1999**, Agonist-inverse agonist characterization at cb1 and cb2 cannabinoid receptors of 1759633, 1759656, and am630, *126*, 665-672.
- 32 Bouaboula, M., Rinaldi, M., Carayon, P., Carillon, C., *et al.*, *Eur J Biochem*, **1993**, Cannabinoid-receptor expression in human leukocytes, *214*, 173-180.
- 33 De Zeeuw, R. A., Malingre, T. M. and Merkus, F. W., *J Pharm Pharmacol*, **1972**, 1 - tetrahydrocannabinolic acid, an important component in the evaluation of cannabis products, *24*, 1-6.
- 34 Kelly, P. and Jones, R. T., *J Anal Toxicol*, **1992**, Metabolism of tetrahydrocannabinol in frequent and infrequent marijuana users, *16*, 228-235.
- 35 van Furth, R., *Immunobiology*, **1982**, Current view on the mononuclear phagocyte system, *161*, 178-185.
- 36 Rizzo, M. G., Zepparoni, A., Cristofanelli, B., Scardigli, R., *et al.*, *Br J Cancer*, **1998**, Wt-p53 action in human leukaemia cell lines corresponding to different stages of differentiation, *77*, 1429-1438.
- 37 Berdyshev, E. V., Boichot, E., Germain, N., Allain, N., *et al.*, *Eur J Pharmacol*, **1997**, Influence of fatty acid ethanolamides and delta9-tetrahydrocannabinol on cytokine and arachidonate release by mononuclear cells, *330*, 231-240.
- 38 Kast, R. E., *Int J Immunopharmacol*, **2000**, Tumor necrosis factor has positive and negative self regulatory feed back cycles centered around camp, *22*, 1001-1006.
- 39 Zidek, Z., *Eur Cytokine Netw*, **1999**, Adenosine - cyclic amp pathways and cytokine expression, *10*, 319-328.
- 40 Monick, M. M., Carter, A. B., Gudmundsson, G., Mallampalli, R., *et al.*, *J Immunol*, **1999**, A phosphatidylcholine-specific phospholipase c regulates activation of p42/44 mitogen-activated protein kinases in lipopolysaccharide-stimulated human alveolar macrophages, *162*, 3005-3012.
- 41 Zhang, F., Zhao, G. and Dong, Z., *Int Immunopharmacol*, **2001**, Phosphatidylcholine-specific phospholipase c and d in stimulation of raw264.7 mouse macrophage-like cells by lipopolysaccharide, *1*, 1375-1384.
- 42 Carter, A. B., Monick, M. M. and Hunninghake, G. W., *Am J Respir Cell Mol Biol*, **1998**, Lipopolysaccharide-induced nf-kappab activation and cytokine release in human alveolar macrophages is pkc-independent and tk- and pc-plc-dependent, *18*, 384-391.
- 43 Ho, B. Y., Current, L. and Drewett, J. G., *FEBS Lett*, **2002**, Role of intracellular loops of cannabinoid cb(1) receptor in functional interaction with g(alpha16), *522*, 130-134.
- 44 McRae, B. L., Kennedy, M. K., Tan, L. J., Dal Canto, M. C., *et al.*, *J Neuroimmunol*, **1992**, Induction of active and adoptive relapsing experimental autoimmune encephalomyelitis (eae) using an encephalitogenic epitope of proteolipid protein, *38*, 229-240.
-



# Chapter 8

---

## **Categorization of the anti-inflammatory properties of Cannabis extracts using transcriptomics in combination with multivariate data analysis.**

Kitty C.M. Verhoeckx<sup>1,2</sup>

Sabina Bijlsma<sup>1</sup>

Renger F. Witkamp<sup>1</sup>

Jan van der Greef<sup>1,2</sup>

Richard J.T. Rodenburg<sup>3</sup>

<sup>1</sup> TNO Quality of Life, Zeist, The Netherlands, <sup>2</sup> Leiden University, Leiden/Amsterdam Center for Drug Research, Leiden, The Netherlands, <sup>3</sup> UMC St Radboud, Nijmegen, The Netherlands

## **Categorization of the anti-inflammatory properties of Cannabis extracts using transcriptomics in combination with multivariate data analysis.**

*In the present study we categorized the anti-inflammatory activities of unheated and heated Cannabis extracts according to their mechanism of action. For this purpose we made use of U937 macrophages exposed to LPS in the absence or presence of Cannabis extracts, as well as different classes of anti-inflammatory compounds (e.g.  $\beta_2$ -adrenergic agonists, corticosteroid, MAP kinase inhibitor or proteasome inhibitor). The effects on the transcriptome were investigated using oligonucleotide microarrays in combination with principal component discriminant analysis. We were able to show that heated and unheated Cannabis extracts give rise to different expression patterns, suggesting that their major effects on U937 macrophages are different. Furthermore the results show that although the Cannabis extracts share an inhibitory effect on TNF- $\alpha$  release with the anti-inflammatory compounds tested, their major effects on the U937 transcriptome is different. This might suggest that the Cannabis extracts could be assigned to a class of anti-inflammatory compounds that differs from the compounds tested in the present study.*

---

### **Introduction**

In Chapter 7 we have demonstrated that unheated and, to a lesser extent, heated Cannabis extracts were able to inhibit the LPS induced TNF- $\alpha$  release in U937 macrophages. In the present study we investigated if unheated and heated Cannabis extracts have similar effects on the transcriptome compared to other anti-inflammatory drugs which are known to inhibit the LPS induced TNF- $\alpha$  production (e.g. dexamethasone, proteasome inhibitor (PSI), SB203580 clenbuterol, salbutamol, and zilpaterol). For this purpose, we made use of a screenings system that was previously described in Chapter 3<sup>1</sup>. The screenings system can be used to categorize anti-inflammatory compounds. The system uses the monocytic cell line U937 as a model system. These cells are stimulated with the endotoxin LPS, which induces a broad range of inflammatory pathways. Using oligonucleotide microarrays, the effects of LPS-exposure on the transcriptome can be determined. When this procedure is performed in the presence of an anti-inflammatory compound, this leads to characteristic changes in the U937 mRNA expression pattern. The transcriptome of the anti-inflammatory compound under investigation is matched with that of known inflammatory modulators using a pattern recognition tool, principal component discriminant analysis (PC-DA). Using PC-DA, a supervised data

analysis technique, it is possible to focus on differences between the inflammatory inhibitor groups<sup>2</sup>. In the present study, we have used this screening system to categorize unheated and heated Cannabis extracts.

## **Materials and Methods**

### *Chemicals*

Lipopolysaccharide (LPS, *E.coli* 0111:B4), clenbuterol, salbutamol, formoterol, and dexamethasone were obtained from Sigma (St. Louis, MO, USA). SB203580 and proteasome inhibitor (PSI) were purchased from Omnilabo international B.V. (Breda, The Netherlands) and zilpaterol from Intervet Inc. (Millsboro, US). Two different Cannabis plant cultivars (*Cannabis sativa* and *Cannabis indica*) were obtained from Maripharm (Rotterdam, The Netherlands). Approximately 2.1 g of dried flower tops were extracted twice with 25 mL methanol (sonication for 5 min) and after addition of 2 ml chloroform further extracted for 1 h. The supernatant containing the cannabinoids was evaporated and re-dissolved in ethanol. This extract will be referred to as the ‘unheated’ extract. For the heated extracts, the chloroform/methanol extracts were evaporated, heated for 7 minutes at 200 °C and re-dissolved in an equal volume of ethanol.

### *Cell cultures and incubations*

Human monocyte-like histiocytic lymphoma cells U937<sup>3</sup> obtained from the ATCC (CRL-1593.2) were grown in RPMI-1640 medium, supplemented with 10% (v/v) fetal calf serum and 2 mM L-glutamine (Life technologies, Breda, The Netherlands) at 37 °C, 5% CO<sub>2</sub> in a humidified atmosphere. U937 monocytic cells were differentiated into macrophages using phorbol 12-myristate 13-acetate (PMA, 10 ng/ml, overnight, Omnilabo, Breda, The Netherlands) as described previously<sup>4</sup>. The PMA-differentiated macrophages were allowed to recover from PMA treatment for 48 h, during which the culture medium was replaced daily. At day three after PMA treatment, the macrophages were exposed for 6 h to LPS (*E.Coli*, 1 µg/ml) in the presence or absence of an inflammatory inhibitor. The following inhibitors were used: clenbuterol (1.10<sup>-7</sup> M), salbutamol (1.10<sup>-6</sup> M), zilpaterol (1.10<sup>-6</sup> M), dexamethasone (1.10<sup>-7</sup> M), SB203580 (1.10<sup>-6</sup> M), proteasome inhibitor (PSI, 1.10<sup>-5</sup> M), unheated Cannabis extracts (250 fold diluted) and heated Cannabis extracts (250 fold diluted). The concentrations used give rise to a reduction of the LPS-stimulated TNF-α release of 5-40% compared to the LPS-stimulated TNF-α levels in the absence of inhibitors.

### *Transcriptomics*

Incubations of U937 macrophages with LPS, with or without an inhibitor, were performed in sextuple and pooled afterwards. Total RNA was extracted from stimulated U937 macrophages using Trizol reagent (Life technologies, Rockville, USA) and RNeasy columns (Qiagen, Westburg, Leusden, The Netherlands) according to the manufacturer's protocol. DNase treatment (Qiagen) was performed on the RNeasy column. Each sample was analysed by oligonucleotide microarrays in quadruple, in which LPS was labelled with Cy-3 and LPS + inhibitor was labelled with Cy-5. In addition, a control experiment was performed simultaneously by comparing LPS-Cy-5 with LPS-Cy-3 on the same array, to check the differences in labelling efficiency. Subsequently, the microarray experiments and data processing were performed as described before<sup>5</sup>. The resulting list of genes with their normalized log transformed spot volumes per array were mean-centered and subsequently analyzed with principal component discriminant analysis (PC-DA) using an in house developed function for Matlab (version 6.5.1, release 13, The Mathworks, Inc., 2003).

### **Results**

To investigate the effect of unheated and heated Cannabis extracts on the mRNA expression levels in LPS treated U937 macrophages, we used the same experimental setup as described in chapter 3<sup>1</sup>. Two Cannabis cultivars (1 and 2) containing comparable concentrations of  $\Delta^9$ -tetrahydrocannabinoid acid were investigated. Figure 1 shows the results of the PC-DA of the microarray dataset containing 21,529 oligonucleotides which correspond to 21,316 genes. After data pre-processing and normalisation, a dataset of 10,588 genes remained that was used in the PC-DA.

The close proximity in the PC-DA scoreplot of the data points representing the microarray data of incubations with the two types of heated Cannabis extracts indicate that the mRNA expression patterns of the two heated Cannabis extracts were similar. The same can be concluded for the mRNA patterns obtained after incubation with the two unheated Cannabis extracts. The array data obtained with the unheated Cannabis extracts were positioned at a greater mutual distance from the heated Cannabis extract array data, indicating that unheated and heated Cannabis extracts induced different effects. Moreover, the array data obtained with the Cannabis extracts were positioned at completely different locations than the array data obtained with the other anti-inflammatory compounds,  $\beta_2$ -agonists (clenbuterol, zilpaterol, and salbutamol), proteasome inhibitor (PSI), MAP kinase inhibitor (SB203580) or corticosteroid (dexamethasone). These results suggest that the Cannabis extracts exert their

TNF- $\alpha$  inhibitory effect via a different metabolic pathway than the other anti-inflammatory compounds under investigation.

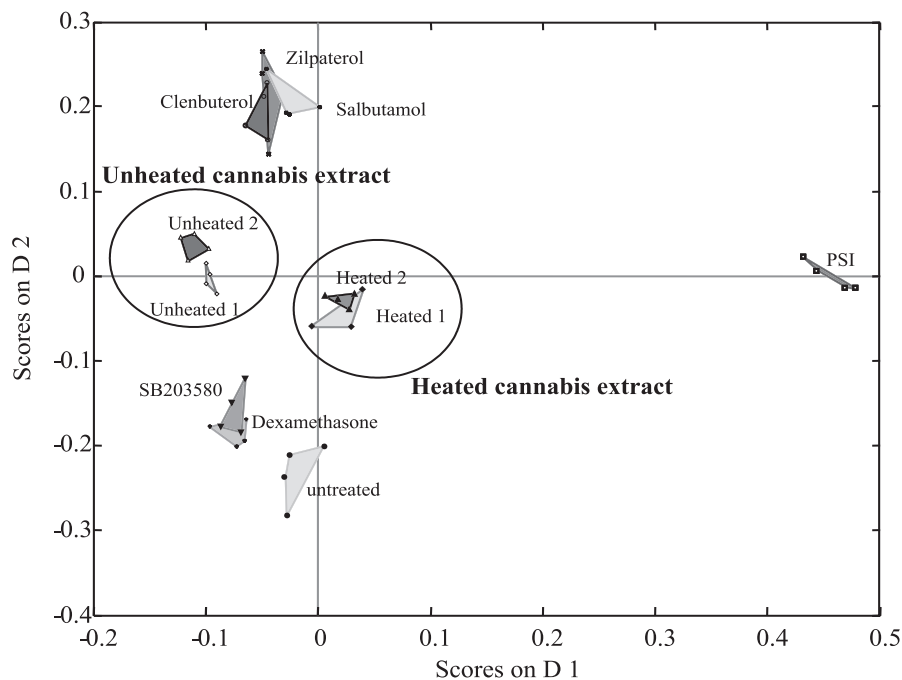


**Figure 1** Graphical presentation of the microarray data analyzed by PC-DA. The results of the arrays of untreated U937 macrophages (●), and macrophages treated with LPS in combination with zilpaterol (×), clenbuterol (○), salbutamol (\*) SB203580 (▼), dexamethasone (+), proteasome inhibitor (PSI □), unheated Cannabis extract (1: ◇ and 2: Δ), and heated Cannabis extract (1: ◆ and 2: ▲) are shown. Each data point represents a separate microarray.

## Discussion

In this study we demonstrate that unheated and heated Cannabis extracts give rise to distinct and characteristic mRNA patterns in our screenings system. Furthermore, our screenings system shows that unheated and heated Cannabis extracts, give rise to a mRNA pattern that is completely different from that of the other anti-inflammatory compounds under investigation. The anti-inflammatory compounds used belong to four different classes with anti-inflammatory properties, each of which has its own specific, partially overlapping inhibitory effect; dexamethasone, a corticosteroid<sup>6-9</sup>, a proteasome inhibitor (PSI)<sup>10-12</sup>, the MAP kinase inhibitor SB203580<sup>13</sup> and three  $\beta_2$ -adrenoreceptor agonists, clenbuterol<sup>14,15</sup>, salbutamol<sup>16</sup>, and zilpaterol<sup>17</sup>. The results presented here demonstrate that heated and unheated Cannabis extracts exert their effect via different pathways, which is in line with our findings presented in Chapter 7. However, the mechanism of action could not be assigned to one of the classes of inflammatory inhibitors mentioned above.

## References

- 1 Verhoeckx, K. C., Bijlsma, S., Jespersen, S., Ramaker, R., *et al.*, *Int Immunopharmacol*, **2004**, Characterization of anti-inflammatory compounds using transcriptomics, proteomics, and metabolomics in combination with multivariate data analysis, *4*, 1499-1514.
- 2 Hoogerbrugge, R., Willig, S. J. and Kistemaker, P. G., *Analytical Chemistry*, **1983**, Discriminant analysis by double stage principal component analysis, *55*, 1710-1712.
- 3 Sundstrom, C. and Nilsson, K., *Int J Cancer*, **1976**, Establishment and characterization of a human histiocytic lymphoma cell line (u-937), *17*, 565-577.
- 4 Izeboud, C. A., Vermeulen, R. M., Zwart, A., Voss, H. P., *et al.*, *Naunyn Schmiedebergs Arch Pharmacol*, **2000**, Stereoselectivity at the beta2-adrenoceptor on macrophages is a major determinant of the anti-inflammatory effects of beta2-agonists, *362*, 184-189.
- 5 Verhoeckx, K. C., Bijlsma, S., de Groene, E. M., Witkamp, R. F., *et al.*, *Proteomics*, **2004**, A combination of proteomics, principal component analysis and transcriptomics is a powerful tool for the identification of biomarkers for macrophage maturation in the u937 cell line, *4*, 1014-1028.
- 6 Almawi, W. Y. and Melemedjian, O. K., *J Mol Endocrinol*, **2002**, Negative regulation of nuclear factor-kappa activation and function by glucocorticoids, *28*, 69-78.
- 7 Joyce, D. A., Gimblett, G. and Steer, J. H., *Inflamm Res*, **2001**, Targets of glucocorticoid action on tnf-alpha release by macrophages, *50*, 337-340.
- 8 Steer, J. H., Kroeger, K. M., Abraham, L. J. and Joyce, D. A., *J Biol Chem*, **2000**, Glucocorticoids suppress tumor necrosis factor-alpha expression by human monocytic thp-1 cells by suppressing transactivation through adjacent nf-kappa b and c-jun-activating transcription factor-2 binding sites in the promoter, *275*, 18432-18440.
- 9 Joyce, D. A., Steer, J. H. and Abraham, L. J., *Inflamm Res*, **1997**, Glucocorticoid modulation of human monocyte/macrophage function: Control of tnf-alpha secretion, *46*, 447-451.
- 10 Adams, J., *Curr Opin Oncol*, **2002**, Proteasome inhibitors as new anticancer drugs, *14*, 628-634.
- 11 Wojcik, C., *Cell Mol Life Sci*, **1999**, Proteasomes in apoptosis: Villains or guardians? *56*, 908-917.
- 12 Griscavage, J. M., Wilk, S. and Ignarro, L. J., *Proc Natl Acad Sci U S A*, **1996**, Inhibitors of the proteasome pathway interfere with induction of nitric oxide synthase in macrophages by blocking activation of transcription factor nf-kappa b, *93*, 3308-3312.
- 13 Lee, J. C., Kassis, S., Kumar, S., Badger, A. and Adams, J. L., *Pharmacol Ther*, **1999**, P38 mitogen-activated protein kinase inhibitors--mechanisms and therapeutic potentials, *82*, 389-397.
- 14 Izeboud, C. A., Monshouwer, M., van Miert, A. S. and Witkamp, R. F., *Inflamm Res*, **1999**, The beta-adrenoceptor agonist clenbuterol is a potent inhibitor of the lps-induced production of tnf-alpha and il-6 in vitro and in vivo, *48*, 497-502.
- 15 Izeboud, C. A., Mocking, J. A., Monshouwer, M., van Miert, A. S. and Witkamp, R. F., *J Recept Signal Transduct Res*, **1999**, Participation of beta-adrenergic receptors on macrophages in modulation of lps-induced cytokine release, *19*, 191-202.
- 16 Libretto, S. E., *Arch Toxicol*, **1994**, A review of the toxicology of salbutamol (albuterol), *68*, 213-216.
- 17 Intervet, **1998**, Zilmax technical brochure.





# Chapter 9

---

**Concluding remarks and future perspectives**

**Summary**

**Samenvatting**

### **Concluding remarks and future perspectives**

The studies performed in this thesis show that holistic analytical strategies, based on transcriptomics, proteomics and metabolomics in combination with multivariate data analysis tools are very powerful in finding specific markers for cellular processes and effects of biologically active compounds. This approach was used to categorize anti-inflammatory drugs based on their mRNA, protein and/or lipid expression patterns. The outcome of the categorization depends on the availability and choice of compounds that can be used as reference compounds in the experiment. The approach that was developed enabled us to classify zilpaterol as a  $\beta_2$ -adrenergic receptor agonist based on a transcriptomic and metabolomic analysis. In addition, although we could not fully elucidate the mechanism of the anti-inflammatory effect of *Cannabis sativa* extracts, we were able to show that this mechanism does not overlap with that of several known anti-inflammatory compounds, including corticosteroids, MAP kinase inhibitor,  $\beta_2$ -adrenergic receptor agonist, and proteasome inhibitor. Moreover, our results suggest that unheated and heated Cannabis extracts use a different mechanism to exert their anti-inflammatory action.

The transcriptomics data showed to be the most suitable dataset to categorize anti-inflammatory drugs, using the U937 cell line. The categorization was less successful when the proteomics data of the applied 2-D gel technology was used. Microarray technology is a straight-forward method. In one experiment ten thousands of genes (from approx. 30.000) can be analysed simultaneously. The possibility to measure almost all genes at once makes transcriptomics a favourable method for holistic approaches at this moment.

Proteomics methods are less suitable for holistic approaches because in a proteomics experiment only a fraction of the total number of proteins in a biological sample (approximately 1000 out of estimated 50.000-500.000 proteins) with more or less the same physiological characteristics (e.g. concentration range, hydrophobicity,) can be observed simultaneously. These proteins are often high abundant proteins, while low abundant proteins that are important in many metabolic pathways, e.g. those involved in the inflammatory response, are not readily seen. Hence the chance of missing crucial regulatory proteins, e.g. those involved in the action of anti-inflammatory drugs, is present. A more in-depth investigation of the proteome is therefore necessary. Pre-fractionation of the sample and enrichment strategies (e.g. immunoaffinity chromatography, subcellular fractionation, and sequential extraction) will improve the chance to find interesting proteins other than the

common ‘housekeeping’ proteins, as was demonstrated by analysing the secreted protein fraction in Chapter 4. Applying more than one proteomics technique (e.g. 2-D gel electrophoresis, LC-MS, protein arrays) within a proteomics study will improve the recovery of a wide range of diverse proteins. None of the above-mentioned proteomics techniques is preferable over the other, instead these techniques are complementary. The analysis of protein samples separated into many different fractions and the application of different analytical techniques makes the analysis of only one sample a time-consuming task. Nevertheless, the protein level remains one of the most interesting levels to investigate biological functions and disease states. In practice it is therefore advisable to focus solely on a specific part of the proteome that is closely related to the biological question, instead of analysing the whole proteome. For example, when there is an interest in G-protein coupled receptors, the membrane fraction has to be investigated rather than the whole cell lysate. For this reason, in future research it is important to focus on pre-fractionation techniques that are reproducible and yield high protein content.

Another important issue in proteomics is protein identification. Insufficient amounts of peptides being generated after in-gel digestion and their low signal intensity makes it difficult to identify proteins with high confidence. These drawbacks have to be improved especially when low abundant or proteins with low molecular masses have to be identified. With LC-MS methods this problem is less pronounced but in some methods the proteins have to be identified using a minimal number of peptides, especially in cases where peptides have been tagged and subsequently pre-fractionated (e.g. cysteins) for quantification purposes. Moreover, information on post-translational modifications, such as phosphorylation, are easily missed. Furthermore, mass accuracy is an important issue in protein identification. The more accurate the peptide mass, the larger the chance that a protein or peptide will be identified with high confidence. The introduction of the Fourier transform mass spectrometer (FT-MS), a high resolution mass spectrometer, in the proteomics platform will significantly improve protein identification.

The analysis of the metabolome is hampered by similar problems as encountered during proteome analysis. The diverse properties and vast concentration ranges of molecules forces the investigator to use many different methods to analyse, if possible at all, the whole metabolome. Using only the lipid data we were able to categorize the anti-inflammatory drugs based on their mechanisms of action. The separation by PC-DA could not be assigned to one

or more specific biomarkers. This means that the combined regulation of several lipids is responsible for the differences found in the lipid expression patterns by PC-DA. This underlines the power of multivariate data analysis tools to find hidden correlations and trends in large datasets.

Multivariate data analysis tools proved to be powerful in classifying samples according to their differentiation state (Chapter 2), anti-inflammatory effect (Chapter 3) and disease state (inflammation, inhibition of inflammation) in Chapter 4. Moreover, the use of multivariate data analysis tools enabled us to find specific biomarkers for differentiation (Chapter 2), anti-inflammatory effects of different anti-inflammatory drugs (Chapter 3) and biomarkers that were linked to anti-inflammation and the  $\beta_2$ -adrenergic receptor (Chapter 4). The datasets obtained by proteomics, transcriptomics and metabolomics was in most cases based on a limited number of samples, compared to the number of variables. Multivariate data analysis tools are mathematical tools, and therefore, finding false positive results can not be excluded, especially when the number of data points is at the lower limit. It is therefore important to regard the statistical tools employed as explorative tools and all findings have to be biologically validated, for example by using traditional biochemical methods like real time PCR, Western blot, or immunoassays. When the observed differences can not be validated univariately, other more comprehensive methods have to be used (e.g. a comparison of the transcriptome with the proteome of the same sample). In any case, the modern technologies used in transcriptomics, proteomics and metabolomics research yield vast amounts of data, and the statistical tools currently available are not optimally designed to meet this challenge. Therefore, extensive validation of any result found by statistical analysis is essential. Hopefully, in the future statisticians and biologists can find more suitable methods to cope with these large datasets. Statisticians have to develop methods that can cope with a smaller number of samples and biologists have to find a way to reduce the number of variables by filtering the datasets to remove the 'noise'. Unfortunately, it is not possible to filter the datasets by using univariate data analysis tools, because these tools do not take into account the possible correlations between two or more variables. Although the use of smaller datasets or microarrays which contain less genes could be an alternative to overcome these issues, but this may possibly narrow down the research to already well known pathways. This contradicts with the idea of the holistic approach of systems biology, which aims to investigate all cellular pathways, and to identify the web of interactions between these pathways.



of great importance. Minor variations in procedures, reagents, or environment may already have a great impact on the biological system under investigation.

Systems biology is a powerful tool but the success of this technology can be greatly enhanced by an efficient cooperation of many scientists of different disciplines, as well as of the universities and companies involved in systems biology.

## Summary

The introduction of the ‘omics’ techniques (transcriptomics, proteomics, and metabolomics) and systems biology, has caused fundamental changes in the drug discovery process and many other fields in the life science area. In this thesis we explored the possibilities to apply these holistic technologies to investigate the effects of known and potential anti-inflammatory compounds on macrophages. For this purpose we made use of a monocyte-like human histocytic lymphoma cell line U937. U937 cells can be induced by phorbol 12-myristate 13-acetate (PMA) to undergo differentiation into a macrophage-like phenotype. The two differentiation stages, monocyte and macrophage, were compared by using oligonucleotide microarrays and 2-D gel electrophoresis in combination with principal component analysis (PCA). This differentiation study is described in Chapter 2. The differential expression of three protein biomarkers, gamma interferon inducible lysosomal thiol reductase (GILT), cathepsin D and adipocyte-fatty acid binding protein (A-FABP) were biologically validated by Western blot and real time polymerase chain reaction (real time PCR). GILT and A-FABP were also found to be differentially expressed at the mRNA level as indicated by the results of the microarray experiment. Moreover, the transcriptomics data revealed a large number of additional putative differentiation markers in U937 macrophages, many of which are known to be expressed in peripheral blood-derived macrophages. From the results presented in Chapter 2 can be concluded that the U937 cell line is an excellent model system for the blood-derived macrophage and that microarrays and 2-D gel electrophoresis are suitable methods to identify biomarkers for differentiation.

Chapter 3 describes the use of a systems biology approach to categorize anti-inflammatory drugs based on their mRNA, protein and lipid expression pattern, as determined by oligonucleotide microarrays, 2-D gel electrophoresis and a LC-MS method for lipids, in combination with principal component discriminant analysis (PC-DA). The results described in this chapter demonstrate that different classes of anti-inflammatory compounds show distinct and characteristic mRNA, protein, and lipid expression patterns, which can be used to categorize known anti-inflammatory drugs, as well as to discover and classify new leads. The latter was exemplified by the categorization of zilpaterol, a poorly characterized  $\beta_2$ -agonist. Exposure to zilpaterol gives rise to an almost identical expression pattern as that observed after exposure to the well-characterized  $\beta_2$ -agonists clenbuterol and salbutamol, suggesting that zilpaterol is indeed a  $\beta_2$ -agonist. In addition, this study revealed potential biomarkers for

the different anti-inflammatory drugs under investigation. The categorization of the anti-inflammatory drugs on the basis of proteomics data alone was not successful. The most likely explanation for this is that by the analysis of whole cell lysates, only highly abundant proteins can be visualized, while the low abundant proteins, which are often involved in important metabolic pathways, are not. Therefore, a more focused approach was used to investigate the mechanism of action of zilpaterol, which is described in Chapter 4.

In Chapter 4, U937 macrophages were stimulated with LPS to induce an inflammatory response. This response was inhibited by the addition of zilpaterol (LZ) and this inhibition was antagonized by the  $\beta_2$ -adrenergic receptor antagonist propranolol (LZP). Two-dimensional difference gel electrophoresis (DIGE) in combination with Student's *t*-test and two multivariate data analysis tools (PCA and partial least squares discriminant analysis PLS-DA) were used to examine the secreted proteome induced by the three treatments. This revealed 8 potential protein biomarkers. The protein spots were identified using nano LC-MS-MS. Only two of the identified proteins, namely macrophage inflammatory protein-1 $\beta$  (MIP-1 $\beta$ ) and macrophage inflammatory protein-1 $\alpha$  (MIP-1 $\alpha$ ) are known to be secreted proteins. The inhibition of MIP-1 $\beta$  by zilpaterol and the involvement of the  $\beta_2$ -AR and cyclic adenosine-3',5'-cyclic monophosphate (cAMP) were confirmed using a specific immuno-assay. The experiments described in this chapter demonstrate the importance of pre-fractionation of complex protein samples before performing proteomics studies.

The categorization of zilpaterol in Chapter 3 as a  $\beta_2$ -adrenergic receptor agonist was further explored in Chapter 5. In this chapter we investigated the binding affinity of zilpaterol to the  $\beta_1$ - and  $\beta_2$  receptor by using a receptor binding assay. Furthermore, we examined the role of the  $\beta_1$ - and  $\beta_2$  adrenoceptor in the inhibition of the LPS induced tumor necrosis factor-alpha (TNF- $\alpha$ ) production and the induction of cAMP by U937 macrophages. For this purpose we made use of a selective  $\beta_1$ -receptor antagonist (atenolol), a selective  $\beta_2$ -antagonist (ICI 118551) and a non-selective  $\beta$ -antagonist (propranolol). Finally, the inhibitory effect of zilpaterol on the TNF- $\alpha$  production was investigated in LPS-treated male Wistar rats. The results obtained in this way clearly show that zilpaterol is a  $\beta_2$ -adrenergic agonist and a inhibitor of the LPS-induced TNF- $\alpha$  production by macrophages both *in vivo* and *in vitro*.

The three  $\beta_2$ -agonists specific biomarkers, Granulocyte Chemotactic Protein-2 (GCP-2/CXCL6), Oncostatin M (OSM), and Vascular Endothelial Growth Factor (VEGF) that were

identified in Chapter 3, were further examined in Chapter 6. The three markers were significantly up-regulated both in U937 macrophages and in blood-derived macrophages exposed to a  $\beta_2$ -agonist (clenbuterol and zilpaterol) in the absence or presence of LPS, as determined by a specific enzyme-linked immunosorbent assays (ELISA). Moreover, this up-regulation was also accomplished by other cyclic AMP elevating agents (forskolin, prostaglandins  $E_2$ , and dibutyryl cAMP), suggesting a role of cAMP in the up-regulation of GCP-2/CXCL6, VEGF and OSM. We hypothesize that these proteins may be involved in some of the adverse effects in the treatment of asthma with  $\beta_2$ -adrenergic receptor agonists.

In the second part of this thesis we focussed on a multi-component drug, namely *Cannabis sativa*. In Chapter 7, the immuno-modulating effects of unheated and heated Cannabis extracts were investigated. This study revealed that unheated Cannabis extracts and its major non-psychoactive compound  $\Delta^9$ -tetrahydrocannabinolic acid (THCa) were able to inhibit the LPS induced TNF- $\alpha$  production both in U937 macrophages and in blood-derived macrophages. The inhibitory effect on TNF- $\alpha$  was not mediated by the cannabinoid receptors CB<sub>1</sub> and CB<sub>2</sub>. Furthermore, this study showed that unheated Cannabis extracts and THCa exert their inhibitory effect on the TNF- $\alpha$  production via a mechanism that is different from that of heated Cannabis extract and its main constituent the psychoactive compound  $\Delta^9$ -tetrahydrocannabinol (THC). The inhibition of TNF- $\alpha$  release by unheated Cannabis extract and THCa was prolonged over a relatively long period of time. By contrast, although THC and heated extracts initially inhibit the release of TNF- $\alpha$ , after longer incubation times they seem to increase TNF- $\alpha$  production to levels that are even higher than in the absence of THC or Cannabis extract. This difference in response of the U937 macrophages to THC and THCa was also observed in an experiment in which we examined the effects on phosphatidylcholine specific phospholipase C (PC-PLC) activity. Unheated Cannabis extract and THCa inhibited the PC-PLC activity in a dose-dependent manner, while THC induced PC-PLC activity at high concentrations. Finally, we studied the effect of THCa and unheated Cannabis extract in a pilot study using an Experimental Autoimmune Encephalomyelitis (EAE) mouse model. Unheated Cannabis extract and THCa had a favourable effect on the clinical and histological signs of EAE. However, these results are preliminary and not clearly significant, therefore further investigation is necessary.

Chapter 8 describes the categorization of unheated and heated Cannabis extracts using the same model system as described in Chapter 3. The mRNA patterns obtained from U937

macrophages exposed to LPS in the absence or presence of different anti-inflammatory drugs and unheated and heated Cannabis extracts were analysed using PC-DA. The study revealed that heated and unheated Cannabis extracts give rise to different expression patterns, which is in agreement with the observations made in Chapter 7 that they exert their TNF- $\alpha$  inhibitory effect via different pathways. Moreover, their expression patterns did not overlap with that of other classes of anti-inflammatory compounds known to inhibit the TNF- $\alpha$  production. These results suggest that the Cannabis extracts can not be assigned to one of the above mentioned classes of inflammatory inhibitors. Further investigation is necessary to unravel the exact mechanism of action of unheated and heated Cannabis extracts.

In conclusion, the studies in this thesis show that the application of systems biology approaches are very useful in the categorization of anti-inflammatory compounds based on their mRNA and lipid expression patterns and to find specific biomarkers for these compounds. The categorization based on the protein expression pattern was less successful. This is most probably due to the fraction of proteins that was analysed on the gel. With proteomics techniques only a small fraction of proteins can be analysed simultaneously. Pre-fractionation, enrichment techniques and different analytical methods are therefore necessary to analyse a wide range of proteins with diverse physiological properties and dynamic range. The datasets obtained by transcriptomics, proteomics and metabolomics were analysed using statistical and pattern recognition tools. The datasets often contained a limited number of samples with respect to the large number of variables. It is therefore important to use these techniques as an explorative tool only and to validate the potential biomarkers found by additional individual measurements.

Taken together, the use of systems biology for the investigation of anti-inflammatory drugs yielded very promising results, even though only a small part of the systems biology circle (Fig. 1) was used.

## Samenvatting

De ontwikkelingen op het gebied van genomics, systeembioïogie, en de verschillende afzonderlijke ‘omics’-disciplines (transcriptomics, proteomics en metabolomics) hebben ingrijpende veranderingen te weeg gebracht in het biomedisch onderzoek. Dit geldt zeker ook voor het onderzoek en de ontwikkeling van nieuwe geneesmiddelen.

Bij het onderzoek beschreven in dit proefschrift werden onder andere de mogelijkheden bestudeerd om deze ‘holistische’ technieken toe te passen bij studies naar de eigenschappen van bestaande en nieuwe ontstekingsremmende verbindingen. In de studies werd gebruik gemaakt van de U937 cellijn, welke is afgeleid van humane monocytën. U937 cellen kunnen na blootstelling aan phorbol 12-myristate 13-acetaat (PMA) differentiëren naar een cel met een macrofaag-achtig fenotype. De twee differentiatiestadia (monocyte en macrofaag) werden met elkaar vergeleken door middel van oligonucleotide microarrays en 2-dimensionale gelelectroforese in combinatie met principale component analyse (PCA). Deze differentiatiestudie wordt beschreven in hoofdstuk 2. De differentiële expressie van drie eiwit biomarkers, gamma interferon inducible lysosomal thiol reductase (GILT), cathepsin D en adipocyte-fatty acid binding protein (A-FABP) werden biologisch gevalideerd met behulp van Western blot en real time polymerase chain reaction (real time PCR). De inductie van GILT en A-FABP werd ook op mRNA niveau gevonden met behulp van microarrays. Naast deze markers leverde het microarray experiment nog meer mogelijke biomarkers op, waarvan er diversen al beschreven waren voor perifere bloedmacrofagen. De resultaten beschreven in hoofdstuk twee laten zien dat de U937 cellijn een geschikt modelsysteem is voor de uit bloed geïsoleerde macrofaag en dat microarrays en 2-D gelelectroforese geschikte technieken zijn om differentiatie biomarkers te identificeren.

Hoofdstuk 3 beschrijft een systeembioïogische aanpak om ontstekingsremmende verbindingen te karakteriseren op basis van hun mRNA-, eiwit- en lipide- expressiepatroon. Deze expressiepatronen werden geanalyseerd met behulp van oligonucleotide microarrays, 2-D gelelectroforese en een LC-MS methode voor lipiden, in combinatie met principale component discriminant analyse (PC-DA). De resultaten gepresenteerd in dit hoofdstuk laten zien dat verschillende klassen van ontstekingsremmers verschillende en karakteristieke mRNA-, eiwit- en lipide- expressiepatronen induceren, die gebruikt kunnen worden om bekende en nieuwe ontstekingsremmers te classificeren. De methode werd getoetst met behulp van zilpaterol, een nog relatief weinig beschreven en gekarakteriseerde  $\beta_2$ -agonist. De

blootstelling van U937 macrofagen aan zilpaterol resulteerde in een bijna identiek expressiepatroon als wanneer de U937 macrofagen blootgesteld werden aan klassieke  $\beta_2$ -agonisten. Daarnaast leverde deze aanpak mogelijke biomarkers op, voor de verschillende klassen ontstekingsremmers gebruikt in het experiment. Het karakteriseren van ontstekingsremmers op basis van de proteomics resultaten alleen was minder succesvol. De meest waarschijnlijke verklaring hiervoor is dat wanneer er gekeken wordt naar extracten verkregen uit hele cellen, alleen de eiwitten die in sterke mate tot expressie komen zichtbaar zijn. De eiwitten die in lage concentratie aanwezig zijn en vooral betrokken zijn bij belangrijke metabole routes worden hierdoor overschaduwd. Daarom werd in hoofdstuk 4 een meer gefocuste methode toegepast om de werking van zilpaterol te bestuderen.

In hoofdstuk 4 werden U937 macrofagen blootgesteld aan LPS om een ontstekingsreactie te induceren. Deze ontsteking werd vervolgens geremd door de toevoeging van zilpaterol. De werking van zilpaterol werd weer opgeheven door de toevoeging van een  $\beta_2$ -antagonist, propranolol. De DIGE technologie (difference gel electrophoresis) in combinatie met de Student's *t*-test en twee multivariate data analyse methoden (PCA en partial least squares discriminant analysis (PLS-DA)) werden gebruikt om de uitgescheiden eiwitfractie van de hierboven beschreven behandelingen te bestuderen. Deze methode leverde 8 mogelijke biomarkers op. De eiwitten werden met behulp van nanoLC-MS geïdentificeerd. Slechts 2 van de 8 eiwitten werden geïdentificeerd als een uitgescheiden eiwit, namelijk macrophage inflammatory protein-1beta (MIP-1 $\beta$ ) en macrophage inflammatory protein-1alpha (MIP-1 $\alpha$ ). De remming van MIP-1 $\beta$  door zilpaterol en de betrokkenheid van de  $\beta_2$ -receptor en cyclic adenosine-3',5'-cyclic monophosphate (cAMP) werd bevestigd met behulp van een immunoassay. De experimenten beschreven in dit hoofdstuk laten zien dat het voor proteomics studies van belang is om complexe eiwitmonsters vooraf te pre-fractioneren.

De karakterisering van zilpaterol als een  $\beta_2$ -agonist in hoofdstuk 3 werd verder onderzocht in hoofdstuk 5. In dit hoofdstuk werd eerst de bindingsaffiniteit van zilpaterol tot de  $\beta_1$ - en  $\beta_2$ -receptor bepaald met behulp van een receptor bindingstudie. Vervolgens werd de betrokkenheid van de  $\beta_1$ - en  $\beta_2$ -adrenoceptor bestudeerd bij de remming van de tumor necrosis factor alpha (TNF- $\alpha$ ) productie door cellen blootgesteld aan LPS. Hiervoor werd gebruik gemaakt van een selectieve  $\beta_1$ -receptor antagonist (atenolol), een selectieve  $\beta_2$ -antagonist (ICI 188551) en een niet-selectieve  $\beta$ -antagonist (propranolol). Als laatste werd het remmende effect van zilpaterol op de TNF- $\alpha$  productie onderzocht in mannelijke Wistar ratten

behandeld met LPS. De verkregen resultaten laten zien dat zilpaterol een  $\beta_2$ -agonist is en een potente remmer van de LPS-geïnduceerde TNF- $\alpha$  productie door macrofagen *in vivo* en *in vitro*.

Drie  $\beta_2$ -agonisten biomarkers geïdentificeerd in hoofdstuk 3, Granulocyte Chemotactic Protein-2 (GCP-2/CXCL6), Oncostatin M (OSM) en Vascular Endothelial Growth Factor (VEGF) werden verder onderzocht in hoofdstuk 6 met behulp van specifieke immunoassays. De drie markers werden significant geïnduceerd in U937 macrofagen en in bloedmacrofagen door  $\beta_2$ -agonisten (clenbuterol en zilpaterol) in de aan- en afwezigheid van LPS. De inductie van deze markers werd ook bewerkstelligd door andere cAMP verhogende verbindingen (forskolin, prostaglandine E2 en dibutyryl cAMP). Deze resultaten suggereren een mogelijke rol van cAMP in de inductie van GCP-2/CXCL6, OSM en VEGF. Ook wordt een mogelijke rol van deze eiwitten bediscussieerd bij enkele nadelige bijeffecten die kunnen optreden tijdens de behandeling van astma met  $\beta_2$ -agonisten.

In het tweede deel van dit proefschrift werd een geneesmiddel bestudeerd dat uit meerder bio-actieve componenten bestaat, namelijk *Cannabis Sativa*. In hoofdstuk 7 werd het immunomodulerende effect van onverhit en verhit Cannabis extract onderzocht. Deze studie laat zien dat zowel onverhitte Cannabis extracten als de voornaamste component die in de plant aanwezig is,  $\Delta^9$  – tetrahydrocannabinolic acid (THC-zuur) de productie van LPS geïnduceerde TNF- $\alpha$  productie kan remmen in U937 macrofagen en in bloedmacrofagen. THC-zuur is zelf niet psychoactief en de cannabinoid receptors CB1 en CB2 bleken niet betrokken te zijn bij het TNF- $\alpha$  remmende effect. Verder kwam uit deze studie naar voren dat onverhitte Cannabis extracten en THC-zuur hun TNF- $\alpha$  remmende effect via een ander mechanisme bewerkstelligen dan verhitte Cannabis extracten. Dit gold ook voor het hoofdbestanddeel van verhit Cannabis, de psychoactieve component  $\Delta^9$ -tetrahydrocannabinol (THC). Onverhit Cannabis extract en THC-zuur remde de TNF- $\alpha$  productie gedurende een langere tijd, terwijl verhit Cannabis extract en THC de TNF- $\alpha$  productie na langere tijd juist stimuleerden tot een niveau dat hoger was dan verkregen na blootstelling aan LPS alleen. In de studie werd ook gekeken naar het effect van Cannabis op de fosfatidylcholine specifieke phospholipase C (PC-PLC) activiteit in U937 macrofagen. Hierbij werd een belangrijk verschil gevonden tussen THC en THC-zuur. Onverhit Cannabis extract en THC-zuur remde de PC-PLC activiteit op een concentratie afhankelijk manier, terwijl THC bij hogere concentraties juist de PC-PLC activiteit stimuleerde. Uiteindelijk werd het effect van onverhit Cannabis extract en

THC-zuur bestudeerd in een EAE (Experimental Autoimmune Encephalomyelitis) muis model. Onverhit Cannabis extract en THC-zuur vertoonden een gunstig effect op de klinische en histologische verschijnselen van EAE. De *in vivo* waargenomen effecten waren echter niet eenduidig en verder onderzoek is hier noodzakelijk.

Hoofdstuk 8 beschrijft de karakterisering van onverhitte en verhitte Cannabis extracten met behulp van het modelsysteem dat beschreven staat in hoofdstuk 3. De mRNA expressiepatronen van U937 macrofagen blootgesteld aan LPS in de aan- en afwezigheid van verschillende ontstekingsremmende verbindingen en verhitte en onverhitte Cannabis extracten werden geanalyseerd met behulp van PC-DA. De studie laat zien dat verhit en onverhit Cannabis extract een verschillend mRNA expressiepatroon induceert. Dit is in overeenstemming met de resultaten van hoofdstuk 7, waar werd gevonden dat onverhitte en verhitte Cannabis extracten op verschillende manieren de TNF- $\alpha$  productie remmen. Bovendien vertoonden de mRNA expressiepatronen geen overlap met de expressiepatronen van bekende klassen van ontstekingsremmers, waarvan bekend is dat zij de TNF- $\alpha$  productie remmen. Dit zou kunnen betekenen dat de Cannabis extracten niet ingedeeld zouden kunnen worden bij de in dit onderzoek gebruikte klassen van ontstekingsremmers. Meer onderzoek is nodig om de precieze werkingsmechanismen van onverhitte en verhitte Cannabis extracten te ontrafelen.

Uit de studies beschreven in dit proefschrift kunnen we concluderen dat toepassing van systeembioïologie een belangrijke bijdrage leveren aan het ontdekken en karakteriseren van ontstekingsremmende verbindingen, wanneer de mRNA- en lipide- expressiepatronen en het vinden van specifieke biomarkers worden geïntegreerd. De resultaten verkregen uit de proteomics studie waren minder goed bruikbaar voor het classificeren van ontstekingsremmers, waarbij gebruik werd gemaakt van het U937 modelsysteem. Een mogelijke verklaring hiervoor zou kunnen zijn dat er slechts een beperkte eiwitfractie op de 2-D gel geanalyseerd kon worden. Prefractionering, eiwit-verrijkingstrategieën en de toepassing van verschillende analytische methoden tegelijkertijd zijn daarom nodig om een grotere verscheidenheid aan eiwitten, met verschillende fysiologische eigenschappen en dynamisch bereik te kunnen analyseren. De transcriptomics, proteomics en metabolomics datasets werden geanalyseerd met behulp van patroonherkenningsmethoden. De datasets bevatten vaak een gelimiteerd aantal monsters ten opzichte van het aantal variabelen. Het is daarom

belangrijk om deze methoden slechts verkennend te gebruiken. Daarnaast moeten de gevonden biomarkers biologisch gevalideerd worden door middel van additionele metingen.

Ten slotte dient te worden opgemerkt dat bij het hier beschreven onderzoek nog maar een deel van de methoden en technieken uit de systeembio­logie cirkel is toegepast (figuur 1, hoofdstuk 9). Desondanks vormen de resultaten van het onderzoek een onderbouwing voor de stelling dat de principes en de aanpak van de systeembio­logie het onderzoek en de ontwikkeling van nieuwe geneesmiddelen blijvend zullen beïnvloeden.



---

## Curriculum vitae

Kitty Catharina Maria Verhoeckx werd geboren op 14 augustus 1970 te Utrecht. Na het behalen van het H.A.V.O. diploma aan de katholieke scholengemeenschap St. Gregorius te Utrecht in 1987, heeft zij het vijfde jaar van het V.W.O aan het Bonifatius college te Utrecht met goed gevolg doorlopen (1988). In datzelfde jaar startte zij met de propedeuse van het HLO (hoger laboratorium onderwijs) aan de hogeschool van Utrecht te Utrecht. In 1989 vervolgde zij haar HLO opleiding met als studie richting Analytische Chemie. Haar 9 maanden durende stage volbracht zij in 1991 bij de divisie Analyse van TNO Voeding te Zeist. Onder leiding van C.G. van der Paauw deed zij onderzoek naar planaire polychloorbifenylen (PCB's) in botlevers met behulp van vloeistof- en gaschromatografische technieken. De HLO opleiding werd in 1992 met succes voltooid. Na haar stage bleef zij werkzaam bij dezelfde werkgroep als research medewerker. In 1997 werd haar loopbaan voortgezet bij de afdeling Bioanalyse van TNO Voeding te Zeist, waar zij zich biochemische technieken eigen maakte. Ondertussen volgde zij de cursus Biochemie en Toxicologie aan de Open Universiteit te Utrecht. Van 1 mei 2000 tot 1 mei 2005 was zij als assistent in opleiding (AIO) werkzaam bij dezelfde afdeling, alwaar het in dit proefschrift beschreven onderzoek werd uitgevoerd onder leiding van Prof. Dr. J. van der Greef, Dr. R.J.T Rodenburg en Dr. R.F. Witkamp. Sinds 1 mei 2005 is zij werkzaam als wetenschappelijk medewerker bij de afdeling Analytical Sciences van TNO Quality of Life te Zeist.



---

## Nawoord

De vijf jaren van mijn promotieonderzoek zijn voorbij gevlogen. Het lijkt alsof ik gisteren nog aan Els de Groene vroeg of het iets voor mij was: AIO zijn. Ik ben erg blij dat zij vol enthousiasme reageerde en voordat ik het wist was ik AIO. Helaas verliet Els al snel daarna TNO om haar carrière voort te zetten bij Unilever. Els, ik vond en vind het nog steeds jammer dat je niet bij ons bent gebleven. Ik bewonder je enthousiasme en positieve instelling, dat gaf mij een enorme impuls om een promotieonderzoek te starten. Eén van de belangrijkste taken van mijn onderzoek was het opzetten van proteomics technieken. Samen met o.a. Sonja Jespersen en Marco Gaspari hebben we het klaargespeeld om dit bij TNO op de rails te zetten. Sonja, je hebt me erg veel geleerd op het gebied van eiwitidentificatie, soms tot in de late uurtjes. Als je er eenmaal in zit dan raak je er aan verslaafd. Ik vind het jammer dat je TNO hebt verlaten, ik mis je gezelligheid en had graag nog meer van je geleerd. (mange lykke og kærlighed). Marco, ik vond het ook erg leuk om met jou samen te werken, maar helaas ben jij ook weer naar huis teruggegaan. In de loop der jaren was je niet alleen een collega AIO, maar ben je ook een goede vriend geworden. Ik hoop dat we in de toekomst contact blijven houden zowel privé als op proteomics gebied. (ringraziare e molto contentezza).

Daarnaast wil ik ook graag mijn kamergenoten benoemen. Gina Bottger, Barry Blankvoort en Robert Doornbos, ik vond het erg prettig om af en toe als analyticus even hardop te kunnen brainstormen over biochemische problemen. Robert, ik stel het erg op prijs dat je in de laatste jaren van mijn AIO onderzoek alle financiën hebt geregeld. Het langste heb ik samengewerkt met Angélique van Meeteren en Linda Le Noble. Ik waardeer jullie interesse en hulp bij het tot stand komen van dit proefschrift.

Buiten mijn eigen productgroep hebben ook vele anderen aan mijn onderzoek bijgedragen. Sabina Bijlsma, je hebt me een hoop geleerd over patroonherkenning. Ik vond je uitleg altijd erg duidelijk en de samenwerking heb ik altijd als erg prettig ervaren. Ik hoop dat we dit in de toekomst zullen voortzetten. Raymond van Hilten, ondanks dat je me helemaal hebt lek geprikt, ben ik je erg dankbaar voor al die keren dat je direct klaar stond om bloed te prikken. De stagiaires, Maarten Notenboom, Petra Blom en Danielle Broekhuizen, ik vond het erg leuk dat jullie bij mij stage wilden lopen. Bovendien was het een uitdaging om jullie wat te leren en te begeleiden. Ook de input van de mensen van de afdeling Analytical Services, in het bijzonder Martin Baak, Robert Schilt, Natascha van Heeringen-Overmars voor hun kennis op het gebied van beta-agonisten en radioactiviteit en de mensen van TNO-PG, Henrie Korthout, Mei Wang en Lex Nagelkerken voor hun cannabis kennis, wil ik niet vergeten te noemen.

---

Daarnaast wil ik de gastvrijheid van de afdeling Toxicology en Analytical Biosciences van de Universiteit Leiden vermelden en metname Marjo de Graauw, Ine Tijdens, en Bertil Hofte voor het gebruik van de apparatuur en jullie uitleg daarbij. Loes Beijersbergen wil ik graag bedanken voor haar goede zorgen en al het regelwerk.

Als laatste wil ik graag mijn familie en vrienden (V'96 en karetrekkers) bedanken voor de interesse die ze de afgelopen jaren in mij en mijn werk hebben getoond. Hierbij wil ik in het bijzonder Maurien Olsthoorn bedanken voor het doorlezen van het manuscript en het interessante congresbezoek in Sienna. Pa en Ma bedankt voor jullie steun bij alle stappen die ik tot nu toe genomen heb. Jullie stonden en staan altijd voor me klaar en dat zal ik nooit vergeten. Als aller laatste wil ik Jeroen bedanken voor zijn geduld, liefde, kopjes thee en lekkere maaltijden als ik weer laat thuis kwam of druk bezig was achter de computer. Ook je AIO-dip-film was erg opbeurend. Zonder jou steun en vertrouwen, was ik niet zover gekomen. Het is bijna achter de rug. Daarna kunnen we weer gezellig in de tuin werken, klussen en vele andere leuke dingen doen.

Kitty

---

## List of publications

Stierum, R., Gaspari, M., Dommels, Y., Ouatas, T., Pluk, H., Jespersen, S., Vogels, J., Verhoeckx, K., Groten, J. and van Ommen, B. (2003). Proteome analysis reveals novel proteins associated with proliferation and differentiation of the colorectal cancer cell line Caco-2. *Biochim Biophys Acta*, 1650, 73-91.

Verhoeckx, K.C., Bijlsma, S., de Groene, E.M., Witkamp, R.F., van der Greef, J. and Rodenburg, R.J.T. (2004). A combination of proteomics, principal component analysis and transcriptomics is a powerful tool for the identification of biomarkers for macrophage maturation in the U937 cell line. *Proteomics*, 4, 1014-28.

Verhoeckx, K.C., Bijlsma, S., Jespersen, S., Ramaker, R., Verheij, E.R., Witkamp, R.F., van der Greef, J. and Rodenburg, R.J.T. (2004). Characterization of anti-inflammatory compounds using transcriptomics, proteomics, and metabolomics in combination with multivariate data analysis. *Int Immunopharmacol*, 4, 1499-514.

Korthout, H.A.A.J., Verhoeckx, K.C.M., Witkamp, R.F., Doornbos, R.P., and Wang, M. (2005). Medicinal acidic cannabinoids. Patent number; WO2005072719 and EP1559423 (A1).

Verhoeckx, K.C.M., Doornbos, R.P., Witkamp, R.F., van der Greef, J., and Rodenburg, R.J.T. (2005) Beta-adrenergic receptor agonists induce the release of Granulocyte Chemotactic Protein-2, Oncostatin M, and Vascular Endothelial Growth Factor from macrophages. Accepted for publication in *Int Immunopharmacol*.

Verhoeckx, K.C.M., Gaspari, M., Bijlsma, S., Doornbos, R.P., van der Greef, J., Witkamp, R.F., and Rodenburg, R.J.T. In search of secreted protein biomarkers for the anti-inflammatory effect of  $\beta_2$ -adrenergic receptor agonists: application of DIGE technology in combination with multivariate and univariate data analysis tools. Accepted for publication in *J. Proteome Res.*

---

Verhoeckx, K.C.M., Doornbos, R.P., Witkamp, R.F., van der Greef, J., and Rodenburg, R.J.T. Inhibitory effects of the  $\beta_2$ -adrenergic receptor agonist Zilpaterol on the LPS-induced production of TNF- $\alpha$  *in vitro* and *in vivo*. Accepted for publication in J. Vet Pharmacol Ther.

Verhoeckx, K.C.M., Korthout, H.A.A.J., Lagerweij, T., Nagelkerken, N., Wang, M., van der Greef, J., Rodenburg, and R.J.T., Witkamp, R.F. Unheated *Cannabis sativa* extracts and its major compound THC-acid have potential anti-inflammatory properties not mediated by CB 1 and CB 2 receptor coupled pathways. Submitted for publication.

Gaspari, M., Verhoeckx, K.C.M., Verheij, E., and van der Greef, J. Integration of two-dimensional LC-MS with multivariate statistics for comparative analysis of proteomic samples. Submitted for publication.

---

## List of abbreviations

<b>A-FABP</b>	adipocyte-fatty acid binding protein
<b><math>\beta_2</math>-AR</b>	beta <sub>2</sub> -adrenergic receptor
<b>cAMP</b>	cyclic adenosine-3',5'-cyclic monophosphate
<b>CB</b>	cannabinoid
<b>CBD</b>	cannabidiol
<b>CBDa</b>	cannabidiolic acid
<b>CFU-G</b>	colony-forming unit granulocyte (granulocyte progenitor cell )
<b>CFU-GM</b>	colony-forming unit granulocyte-macrophage
<b>CFU-M</b>	colony-forming unit monocyte (monocyte progenitor cell)
<b>CNS</b>	central nervous system
<b>CXCL6</b>	granulocyte chemotactic protein-2
<b>CSA</b>	cross stain analysis
<b>D609</b>	tricyclodecan-9-yl-xanthogenate
<b>DIGE</b>	difference gel electrophoresis
<b>Ds</b>	discriminants
<b>EAE</b>	experimental autoimmune encephalomyelitis
<b>ELISA</b>	enzyme-linked immunosorbent assay
<b>ESI</b>	electrospray ionisation
<b>FBS</b>	fetal bovine serum
<b>FT-MS</b>	fourier transform mass spectrometer
<b>GCP-2</b>	granulocyte chemotactic protein-2
<b>GILT</b>	gamma interferon inducible lysosomal thiol reductase
<b>GPCRs</b>	GTP-binding protein-coupled receptors
<b>HPLC-IT-MS</b>	high performance liquid chromatography ion trap mass spectrometry
<b>ICAT</b>	isotopic coded affinity taq
<b>IFN<math>\gamma</math></b>	interferon gamma
<b>IL-1</b>	interleukine-1
<b>IP<sub>3</sub></b>	inositol 1,4,5-triphosphate
<b>LDH</b>	lactate dehydrogenase
<b>LPC</b>	lysophosphatidylcholine
<b>LPS</b>	lipopolysaccharide
<b>MALDI</b>	matrix assisted laser desorption ionisation
<b>MDLC</b>	multidimensional liquid chromatography

---

<b>MIP-1<math>\beta</math></b>	macrophage inflammatory protein-1beta
<b>MHC</b>	major histocompatibility complex
<b>MVDA</b>	multivariate data analysis
<b>MS</b>	multiple sclerosis
<b>MUDPIT</b>	Multi Dimensional Protein Identification Technology
<b>NMR</b>	nuclear magnetic resonance
<b>NO</b>	nitric oxide
<b>11-OH-THC</b>	11-hydroxy- $\Delta^9$ - tetrahydrocannabinol
<b>OSM</b>	oncostatin M
<b>RP</b>	reverse-phase
<b>PB-M<math>\emptyset</math></b>	peripheral blood macrophages
<b>PB-MO</b>	peripheral blood monocytes
<b>PBS</b>	phosphate buffered saline
<b>PC</b>	principal component
<b>PCA</b>	principal component analysis
<b>PC-DA</b>	principal component discriminant analysis
<b>PCR</b>	polymerase chain reaction
<b>PCs</b>	principal components
<b>PC-PLC</b>	phosphatidylcholine phospholipase C
<b>PGE<sub>2</sub></b>	prostaglandin E <sub>2</sub>
<b>PMA</b>	phorbol 12- myristate 13-acetate
<b>PLA<sub>2</sub></b>	phospholipase A <sub>2</sub>
<b>PLS-DA</b>	partial least squares discriminant analysis
<b>RT</b>	reversed transcription
<b>SCX</b>	strong cation exchange
<b>SELDI</b>	surface enhanced laser desorption ionisation
<b>SILAC</b>	stable isotope labelling by amino acids in cell cultures
<b>TBST</b>	tris-buffered saline tween-20
<b>THC</b>	$\Delta^9$ -tetrahydrocannabinol
<b>THCa</b>	$\Delta^9$ -tetrahydrocannabinoid acid
<b>THC-COOH</b>	11-nor-9-carboxy- $\Delta^9$ - tetrahydrocannabinol
<b>TNF-<math>\alpha</math></b>	tumor necrosis factor alpha
<b>TNF-<math>\beta</math></b>	tumor necrosis factor beta.
<b>VEGF</b>	vascular endothelial growth factor

---